Using Modelling to Optimise the Use of Biological Control Agents Against Soil-Borne Plant Pathogens

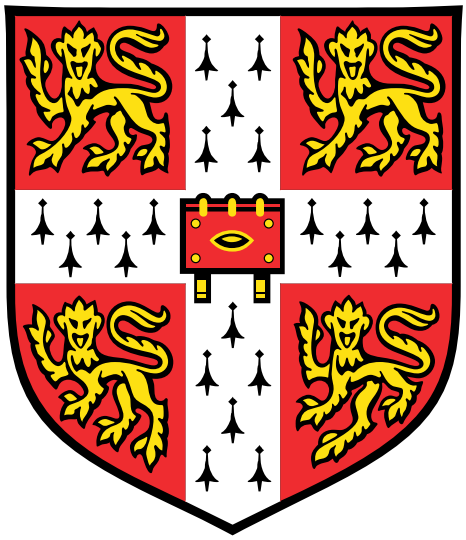

Sarah Joanne Mitchell

Department of Plant Sciences

University of Cambridge

This dissertation is submitted for the degree of

Doctor of Philosophy

Gonville and Caius College

April 2021

Declaration

This thesis is the result of my own work and includes nothing which is the outcome of work done in collaboration except as declared in the preface and specified in the text.

This thesis is not substantially the same as any that I have submitted, or, is being concurrently submitted for a degree or diploma or other qualification at the University of Cambridge or any other University or similar institution except as declared in the Preface and specified in the text.

This thesis does not exceed the prescribed word limit of 60,000 words (excluding bibliography, figures and appendices) as specified by the Degree Committee of the Faculty of Biology.

Sarah Joanne Mitchell

April 2021

Abstract

There is considerable interest in the use of biological control agents as a control strategy against plant pathogens. However, significant variability in their success at pathogen suppression across field trials has resulted in them often not being seen as commercially viable. This thesis uses mathematical modelling to explore the interactions between a soil-borne biocontrol agent, a soil-borne pathogen, and the roots of a host plant. Understanding the dynamics of these organisms in more detail can allow us to optimise the use of biological control agents.

We construct a model that focuses on the roots of a plant and whether they are infected by a pathogen or colonised by a biocontrol agent, as well as including any free-living pathogen and biocontrol agent in the surrounding soil. Although this model can be used across multiple systems, this thesis focuses on modelling the infection of winter wheat by *Gaeumannomyces graminis* var. *tritici* and suppression by the biocontrol agent 2,4-DAPG fluorescent *Pseudomonas* spp. Parameter values are obtained for the model through fitting it to data from this system.

Application timing and amount of application were both found to affect the ability for a biocontrol agent to suppress a pathogen. Including a break crop into a simulation had a negative impact on both the pathogen and biocontrol agent, suggesting that combining multiple strategies for epidemic suppression may not always be effective. Planting a crop with even spaces between plants, or in rows with 12cm between each row, was found to reduce epidemic severity more than if rows were spaced further apart for the first year of an epidemic. However, large-scale dispersal of free-living material between growing seasons from agricultural machinery reduced any benefit of specific spatial arrangements of a crop in the second year of an epidemic. Aggregation of the pathogen and biocontrol agent were found to affect epidemic severity, with the greatest reduction from a highly aggregated pathogen and a uniformly distributed biocontrol agent. We suggest that a greater focus on optimising application, as well as a detailed understanding of how the spatial dynamics of a biocontrol agent and pathogen can affect this application, may enhance the success of biocontrol agents and allow them to be seen as a viable control strategy.

Acknowledgements

Firstly, I would like to thank my supervisor, Nik Cunniffe. Thank you for all of your support and guidance throughout my PhD. Your kindness and encouragement have been greatly appreciated.

I would like to thank all the members, both past and present, of the Epidemiology and Modelling group and the Theoretical and Computational Epidemiology group. It has been wonderful spending time with all of you. My co-supervisor, Chris Gilligan, also deserves thanks for his useful insights and discussions about take-all disease with me.

I am very grateful to the BBSRC for funding my PhD, and to the Department of Plant Sciences for being such a welcoming place to work. I must also thank my college, Gonville and Caius, for organising countless formals and social events that I always looked forward to attending.

Finally, I would like to thank all of my friends and family for their love and support throughout my time in Cambridge. I could not have managed without such an incredible group of people to make every day a little bit better. Special thanks should go to my parents and my sister for inspiring me and encouraging me throughout my life. Thank you to all of my friends from college for brightening my days in the library and providing me with many enjoyable breaks from my work. I am also incredibly grateful to all the residents of 27 Ross Street, both past and present. Especially during the final few months of my PhD, you have been absolutely amazing.

Table of contents

List of figures

List of tables

Chapter 1: Introduction

1.1 The global effect of plant diseases

Plant pathogens across the world cause approximately 10% of crop production to be lost to disease (Oerke, 2006; Savary et al., 2019; Strange and Scott, 2005). The impact of root diseases in particular is constantly increasing, with the presence of certain soil-borne diseases like Rhizoctonia, Pythium and Fusarium root rots so ubiquitous that their presence is considered normal when growing crops such as wheat (Cook, 2001). With an estimated 800 million people worldwide currently undernourished (von Grebmer et al., 2008), it is vital that we can learn how to successfully control these diseases and reduce their impacts.

There are many control methods against plant pathogens already in use, but they all have disadvantages and variable success rates. Concerns about possible detrimental environmental impacts are leading to increased legislative constraints on chemical controls and are limiting their uses (Handford et al., 2015). For many crops including wheat, there are a lack of pathogen-resistant crop varieties, and there has also been mixed success for cultural control methods such as tilling and crop rotations (López-Bellido et al., 1996; Sieczka, 1988). The often rapid evolution of resistant pathogens to chemical controls and new crop varieties can also make chemical and genetic control economically unviable (Cook, 2003; Parnell et al., 2008; van den Bosch and Gilligan, 2008). Due to these factors, there is a growing interest in the use of biological control agents as an alternative strategy to aid in reducing the impact of crop diseases.

1.2 The use of biological control agents as a control strategy against plant pathogens

The definition of a biological control agent is given in Eilenberg et al. (2001) as "The use of living organisms to suppress the population density or impact of a specific pest organism, making it less abundant or less damaging than it would otherwise be". The terms "biocontrol agent" and "biological control agent" are used interchangeably in the literature and both refer to the same thing. The earliest known use of a biocontrol agent dates back to 304 A.D. where nests of the ant *Oecophylla smaragdina* were used in China to suppress insect pests of citrus (Huang and Yang, 1987). Since then, there have been many introductions of biocontrol agents to suppress weeds, animals, and pathogens (Tjamos et al., 1992; van den Bosch et al., 1982). Past introductions have often involved trial and error and minimal planning, with no consideration about potential long-term impacts. Today there is a significant amount of legislation across the UK and Europe that requires the introduction of any living organism to undergo risk assessments based on its persistence in the environment after introduction, as well as any potentially detrimental impacts it may have (Köhl et al., 2019a; Scheepmaker and Butt, 2010; Sundh and Goettel, 2013).

The focus of this thesis is the use of soil-borne biocontrol agents against soil-borne plant pathogens. Screening for potential soil-borne biocontrol agents requires the identification of microorganisms in the soil that seem to suppress one or several plant diseases. Once identified, experiments can be performed to determine how well they can suppress specific plant diseases and how viable they may be for use commercially (Pliego et al., 2011). Many soil-borne microorganisms that are suppressive to plant pathogens and have the potential to be successful biocontrol agents have been identified. Examples include *Bacillus subtilis* (Shoda, 2019), *Pseudomonas* spp. (Weller, 2007), *Sporidesmium sclerotivorum* (Adams and Ayers, 1981), *Gliocladium catenulatum* (Mcquilken et al., 2001), *Streptomyces*

spp. (Vurukonda et al., 2018), *Coniothyrium minitans* (Whipps and Gerlagh, 1992), *Purpureocillium lilacinum* (Lan et al., 2017), *Trichoderma* spp. (Harman, 2006), and *Fusarium* spp. (Fravel et al., 2003).

However, there is still minimal commercial uptake of biocontrol agents as a control strategy against plant pathogens. For example, the use of biopesticides only represents about 1% of agricultural chemical sales (Lidert, 2001). This is due to high variability in their success across different field trials and environmental conditions (Fravel, 2005; Mathre et al., 1999). Biocontrol agents are living organisms and needs suitable conditions to survive and persist. Highly controlled greenhouse studies often provide optimal conditions for their survival, whereas field trials will vary across conditions such as soil type, temperature, and precipitation. There is also considerable variation in factors such as application timing and amount, as well as how a patchy dispersal of the pathogen and biocontrol agent can affect epidemic suppression. The uptake of biocontrol agents as a viable control strategy will only be possible if their success can be consistent regardless of external factors. This requires the identification of such factors and an analysis of how they impact specific biocontrol agents. Additional research is then required to identify how these biocontrol agents can be applied to overcome such limitations, as well as how their use as a control strategy can be optimised across a variety of different conditions (Spadaro and Gullino, 2005).

1.3 Challenges of using soil-borne biocontrol agents

There is an additional challenge when using soil-borne biocontrol agents compared to other biocontrol agents. This comes from their introduction into the soil surrounding a plant, which is called the rhizosphere. The rhizosphere is defined as the area around a plant root that is inhabited by a diverse population of microorganisms, and in which the root and these microorganisms can interact (Bakker et al., 2013). There is a mutualistic relationship between many soil-borne microorganisms and plants, resulting in microbial

population densities in the rhizosphere between 10 to 20 times greater than in the bulk soil (Dandurand and Knudsen, 1997; Weller and Thomashow, 1994). Roots exude a variety of metabolites into the rhizosphere, including up to 10–50% of a plants' fixed carbon (Jones et al., 2009; Kuijken et al., 2015; Massalha et al., 2017). In return, microorganisms can provide the plant with benefits such as fixing atmospheric nitrogen for plant use, and suppressing pathogens. The rhizosphere is incredibly diverse, and interactions between roots and microorganisms can significantly benefit plant health and growth. However, it also provides a highly competitive environment for any introduced biocontrol agent. The composition of microorganisms in the rhizosphere will have a significant impact on the success and prevalence of a biocontrol agent. This can be through competition for space and nutrients, as well as antagonistic behaviour such as the release of toxic chemicals (Ciancio et al., 2019; Nyaku et al., 2017).

There are considerable changes to the rhizosphere during a growing season as a plant and its roots grow. As well as the growth of a root proving more space for colonisation by microorganisms, the metabolites exuded by a root change throughout the season and are heavily affected by external factors. There is also a significant change in rhizosphere dynamics for crops that are planted and harvested each year. In between harvesting a crop and planting the next, any microorganisms in the soil must survive on decaying organic matter without a host. Although this is not a problem for a biocontrol agent that decays rapidly and would not be expected to survive more than one growing season, this temporal heterogeneity can significantly affect the populations of other microorganisms. This will in turn impact the success of any biocontrol agent applied during the following growing season (Angus et al., 2015; Ashworth et al., 2017).

There are also considerable practical challenges affecting the success of soil-borne biocontrol agents. One example is trying to identify microorganisms that may be suitable candidates for use as biocontrol agents. It is often difficult to identify which microorganisms

in the rhizosphere are responsible for the suppression of a pathogen (Knudsen et al., 1997; Pliego et al., 2011). However, recent advances in technology have led to the development of ways in which microbial populations can be identified and examined over time (Lievens et al., 2006; Lievens and Thomma, 2005; Tsui et al., 2011). A microorganism that has an increasing population density whilst a pathogen is experiencing increased suppression may be a key player in epidemic suppression. Likewise, a microorganism that is frequently found in soil that seems to suppress a particular disease may be a suitable target for future research. As discussed later in Section 1.4, epidemic suppression may in fact be due to a combination of interactions between different microorganisms within the rhizosphere rather than one particular species (Weller et al., 2002). It would not be possible to use the microorganisms from this soil as biocontrol agents together because there are too many microorganisms involved in this suppression. Instead, the application of a biocontrol agent often involves a single species.

1.4 Suppressive soils

The ability for certain soils to suppress pathogen activity is well known and has been researched extensively. This suppressive behaviour is attributed to microbial activity in the rhizosphere, with plants supporting specific microorganisms that are able to negatively affect pathogens. Suppressive soils can be divided into two categories – general suppression and specific suppression. General suppression is attributed to the collective activity of all the microorganisms in the rhizosphere, where competition for space and nutrients, or other antagonistic interactions, result in a reduction in pathogen severity. All soils can be assumed to have some level of general suppression. Specific suppression is instead attributed to the activity of a single or select group of microorganisms. These microorganisms will have a higher impact on epidemic suppression than would be exhibited by general suppression and will often have significantly greater population sizes than other microorganisms in the

rhizosphere. The difference between general and specific suppression can be determined through the transferability of suppression. General suppression cannot be transferred from one soil to another, whereas specific suppression can be transferred by adding a small amount of this suppressive soil to a conductive soil. The location of general suppression extends out into the bulk soil, whereas specific suppression will be concentrated in the rhizosphere that directly surrounds a plant's roots (Schlatter et al., 2017; Weller et al., 2002).

There are many different mechanisms that biocontrol agents can use to negatively affect a pathogen, regardless of whether they are involved in general or specific suppression. Many extensive reviews of these mechanisms exist, as well as examples of how they relate to specific biocontrol agents (Jamalizadeh et al., 2011; Köhl et al., 2019b; Mitchell, 1973; Pal and McSpadden Gardener, 2006; Reddy and Reddy, 2014). The main mechanisms are briefly described below.

Competition for space

A biocontrol agent may be able to protect a root by colonising any sites of potential infection and blocking the pathogen from accessing them. Colonisation is widely believed to play a role in the success of soil-borne biocontrol agents. However, there often seems to be minimal correlation between population size and the ability of a biocontrol agent to suppress a pathogen (Handelsman and Stabb, 1996). Even when there is a correlation, such as between wheat roots colonised by *Pseudomonas fluorescens* spp. and suppression of take-all disease, *Pseudomonas fluorescens* spp. is thought to occupy at most 0.1% of the total space on a plant's roots (Haas and Keel, 2003). It therefore seems likely that competition for space is combined with other mechanisms of pathogen suppression by most or all biocontrol agents.

Competition for nutrients

The rhizosphere is a highly competitive environment, and competition for nutrients between microorganisms is common. One example of this is with iron, which is one of the most limited substances in the rhizosphere, and there is therefore strong competition for acquiring it. Some biocontrol agents can secrete iron-binding ligands called siderophores which allows them to sequester iron into their cells and and limit others microorganisms from accessing it. Depriving pathogens of iron can reduce their growth and result in their suppression.

Antibiosis

The production of one or more antibiotics is a common strategy used by biocontrol agents. These compounds can reduce the growth and increase the death rate of pathogens. The effectiveness of an antibiotic requires the production of a sufficient amount of the chemical to have a detrimental impact.

Parasitism and lysis

It is possible for some biocontrol agents to parasitise pathogens. This requires direct contact between the two organisms and the production of lytic enzymes that can digest a pathogen's cell wall. Parasitism by a biocontrol agent is often specific to a single pathogen and is therefore more likely to be involved in specific suppression rather than general suppression.

Induced resistance

The interactions between a biocontrol agent and a plant can induce a change in the plant to increase its defences against a variety of pathogens. When the plant's natural defences have been induced, it can respond more effectively to any infection to reduce the impact of any pathogens.

1.5 Take-all and the phenomenon of take-all decline

1.5.1 Take-all disease

Wheat provides 20% of all food calories consumed globally (Breiman and Graur, 1995), and a 60% worldwide increase in demand is expected by 2050 (Alexandratos and Bruinsma, 2012). The production value of wheat in the UK alone is £1.7 billion, with the crop grown across 1.8 million hectares. Take-all is believed to be the most damaging disease to wheat worldwide, with the UK estimating losses between £85 million and £340 million each year (Osbourn and Ridout, 2013).

Take-all disease is caused by the soil-borne fungus *Gaeumannomyces graminis* var. *tritici* (*Ggt*) (Kwak and Weller, 2013). It causes blackening and rotting of the roots and base of the stem, disrupting nutrient-intake and the flow of water through the crop. This can lead to shrivelling of the grain and sometimes premature death (Cook, 2003). The pathogen has two distinct stages, referred to as the primary and secondary stages. The primary stage is the sporophyte stage, in which the pathogen lives on infected root residues in the soil. This allows it to persist in the soil even after the crop has been harvested. Most pathogen inoculum decays rapidly, but it has been found to persist at low levels even after a year's break from growing wheat (Hornby, 1975). The secondary stage involves the pathogen living on the roots of a plant, where the pathogen infects the wheat root tissue and can then spread within or between plants through infected and uninfected roots within close proximity of each other (Bailey and Gilligan, 1999; HGCA, 2006; Wiese, 1987). This leads to two distinct types of infection - primary infection through soil-borne inoculum, and secondary infection from other infected roots (Brassett and Gilligan, 1988).

The pathogen is most severe when wheat is grown in wet conditions, either due to high irrigation or rainfall. It will often form patches of severely infected plants under these conditions. A single piece of inoculum will infect a plant through primary infection,

and secondary infection will spread the disease to nearby plants through root-to-root contact, radiating the infection out from this central point (Cook, 2003; Kwak et al., 2012). However, take-all can still cause infection under low precipitation in countries such as Australia (Paulitz et al., 2002). These conditions severely limit secondary infection, and each plant will typically have to be infected from a different source of free-living inoculum. Patches of infection are usually absent under these dry conditions. The pathogen favours alkaline, light soils, and a high concentration of nitrogen in the soil (Alford, 2008; Gareth, 1983; Kwak and Weller, 2013).

There are no resistant cultivars and chemical control is only partially successful (Cook, 2003). Although crop rotations and tillage can be effective, the reduction in crop yield from low or no tillage, and the economic impacts of growing wheat continuously, severely reduce the benefits of using them. Take-all can be completely suppressed by the use of soil fumigants, but the cost of these makes them an economically unviable control method for farmers (Weller, 2007; Weller et al., 2002). The fungicide silthiofam has shown promising results in field trials when applied as a seed treatment. However, it is not able to completely suppress the pathogen (Bailey et al., 2005; Huang et al., 2001; Spink et al., 2004).

1.5.2 Take-all decline

Despite the above unsuccessful control methods, there is a naturally occurring phenomenon called take-all decline that results in the epidemic suppression of take-all on wheat globally. Take-all decline is defined as the reduction in incidence and severity of take-all disease after a severe outbreak of the disease during continuous wheat monoculture. It is one of the most well-known and highly studied examples of specific suppression in the soil and occurs across a multitude of different environmental conditions. It has been found throughout Europe, Australia, and North America, and follows a similar pattern in each of these locations (Asher and Shipton, 1981; Campbell, 1989; Gerlagh, 1968; Hornby, 1998;

Kwak and Weller, 2013; Shipton, 1972; Simon and Sivasithamparam, 1989; Weller et al., 2002). The peak of the epidemic often occurs in the second or third year of consecutively growing wheat (Baker and Cook, 1982; Gerlagh, 1968; Shipton, 1972; Walker, 1975), but sometimes takes between four to seven years (Cook, 1988; Shipton, 1975).

The first suggestion that there was a decline in take-all severity during continuous wheat cropping was noticed in the 1950s. Several experiments in the 1960s confirmed this pattern of decline, with an extensive amount of research attempting to establish its cause. Until the late 1990s, there were many conflicting theories. These included general suppression, changes to the virulence of the pathogen population across consecutive years of growing wheat, the infection of the take-all pathogen by a virus, as well as a variety of different specific biocontrol agents that may be involved (Hornby, 1979). A large number of microorganisms that exhibit antagonism towards *Ggt* have been identified in soils exhibiting suppression to take-all. Due to this, multiple different organisms have been proposed as being responsible for take-all decline (Chng et al., 2015; Dewan and Sivasithamparam, 1989; Sanguin et al., 2009; Simon, 1989; Weller et al., 2002; Weller, 1988; Yang et al., 2011).

However, there is now an abundant amount of research showing that fluorescent *Pseudomonas* spp. which produce the antibiotic 2,4-diacetylphloroglucinol (DAPG) have a key role in take-all decline. Although most of this research has been carried out in the United States and the Netherlands, there is strong evidence that these species are the main biocontrol agent involved in take-all decline across the world (De Souza et al., 2003; Landa et al., 2006; Raaijmakers et al., 1999; Raaijmakers and Weller, 1998; Raaijmakers et al., 1997). Antagonistic *Pseudomonas* spp. are well adapted to the rhizosphere, produce a variety of different antibiotics, and are consistently found in fields where wheat is grown.

The importance of 2,4-DAPG fluorescent *Pseudomonas* spp. in take-all decline has been established across multiple experiments. Elimination 2,4-DAPG fluorescent *Pseudomonas* spp. from soil exhibiting take-all decline by pasteurization or crop rotation has resulted in a

loss of take-all suppression (Raaijmakers and Weller, 1998). DAPG is highly effective against *Ggt* and affects multiple cellular pathways (Kwak et al., 2009, 2011). A mutant strain of fluorescent *Pseudomonas* spp. that cannot produce DAPG is no longer able to suppress take-all (De Souza et al., 2003; Raaijmakers and Weller, 1998, 2001). Over consecutive years of growing wheat, the population size of 2,4-DAPG fluorescent *Pseudomonas* spp. increase in the soil from often undetectable levels to levels as high as 10^9 CFU g^{-1} root. A threshold level of 10^5 CFU g^{-1} root is required to maintain take-all suppression, and fields where take-all decline has occurred will consistently have population sizes of 2,4-DAPG fluorescent *Pseudomonas* spp. above this threshold (Raaijmakers et al., 1999; Raaijmakers and Weller, 1998; Weller, 2007). This relationship between epidemic severity and population size of 2,4-DAPG fluorescent *Pseudomonas* spp. across several years of consecutively growing winter wheat is visualised in Figure 1.1. The epidemic severity increases over two or more consecutive years of growing winter wheat, with a low but slowly increasing population size of 2,4-DAPG fluorescent *Pseudomonas* spp. during this time. As this population size increases over the threshold value needed for suppression, disease severity is suppressed to a lower level. After take-all decline has occurred, disease severity remains low and the population size of 2,4-DAPG fluorescent *Pseudomonas* spp. remains above this threshold level.

As required for specific suppression, transferring soil containing 2,4-DAPG fluorescent *Pseudomonas* spp. to a conductive soil results in suppression of take-all (Raaijmakers and Weller, 1998). Even an addition of 0.001% by weight of soil exhibiting take-all decline to conductive soil can result in up to a 50% decrease in take-all on a wheat crop and the establishment of a population size greater than the threshold value (Pope and Hornby, 1975).

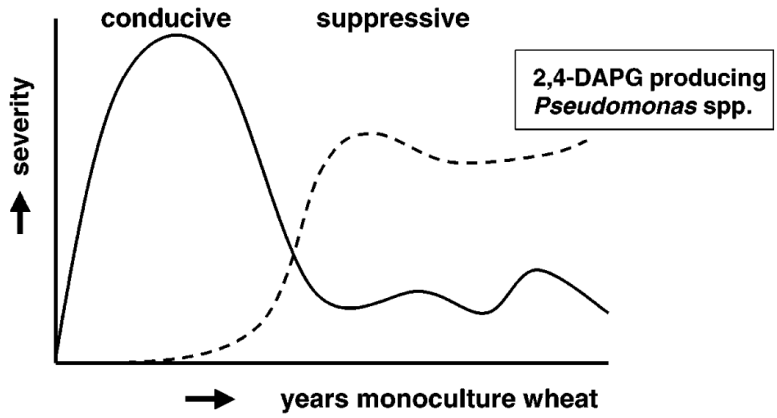

Fig. 1.1 Example of the epidemic severity and population size of 2,4-DAPG fluorescent *Pseudomonas* spp. during take-all decline. The epidemic severity of wheat grown during continuous monoculture is shown by the solid line, whereas the population size of 2,4-DAPG fluorescent *Pseudomonas* spp. is shown by the dashed line. Figure was obtained from Weller et al. (2002).

1.5.3 Distinguishing take-all decline from a decline in take-all

As mentioned in Section 1.5.2, although take-all decline is widely attributed to 2,4-DAPG producing *Pseudomonas fluorescens* spp., some studies have noticed a decline in take-all severity without this biocontrol agent present. This has led many to question whether in fact this biocontrol agent is responsible for take-all decline, or whether the biocontrol agent or agents involved may differ across countries and environmental conditions.

The evidence in support of 2,4-DAPG producing *Pseudomonas fluorescens* spp. playing a key role in take-all decline is overwhelming. Other microorganisms in the rhizosphere will play a part in take-all suppression through general suppression (Section 1.4). However, the activity of 2,4-DAPG producing *Pseudomonas fluorescens* spp. exhibits a prime example of specific suppression (Weller et al., 2002). This therefore produces the question – why is there so much variability in the biocontrol agents involved in the decline of take-all across different experiments? The answer to this comes from Walker (1975), who determined that the phenomenon of take-all decline was only one of six ways that the severity of take-all

could be reduced. "Take-all decline" requires specific criteria to be met, and reductions in epidemic severity that do not match these criteria are not examples of take-all decline. The six categories of suppression stated by Walker (1975) are:

1. Suppression of the pathogen in the first few years of consecutively growing severely diseased wheat. This is "take-all decline"
2. Suppression of the pathogen over a longer period of growing wheat consecutively
3. Suppression developed whilst growing wheat consecutively, but without severe disease required
4. Suppression developed in the presence of non-host plants. This is the same suppression as would occur if a break crop was grown
5. Suppression of the pathogen without a host plant. This suppression therefore occurs in the bulk soil rather than the rhizosphere.
6. General suppression exhibited by many soils

The phenomenon of "take-all decline" is therefore not associated with all decline of the take-all pathogen. Three conditions are regularly stated as necessary for the occurrence of "take-all decline": 1) the monoculture of wheat, 2) the presence of the take-all pathogen, *Gaeumannomyces graminis* var. *tritici*, and 3) at least one severe year of disease (Gerlagh, 1968; Hornby, 1979). Although there is little idea of what constitutes "severe" in the literature, the percentage of infected roots regularly reaches over 35% at the peak of infection (Bailey and Gilligan, 1999; Bailey et al., 2005; Hornby, 1979; Werker et al., 1991). If any of these conditions are not met, the reduction in epidemic severity should not be attributed to "take-all decline".

The distinction between these categories of suppression was popular in the 1970s and 1980s, when significant advances were being made into the research of take-all and the

use of biocontrol agents in disease suppression (Hornby, 1979). However, more recent research has ignored this distinction and often groups all decline of take-all into one category. Although this division of epidemic suppression into six categories may seem complicated, it can also help to explain the variability in biocontrol agents thought to cause take-all decline. The phenomenon of take-all decline is therefore caused by the single biocontrol agent, 2,4-DAPG producing *Pseudomonas fluorescens* spp. The suppression of take-all by any other biocontrol agent can be attributed to categories 2-6 from Walker (1975) and are not related to take-all decline. Creating this distinction allows for an explanation of the differences between the suppression of take-all by different biocontrol agents.

1.6 Conditions affecting the successful decline in take-all disease

Environmental conditions are well known to have significant impacts on microorganisms living in the soil. A decline in take-all severity has been observed with an increase in soil temperature (Dewan and Sivasithamparam, 1989), addition of organic material to the soil (Fellows and Ficke, 1932), fertilisation with NH_4^+ rather than NO_3^- (Sanguin et al., 2009; Smiley, 1973, 1979), and the use of tillage (Brooks and Dawson, 1968). There are different genotypes of 2,4-DAPG producing *Pseudomonas fluorescens* spp. strains that differ in their ability to suppress *Ggt* (Kwak et al., 2012; Okubara and Bonsall, 2008). Different cultivars of wheat are able to support these genotypes to different extents, and some cannot sustain large population sizes of 2,4-DAPG producing *Pseudomonas fluorescens* spp. (Meyer et al., 2010; Okubara et al., 2004; Raaijmakers and Weller, 1998). There are also genetically distinct populations of *Ggt* that are affected by 2,4-DAPG producing *Pseudomonas fluorescens* spp. differently (Daval et al., 2010).

All the factors above can also affect the specific phenomenon of take-all decline, causing differences to the duration before epidemic suppression occurs as well as the longevity of this suppression. Even a single year of detrimental conditions or the introduction of a break crop may result in a severe decrease in the population of *Pseudomonas* spp. to densities similar to their naturally occurring levels. Hornby (1992) postulated a potential link between the presence of take-all decline and high fertility/inputs. For systems with high fertility/inputs due to high use of fertilisers and irrigation, take-all decline is common. Lower fertility/input systems often exhibit a weaker trend of take-all, the complete absence of take-all, or only a short number of years where epidemic suppression occurs after take-all decline before severity increases again. The presence of a nutrient rich soil that is able to sustain a large number of microorganisms may therefore be important for the initiation and prevalence of take-all decline.

One of the important questions about take-all decline is whether it can be sped up to allow epidemic suppression to occur earlier. It would be significantly beneficial if there were a way to induce suppression without the need for at least one year of severe disease. Similarly, a guarantee of a specific level of suppression after a certain number of years of wheat monoculture would be highly advantageous. Although take-all decline is one of the most successful examples of biological control worldwide, it is limited by variability in its behaviour across different fields and environmental conditions. Experiments have been performed where 2,4-DAPG producing *Pseudomonas fluorescens* spp. is applied to a field in the hope that it can speed up take-all decline and enhance suppression compared to natural levels of the biocontrol agent (Cook, 2001; Mathre et al., 1999; Weller and Cook, 1982). However, there were problems with identifying the optimal application dose, and only minimal improvements to crop yield were found. The presence of other soil-borne diseases across field trials also made it difficult to determine the effects of 2,4-DAPG producing *Pseudomonas fluorescens* spp. on take-all only. Enhancing the suppressive behaviour of

2,4-DAPG producing *Pseudomonas fluorescens* spp. would be incredibly influential in the control of take-all and the potential success of biocontrol agents.

1.7 Optimising the use of biocontrol agents for disease suppression

The commercial use of biocontrol agents is severely limited by their variability in effectiveness across different experiments. This variability is often partially attributed to the significant impact of environmental conditions on biocontrol survival and persistence (Fravel et al., 1999; Mathre et al., 1999; Pliego et al., 2011). Due to the living nature of biological control agents, they will always be more influenced by such conditions than other non-biological methods. There is also little know about the optimal application frequency and dosage, as well as how the spatial distribution of a pathogen and biocontrol agent can affect the success of a biocontrol agent. However, the widespread presence of take-all decline in fields across the world (Cook, 2003; Kwak and Weller, 2013), as well as successful epidemic suppression by many other biocontrol agents, demonstrate that it should be possible for them to be seen as viable control strategies. Although changes to environmental factors and application strategy have an effect on the prevalence and population sizes of biocontrol agents, they are still often able to survive and persist. There should therefore be a focus on how we can optimise the use of biocontrol agents regardless of external factors.

Although significant research has been carried out on when to apply chemical control methods and what the optimal doses are (Beres et al., 2016; Cook et al., 1999; Sharma et al., 2015; Turkington et al., 2016), little has been performed for biocontrol agents (Spadaro and Gullino, 2005). A biocontrol agent that decays rapidly may not be successful if applied as a seed treatment as it will not be present for most of the growing season when the pathogen is present. Likewise, a biocontrol agent that requires time to bulk-up

in the rhizosphere before it can successfully suppress a pathogen may benefit from earlier application. The mechanisms that a biocontrol agent uses to suppress a pathogen may significantly affect the optimal time of application too. For example, a biocontrol agent acting through niche exclusion, where it occupies key sites on the root to prevent infection, would benefit from early application before any roots have already been infected. The amount of application is also important, with a low dose unable to effectively suppress the pathogen, whilst a high dose may become phytotoxic or may result in the biocontrol agent out-competing other beneficial microorganisms. This would result in decreased general suppression and may lead to an increase to epidemic severity. The specific behavioural dynamics of a biocontrol agent, as well as how they interact with the host and pathogen, need to be understood before successful application can occur.

Microbial populations within the soil are known to have patchy distributions which vary significantly in size with environmental conditions (Abbott et al., 2015; Clarkson and Polley, 1981; Hornby et al., 1989; White and Gilligan, 1998). Diseases such as take-all often produce patches of infected plants. Initial infection occurs from pathogen inoculum living in the soil, and the pathogen then spreads radially outwards between the interconnected roots of different plants. The impact of some soil-borne pathogens is therefore incredibly dependent on their distribution across a field, and how far they can spread through the soil. Xu and Hu (2020) used a model to simulate the effect of aggregation of a pathogen and biocontrol agent on biocontrol potential. They found that increased aggregation of a biocontrol agent can lead to both a reduction in the ability for it to suppress a pathogen, as well as increased variability in its success at suppression. The successful suppression of a pathogen therefore depends on the spatial distribution of both the pathogen and the biocontrol agent. As soil-borne biocontrol agents often cannot travel far, their successful application is dependent on close contact with the pathogen directly after application.

The use of biocontrol agents on their own is often not enough to fully suppress a pathogen. Take-all decline is commonly seen as the most successful example of epidemic suppression by a soil-borne biocontrol agent, but it only ever reduces epidemic severity rather than completely eliminating the pathogen (Bailey et al., 2009; Hornby, 1979; Werker et al., 1991). It is therefore often suggested that biocontrol agents should be combined with other control strategies to enhance their suppressive abilities (Guetsky et al., 2002; Mazzola and Freilich, 2017; Spadaro and Gullino, 2005). The idea behind this is that the combination of two moderately suppressive control strategies can result in a highly suppressive strategy.

However, there is the possibility for control strategies to negatively impact each other and reduce their ability to suppress a pathogen. The use of a break crop, where a different crop is grown that is not susceptible to the same diseases as the main crop, is often suggested. The break crop causes the free-living pathogen to decay in the absence of a host plant, reducing the epidemic severity or even eliminating the pathogen in the next growing season. The potential impact of a break crop on the population size of a free-living biocontrol agent, and its ability to suppress a pathogen after this break, should therefore be examined in more detail.

The combined use of biocontrol agents that use different mechanisms to suppress a pathogen is also a common suggestion. It is common to apply more than one biocontrol agent at the same time, assuming that they will work together to cause higher pathogen suppression (Abeysinghe, 2009; Manasfi et al., 2018; Pertot et al., 2017; Singh et al., 2012; Spadaro and Gullino, 2005). However, Xu and Jeger (2011) found that the combined use of two biocontrol agents to control a foliar disease was less effective than expected and suggested antagonistic interactions between the biocontrol agents. Many published studies agree with these results, where the ability of a biocontrol agent to suppress a pathogen may be reduced through the introduction of another (Xu et al., 2011). As mentioned in

Section 1.3, the rhizosphere is a diverse and competitive habitat. It is not surprising that soil-borne biocontrol agents will compete with and negatively affect any others, especially if both are applied at high doses that cannot be sustained by a plant's roots.

The most important factor for successfully applying a biocontrol agent is acquiring detailed knowledge about the biological system. A biocontrol agent that is significantly impacted by temperature or soil type is unlikely to ever be widely successful as a control strategy. Likewise, crop cultivars that are able to sustain high microbial populations are required, and fertilisers that benefit the biocontrol agent more than the pathogen should be used. Information about the mechanisms of infection for the pathogen, and the mechanisms of antagonism towards the pathogen for the biocontrol agent, need to be understood. How the pathogen and biocontrol agents interact within the rhizosphere and across a variety of different conditions must be explored and understood. Without this knowledge, the use of biocontrol agents for pathogen suppression will always be variable and prone to failure.

1.8 Modelling soil-borne biocontrol agents

It is estimated that the production of a new synthetic pesticide takes 10 years and $200 million from development to production. Although these values will vary between different control methods, there is always a substantial amount of time and cost required. Even after this, variables such as dose amount, application time, and environmental variation must be analysed to ensure effective disease control (Popp et al., 2013). The variable success of biocontrol agents across field trials often results in a lack of solid conclusions that can be generalised between experiments. However, additional experimental work, especially for soil-borne systems, can often require time consuming and challenging data collection.

The use of mathematical models can allow for a quick and inexpensive way for epidemic spread and the effectiveness of control methods to be examined across a variety of different conditions. These models can either be completely theoretical, or focus on a specific

biological system. There are a large number of models that simulate the interactions between two biological systems, either host-pathogen or pathogen-biocontrol agent. A summary of some of these models that can be found in Tables 1.1 and 1.2, with more extensive literature reviews existing elsewhere (Cunniffe and Gilligan, 2020; Gilligan, 2002; Gilligan and van den Bosch, 2008; Mills and Getz, 1996).

A smaller number of models examine the interactions between a host plant, a pathogen, and a biocontrol agent (Tables 1.3 and 1.4). The biocontrol agent is often not explicitly modelled and instead its effects are analysed either by varying certain rate parameters over time, or through fitting a plant-pathogen model to experimental data when a biocontrol agent is or is not present.

The exclusion of an explicitly modelled biocontrol agent in such models will often be to reduce model complexity. There is always a trade-off between capturing the biological complexity of a system and making it simple enough to fit to data and understand any results (Peck, 2004). Complex models will be prone to overfitting (Gomez-Cabrero et al., 2011; Pullen and Morris, 2014) and result in conclusions that are heavily dependent on the data and parameter values used. However, the explicit modelling of a biocontrol agent can allow for its impact on a host and pathogen to be explored in more detail.

The success of a biocontrol agent on epidemic suppression is known to be highly dependent on the mechanisms that it uses to negatively impact the pathogen (Handelsman and Stabb, 1996; Köhl et al., 2019b). Xu et al. (2010) used a model to demonstrate that a biocontrol agent was able to suppress a foliar pathogen more effectively if its main mode of action was competition or induced resistance rather than mycoparasitism or antibiosis. Likewise, Xu and Jeger (2013a) examined how combining biocontrol agents that use different mechanisms for pathogen suppression may result in less effective disease suppression than previous literature assumed. Incorporating a biocontrol agent into a model

allows for its behaviour to be explored in more detail, as well as being able to examine additional factors such as spatial aggregation and application amount on epidemic severity.

There are several papers that examine the interactions between a foliar pathogen and biocontrol agent on a host plant (Fedele et al., 2020; Jeger and Xu, 2015; Xu et al., 2011; Xu and Jeger, 2013a,b; Xu et al., 2010), or between a parasite and hyperparasite on a host plant (Morozov et al., 2007; White and Gilligan, 1998). These focus on the presence or absence of a pathogen and biocontrol agent on the host only. Modelling soil-borne pathogens and biocontrol agents introduces an additional level of complexity, as the pathogen and biocontrol agent can exist in the rhizosphere as well as on the roots of a host plant. This complexity is required to allow for primary and secondary infection to occur, which is well known to have a significant impact on epidemic behaviour (Bailey et al., 2006; Brassett and Gilligan, 1988; Cunniffe and Gilligan, 2010; Gilligan and Kleczkowski, 1997; Madden and van den Bosch, 2002).

Models that focus on soil-borne pathogens and biocontrol agents - the focus of this thesis – are often linked to a specific system. This is commonly the biocontrol agent *Trichoderma viride* against the pathogen *Rhizoctonia solani* on radish (Bailey and Gilligan, 1997; Gibson et al., 1999, 2004; Kleczkowski et al., 1996) or the occurrence of take-all decline on winter wheat (Bailey et al., 2009; Werker et al., 1991). These incorporate large amounts of experimental data and are usually used to make predictions specific to a particular host-pathogen-biocontrol agent system. However, Cunniffe and Gilligan (2011) use a more generalised model to examine the interactions of a soil-borne pathogen and biocontrol agent on the roots of a plant, including both primary and secondary infection as well as multiple mechanisms that the biocontrol agent can use to affect the pathogen. They are able to determine conditions that are necessary for epidemic suppression, as well as how they are influenced by both pathogen and biocontrol agent behaviour. Although

the model is relatively simplistic, it allows for generalised conclusions to be drawn that may assist with future experimental planning or additional modelling work.

Multiple additions to the above models can be made to make them more biologically realistic and address specific research questions. Two of the most important of these are spatial and temporal heterogeneity. There is often a patchy distribution of pathogens and biocontrol agents across a field, resulting in a lack of interaction between the two. Xu and Hu (2020) found that aggregation of a biocontrol agent resulted in less epidemic suppression than if it was homogeneously distributed. Gubbins and Gilligan (1997c) found that the dynamics between *Sporidesmium sclerotivorum*, *Sclerotinia minor*, and lettuce only matched a computational model when spatial heterogeneity was included.

Temporal heterogeneity is important in systems where 1) a host plant is grown and removed by harvesting each year, and 2) a model trajectory longer than a single year is examined (Cunniffe et al., 2015). For crops such as wheat, barley, and potatoes, a large number of seeds are planted at the start of the season, and the matured plants are then removed at the end of the season (Madden et al., 2007). Whilst a crop is present in a field, any pathogen or biocontrol agent can interact with its roots. However, the removal of these plants at harvest leaves the pathogen and biocontrol agent without a host, where they must survive on decaying organic matter until the next crop is planted. Pathogen survival and epidemic severity are highly influenced by this between-season period (Cook, 2003) However, only Gubbins and Gilligan (1997c) and Madden and van den Bosch (2002) incorporated it into their models.

The construction of a biological model can be seen to require careful consideration, with a trade-off between model complexity and biological reality. Any addition or exclusion should be justified, and thought should be put into how these decisions may impact any results obtained.

1.9 Aims of this thesis

Biological control shows a lot of promise as an environmentally-friendly and effective control method against plant pathogens. However, its success is currently too variable for wide commercial uptake. Optimising the use of biocontrol agents requires a detailed understanding of the biological systems that they are being introduced into, as well as looking at factors such as application timing, application dose, and the effects of temporal and spatial heterogeneity. The aim of this thesis is to explore the use of a soil-borne biocontrol agent against a soil-borne pathogen using a model, and to understand how the biocontrol agent can be optimised for use as a control strategy.

In Chapter 2, the models that are used throughout this thesis are described. The first is the SIX model, which focuses on the roots of a plant and whether they are susceptible (S) or infected by the pathogen (I), as well as modelling any free-living pathogen in the soil (X). The distinction between the pathogen on the roots of a plant and free-living in the soil allows for both primary and secondary infection to be modelled. The SIX model is then extended to incorporate a biocontrol agent, resulting in the SIXCA model. Two additional compartments are added: roots that are colonised by the biocontrol agent (C), and any free-living biocontrol agent in the soil (A). There are multiple mechanisms that are included in the SIXCA model to represent different ways that the biocontrol agent can negative impact the pathogen.

Parameter values are obtained for the SIX and SIXCA models in Chapters 3 and 4, where the models are fitted to data from Werker et al. (1991). This data was obtained from field experiments carried out over 10 consecutive years, where winter wheat infected by take-all was grown. The number of infected roots is low in the first year of the experiment, before rising to a peak in the third year, and dropping down to a lower level for all subsequent years. This trend is typical of take-all decline and therefore allows for this suppressive

activity to be modelled and examined in more detail. The difficulties of model fitting, and suggestions as to how future data collection could be improved, are discussed.

Chapter 5 examines how a biocontrol agent can be applied to optimise its ability to suppress a pathogen. Application timing and dosage are explored, as well as how the mechanisms that the biocontrol agent uses to affect the pathogen can impact application success. The effects of primary and secondary infection are further analysed in Chapters 6 and 7, where the SIX and SIXCA model are spatially modelled. The optimal spatial placement of plants to reduce epidemic spread is explored. There is also an examination of the effect of pathogen and biocontrol agent aggregation on epidemic suppression.

In the discussion (Chapter 8), we explore how the above research can be used to improve the use of soil-borne biocontrol agents. We make suggestions for future experimental work to confirm our findings, as well as the potential to extend some of our modelling work further. We discuss what challenges are still facing the commercial use of biocontrol agents, and explain the steps that are needed before we believe that they can be used successfully.

Table 1.1 Key models that represent the interactions between a host plant and pathogen.

Paper	Focus of model	Specific case study
Brassett and Gilligan (1988)	Plant roots and soil-borne pathogen	Plant: cress (*Lepidium sativum*) Pathogen: *Pythium ultimum*
Gilligan and Kleczkowski (1997)	Plant roots and soil-borne pathogen	None
Gubbins and Gilligan (1997b)	Host plant and parasite	None
Gubbins et al. (2000)	Host plant and parasite	None
Park et al. (2001)	Host plant and parasite	None
Madden and van den Bosch (2002)	Plant and pathogen	None
Truscott and Gilligan (2003)	Host plant and parasite	Plant: sugar beet Pathogen: *Polymyxa betae*
Bailey and Gilligan (2004)	Plant roots and soil-borne pathogen	Plant: winter wheat (*Triticum aestivum*) Pathogen: *Gaeumannomyces graminis* var. *tritici*
Bailey et al. (2005)	Plant roots and soil-borne pathogen	Plant: winter wheat (*Triticum aestivum*) Pathogen: *Gaeumannomyces graminis* var. *tritici*
Bailey et al. (2006)	Plant roots and soil-borne pathogen	Plant: winter wheat (*Triticum aestivum*) Pathogen: *Gaeumannomyces graminis* var. *tritici*
Cunniffe and Gilligan (2010)	Plant roots and soil-borne pathogen	None
Zhang et al. (2015)	Plant and pathogen	None
Abodayeh et al. (2020)	Plant and vector-borne plant disease	None

Table 1.2 Key models that represent the interactions between a pathogen and biocontrol agent.

Paper	Focus of model	Specific case study
Gubbins and Gilligan (1996)	Parasite and hyperparasite	Parasite: *Sclerotinia minor* Pathogen: *Pythium ultimum*
Gubbins and Gilligan (1997c)	Parasite and hyperparasite	Parasite: *Sclerotinia minor* Pathogen: *Pythium ultimum*
Xu and Hu (2020)	Microbial pathogen and biocontrol agent	

Table 1.3 Key models that represent the interactions between a host plant, pathogen, and biocontrol agent, where the biocontrol agent is not explicitly included in the model. Instead, its effects are analysed either by varying certain rate parameters over time, or through fitting a plant-pathogen model to experimental data when a biocontrol agent is or is not present.

Paper	Focus of model	Specific case study
Gilligan (1990)	A plant, pathogen, and biocontrol agent	Multiple examples, all involving soil-borne pathogens and biocontrol agents
Kleczkowski et al. (1996)	A plant, pathogen, and biocontrol agent	Plant: radish (*Raphanus sativus*) Pathogen: *Rhizoctonia solani* Biocontrol agent: *Trichoderma viride*
Bailey and Gilligan (1997)	Plant roots, soil-borne pathogen, and biocontrol agent	Plant: radish (*Raphanus sativus*) Pathogen: *Rhizoctonia solani* Biocontrol agent: *Trichoderma viride*
Gubbins and Gilligan (1997a)	Host plant, parasite, and hyperparasite	Plant: lettuce Parasite: *Sclerotinia minor* Hyperparasite: *Sporidesmium sclerotivorum*
Gibson et al. (1999)	A plant, pathogen, and biocontrol agent	Plant: radish (*Raphanus sativus*) Pathogen: *Rhizoctonia solani* Biocontrol agent: *Trichoderma viride*
Gibson et al. (2004)	A plant, pathogen, and biocontrol agent	Plant: radish (*Raphanus sativus*) Pathogen: *Rhizoctonia solani* Biocontrol agent: *Trichoderma viride*
Kleczkowski and Gilligan (2007)	A plant, pathogen, and biocontrol agent	Plant: radish (*Raphanus sativus*) Pathogen: *Rhizoctonia solani* Biocontrol agent: *Trichoderma viride*
Bailey et al. (2009)	Plant roots, soil-borne pathogen, and biocontrol agent	Plant: winter wheat (*Triticum aestivum*) Pathogen: *Gaeumannomyces graminis* var. *tritici* Biocontrol agent: not specified

Table 1.4 Key models that represent the interactions between a host plant, pathogen, and biocontrol agent, where the biocontrol agent is explicitly included in the model.

Paper	Focus of model	Specific case study
Knudsen and Hudler (1987)	Plant leaves, foliar pathogen, and biocontrol agent	Plant: red pine (*Pinus resinosa*) Pathogen: *Gremmeniella abietina* Biocontrol agent: *Pseudomonas fluorescens*
White and Gilligan (1998)	Host plant, parasite, and hyperparasite	None
Kessel et al. (2005)	Dead leaf tissue, foliar pathogen, and biocontrol agent	Plant: cyclamen (*Cyclamen persicum*) Pathogen: *Botrytis cinerea* Biocontrol agent: *Ulocladium atrum*
Morozov et al. (2007)	Host plant, parasite, and hyperparasite	Plant: chestnut tree Pathogen: *Cryphonectria parasitica* Biocontrol agent: *Cryphonectria* hypovirus 1
Jeger et al. (2009)	Plant leaves, foliar pathogen, and biocontrol agent	Plant: not specified Pathogen: *Trichoderma* spp. Biocontrol agent: *Botrytis cinerea*
Cunniffe and Gilligan (2011)	Plant roots, soil-borne pathogen, and biocontrol agent	None
Xu et al. (2010)	Plant leaves, foliar pathogen, and biocontrol agent	None
Xu et al. (2011)	Plant leaves, foliar pathogen, and biocontrol agent	None
Xu and Jeger (2013a)	Plant leaves, foliar pathogen, and biocontrol agent	None
Xu and Jeger (2013b)	Plant leaves, foliar pathogen, and biocontrol agent	None
Jeger and Xu (2015)	Plant leaves, foliar pathogen, and biocontrol agent	None
Fedele et al. (2020)	Plant leaves, foliar, pathogen and biocontrol agent	Plant: grapevines Pathogen: *Botrytis cinerea*

Chapter 2: Introducing the SIX and SIXCA models

This chapter introduces the SIX model, as well as several variations of the SIXCA model. The SIX model simulates the interactions between the roots of a plant and a soil-borne pathogen, whereas the SIXCA model simulates the interactions between the roots of a plant, a soil-borne pathogen, and a soil-borne biocontrol agent. The SIX model focuses on the roots of a plant and whether they are susceptible (S) or infected by the pathogen (I), as well as modelling any free-living pathogen in the soil (X). The SIXCA model incorporates two additional compartments to represent the addition of a biocontrol agent. Roots can also be colonised by the biocontrol agent (C), and there is free-living biocontrol agent in the soil (A). The different variations of the SIXCA model are described in Section 2.4 and represent the incorporation of different mechanisms that a biocontrol agent can use to negatively affect a pathogen.

2.1 Seasonality

When growing seasonal crops, there is a temporal disturbance to any within-soil dynamics throughout a year due to planting and harvesting. After a crop is planted, its roots are present in the soil and they can be infected by a pathogen or colonised by a biocontrol agent. After harvest, the crop is removed and all roots die. Any free-living pathogen and biocontrol agent must survive and persist in in the soil without a host until the next crop is planted. These dynamics are included in the models in this chapter to represent the seasonal fluctuations of many commonly grown crops, and to examine what effect they have on the invasion of a pathogen and success of a biocontrol agent over several consecutive years of planting and harvesting. Each year of a simulation is split into three sections:

1. **Within-season dynamics:** the host plant is present and the pathogen and biocontrol agent can infect/colonise its roots. Free-living pathogen and biocontrol agent in the surrounding soil are also present

2. **At the end of a growing season:** this period represents the death of all roots at the end of a growing season due to harvesting, the subsequent transition of infected roots to free-living pathogen in the surrounding soil, and the subsequent transition of colonised roots to free-living biocontrol agent in the surrounding soil

3. **Between growing seasons:** during this period of time between harvesting and replanting, the host plant is not present, whereas the pathogen and biocontrol agent are still present in the soil

2.2 The SIX model

This model focuses on the roots of a plant, as well as any pathogen in the surrounding soil. Roots on a host crop can be in one of two compartments - susceptible (S) or infected by the pathogen (I). Free-living pathogen (X) can also exist in the surrounding soil. The unit of measurement for roots is a fragment that is large enough to host the pathogen, whereas for the pathogen it is a piece that is large enough to cause infection and attach to a root.

Within-season dynamics

The rate equations are

$$\begin{aligned}
\frac{dS}{dt} &= \rho(S+I)\left(\frac{\kappa-(S+I)}{\kappa}\right) - \beta_P SX - \beta_S SI, \\
\frac{dI}{dt} &= \beta_P SX + \beta_S SI - \mu I, \\
\frac{dX}{dt} &= -\lambda_X X + \tau_I^* \mu I,
\end{aligned} \tag{2.1}$$

with a summary of the parameters used and definitions for each included in Table 2.1. A visual representation of the within-season dynamics can be found in Figure 2.1.

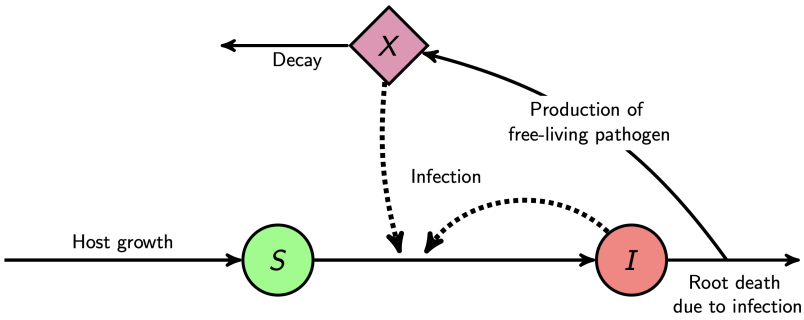

Fig. 2.1 Schematic of the dynamics within a crop growing season for the SIX model of a soil-borne pathogen on the roots of a plant and in the surrounding soil. Plant roots, represented by coloured circles, can be in one of two compartments: susceptible (S) or infected by the pathogen (I). Pathogen inoculum (X) in the surrounding soil is represented by a coloured rhombi. Solid lines represent the transition from one compartment to another, the birth and death of roots, and the decay of material in the soil. Dotted lines represent the necessary interaction between two compartments for a transition from one compartment to the other to occur.

Root growth is logistic, where susceptible (S) and infected (I) roots contribute to the carrying capacity (κ), and the rate of growth is governed by the parameter ρ. Each within-season period starts with one susceptible root to initiate crop growth. The number of infected roots always starts at 0, which means that any initial infection of a plant's roots

has to occur from the free-living pathogen (X). Infected roots die due to infection at rate μ, and any pathogen that was living on the root will now exist as free-living pathogen. The parameter τ_I^* represents the units of pathogen present on an infected root that has died due to severe infection.

The amount of free-living pathogen at the start of the first growing season represents the introduction of a small amount of pathogen into the soil that is capable of initiating infection. This amount varies in subsequent seasons depending on the previous season's level of infection. Free-living pathogen decays at rate λ_X.

Table 2.1 List of parameters and definitions for the SIX model.

Parameter	Definition	Units
S	Number of susceptible roots	
I	Number of roots infected by the pathogen	
X	Density of free-living pathogen	
t	Time (degree days $> 0^\circ$C)	
X_s	Initial amount of free-living pathogen present at the start of the first growing season	
ρ	Rate of root production	t^{-1}
κ	Carrying capacity of root production	
μ	Death rate of roots due to infection	t^{-1}
β_p	Rate of primary infection of roots by free-living pathogen	t^{-1}
β_s	Rate of secondary infection of roots	t^{-1}
λ_X	Rate of decay of pathogen inoculum	t^{-1}
τ_I	Units of pathogen present on an infected root. When the host crop is harvested at the end of a growing season, this parameter determines the amount of free-living pathogen released into the soil from an infected root	
τ_I^*	Units of pathogen present on an infected root that has died due to severe infection	

At the end of a growing season

This period represents the death of all roots at the end of a growing season, and the subsequent transition of infected roots to free-living pathogen in the surrounding soil. This free-living material must persist and survive in the soil until the next crop is planted, where it can then infect the new crop's roots.

The parameter τ_I represents the units of pathogen present on an infected root. When the host crop is harvested at the end of a growing season, this parameter determines the amount of free-living pathogen released into the soil from an infected root. Using similar terminology to Madden and Van Den Bosch (2002), the amount of free-living pathogen at the start of the between growing season period is

$$X(t_b^+) = X(t_w^-) + \tau_I I(t_w^-), \tag{2.2}$$

where t_b^+ represents the time immediately before the start of between-season dynamics, and t_w^- represents the time immediately at the end of within-season dynamics.

Between growing seasons

The rate equations are

$$\begin{aligned} \frac{dS}{dt} &= 0, \\ \frac{dI}{dt} &= 0, \\ \frac{dX}{dt} &= -\lambda_X X, \end{aligned} \tag{2.3}$$

where there are no roots present as the host crop has been harvested. As no infection can occur, the free-living pathogen can only decay.

2.3 The SIXCA model

This model focuses on the roots of a plant, as well as any pathogen and biocontrol agent in the surrounding soil. The unit of measurement for roots is a fragment that is large enough to host the pathogen or biocontrol agent, whereas for the pathogen it is a piece that is large enough to cause infection and attach to a root, and for the biocontrol agent it is a piece that is large enough to cause colonisation and attach to a root. Roots on a host crop can be in one of three compartments - susceptible (S), infected by the pathogen (I), or colonised by the biocontrol agent (C). Free-living pathogen (X) and biocontrol agent (A) can also exist in the surrounding soil.

Within-season dynamics

The rate equations are

$$\begin{aligned}
\frac{dS}{dt} &= \rho(S+I+C)\left(\frac{\kappa-(S+I+C)}{\kappa}\right) - \beta_P SX - \beta_S SI - \alpha_P SA - \alpha_S SC, \\
\frac{dI}{dt} &= \beta_P SX + \beta_S SI - \mu I, \\
\frac{dC}{dt} &= \alpha_P SA + \alpha_S SC, \\
\frac{dX}{dt} &= -\lambda_X X + \tau_I^* \mu I, \\
\frac{dA}{dt} &= -\lambda_A A,
\end{aligned} \tag{2.4}$$

with a summary of the parameters used and definitions for each included in Table 2.2. A visual representation of the within-season dynamics can be found in Figure 2.2.

Root growth is logistic, where susceptible (S), infected (I), and colonised (C) roots contribute to the carrying capacity (κ), and the rate of growth is governed by the parameter

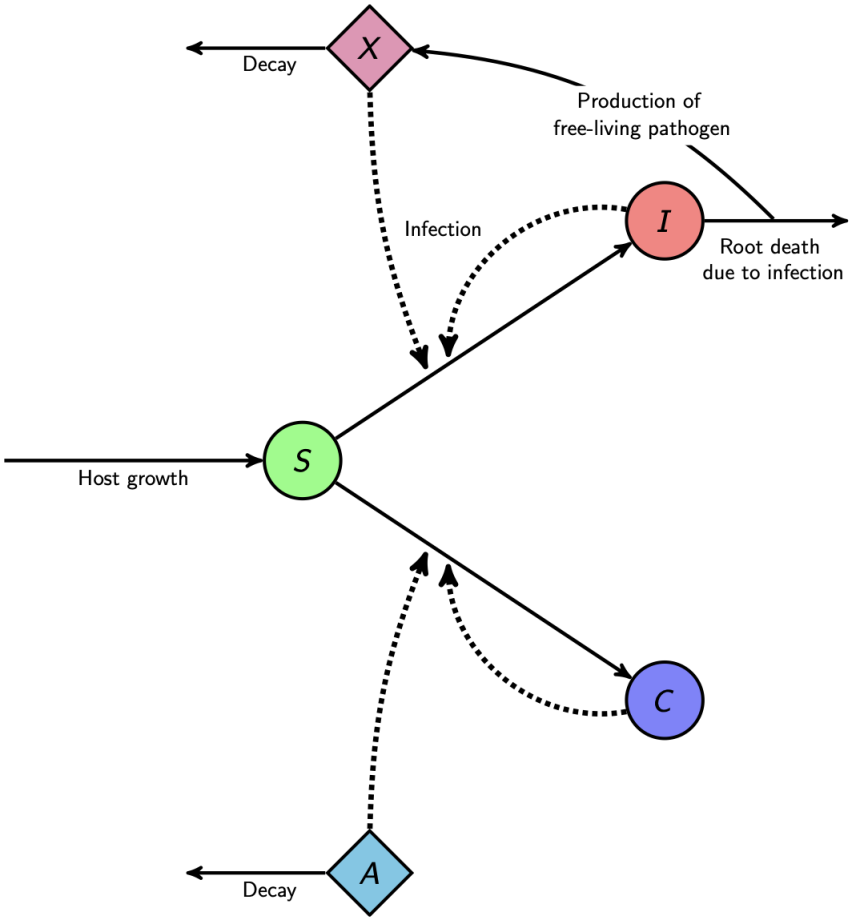

Fig. 2.2 Schematic of the dynamics within a crop growing season for the SIXCA model of a soil-borne pathogen and biocontrol agent on the roots of a plant and in the surrounding soil. Plant roots, represented by coloured circles, can be in one of three compartments: susceptible (S), infected by the pathogen (I), or colonised by the biocontrol agent (C). Pathogen inoculum (X) and free-living biocontrol agent (A) in the surrounding soil are represented by coloured rhombi. Solid lines represent the transition from one compartment to another, the birth and death of roots, and the decay of material in the soil. Dotted lines represent the necessary interaction between two compartments for a transition from one compartment to the other to occur. The biocontrol agent is able to negatively affect the pathogen through competing for space on the crop's roots.

ρ. Each within-season period starts with one susceptible root to initiate crop growth. The number of infected and colonised roots always start at 0, which means that any initial infection or colonisation of the crop roots has to occur from the free-living pathogen (X) or biocontrol agent (A). The amount of free-living pathogen and biocontrol agent at the start of

the first growing season represents the introduction of a small amount of pathogen/biocontrol agent into the soil that is capable of initiating infection/colonisation.These amounts vary in subsequent seasons depending on the previous season's level of infection and colonisation.

Susceptible roots can become infected by the pathogen through primary (β_P) or secondary (β_S) infection, and colonised by the biocontrol agent through primary (α_P) or secondary (α_S) colonisation. Free-living pathogen decays at rate λ_X, and free-living biocontrol agent decays at rate λ_A.

Table 2.2 List of parameters and definitions for the SIXCA model.

Parameter	Definition	Units
S	Number of susceptible roots	
I	Number of roots infected by the pathogen	
C	Number of roots colonised by the biocontrol agent	
X	Density of free-living pathogen	
A	Density of free-living biocontrol agent	
t	Time (degree days $> 0^{\circ}$C)	
X_s	Initial amount of free-living pathogen present at the start of the first growing season	
A_s	Initial amount of free-living biocontrol agent present at the start of the first growing season	
ρ	Rate of root production	t^{-1}
κ	Carrying capacity of root production	
μ	Death rate of roots due to infection	t^{-1}
β_p	Rate of primary infection of roots by free-living pathogen	t^{-1}
β_s	Rate of secondary infection of roots	t^{-1}
λ_X	Rate of decay of pathogen inoculum	t^{-1}
τ_I	Units of pathogen present on an infected root. When the host crop is harvested at the end of a growing season, this parameter determines the amount of free-living pathogen released into the soil from an infected root	
τ_I^*	Units of pathogen present on an infected root that has died due to severe infection	
α_p	Rate of primary colonisation of roots by free-living biocontrol agent	t^{-1}
α_s	Rate of secondary colonisation of roots	t^{-1}
λ_A	Rate of decay of free-living biocontrol agent	t^{-1}
τ_C	Units of biocontrol agent present on a colonised root. When the host crop is harvested at the end of a growing season, this parameter determines the amount of free-living biocontrol agent released into the soil from a colonised root	

At the end of a growing season

This period represents the death of all roots at the end of a growing season, and the subsequent transition of infected roots to free-living pathogen, and colonised roots to free-living biocontrol agent, in the surrounding soil. This free-living material must persist and survive in the soil until the next crop is planted, where it can then infect/colonise the new crop's roots.

The parameter τ_I represents the units of pathogen present on an infected root. When the host crop is harvested at the end of a growing season, this parameter determines the amount of free-living pathogen released into the soil from an infected root. Using similar terminology to Madden and Van Den Bosch (2002), the amount of free-living pathogen at the start of the between growing season period is

$$X(t_b^+) = X(t_w^-) + \tau_I I(t_w^-), \tag{2.5}$$

where t_b^+ represents the time immediately before the start of between-season dynamics, and t_w^- represents the time immediately at the end of within-season dynamics.

Similarly, the parameter τ_C represents the units of biocontrol agent present on a colonised root. The amount of free-living biocontrol agent at the start of the between growing season period is

$$A(t_b^+) = A(t_w^-) + \tau_C C(t_w^-), \tag{2.6}$$

where t_b^+ represents the time immediately before the start of between-season dynamics, and t_w^- represents the time immediately at the end of within-season dynamics.

Between growing seasons

The rate equations are

$$\begin{aligned}
\frac{dS}{dt} &= 0, \\
\frac{dI}{dt} &= 0, \\
\frac{dC}{dt} &= 0, \\
\frac{dX}{dt} &= -\lambda_X X, \\
\frac{dA}{dt} &= -\lambda_A A,
\end{aligned} \tag{2.7}$$

where there are no roots present as the host crop has been harvested. As no infection or colonisation can occur, the free-living pathogen and biocontrol agent can only decay.

2.4 Variations of the SIXCA model

In the version of the SIXCA model described in Section 2.3, the only mechanism that the biocontrol agent could use to negatively affect the pathogen was through competition for space on a crop's roots by primary (α_P) or secondary (α_S) colonisation. However, there are other additional mechanisms that the biocontrol agent could use:

1. Reducing the ability of soil-borne pathogen inoculum to infect susceptible roots through primary infection (ω_P).
2. Reducing the ability of infected roots to infect susceptible roots through secondary infection (ω_S).
3. Reducing the ability of the free-living pathogen to infect non-infected roots due to a level of protection offered by the biocontrol agent on colonised roots (ϵ_P).
4. Reducing the ability of infected roots to infect non-infected roots due to a level of protection offered by the biocontrol agent on colonised roots (ϵ_S).
5. Primary colonisation of infected roots by the free-living biocontrol agent (ψ_P).
6. Secondary colonisation of infected roots by biocontrol agent living on the roots (ψ_S).
7. Causing the death of any pathogen on infected roots (η)
8. Causing the death of any pathogen on infected roots (η), and subsequent bulk-up of the free-living biocontrol agent (ϕ_η).
9. Increasing the rate of decay of free-living pathogen (ν)
10. Increasing the rate of decay of free-living pathogen (ν), and subsequent bulk-up of the free-living biocontrol agent (ϕ_ν).

Focusing on each of these traits individually (by setting the other rates to 0) can allow for an analysis of which characteristics lead to the most effective disease control (Cunniffe and Gilligan, 2011), or which mechanisms are most likely to be involved in pathogen suppression by a biocontrol agent. The differences between the dynamics of these three models within a growing season can be seen in Table 2.3, and will be explained in more detail in Sections 2.4.1 to 2.4.5.

Table 2.3 List of parameters and definitions of additions to the SIXCA model of mechanisms where the biocontrol agent can negatively affect the pathogen. All other parameters for the SIXCA model can be found in Table 2.2.

Parameter	Definition	Units
Model 1: ϵ_P included		
ϵ_P	Proportionate reduction in the rate of primary infection of colonised roots compared to susceptible roots	
Model 2: ϵ_S included		
ϵ_S	Proportionate reduction in the rate of secondary infection of colonised roots compared to susceptible roots	
Model 3: ψ_P included		
ψ_P	Rate of primary colonisation of infected roots by free-living biocontrol agent	t^{-1}
Model 4: ψ_S included		
ψ_S	Rate of secondary colonisation of infected roots by colonised roots	t^{-1}
Model 5: ω_P included		
ω_P	Reduction in the rate of primary infection due to the free-living biocontrol agent	t^{-1}
Model 6: ω_S included		
ω_S	Reduction in the rate of secondary infection due to the free-living biocontrol agent	t^{-1}
Model 7: η included		
η	Death rate of the pathogen on infected roots by the free-living biocontrol agent	t^{-1}
Model 8: η and ϕ_η included		
η	Death rate of the pathogen on infected roots by the free-living biocontrol agent	t^{-1}
ϕ_η	Production of free-living biocontrol agent through consumption of pathogen present on infected roots	t^{-1}
Model 9: ν included		
ν	Increased decay rate of the free-living pathogen by the free-living biocontrol agent	t^{-1}
Model 10: ν and ϕ_ν included		
ν	Increased decay rate of the free-living pathogen by the free-living biocontrol agent	t^{-1}
ϕ_ν	Production of free-living biocontrol agent through consumption of free-living pathogen in the soil	t^{-1}

2.4.1 Including ϵ_P or ϵ_S

Within-season dynamics: The rate equations for within a growing season, with additions to Equation 2.4 highlighted in bold, are

$$\begin{aligned}
\frac{dS}{dt} &= \rho(S+I+C)\left(\frac{\kappa-(S+I+C)}{\kappa}\right) - \beta_P SX - \beta_S SI - \alpha_P SA - \alpha_S SC, \\
\frac{dI}{dt} &= \beta_P SX + \beta_S SI + \boldsymbol{\beta_P \epsilon_P CX} + \boldsymbol{\beta_S \epsilon_S CI} - \mu I, \\
\frac{dC}{dt} &= \alpha_P SA + \alpha_S SC - \boldsymbol{\beta_P \epsilon_P CX} - \boldsymbol{\beta_S \epsilon_S CI}, \\
\frac{dX}{dt} &= \mu \tau_I^* I - \lambda_X X, \\
\frac{dA}{dt} &= -\lambda_A A.
\end{aligned} \tag{2.8}$$

These dynamics can be visualised in Figure 2.3. Colonised roots can offer a level of protection from infection, reducing the ability of the pathogen to cause infection. This happens at a reduced infection rate of $\epsilon\beta_P$ for primary infection, and $\epsilon\beta_S$ for secondary infection infection. The value of the parameter ϵ is therefore a measure of the strength of protection afforded by the biocontrol agent.

At the end of a growing season and between growing seasons: The dynamics at the end of a growing season, as well as the rate equations for between growing seasons, do not change from those mentioned in Section 2.3.

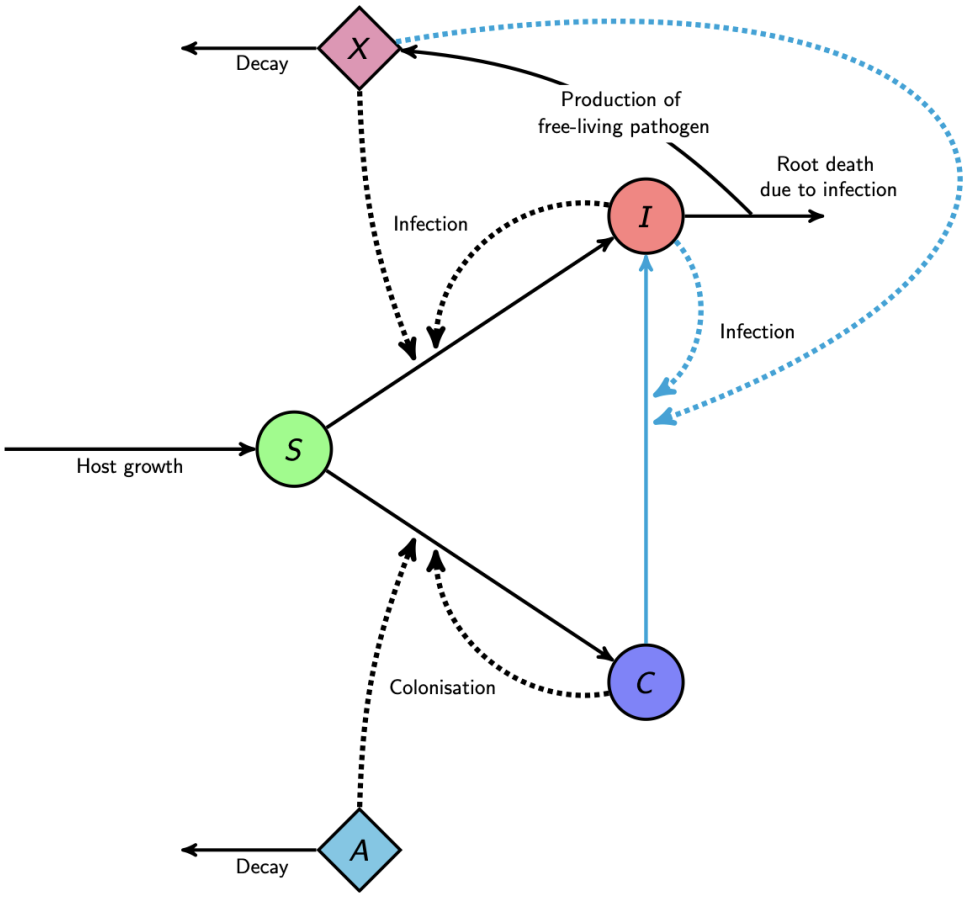

Fig. 2.3 **SIXCA model, with ϵ_P and ϵ_P included**. Schematic of the dynamics within a crop growing season for the SIXCA model of a soil-borne pathogen and biocontrol agent on the roots of a plant and in the surrounding soil. The biocontrol agent is able to negatively affect the pathogen through competing for space on the crop's roots, as well as offering a level of protection from both primary and secondary infection through making colonised roots more difficult to infect than susceptible roots. Plant roots, represented by coloured circles, can be in one of three compartments: susceptible (S), infected by the pathogen (I), or colonised by the biocontrol agent (C). Pathogen inoculum (X) and free-living biocontrol agent (A) in the surrounding soil are represented by coloured rhombi. Solid lines represent the transition from one compartment to another, the birth and death of roots, and the decay of material in the soil. Dotted lines represent the necessary interaction between two compartments for a transition from one compartment to the other to occur. Blue lines represent rates where the pathogen is directly and negatively affected by the presence of the biocontrol agent.

2.4.2 Including ψ_P or ψ_S

Within-season dynamics: The rate equations for within a growing season, with additions to Equation 2.4 highlighted in bold, are

$$\begin{aligned}
\frac{dS}{dt} &= \rho(S+I+C)\left(\frac{\kappa-(S+I+C)}{\kappa}\right) - \beta_P SX - \beta_S SI - \alpha_P SA - \alpha_S SC,\\
\frac{dI}{dt} &= \beta_P SX + \beta_S SI - \mu I - \boldsymbol{\psi_P IA - \psi_S IC},\\
\frac{dC}{dt} &= \alpha_P SA + \alpha_S SC + \boldsymbol{\psi_P IA + \psi_S IC},\\
\frac{dX}{dt} &= \mu\tau_I^* I - \lambda_X X,\\
\frac{dA}{dt} &= -\lambda_A A.
\end{aligned} \tag{2.9}$$

These dynamics can be visualised in Figure 2.4. It is possible for the biocontrol agent to out-compete the pathogen and result in the transition of infected roots to colonised roots. This occurs at a rate of ψ_P for primary colonisation, and ψ_S for secondary colonisation.

At the end of a growing season and between growing seasons: The dynamics at the end of a growing season, as well as the rate equations for between growing seasons, do not change from those mentioned in Section 2.3.

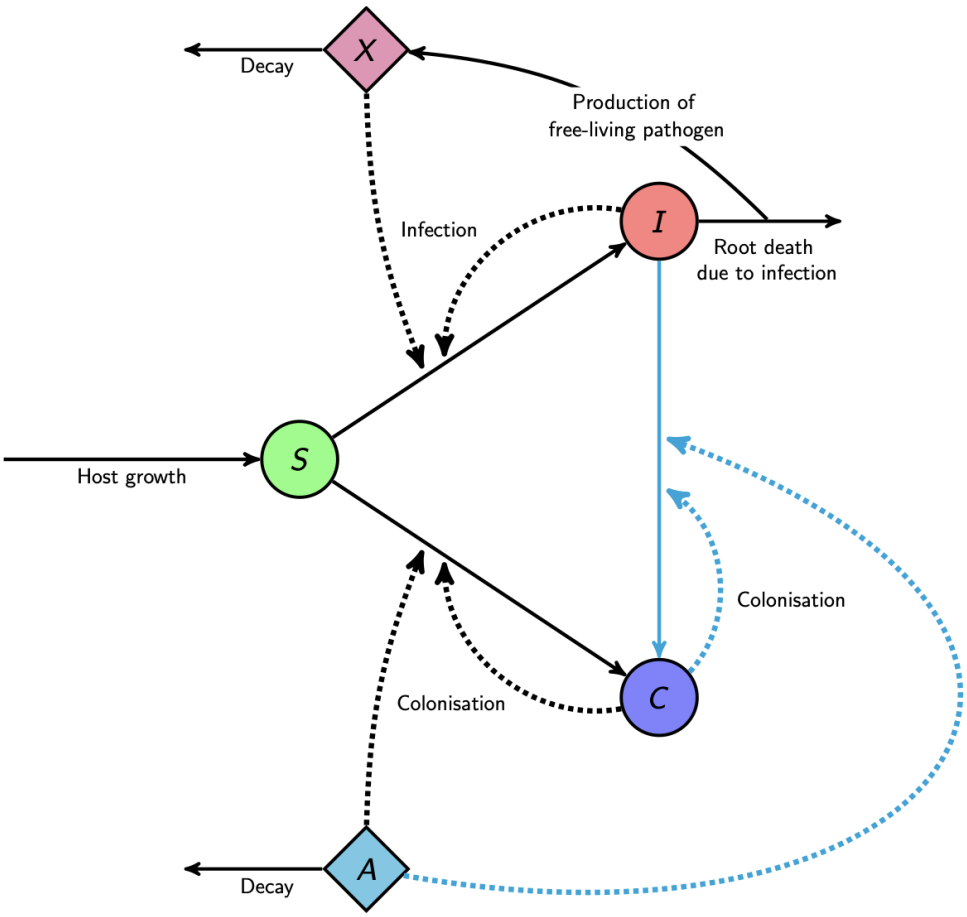

Fig. 2.4 **SIXCA model, with ψ_P and ψ_S included**. Schematic of the dynamics within a crop growing season for the SIXCA model of a soil-borne pathogen and biocontrol agent on the roots of a plant and in the surrounding soil. The biocontrol agent is able to negatively affect the pathogen through competing for space on the crop's roots, as well as being able to outcompete the pathogen and cause a transition of infected to colonised roots. Plant roots, represented by coloured circles, can be in one of three compartments: susceptible (S), infected by the pathogen (I), or colonised by the biocontrol agent (C). Pathogen inoculum (X) and free-living biocontrol agent (A) in the surrounding soil are represented by coloured rhombi. Solid lines represent the transition from one compartment to another, the birth and death of roots, and the decay of material in the soil. Dotted lines represent the necessary interaction between two compartments for a transition from one compartment to the other to occur. Blue lines represent rates where the pathogen is directly and negatively affected by the presence of the biocontrol agent.

2.4.3 Including ω_P or ω_S

Within-season dynamics: The rate equations for within a growing season, with additions to Equation 2.4 highlighted in bold, are

$$\begin{aligned}
\frac{dS}{dt} &= \rho(S+I+C)\left(\frac{\kappa-(S+I+C)}{\kappa}\right) - \frac{\beta_P SX}{\mathbf{1+\omega_P A}} - \frac{\beta_S SI}{\mathbf{1+\omega_S A}} - \alpha_P SA - \alpha_S SC,\\
\frac{dI}{dt} &= \frac{\beta_P SX}{\mathbf{1+\omega_P A}} + \frac{\beta_S SI}{\mathbf{1+\omega_S A}} - \mu I,\\
\frac{dC}{dt} &= \alpha_P SA + \alpha_S SC,\\
\frac{dX}{dt} &= \mu\tau_I^* I - \lambda_X X,\\
\frac{dA}{dt} &= -\lambda_A A.
\end{aligned} \tag{2.10}$$

These dynamics can be visualised in Figure 2.5. Free-living biocontrol agent can negatively affect the fitness of a pathogen, reducing its ability to infect susceptible roots through both primary (ω_P) and secondary (ω_S) infection.

At the end of a growing season and between growing seasons: The dynamics at the end of a growing season, as well as the rate equations for between growing seasons, do not change from those mentioned in Section 2.3.

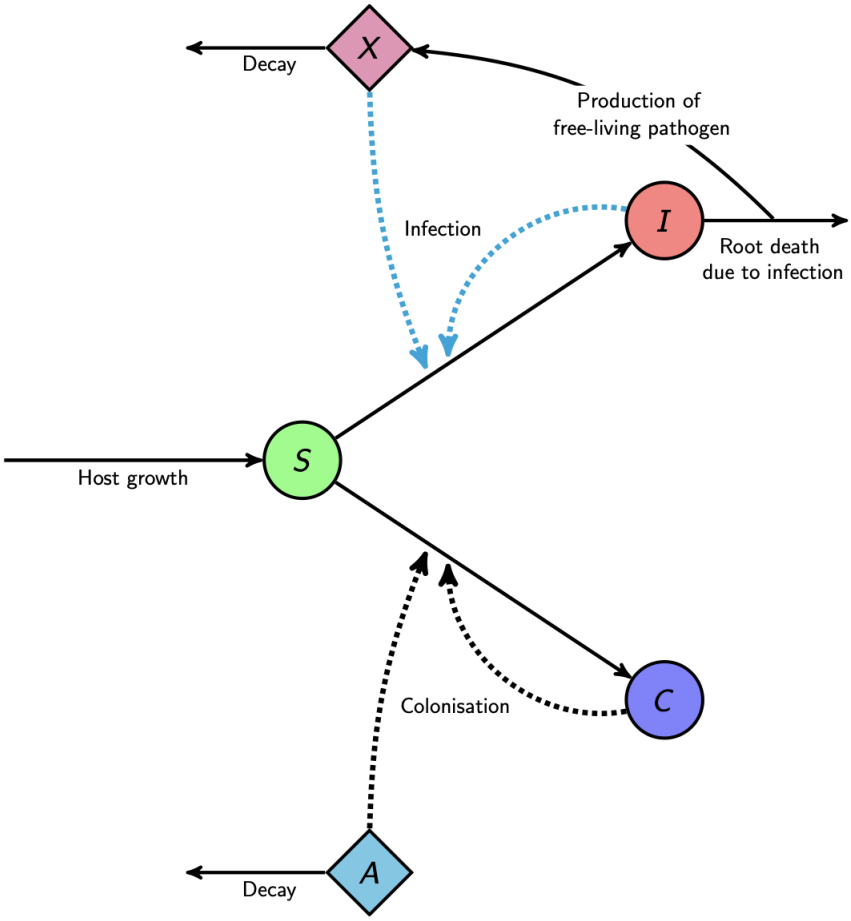

Fig. 2.5 **SIXCA model, with ω_P and ω_S included**. Schematic of the dynamics within a crop growing season for the SIXCA model of a soil-borne pathogen and biocontrol agent on the roots of a plant and in the surrounding soil. The biocontrol agent is able to negatively affect the pathogen through competing for space on the crop's roots, as well as being able to reduce the rate of primary and secondary infection. Plant roots, represented by coloured circles, can be in one of three compartments: susceptible (S), infected by the pathogen (I), or colonised by the biocontrol agent (C). Pathogen inoculum (X) and free-living biocontrol agent (A) in the surrounding soil are represented by coloured rhombi. Solid lines represent the transition from one compartment to another, the birth and death of roots, and the decay of material in the soil. Dotted lines represent the necessary interaction between two compartments for a transition from one compartment to the other to occur. Blue lines represent rates where the pathogen is directly and negatively affected by the presence of the biocontrol agent.

2.4.4 Including η and ϕ_η

Within-season dynamics: The rate equations for within a growing season, with additions to Equation 2.4 highlighted in bold, are

$$\begin{aligned}
\frac{dS}{dt} &= \rho(S+I+C)\left(\frac{\kappa-(S+I+C)}{\kappa}\right) - \beta_P SX - \beta_S SI - \alpha_P SA + \boldsymbol{\eta AI},\\
\frac{dI}{dt} &= \beta_P SX + \beta_S SI - \boldsymbol{\eta AI},\\
\frac{dC}{dt} &= \alpha_P SA,\\
\frac{dX}{dt} &= -\lambda_X X,\\
\frac{dA}{dt} &= -\lambda_A A + \boldsymbol{\phi_\eta \eta AI}\,.
\end{aligned} \tag{2.11}$$

These dynamics can be visualised in Figure 2.6. Free-living biocontrol agent in the soil can attack and kill any pathogen living on a plants' roots, causing them to transition back to susceptible roots at rate η. If the biocontrol agent ingests the pathogen and uses it as a source of food, it can bulk-up at rate ϕ_η.

At the end of a growing season and between growing seasons: The dynamics at the end of a growing season, as well as the rate equations for between growing seasons, do not change from those mentioned in Section 2.3.

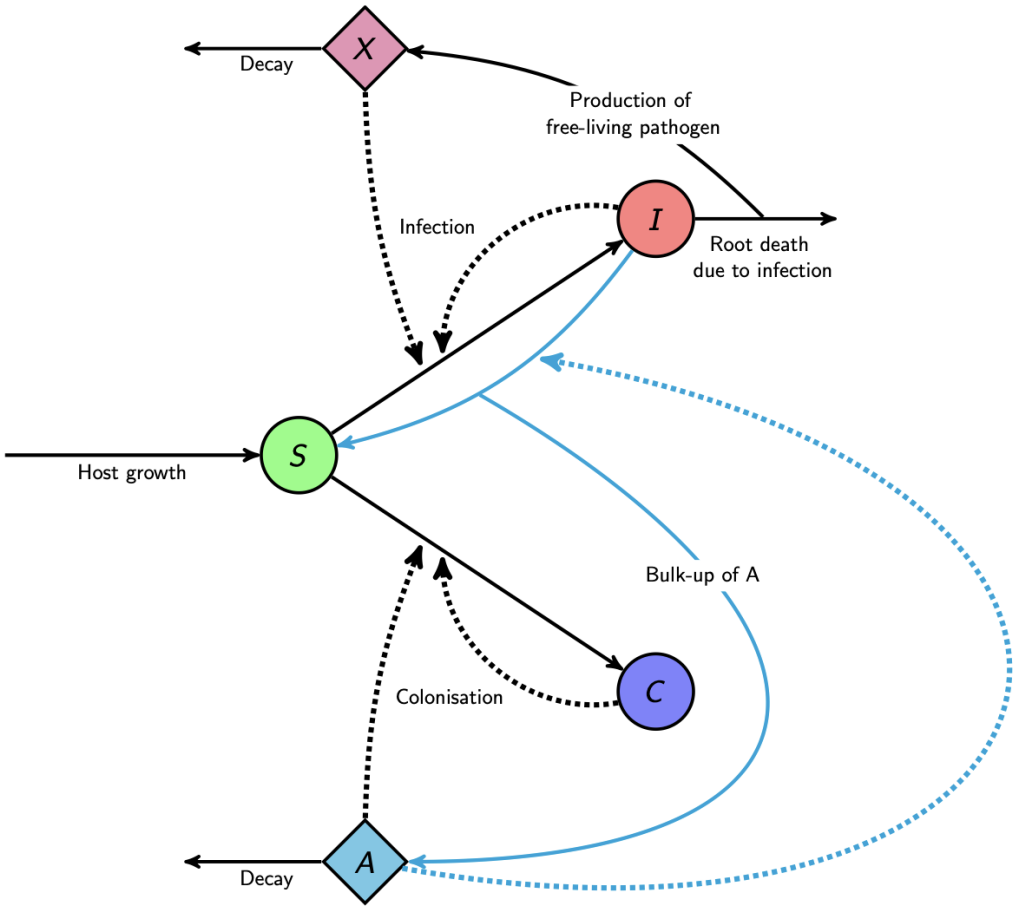

Fig. 2.6 **SIXCA model, with η and ϕ_η included**. Schematic of the dynamics within a crop growing season for the SIXCA model of a soil-borne pathogen and biocontrol agent on the roots of a plant and in the surrounding soil. The biocontrol agent is able to negatively affect the pathogen through competing for space on the crop's roots, as well as causing the death of pathogen on infected roots at rate η. The biocontrol agent can bulk-up from this interaction at rate ϕ_η. Plant roots, represented by coloured circles, can be in one of three compartments: susceptible (S), infected by the pathogen (I), or colonised by the biocontrol agent (C). Pathogen inoculum (X) and free-living biocontrol agent (A) in the surrounding soil are represented by coloured rhombi. Solid lines represent the transition from one compartment to another, the birth and death of roots, and the decay of material in the soil. Dotted lines represent the necessary interaction between two compartments for a transition from one compartment to the other to occur. Blue lines represent rates where the pathogen is directly and negatively affected by the presence of the biocontrol agent.

2.4.5 Including ν and ϕ_ν

Within-season dynamics: The rate equations for within a growing season, with additions to Equation 2.4 highlighted in bold, are

$$\begin{aligned}
\frac{dS}{dt} &= \rho(S+I+C)\left(\frac{\kappa-(S+I+C)}{\kappa}\right) - \beta_P SX - \beta_S SI - \alpha_P SA, \\
\frac{dI}{dt} &= \beta_P SX + \beta_S SI, \\
\frac{dC}{dt} &= \alpha_P SA, \\
\frac{dX}{dt} &= -\lambda_X X \boldsymbol{-\nu AX}, \\
\frac{dA}{dt} &= -\lambda_A A \boldsymbol{+\phi_\nu \nu AX}\,.
\end{aligned} \tag{2.12}$$

These dynamics can be visualised in Figure 2.7. Free-living biocontrol agent in the soil can attack and kill any free-living pathogen, increasing its decay rate by rate ν. If the biocontrol agent ingests the pathogen and uses it as a source of food, it can bulk-up at rate ϕ_ν.

At the end of a growing season and between growing seasons: The dynamics at the end of a growing season do not change from those mentioned in Section 2.3. The rate equations for between growing seasons, with additions to Equation 2.7 highlighted in bold, are

$$
\begin{aligned}
\frac{dS}{dt} &= 0, \\
\frac{dI}{dt} &= 0, \\
\frac{dC}{dt} &= 0, \\
\frac{dX}{dt} &= -\lambda_X X - \boldsymbol{\nu A X}, \\
\frac{dA}{dt} &= -\lambda_A A + \boldsymbol{\phi_\nu \nu A X}\,.
\end{aligned}
\tag{2.13}
$$

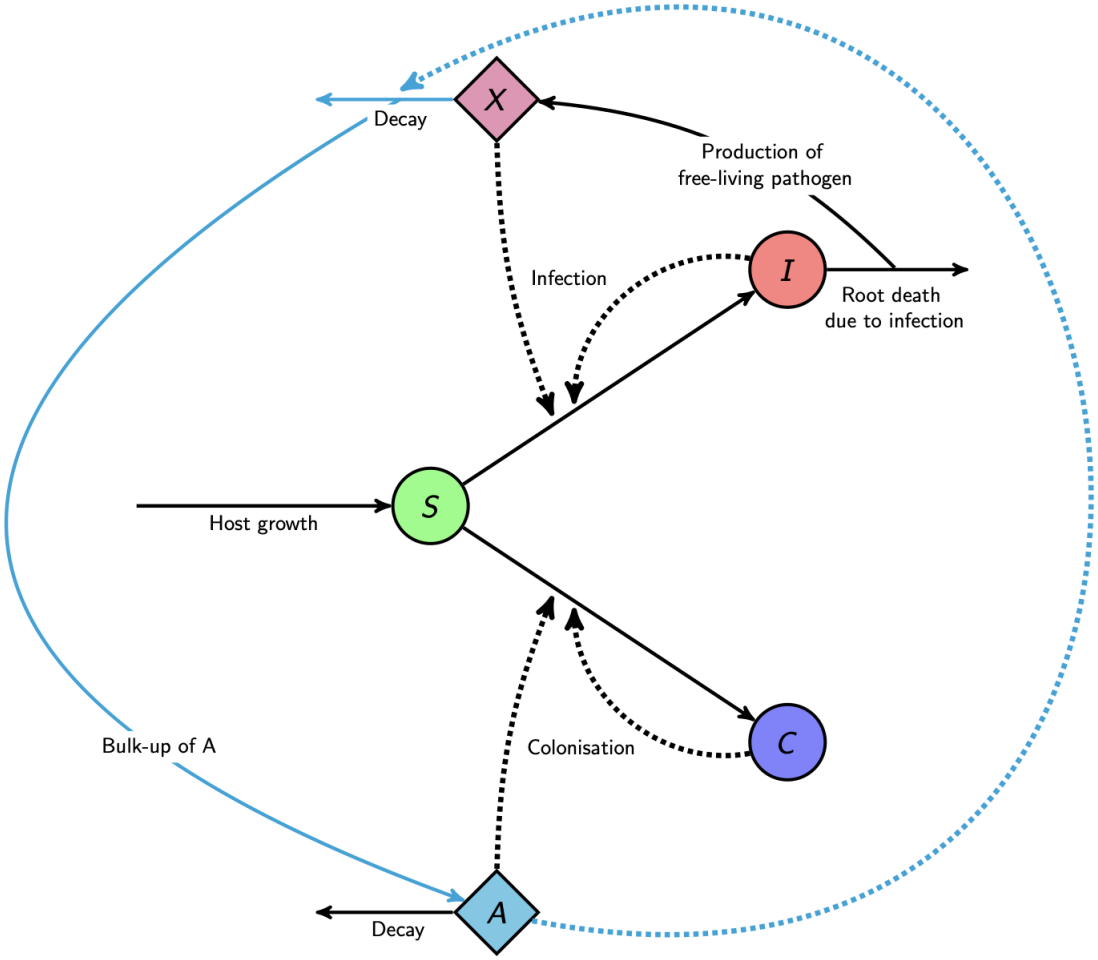

Fig. 2.7 **SIXCA model, with ν and ϕ_ν included**. Schematic of the dynamics within a crop growing season for the SIXCA model of a soil-borne pathogen and biocontrol agent on the roots of a plant and in the surrounding soil. The biocontrol agent is able to negatively affect the pathogen through competing for space on the crop's roots, as well as increasing the decay rate of pathogen inoculum at rate ν. The biocontrol agent can bulk-up from this interaction at rate ϕ_ν. Plant roots, represented by coloured circles, can be in one of three compartments: susceptible (S), infected by the pathogen (I), or colonised by the biocontrol agent (C). Pathogen inoculum (X) and free-living biocontrol agent (A) in the surrounding soil are represented by coloured rhombi. Solid lines represent the transition from one compartment to another, the birth and death of roots, and the decay of material in the soil. Dotted lines represent the necessary interaction between two compartments for a transition from one compartment to the other to occur. Blue lines represent rates where the pathogen is directly and negatively affected by the presence of the biocontrol agent.

Chapter 3: Obtaining parameter values that represent the infection of winter wheat by take-all

3.1 Abstract

It is common practice in biological modelling to obtain parameter values for a model by fitting to experimental data. This allows the model to directly mimic the behaviour of a biological system, and can increase confidence that conclusions drawn through model simulations are applicable to real-world situations. However, the process of model fitting can often be complex, especially when fitting multiple parameters at once or when little data are available. The latter is commonplace in biological systems, where data collection can take multiple years and repeated experiments are constrained by time and cost. Further difficulties arise when examining soil-borne systems due to the complexities with examining below-ground interactions. These issues can lead to difficulties with the model fitting process, resulting in the identification of suboptimal parameters and a poor fit of a model to the data.

This chapter focused on the SIX model, which simulates the interactions between a pathogen and the roots of a plant. Data was obtained from Werker et al. (1991) that examined the proportion of winter wheat roots infected by take-all, *Gaeumannomyces graminis* var. *tritici*, over a growing season. The model was able to fit to this data, providing rate parameter values for primary and secondary infection. The model fitting process was relatively simple due to only two rate parameter values that needed to be

determined, as well as a large amount of experimental data due to repeated experiments over multiple years. However, there was an initial problem with overfitting, and the ability of a fitting attempt to converge on the global optimum was highly dependent on initial starting conditions. There is therefore a need to carefully analyse the results from any model fitting work to ensure that the global optimum is located and that confidence intervals can be obtained for each parameter.

3.2 Introduction

The behaviour of a computational model can significantly vary depending on the values given to any included rate parameters. In a host-pathogen model, values that favour a pathogen could lead to high disease severity and almost definite persistence of the pathogen in the system, whereas parameter values associated with a weak pathogen may lead to minimal infection or spread of disease. Parameter values must be chosen carefully depending on the focus of the research and questions being addressed. Focusing on a specific host and disease requires parameter values to be obtained that accurately reflect the dynamics of that system, whereas a broader focus can allow for a wider range of parameter values to be considered.

For a simple model with few parameters and no focus on a specific biological system, it is possible to perform a sensitivity analysis where the values of individual parameters can be varied, and their effects on the model output separately analysed. Parameter values can then be chosen based on whichever model output best suits the research question. However, more complex models have too many parameters to successfully do this, due to interactions between parameters and the difficulty of analysing the effects of parameters on the model output individually. Instead, analysis of these models will often result in choosing parameter values that allow for several different scenarios to be explored (Cunniffe and Gilligan, 2011; Jeger et al., 2009; Park et al., 2001; Xu et al., 2011; Xu and Jeger, 2013a). For example, a

set of parameters that result in high epidemic severity or low epidemic severity could be compared. However, it is impossible to know whether these parameter values reflect any real life biological systems or not, and this therefore reduces the validity of any conclusions drawn that relate to real-world systems. This is especially important when focusing on a specific host-pathogen system as the individual pathogen's biology will have an impact on the model dynamics. For example, the success of various control methods against a disease will vary significantly depending on how the pathogen interacts with the host and its environment.

Obtaining parameter values that reflect the dynamics of a real-life biological system involves fitting a model to data. There are multiple different methods for model fitting, and the process of model fitting can often be complex, especially when there is little available data or many parameters that need to be fitted (Ashyraliyev et al., 2009; Fernández Slezak et al., 2010; Gutenkunst et al., 2007; Moles et al., 2003). The main issues with model fitting can be split into the following three sections:

1. **Obtaining optimal data**: data should be selected that best represent the real life situation that is attempting to be modelled. A lack of data can reduce the ability of the model fitting process to converge on a single solution, as there may be multiple combinations of parameters that can produce the same output. Difficulties with model fitting are commonplace in biological systems (Ashyraliyev et al., 2009; Gutenkunst et al., 2007; Moles et al., 2003), especially in field experiments set over multiple years where environmental conditions can significantly vary((Bailey et al., 2009; Werker et al., 1991).

2. **Determining how may parameters can be included in the fitting**: models with multiple parameters that need to be fitted together can result in model fitting difficulties. It is possible that pairs of parameters can be codependent, where the value of one parameter can trade off against another without affecting the fitted model

trajectory. The best model fitting solution may also not necessarily be the best from a biological point of view, producing biologically implausible values (Fernández Slezak et al., 2010). The likelihood of these issues occurring increases when less is known about the biological system, reducing the ability to impose tight bounds of the possible range of parameter values in the fitting process. It may be necessary in these cases to reduce the number of parameters included in the model fitting process through fixing some of these parameters at specified values. In some cases, parameters may be included in a model that do not improve the ability of a model to fit to data, and could therefore be discarded.

3. **Ensuring that the "best" model fit has been obtained**: problems with model fitting such as a lack of data or having to fit several parameters at once can lead to a complex model fitting landscape where there are multiple fitting solutions. Depending on which initial parameter values you start the model fitting process at, you may end up with a different answer as to which parameter values best fit to the data. Each of these solutions is called a local optimum, as the model fitting has converged on the optimum solution for a specific area of parameter space, but it may not be the optimum when the whole model fitting landscape is considered. It is therefore necessary to thoroughly scan the model fitting solution landscape to ensure that the global optimum is obtained. This can often be achieved by starting model fitting simulations across a wide range of initial parameter conditions. However, fully scanning across these parameter ranges is incredibly computationally expensive. Instead, randomly selected values within these parameter ranges may be generated multiple times, and hopefully some of these would converge on the global optimum. If a very small range of parameters converge on this optimum, it may be missed and another set of parameters may incorrectly be determined as the global optimum. Even if the optimum is found, it may be difficult to differentiate it from other local

optima that fit almost as well to the data. Exploring the results obtained from model fitting therefore needs to be done carefully.

For biological data, there is also often an overall lack of data due to time, space, and cost constraints that reduce the ability for replicated experiments and frequent data collection times. These problems are exacerbated in soil-borne systems as the processes of assessing disease severity and recording any changes to roots in the soil are challenging and time consuming. The methods used are often destructive and damage both root tissue and soil-borne organisms, limiting the frequency of feasibly possible data collection occasions. Several years of data are often necessary when focusing on soil-borne plant diseases, as inoculum builds up in the soil over multiple crop growing seasons (Cook, 2003).

3.2.1 Case study: take-all

Take-all disease is known to be suppressed by a wide range of microorganisms in the rhizosphere of wheat plants. One example of this is with take-all decline (Section 1.5.2). It is one of the most researched examples of specific suppression by a biocontrol agent, and multiple experiments have been performed that examine the interactions between the roots of a wheat plant, take-all disease, and 2,4-DAPG fluorescent *Pseudomonas* spp. It was therefore chosen as the case study for this thesis, where the SIX and SIXCA models could be fitted to data representing take-all infection and take-all decline. This chapter focuses on fitting the SIX model to data from the first year that winter wheat is grown in the presence of take-all. Chapter 4 expands upon this model fitting to include the biocontrol agent, fitting the remaining parameters of the SIXCA model to data that shows the occurrence of take-all decline. The model fitting process was split into these two sections due to the complexity of the SIXCA model coupled with the small amount of data available that shows a convincing trend of take-all decline. Initial tests also showed that attempting to fit all the parameters at once resulted in multiple model fitting solutions and very little confidence in

any one fitting attempt being the optimal solution. Splitting the fitting process into two smaller stages allowed fewer parameter values to be fitted at the same time.

3.2.2 Potential problems with model fitting

A large problem with biological models is determining how complex they need to be. On one hand, biological systems are intricate and contain a huge number of interactions and processes. On the other hand, not all of these interactions and processes need to be modelled to address specific research questions, and the model fitting process gets significant more difficult as the number of parameters increases. There is therefore a trade-off between capturing the biological complexity of a system and making it simple enough to fit to data and understand any obtained results (Peck, 2004).

If a model is overfitted to data, it captures too much detail from the data without gaining any additional insights. It may capture some of the noise from a dataset and may result in conclusions that are overly specific to the dataset used. It may also contain parameters that do not improve the fit of the model to the data. If a model is underfitted, it is not able to capture all of the key biological processes occurring, resulting in overly generalised conclusions and parameter values that do not reflect real life processes (Peck, 2004; Pullen and Morris, 2014). Biological models are often over-parameterised due to the difficulty in determining which interactions are vital to the model dynamics and which can be ignored (Gomez-Cabrero et al., 2011). Fitting the SIX model to data therefore requires an examination of the rate parameters included, and a determination of whether they are necessary to simulate the interactions between *Gaeumannomyces graminis* var. *tritici* and the roots of a wheat plant.

The data must also not be too noisy to hide any interactions between the plant and pathogen, and must contain enough data points to allow a model to be fitted to it. A lack of data can reduce the ability of the model fitting process to converge on a single solution,

as there may be multiple combinations of parameters that have the same deviation from the data. Noisy data will need to be offset with a greater number of data points.

The data must examine the roots of a plant rather than an above-ground assessment of the number of infected plants. Werker et al. (1991) collected data on both the percentage of infected plants and the percentage of roots per plant infected by take-all. The mean percentage of infected plants was consistently higher than the mean percentage of infected roots per plant over the eight years of data collection, suggesting that focusing on infected plants rather than roots could overestimate the disease severity of the plants' roots. Focusing on infected plants rather than roots also ignores important aspects of soil-borne infection, including the effects of primary and secondary infection, and the rapid decay of free-living material (Bailey and Gilligan, 1999; Bailey et al., 2006, 2000).

3.2.3 Key questions

This chapter will focus on the following key questions:

1. Can rate parameters for the SIX model be obtained through fitting to data from a take-all epidemic?
2. How complex is the model fitting landscape?
3. What issues increase the difficulty of this model fitting problem, and how can they be minimised?

3.3 The model

The SIX model is described in detail in Section 2.2. It focuses on the roots of the plant and whether they are susceptible or infected by a pathogen, as well as including free-living pathogen in the surrounding soil.

3.4 Obtaining data for model fitting

3.4.1 Identifying a suitable dataset

Obtaining suitable data for use during the model fitting process required the identification of a dataset that examined the roots of winter wheat plants infected by take-all throughout a growing season. Data must be collected at multiple times throughout the growing season to examine how the number of infected roots changes over time. The crop should be planted and harvested at times that are common for winter wheat, and the previous crop should not have been susceptible to take-all. Without knowing the crop that was planted in the previous season, it is impossible to know how much of an impact it will have had on the population sizes of the pathogen and biocontrol agent. Planting a crop that is not susceptible to take-all, or having an empty field, for at least one previous season is required to ensure that the population sizes of the pathogen or biocontrol agent have not been affected by previous cropping history. Information about the population size of the free-living pathogen would also be helpful. There are several experiments that examine winter wheat roots infected by take-all over a single growing season. However, there is often no mention of previous cropping history, or data collection is only performed once. No experiments could be found that examined the pathogen both on the roots of a plant and free-living in the soil in the same experiment.

The dataset that was chosen for the model fitting process was from Werker et al. (1991). It contains two sets of data where winter wheat infected by take-all was grown between 1978-1987. The first set of data was from eight experiments where winter wheat infected by take-all was grown for two consecutive years, with a break crop (spring beans) planted the years before and after. The data from the first year that winter wheat is grown for each experiment is shown in Figure 3.1. Between 1979 and 1986, the first year of planting occurred for each of the eight experiments. The break crop should remove any build up of

pathogen inoculum from the previous season, and therefore each two year period of winter wheat growth can be treated independently (Cook, 1981; Shipton, 1975). The second set of data was from a single experiment where winter wheat infected by take-all was grown for ten consecutive years. This data is discussed in Chapter 4.

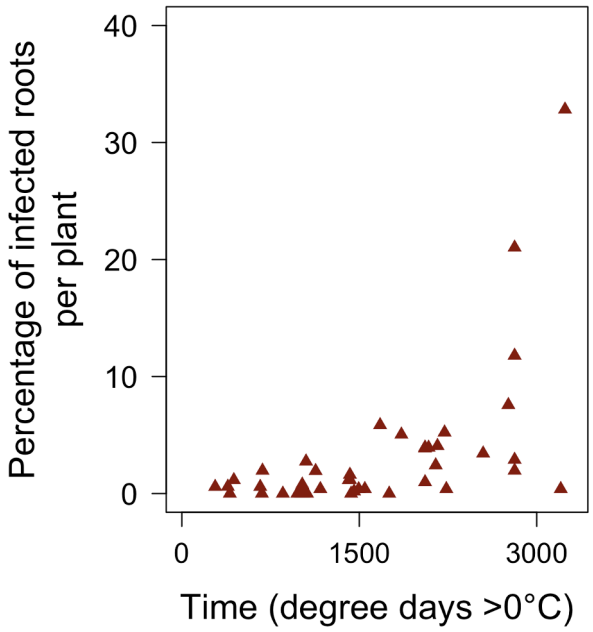

Fig. 3.1 Data from Werker et al. (1991) used in the model fitting process. Data is from the first year of eight experiments where winter wheat infected by take-all was grown over two consecutive years. The experiments took place between 1979-1987. Time is given in degree days $> 0°C$, and the percentage of infected roots per plant (red) was recorded.

The data from Werker et al. (1991) was chosen for several reasons. Firstly, it examines the proportion of infected roots several times each season. The eight repeated experiments give a large amount of data to fit to and will hopefully reduce the effect of environmental variation on the obtained parameter values. The previous cropping history is known, and the break crop used in the previous season is not susceptible to take-all infection. As the second dataset examines the infection of winter wheat over ten consecutive growing seasons, data that has been collected in the same way and with the same environmental conditions can be used to obtain parameter values for both the SIX and SIXCA models.

3.4.2 Converting percentages of infected roots in Werker et al. (1991) to numbers of infected roots

The data in Werker et al. (1991) gives the percentage of infected roots rather than the number, which does not allow for parameters involved in the growth and death of roots to be obtained. This data therefore needed to be converted to represent the number of infected roots. This required data to be obtained that records the total number of roots at multiple time points across a season. The data chosen for this comes from Bailey et al. (2009), which examines winter wheat roots that have been infected by take-all (Figure 3.2). As the data is collected across six seasons, there will be less impact of variability in the rate of root production. Bailey et al. (2009) states that there was no impact of epidemic severity on the rate of root growth or on the carrying capacity of roots. It was therefore assumed that the growth dynamics between Bailey et al. (2009) and Werker et al. (1991) were comparable, which allowed for the data in Werker et al. (1991) to be transformed from the percentage of infected roots into the number of infected and susceptible roots.

The dynamics for root growth were assumed to be

$$\frac{dN}{dt} = \rho N\left(\frac{\kappa - N}{\kappa}\right), \tag{3.1}$$

where root growth is logistic and there is no root death. Both the use of logistic growth and the lack of host death are commonly seen when modelling soil-borne root dynamics (Bailey et al., 2006, 2004, 2005; Cunniffe and Gilligan, 2010; Gilligan and Kleczkowski, 1997; Gubbins and Gilligan, 1997d; Park et al., 2001; Truscott et al., 1997). The latter is often due to necessity, as the co-dependence between birth and death rates results in an impossible model fitting problem unless prior knowledge is known about the relevant rate

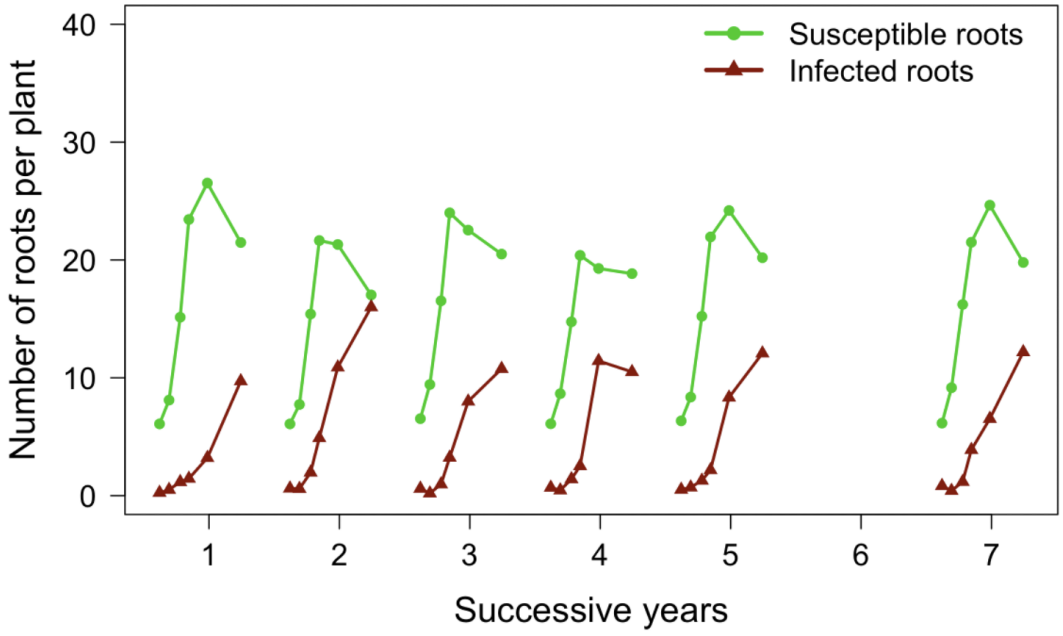

Fig. 3.2 Data obtained from Bailey et al. (2009). Winter wheat infected by take-all was grown over seven consecutive years, although no data was collected in the sixth year. The number of susceptible (green) and infected (red) roots per plant were recorded.

parameters. For a simple model with logistic host growth and death,

$$\frac{dN}{dt} = \rho N\left(\frac{\kappa - N}{\kappa}\right) - \delta N, \tag{3.2}$$

any change to ρ can be offset by changing δ or κ. If this equation were to be fitted to biological data, there would be an infinite number of rate parameter values for ρ, δ, and κ that fit just as well to the data. To remove this problem, death is removed from the model and it is assumed that there is no natural root death during a growing season.

The data in Bailey et al. (2009) for susceptible and infected roots was added together at each time point to produce the total number of roots ($N = S + I$) at each time point. This produced six data points per season, which can be visualised in Figure 3.3. Equation 3.1 was fitted to this data using maximum likelihood estimation, which was implemented using the *optim* function in R (R Core Team, 2019). The *optim* function was chosen due to

clear documentation and frequent use in biological modelling (Bolker, 2008; Nash, 2014). The model fitting process produced the values $\rho = 3.27 \times 10^{-3}\ t^{-1}$ and $\kappa = 31.4$.

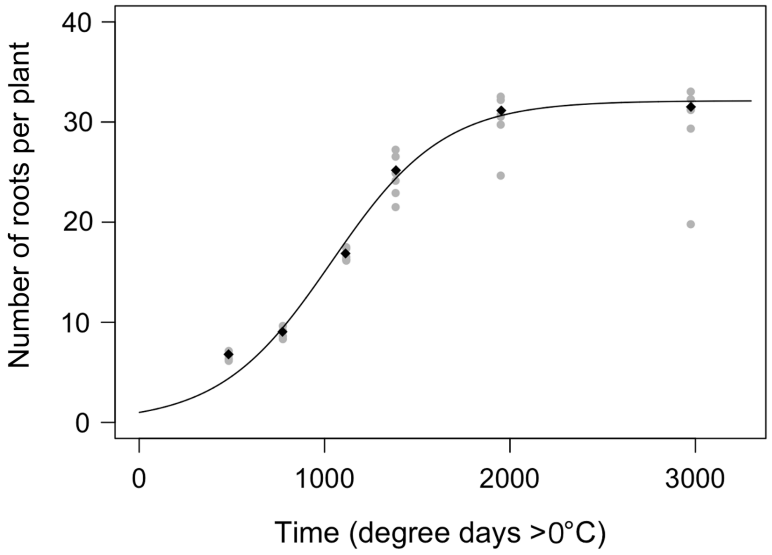

Fig. 3.3 Calculating the carrying capacity (κ) and growth rate (ρ) of the roots of a winter wheat plant across a growing season, using data from Bailey et al. (2009). The growing season lasts 3250 degree days $> 0°$C. Data was collected on the same six dates over six seasons of growing winter wheat that had been infected by the take-all pathogen. Each data point is shown by grey circles, and the mean of these for each time is shown by black diamonds. A logistic growth curve is plotted, shown with a black line, using the values $\rho = 3.27 \times 10^{-3}\ t^{-1}$ and $\kappa = 31.4$.

These parameter values were then substituted into Equation 3.1 to calculate the number of roots for every degree day $> 0°$C throughout a crop growing season. This data couln't directly be used to calculate the total number of roots per time point for the data in Werker et al. (1991). This was because the baseline temperature used to calculate the number of degree days per season was different for Bailey et al. (2009) and Werker et al. (1991). A crop growing season lasts approximately 3000 degree days in Bailey et al. (2009) and approximately 1750 degree days in Werker et al. (1991). Bailey et al. (2009) states that they used degree days $> 3°$C, but calculation of degree days per season using Met Office data suggests that degree days $> 0°$C were used instead. Data from the Met Office was obtained for Southern England and provided a maximum and minimum temperature for

each month, averaged over each year between 1981-2010. The experimental site that data was collected from in Werker et al. (1991) was in the south of England, and therefore the Met Office data was chosen that would best represent this data.

Over a typical growing season for winter wheat (mid October - mid August), the number of degree days calculated using the Met Office data is approximately 3250 for $> 0°C$, 1750 for $> 3°C$, and 1500 for $> 4°C$. This is further confirmed in AHDB (2018), which calculates that the number of degree days $> 0°C$ per winter wheat growing season is similar to that found in Bailey et al. (2009) (roughly 3100 degree days $> 0°C$). It is therefore assumed that degree days $> 0°C$ are used in Bailey et al. (2009), and that degree days $> 3°C$ are used in Werker et al. (1991) as stated. The data in Werker et al. (1991) was converted to degree days $> 0°C$ rather than converting the data in Bailey et al. (2009) to degree days $> 3°C$. This was due to the frequent use of degree days $> 0°C$ in experiments where winter wheat is grown, under the assumption that there is no growth of winter wheat when the temperature is less than $0°C$ (Bauer et al., 1984; Klepper et al., 1988; Stapper and Harris, 1989; Undersander and Christiansen, 1986).

Conversion of the data in Werker et al. (1991) for each time point gave a series of time points that ranged between 282-3239 degree days $> 0°C$. The crop growing period was fixed at 3250 degree days $> 0°C$, and the period between harvesting and replanting (mid August - mid October) was fixed at 750 degree days $> 0°C$. This resulted in a whole year composed of 4000 degree days $> 0°C$. The total number of roots for each time point (measured in degree days $> 0°C$) from Werker et al. (1991) was then calculated using the data shown in Figure 3.3. These could be used to calculate the number of susceptible and infected roots for each time point, which are represented in Figure 3.4.

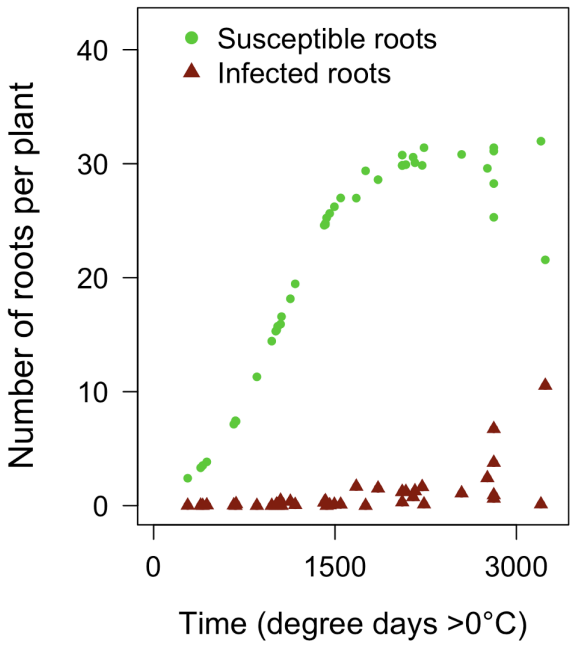

Fig. 3.4 Data obtained from Werker et al. (1991) that has been converted from percentage of infected roots to number of susceptible and infected roots using data from Bailey et al. (2009) to determine the growth rate and carrying capacity. Data is from eight experiments where winter wheat infected by take-all was grown over a single year.

3.5 Methods

3.5.1 Selecting the model and data

The data in Werker et al. (1991) spans 10 years, during which take-all decline occurs. It is assumed that the mechanism of take-all decline occurs due to naturally occurring biocontrol agents building up in the soil over several successive years of take-all decline. This increase in biocontrol agents is assumed to be gradual, with insignificant levels during the first year of winter wheat sowing when disease severity is still low. Data in the first year is therefore assumed to only reflect the dynamics between the crop and the pathogen causing take-all disease, excluding any interactions that involve the biocontrol agent. This allows

for the SIX model, and therefore a smaller number of parameters, to be fitted, reducing the complexity of the model fitting problem.

The initial attempt at fitting the model to data from Werker et al. (1991) required four parameter to be included in the fitting process (Appendix A.1). Due to a lack of data and high collinearity between these parameters, this model fitting attempt was not able to successfully converge on a single optimum fitting solution. However, a parameter was identified as being possible to fix at a specific value and therefore could be removed from the model fitting process, reducing the complexity of the fitting problem. This was τ_I^*, which represents the units of free-living pathogen that are released into the soil when a root dies due to severe infection. As the model fitting results suggested that this rate parameter had a level low enough to be negligible to the overall model dynamics, it was set at $0t^{-1}$. The second attempt at model fitting came across the same problem for μ, which represents the death rate of roots due to infection (Appendix A.2). This parameter value was therefore also fixed at $0t^{-1}$.

The parameter λ_X, which represents the rate of decay of free-living pathogen, was fixed for all model fitting attempts. Previous experimental work on the rate of decay of free-living *Gaeumannomyces graminis* var. *tritici* in the soil had determined this to be 3.32×10^{-3} t^{-1} (Bailey et al., 2005) and 3.74×10^{-3} t^{-1} (Bailey et al., 2009) for a growing season with the same number of degree days as used here. The value of λ_X was fixed at the mean value of these two values, which is $3.53 \times 10^{-3} t^{-1}$. This meant that two parameters were left to be included in the subsequent model fitting process. These were the parameters for the rate of primary infection (β_P) and the rate of secondary infection (β_P).

The parameters for the carrying capacity of root production (κ) and for the growth rate of roots (ρ) were not included in the model fitting process as they had already been established through the process of calculating the number of infected roots, which is described in Section 3.4.2. The initial amount of free-living pathogen was fixed at 0.1 to

represent the introduction of a small amount of pathogen to the soil. Initial model fitting work determined that this value had to be fixed due to strong collinearity between it and the rate of primary infection, β_P. All of the parameters included in the SIX model can be found in Table 3.1.

Table 3.1 List of parameters and definitions for the SIX model. The rate of decay of the free-living pathogen (λ_X) was obtained from Bailey et al. (2005) and Bailey et al. (2009). The rate of root production (ρ) and the carrying capacity of root production (κ) were determined through prior model fitting in Section 3.4.2. The initial amount of free-living pathogen present at the start of the simulation (X_s) is fixed to simplify the model fitting problem and to reduce collinearity between the parameters included in the model fitting process. Any parameters that do not have a default value will be determined in the subsequent model fitting process.

Parameter	Definition	Default value	Units
S	Number of susceptible roots	Variable	
I	Number of roots infected by the pathogen	Variable	
X	Density of free-living pathogen	Variable	
t	Time (degree days $> 0^{\circ}$C)	Variable	
X_s	Initial amount of free-living pathogen present at the start of the first growing season start of the first growing season	1.00×10^{-1}	
ρ	Rate of root production	3.31×10^{-3}	t^{-1}
κ	Carrying capacity of root production	32.1	
β_p	Rate of primary infection of roots by free-living pathogen	-	t^{-1}
β_s	Rate of secondary infection of roots	-	t^{-1}
λ_X	Rate of decay of pathogen inoculum	3.53×10^{-3}	t^{-1}

There were no data collected in the first growing season for the 10 year continuous dataset in Werker et al. (1991). The SIX model was instead fitted to the first year of the two-year experimental plots that grew winter wheat for two consecutive years. These plots occurred over the same time period and under the same growing conditions as the continuous wheat plot. Using this data significantly increased the amount of data available for fitting, and would help to account for variability due to environmental conditions.

3.5.2 Model fitting

Maximum likelihood estimation is used to fit the SIX model to the data shown in Figure 3.4. It was implemented through the *optim* function in R (R Core Team, 2019) and is a commonly used method for model fitting (Bolker, 2008; Nash, 2014). It works by calculating a likelihood function which determines how well a model with a specific set of parameters fits to a dataset. The set of parameters that maximise the likelihood are those that allow the model to fit best to the data. For a set of observed data $\{y_1, \ldots, y_n\}$, with the assumption that errors are normally distributed, the likelihood function that we are trying to maximise is

$$L(\theta) = \left(\frac{1}{\sqrt{2\pi}\sigma}\right)^n e^{-\sum_{i=1}^{n} \frac{(y_i - x_i)^2}{2\sigma^2}}, \tag{3.3}$$

using measured data points y_i and model output values x_i. The standard deviation, σ, needs to be determined through the model fitting process.

For a single model fitting attempt, a random value for each parameter included in the fitting process was generated as an initial condition for an exploration of parameter space. The biologically feasible values of these parameters were unknown and were therefore chosen from a significantly wider range than the hypothesised feasible parameter limits. These limits can be seen in Table 3.2.

The randomly selected parameter values were used as the initial values for the model fitting process, which are required by the *optim* function. In order to allow for the global solution space to be fully explored, and for the global optimum to be located, the model fitting process was performed 5,000 times under different sets of initial parameter values. The best model fit (the fit that produces the greatest log likelihood value) could then be obtained. The log likelihood is used rather than just the likelihood because it simplifies the

mathematical analysis and reduces the problem of small likelihood values that can easily underflow the numerical precision of a computer.

Table 3.2 Range of numbers that initial parameter values were chosen from when fitting the SIX model to the data in Werker et al. (1991).

Parameter	Lower bound	Upper bound
β_P	0	1
β_S	0	1
σ	0	10

3.5.3 Analysing the model fitting output

Although it is easy to obtain the single model fitting solution with the highest log likelihood (LL) from many simulations, there may be multiple other solutions with very similar LL values. It is therefore necessary to examine the other model fitting solutions to explore any local optima in the model fitting landscape, as well as determining the range of parameter values that compose the global optimum. This was carried out over multiple steps:

1. **Exploring variation in the log likelihood values:** bar plots were constructed showing the variation in the LL value for each of the 5,000 model fitting attempts

2. **Collinearity:** the *collin* function in the *FME* package (Soetaert and Petzoldt, 2010) measures how related parameters are to each other. The more related a combination of parameters are, the more likely that different combinations of parameter values can produce the same output. This increases the likelihood of a model fitting problem having multiple solutions, and high collinearity values should therefore be avoided wherever possible (Omlin et al., 2001). The *collin* function analyses the proposed model and calculates a collinearity value for the whole model, as well as calculating values for reduced models with fewer of the proposed parameter values. Omlin et al.

(2001) and Brun et al. (2001) estimate that a collinearity value of greater than 20 results in a model that will be difficult or impossible to estimate a single set of optimal parameter values for. Any model with a collinearity value exceeding 20 should therefore be analysed to see whether it is possible to reduce this value.

3. **Visualising the fitting landscape:** depending on the complexity of the model fitting landscape, it is possible that there will be multiple local optima. Model fitting attempts can get caught in these local optima rather than locating the global optimum. It is also possible that the global optimum will be located within a wide space of parameter values, within which small changes to parameters can lead to very similar log likelihood (LL) values. Visualising this landscape can allow for complexities with the fitting problem to be located, and may help to explain variation in model fitting results. As only two parameters were involved in this model fitting process, variation between their values, and how this has an impact on the LL value, can easily be visualised. The rates of primary infection (β_P) and secondary infection (β_S) can be plotted on the x- and y-axes, and the corresponding LL value can be distinguished based on colour. Variation in the value of σ was not included in this analysis as the aim was to examine the effect of the two rate parameters in the SIX model in more detail. This can allow for the model fitting landscape to be explored, for any local optima to be identified, and for an examination of the global optimum and how easily it can be distinguished from the rest of the fitting solutions.

4. **Constructing profile likelihood plots**: model fitting using maximum likelihood estimation returns an individual set of parameter values. This output is heavily dependent on the initial parameter values included in the model fitting input, and fitting solutions may get caught at local optima. It is therefore necessary for complex fitting problems to perform the model fitting multiple times at different initial parameter values to ensure that the global optimum is found. However, this output

does not give any information about what range of parameters can produce a similar fit to the data. The precision of these parameter estimates can be calculated using profile likelihood, which produces upper and lower confidence intervals for each parameter. A parameter is determined to be identifiable if the upper and lower confidence intervals of its estimate are finite. Parameters that have infinite upper or lower bounds are problematic as they mean that a large range of values for that parameter can produce a similar model output, reducing any confidence in the values obtained through model fitting. If possible, any non-identifiable parameters should be fixed or removed to increase confidence in the fitted solution. For parameters with a finite upper bound but infinite lower bound, it may be possible to remove this parameter from the model. For parameters with a finite lower bound but infinite upper bound, strong collinearity between parameters should be examined. If two parameters are highly collinear, increasing the value of one whilst decreasing the value of the other may give a similar model output. In this case, it may be sensible to fix one of these parameters so that the model can be made identifiable. For all parameters that are identifiable, the upper and lower confidence intervals show the range of parameters that can produce a similar model output, and therefore how much confidence we can have in the parameter values obtained through model fitting. Profile likelihood allows for confidence intervals to be calculated for nonlinear and complex models (Fischer and Lewis, 2021; Royston and Groups, 2007; Venzon and Moolgavkar, 1988). A parameter (θ_i) is determined to be identifiable if the upper and lower confidence intervals of its estimate ($\hat{\theta}_i$) are finite. If a parameter does not have a finite upper or lower confidence interval, it is determined to be unidentifiable. The profile for a parameter (θ_i) is calculated by scanning across a range of values for this parameter and, for each value, using maximum likelihood to reoptimise all other

parameters ($\theta_{j\neq i}$). The profile likelihood for parameter θ_i can therefore be written as

$$PL(\theta_i) = \max_{\theta_{j\neq i}} L(\theta). \tag{3.4}$$

This creates a range of parameter values for θ_i, which will all have a corresponding likelihood value. For parameter values of θ_i, any profile likelihood values where

$$PL(\theta_i) - L(\hat{\theta}) \leq \chi^2_{\alpha,1}, \tag{3.5}$$

is true sit below the confidence limit, where α is the chosen confidence level. Any parameter that is not identifiable should be examined further to see if can be removed or fixed at a specific value. The 95% confidence interval is used in this chapter to determine if parameters are identifiable or not.

3.6 Results

The model fitting process was performed 5,000 times under randomly selected initial parameter values, and the fitting attempt that provided the parameters that fit best to the data can be seen in Table 3.3. Using these parameter values to run a simulation of the SIX model over a single growing year gives the model trajectory seen in Figure 3.5. The number of infected roots increases gradually over the growing season, resulting in a peak of 5.75 infected roots at 3250 degree days >0°C. The amount of free-living pathogen decays exponentially throughout a growing season, resulting in less than 1% remaining at 2000 degree days >0°C.

The proportion of infected roots throughout the season has two separate peaks (Figure 3.6). The first is towards the start of the growing season, when there is a large amount of pathogen inoculum in the soil to cause high levels of primary infection. However, the rapid

decay of inoculum means that primary infection begins to drop and causes a reduction in the proportion of infected roots. As the season progresses, secondary infection begins to dominate and this causes the second much larger peak in the proportion of infected roots. At the end of the growing season, 18% of roots are infected.

Table 3.3 Parameter values and their 95% confidence intervals for primary (β_P) and secondary (β_S) infection obtained through fitting the SIX model to data over one year of growing winter wheat crop infected by take-all. Maximum likelihood model fitting was used, and the standard deviation (σ) that was calculated during this process is shown in the table. Data was obtained from Werker et al. (1991). Out of 5,000 model fitting simulations starting with different initial parameter values, these parameter values produced the highest log likelihood (LL) value.

		Confidence interval (95%)		
Parameter	Value	Lower	Upper	Units
β_P	1.35×10^{-3}	2.10×10^{-4}	3.59×10^{-3}	t^{-1}
β_S	5.92×10^{-5}	4.23×10^{-5}	8.90×10^{-5}	t^{-1}
σ	1.25	1.08	1.49	
LL	-118			

Using the parameter values found in Table 3.3, the SIX model fitted to the data from Werker et al. (1991) produced a collinarity value of 1.82. This is significantly below the threshold value determined by Omlin et al. (2001) and Brun et al. (2001), suggesting that the model is strongly identifiable using this data. More complex versions of the SIX model, discussed in Appendix Sections A.1 and A.2, have much higher collinearity values and are deemed not identifiable.

The profile likelihoods were calculated for both fitted parameters (Figure 3.7). Upper and lower 95% confidence intervals were obtained for β_P and β_S (Table 3.3), meaning that they are both identifiable. Both parameters have relatively narrow confidence intervals and a distinguishable minimum value, strengthening the support for the parameter values in Table 3.3 being the global optimum.

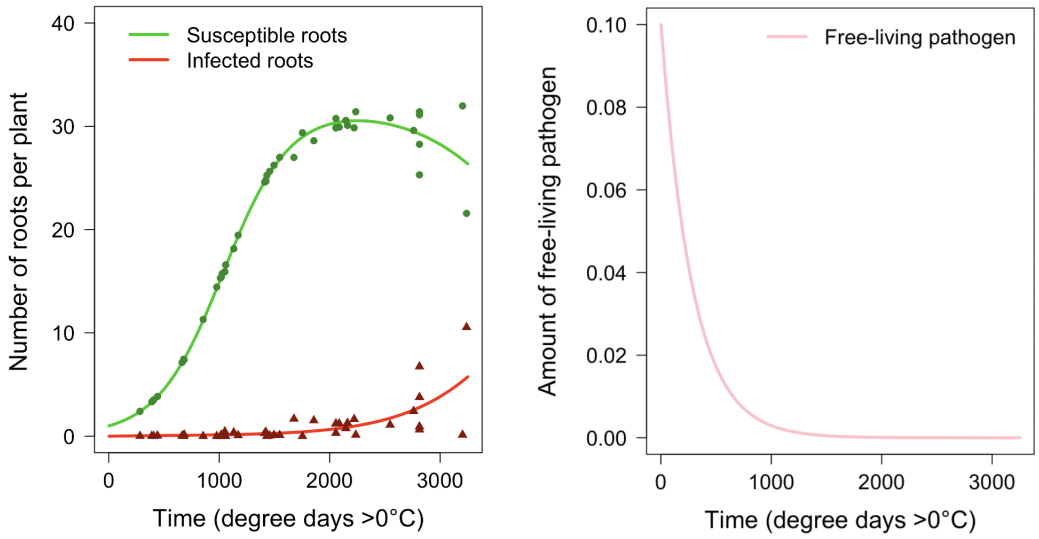

Fig. 3.5 Simulation of the SIX model over a growing season using the best fitting parameter values in Table 3.3. Solid lines show the number of susceptible (green) and infected (red) roots per plant, as well as the amount of free-living pathogen (pink) in the surrounding soil. Data was obtained from field experiments carried out over a year where winter wheat infected by take-all decline was grown (Werker et al. 1991). The data is shown for susceptible roots (green circles) and infected roots (red triangles).

Over the 5,000 simulations, the log likelihood value varied between -118 and -327 (Figure 3.8). A log likelihood value of -118 was obtained for 2496 of the solutions, which represents just under 50% of the total. The variation in log likelihood values across the solutions is further explored in Figure 3.9, where the variation in the values of β_P, β_S, and the log likelihood value are visualised. The range of values for β_P is significantly greater than for β_S, but both have a single distinct peak that represents the global optimum when looking across the whole of parameter space (Figure 3.9A). The area of parameter space that included this peak was more closely analysed by focusing on log likelihood values greater than -130 (Figure 3.9B). There is still a distinct peak of solutions representing the global optimum. However, there is some spread of β_P and β_S values away from this peak that have relatively high log likelihood values. The clustering of solutions towards either β_P or β_S at 0 is due to the model fitting process, where fitted values were required to be

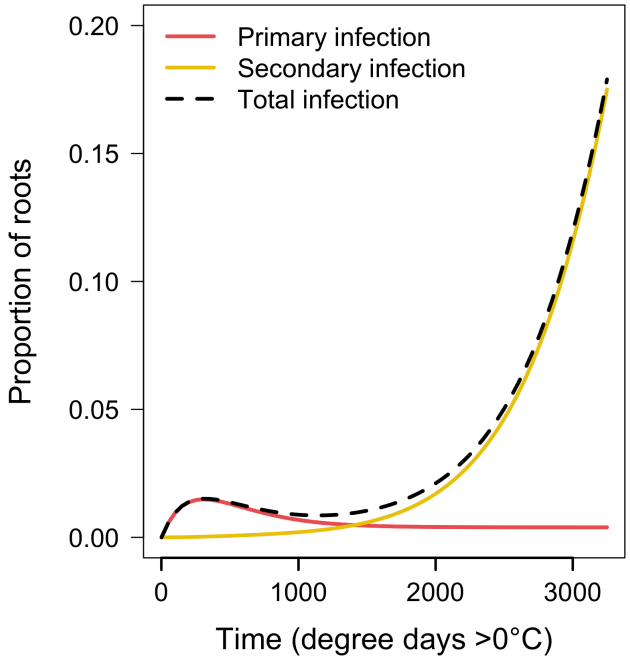

Fig. 3.6 Change in the proportion of infected roots that occur through primary and secondary infection over a growing season using the SIX model and the parameter values in Table 3.3. The proportion of roots that are infected by primary infection is shown by a red line, whereas the proportion of roots that are infected by secondary infection is shown by a yellow line. The total proportion of infected roots is shown by a black dashed line.

positive. The difference in the spatial arrangement of parameters when they are allowed to be positive is shown in Appendix Figure A.5 There is still a distinctive global optimum and there is no difference in the values of β_P and β_S that maximise the log likelihood value. However, all solutions with a log likelihood value of greater than 130 have visibly identical values rather than the spread seen in Figure 3.9B. Both Figure 3.9 and Figure A.5 show that the model fitting process either converges on a solution that doesn't fit well to the data at all, or it converges on the optimal solution. There are no other significant global optima.

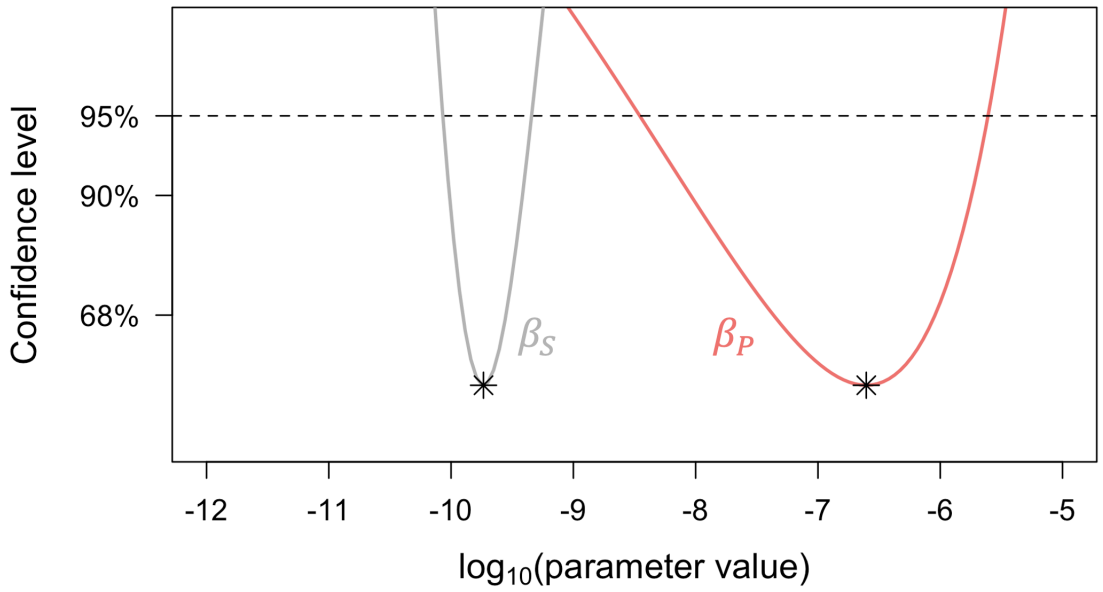

Fig. 3.7 Profile likelihood plots of the rate parameters for primary (β_P) and secondary (β_S) infection in the SIX model. Both parameters are identifiable to the 95% confidence level. The best fitting parameter values from Table 3.3 are marked on each profile likelihood curve by an asterisk. The 95% confidence intervals for σ are 1.08-1.49.

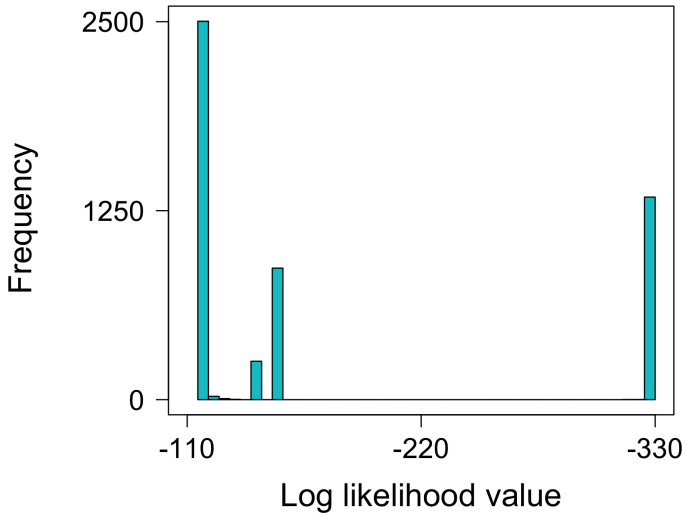

Fig. 3.8 Variation in the log likelihood value for 5,000 model fitting simulations of the SIX model. Data was obtained from Werker et al. (1991) and focuses on the percentage of infected roots across a single growing season for winter wheat.

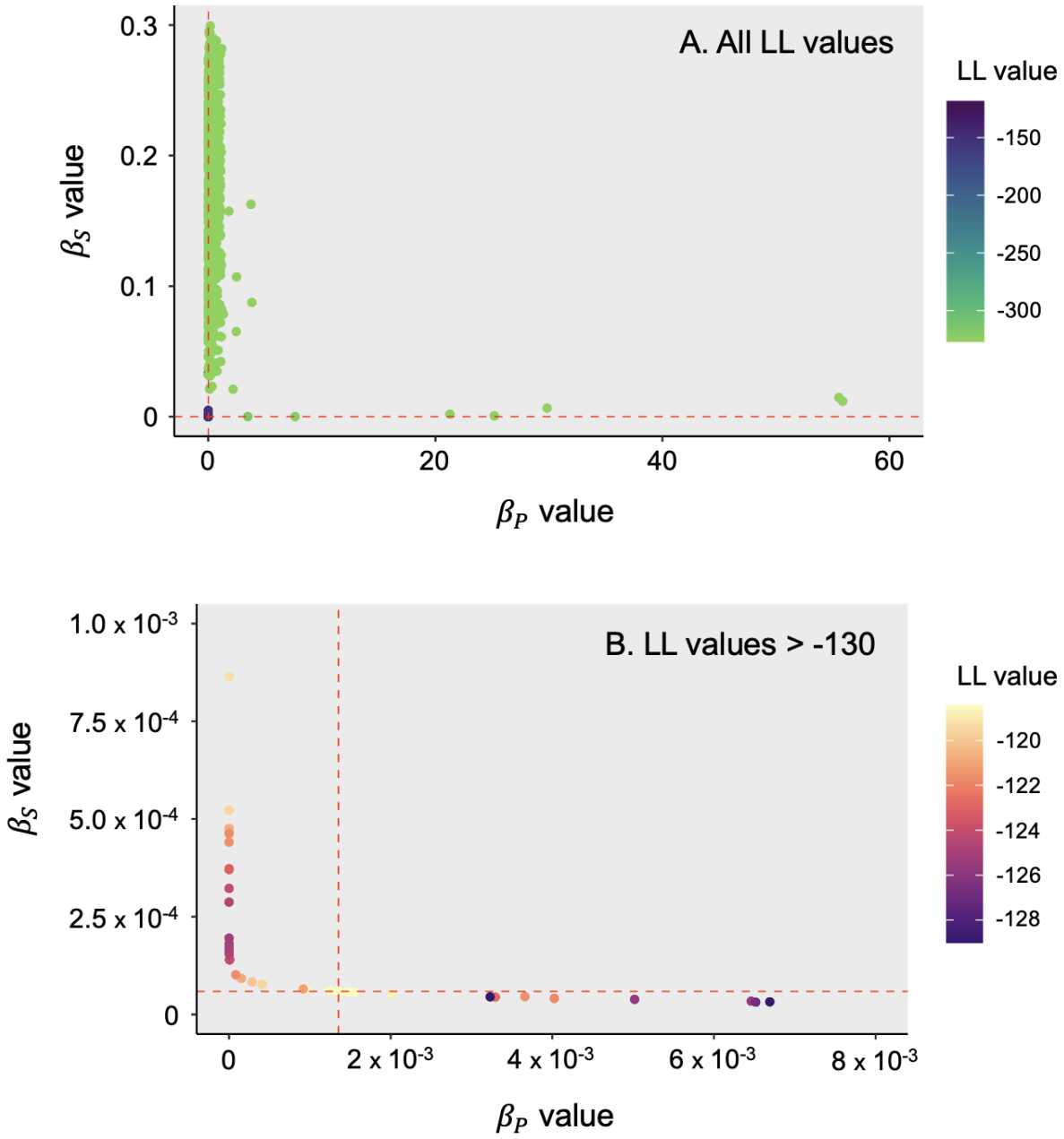

Fig. 3.9 Variation in the values of β_P, β_S, and the log likelihood value across 5,000 model fitting attempts. Either (A) all solutions, or (B) solutions with a log likelihood value greater than -130 are focused on. Out of all fitting attempts, the values of β_P and β_S that produced the highest log likelihood value are shown by red dashed lines.

3.7 Discussion

Before the analysis in this chapter occurred, the SIX model contained two additional rate parameters. These were included in the model as they were believed to have an important role in the interactions between a soil-borne pathogen and a host plant. It is common for biological models to contain more complexity than is needed to fit to a data set. It can be difficult to determine which biological processes are required to model the interactions between organisms accurately, and which can be ignored. Biological models therefore often struggle with the problem of over-fitting, and initial analysis must be carried out to determine whether all the included processes are required. For the SIX model, there was no change to the log likelihood value when two parameters were removed from the model. This means that the model could fit just as well to the data without these parameters, and they therefore were not required. Removing these parameters also resulted in identifiable 95% confidence intervals for the two rate parameters still included in the model fitting. This allowed us to examine the range of parameter values that produced a similar model output, and made any chance of further overfitting less likely.

The rate of pathogen decay was fixed at a value determined in Bailey et al. (2005) and Bailey et al. (2009). This rapid decay of free-living material is known to affect the mechanisms of infection during each growing season. Primary infection dominates at the start of the growing season whilst there is still a significant amount of free-living pathogen present, before secondary infection takes over as more roots become infected and the free-living pathogen decays to lower levels (Bailey and Gilligan, 1999; Bailey et al., 2005; Brassett and Gilligan, 1988; Schoeny and Lucas, 1999). This switch between primary to secondary infection is known to often produce a plateau in the proportion of infected roots in between inoculum decaying to low levels and secondary infection accelerating (Bailey et al., 2009, 2005; Werker et al., 1991). This was also found during the first growing season for the

SIX model (Figure 3.6), strengthening the importance of a distinction between primary and secondary infection when modelling soil-borne plant diseases that have free-living inoculum.

Although the data from the first growing season of winter wheat in Werker et al. (1991) is noisy, the SIX model is still able to fit well and give sensible parameter values. These parameter values ($\beta_P = 1.35 \times 10^{-3}$ and $\beta_S = 5.92 \times 10^{-5}$) are similar to those found in Bailey et al. (2005) ($\beta_P = 9.00 \times 10^{-4}$ and $\beta_S = 7.35 \times 10^{-5}$), which also looks at winter wheat roots infected by take-all during the first growing season. Although it is well known that environmental conditions can have a significant impact on parameter values (Bossio et al., 1998; Smit et al., 2001; Weller, 1988), it is reassuring that the calculated parameter values from two separate data sets produced similar results.

It can be confidently assumed that the obtained parameter values represent the global optimum across parameter space. No other local optima were located that had a similar log likelihood value to the best fitting solution, and 50% of model fitting attempts converged on this solution. However, it is worth noting that 50% of solutions had a log likelihood value of -130 or less and did not fit well to the data. Even for a simple model with two parameters and minimal collinearity between them, the model optimisation was not always able to converge on parameter values that fit well to the data. There was significant variation in the rate parameter values for primary and secondary infection depending on what the initial conditions for the model fitting were.

This is likely due to the fact that initial parameter values that were used to initiate the model fitting process were chosen from a wide range of values. Knowledge about the biological constraints on these parameters would have been likely to result in a greater proportion of fitting solutions converging on the global optimum. It is worth noting that, when little is known about parameter values, the global optimum may not always be located, even for a simple model. There is therefore a requirement for multiple simulations to be performed before determining the solution that is at the global optimum, or for the use of

a more complex optimisation method that is not as constrained by the initial parameter values.

The SIX model focused on the interactions between a pathogen and the roots of a plant. When fitting to the data from Werker et al. (1991), an assumption was made that there will be minimal biocontrol activity in the first growing season. This allows parameters related to the pathogen to be calculated separately to those related to the biocontrol agent, reducing the number of parameters that have to be fit at the same time. Initial research determined that it was not possible to fit parameters for the pathogen and the biocontrol agent at the same time due to a lack of data, as well as strong collinearity between some of the parameters. Using the first season of data from Werker et al. (1991) to only fit parameter values relating to the pathogen therefore allowed for a simpler optimisation problem.

3.7.1 Conclusions

The SIX model was able to successfully fit to the data from Werker et al. (1991) that examined the proportion of winter wheat roots infected by take-all, *Gaeumannomyces graminis* var. *tritici*, over a growing season. However, even with a relatively large amount of data and only two parameters included in the model fitting process, there were problems with over-fitting and convergence on the global optimum. The model fitting process could have been optimised by knowing the potential bounds for the parameter values, as well as having access to data on the free-living pathogen.

Chapter 4: Obtaining parameter values that represent take-all decline

4.1 Abstract

This chapter follows on from initial model fitting work in Chapter 3, where parameter values relating to the take-all pathogen were determined. There is now a focus on incorporating a biocontrol agent into the model and using additional model fitting to determine parameter values to represent its behaviour. This uses the SIXCA model, which simulates the interactions between a pathogen and a biocontrol agent on the roots of a plant and as free-living material in the soil.

This research aimed to fit several variations of the SIXCA model to data that shows take-all decline. These model variations differed in the mechanisms that the biocontrol agent could use to negatively affect the pathogen. Take-all decline is a natural phenomenon where the disease severity of take-all (caused by the soil-borne fungus *Gaeumannomyces graminis* var. *tritici*) decreases after several successive years of planting winter wheat due to the natural build up of biocontrol agents in the soil. Data from Werker et al. (1991) showed a convincing trend of take-all decline, although a lack of data collection times, as well as an absence of data recorded on the densities of the biocontrol agent and free-living pathogen, resulted in a complex model fitting problem.

A set of parameters was obtained for each model variation through model fitting. Five of the mechanisms that the biocontrol agent could use to negatively affect the pathogen were found to be capable of causing take-all decline. These were 1) competition for space on the crop's roots, 2) colonisation of infected roots by the free-living biocontrol agent, 3)

colonisation of infected roots by the biocontrol agent on other colonised roots, 4) death of the pathogen on infected roots and subsequent bulk up of the biocontrol agent, and 5) death of free-living pathogen and subsequent bulk up of the biocontrol agent. The complexities of this model fitting problem are discussed.

4.2 Introduction

The process of fitting a model to a data set allows for values of rate parameter to be obtained that represent a biological system. This process can be complex if there are many parameters that need to be included in the fitting process, of if there is little or noisy data. The main issues with model fitting are discussed in Chapter 3 and will therefore not be explored further here.

4.2.1 Case study: take-all decline

Take-all decline demonstrates an example of successful disease suppression of a soil-borne pathogen through interactions with a naturally occurring biocontrol agent (Section 1.5.2). In order to successfully fit a model to data showing take-all decline, two conditions have to be met. First, the model must be capable of replicating this trend in disease severity. Secondly, the data must not be too noisy to hide this trend, and must contain enough data points to allow a model to be fitted to it. These two points are explored in more detail in Section 3.2.2. Unlike with the SIX model, additional criteria need to be met in order to successfully fit the SIXCA model to data. The first is that the data must be collected from consecutive years of growing wheat. A break in growing this crop, either through leaving the field empty or growing another type of crop, is long enough to cause significant changes to the free-living pathogen and biocontrol agent populations (Cook, 1981; Shipton, 1975).

Data collection must also span enough years for take-all decline to be able to occur, which involves an initial peak in epidemic severity before this severity starts to decline over subsequent years. This initial peak often occurs between two and three years of consecutively growing winter wheat (Gerlagh, 1968; Schlatter et al., 2017; Shipton, 1972; Weller et al., 2002), but this timing can vary considerably (Cook, 1988; Shipton, 1975).

Finally, the data must show a convincing trend of take-all decline, where several successive years of take-all disease culminates in a peak of disease severity, followed by a subsequent reduction in disease for all successive years. This trend is likely to be affected by environmental variability, which might affect the characteristic take-all decline trend or prevent it from occurring altogether.

4.2.2 Key questions

This chapter will focus on the following key questions:

1. Can data be found that represents the phenomenon of take-all decline?
2. Can the above data be used to obtain rate parameter values that represent take-all decline?
3. What mechanism or mechanisms does the biocontrol agent seem to be using to negatively affect the take-all pathogen?
4. How complex is the model fitting landscape, examining local optima and confidence intervals for rate parameters included in the model fitting process?
5. What issues increase the difficulty of this model fitting problem, and how can they be minimised?

4.3 The model

The SIXCA model is described in detail in Chapter 2. It focuses on the roots of the plant and whether they are infected by a pathogen or colonised by a biocontrol agent, as well as including free-living pathogen and biocontrol agent in the surrounding soil. There are 10 different mechanisms that the biocontrol agent can use to negatively and directly affect the pathogen. Each of these is included into the SIXCA model separately, fixing the values for all other mechanisms at 0. This means that each individual mechanism can be examined separately, identifying whether they significantly improve the ability of the SIXCA model to fit to the data, as well as how likely they are to be a mechanism of disease suppression during take-all decline.

All of these models include primary and secondary colonisation by the biocontrol agent. Including a variation of the SIXCA model where none of the 10 mechanisms are present (all fixed at 0, but with primary and secondary colonisation still included), gives 11 different variation of the model. These will be fitted separately to the data, analysing whether certain mechanisms can 1) cause take-all decline to occur, and 2) improve the fit of the model to the data.

4.4 Obtaining data for model fitting

4.4.1 Identifying a suitable data set

Experiments that assess the severity of take-all on a crop's roots often only examine take-all across one or two years (Brassett and Gilligan, 1989; Weller and Cook, 1982; Raaijmakers and Weller, 1998), or examine it across multiple years but only collect data on disease severity once at the end of each year (Shipton, 1975). This data does not provide enough information to allow for accurate model fitting of the SIXCA model to occur.

Only two experiments were identified that recorded the amount of infected roots per season, both at multiple data points per season, as well as across enough years for take-all decline to have been able to occur (Bailey et al., 2009; Werker et al., 1991). The relevant data from Bailey et al. (2009) and Werker et al. (1991) are included in Figures 4.1 and 4.2. The dates that data collection occurred were stated in the text for both experiments. Data on the crop's roots was obtained through digitising Figure 1 from Bailey et al. (2009) and Figure 2 from Werker et al. (1991).

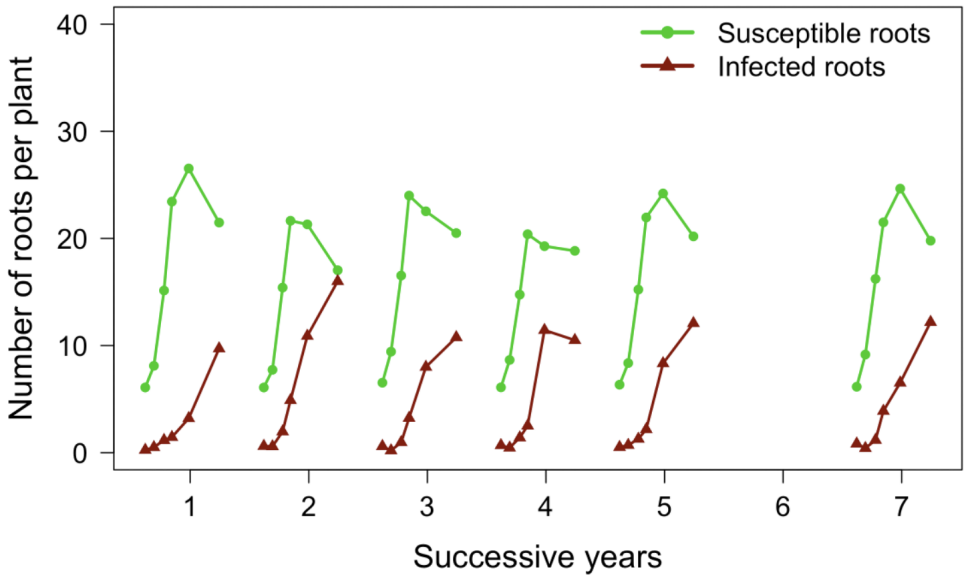

Fig. 4.1 Data obtained from Bailey et al. (2009). Winter wheat infected by take-all was grown over seven consecutive years, although no data was collected in the sixth year. The number of susceptible (green) and infected (red) roots were recorded.

The experiment discussed in Bailey et al. (2009) spanned seven consecutive years, although no data was collected in the sixth year (Figure 4.1). Data was collected at six time points each year, and the number of roots that were either susceptible or infected was recorded.

Werker et al. (1991) contained two sets of data where winter wheat infected by take-all was grown between 1978-1987. The first set of data was from eight experiments where winter wheat infected by take-all was grown for two consecutive years. This data is described

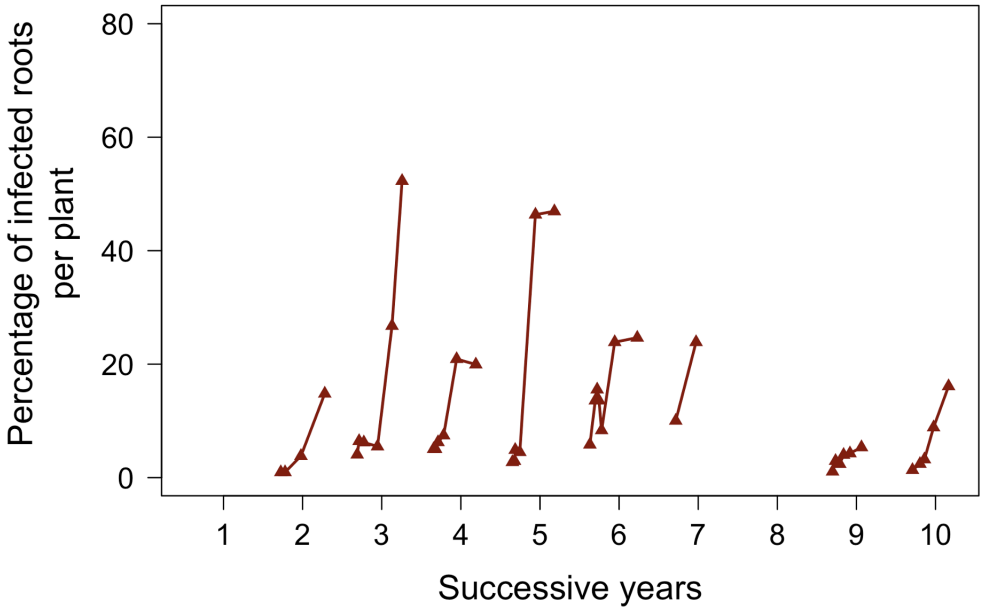

Fig. 4.2 Data from Werker et al. (1991) used in the model fitting process. Data was collected from a single experiment where winter wheat infected by take-all was grown over ten consecutive years. No data was collected in the first and eighth years. For both experiments, the percentage of infected roots (red) was recorded.

in Section 3.4 where the SIX model was fitted to the first year of this data to obtain parameter values relating to the pathogen and crop roots. The second set of data was from a single experiment where winter wheat infected by take-all was grown for ten consecutive years (Figure 4.2). For this experiment, no data was collected in the first and eighth years (1978 and 1985, respectively). The number of sampling occasions varied between years, spanning from two to seven data points per season. The percentage of infected roots on each plant was recorded.

The authors of both of these papers state that, for each of their experiments, the variation in take-all severity across successive years is likely due to the phenomenon of take-all decline. For both of these experiments, no data was collected on the presence or absence of any biocontrol agent on the crop roots, or for any free-living pathogen or biocontrol agent in the surrounding soil. The number of infected roots in the data from Bailey et al. (2009) peaks in season two, and there is no dramatic increase and subsequent

decrease of disease severity as would be expected if take-all decline had occurred. This might suggest that the soil did not contain the biocontrol agent (or agents) needed for take-all decline to occur, or that environmental conditions were not conducive to allowing disease suppression to occur. Instead, changes in the levels of disease could be due to general suppression from soil-borne biocontrol agents, or changes in environmental conditions over subsequent seasons. This is explained further in Section 1.4.

The data in Werker et al. (1991) shows a more classic trend of take-all decline, with low disease severity in season two, rising to a peak in season three, followed by a decrease in disease across all subsequent seasons. However, the disease severity in season four is lower than would be expected. This is likely to be due to environmental variation, and a convincing trend of take-all decline can still be seen. However, this makes the data more complex to fit a model to and could lead to problems with convergence of model fitting attempts. As it seems likely that take-all decline did not occur in Bailey et al. (2009), the data from Werker et al. (1991) was chosen for model fitting.

4.4.2 Converting percentages of infected roots in Werker et al. (1991) to numbers of infected roots

The data in Werker et al. (1991) gives the percentage of infected roots rather than the number, which does not allow for parameters involved in the growth and death of roots to be obtained. It was therefore assumed that the growth dynamics between Bailey et al. (2009) and Werker et al. (1991) were comparable, which allowed for the data in Werker et al. (1991) to be transformed from the percentage of infected roots into the number of infected and susceptible roots. This process is explained in detail in Section 3.4.2, with the resulting data shown in Figure 4.3.

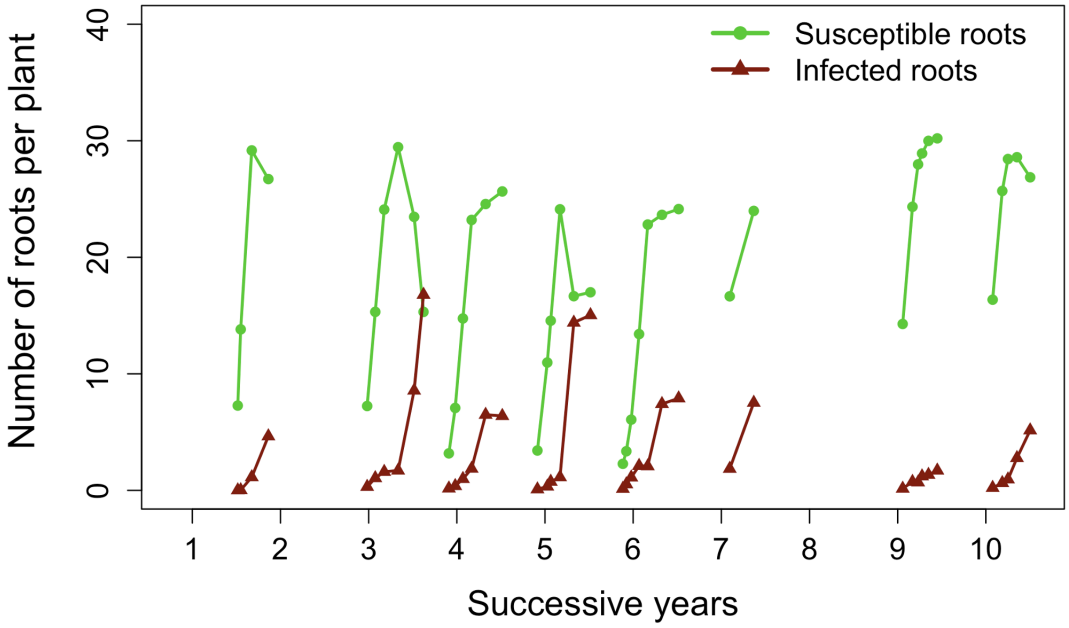

Fig. 4.3 Data obtained from Werker et al. (1991) that has been converted from percentage of infected roots to number of susceptible and infected roots using data from Bailey et al. (2009) to determine the growth rate and carrying capacity. This process is explained in Section 4.4.2. Data was collected from a single experiment where winter wheat infected by take-all was grown over ten consecutive years. No data was collected in the first and eighth years.

4.5 Methods

4.5.1 Selecting the model and data

The SIXCA model focuses on the roots of a plant, as well as free-living pathogen and biocontrol agent in the surrounding soil. More information about this model can be found in Chapters 2 and 3. A growing season where the crop is present lasts 3250 degree days >0°C, where crop roots, pathogen and biocontrol agent living on the roots, and free-living pathogen and biocontrol agent, are present. The crop is harvested at 3250 degree days and is removed from the system, resulting in only the free-living pathogen and biocontrol agent present for the between growing season period (750 degree days >0°C). A whole year lasts 4000 degree days >0°C. The parameters for root growth and for pathogen activity have

already been determined through model fitting (Chapter 3) and are therefore not included in the subsequent model fitting process. The parameters that are included in this fitting process relate to the biocontrol agent and can be found in Tables 4.1 and 4.2. To assist with the model fitting, a single data point for infected roots was added at the final time point for seasons 11-20 to represent 20% of all roots being infected. The value of 20% was chosen because the proportion of infected roots after suppression from take-all decline is known to be similar to that in the first year that winter wheat is infected by take-all (Hornby, 1979, 1998; Pope and Hornby, 1973; Werker et al., 1991; Zogg and Jäggi, 1974), and this was determined to be 18% for the SIX model through the model fiting process (Chapter 3). Including this data increased the chance of disease plateauing at a low level as seen with take all-decline, rather than being completely eliminated from the system as was seen with initial fitting attempts.

4.5.2 Model fitting

The process of model fitting is the same as for the SIX model and is described in Section 3.5.2. However, the parameters that are included in the model fitting are different. There is also a variation in which parameters are included in the model fitting process depending on which mechanisms that the biocontrol agent can use to negatively impact the pathogen are included in the model. A description of the parameters included in all model variations can be found in Table 4.1. All additional mechanisms that can be incorporated into the SIXCA model are listed in Table 4.2 and are explained in more detail in Section 2.4. The difference between the parameters included in each model variation are listed in Table 4.3.

As the SIX model was only fitted to data from a single season of growing winter wheat (Chapter 3), no between-season dynamics were included in the model fitting. This means that the rate parameter τ_I, which represents the units of pathogen present on an infected root, had not been determined. This was therefore included in the rate parameters that

Table 4.1 List of parameters and definitions for the SIXCA model, where the biocontrol agent can only negatively affect the pathogen through competition for space on a plant's roots by primary (α_P) and secondary (α_S) colonisation. The initial amount of free-living pathogen (X_s) and biocontrol agent (A_s) present at the start of a simulation are fixed to simplify the model fitting problem and to reduce collinearity between the parameters included in the model fitting process. Parameters marked with an asterisk were obtained through prior model fitting in Chapter 3. The rate of decay of free-living pathogen (λ_X) was obtained from Bailey et al. (2005) and Bailey et al. (2009), and the rate of decay of free-living biocontrol agent (λ_A) was obtained from Elsas et al. (1986) and Weller (1983). Any parameters that do not have a default value will be determined in the subsequent model fitting process.

Parameter	Definition	Default value	Units
S	Number of susceptible roots	Variable	
I	Number of roots infected by the pathogen	Variable	
C	Number of roots colonised by the biocontrol agent	Variable	
X	Density of free-living pathogen	Variable	
A	Density of free-living biocontrol agent	Variable	
t	Time (degree days $> 3^{\circ}$C)	Variable	
X_s	Initial amount of free-living pathogen present at the start of the first growing season	1.00×10^{-1}	
A_s	Initial amount of free-living biocontrol agent present at the start of the first growing season	2.50×10^{-2}	
ρ	Rate of root production	3.31×10^{-3}*	t^{-1}
κ	Carrying capacity of root production	32.1*	
β_p	Rate of primary infection of roots by free-living pathogen	1.35×10^{-3}*	t^{-1}
β_s	Rate of secondary infection of roots	5.92×10^{-5}*	t^{-1}
λ_X	Rate of decay of pathogen inoculum	3.53×10^{-3}*	t^{-1}
τ_I	Number of root fragments produced from a dead infected root when the host crop is harvested	-	
α_p	Rate of primary colonisation of roots by free-living biocontrol agent	-	t^{-1}
α_s	Rate of secondary colonisation of roots	-	t^{-1}
λ_A	Rate of decay of free-living biocontrol agent	5.13×10^{-3}	t^{-1}
τ_C	Number of root fragments produced from a dead colonised root when the host crop is harvested	-	

were determined during this process of model fitting. All other parameters included in the model fitting are related to the biocontrol agent.

Initial model fitting attempts revealed that there was strong collinearity between parameters included in the model fitting. To reduce this, the rate of decay of the free-living

Table 4.2 List of parameters and definitions of additions to the SIXCA model of mechanisms where the biocontrol agent can negatively affect the pathogen. More information about these models can be found in Section 2.4.

Parameter	Definition	Units
ϵ_P	Proportionate reduction in the rate of primary infection of colonised roots compared to susceptible roots	
ϵ_S	Proportionate reduction in the rate of secondary infection of colonised roots compared to susceptible roots	
ψ_P	Rate of primary colonisation of infected roots by free-living biocontrol agent	t^{-1}
ψ_S	Rate of secondary colonisation of infected roots by colonised roots	t^{-1}
ω_P	Reduction in the rate of primary infection due to the free-living biocontrol agent	t^{-1}
ω_S	Reduction in the rate of secondary infection due to the free-living biocontrol agent	t^{-1}
η	Death rate of the pathogen on infected roots by the free-living biocontrol agent	t^{-1}
ϕ_η	Production of free-living biocontrol agent through consumption of pathogen present on infected roots	t^{-1}
ν	Increased decay rate of the free-living pathogen by the free-living biocontrol agent	t^{-1}
ϕ_ν	Production of free-living biocontrol agent through consumption of free-living pathogen in the soil	t^{-1}

biocontrol agent was fixed. A rate of decay for *Pseudomonas fluorescens*, the biocontrol agent believed to cause take-all decline (Cook, 2003; Kwak and Weller, 2013), could not be found in the literature. However, two papers did record its decay after being introduced to the rhizosphere of winter wheat plants (Elsas et al., 1986; Weller, 1983). Elsas et al. (1986) recorded the decay of *Pseudomonas fluorescens* over 120 days, whereas Weller (1983) recorded this decay over 240 days. Both papers reported a rapid decay of free-living material over time. Each set of data was separately fitted to an exponential decay curve,

$$\frac{dA}{dt} = -\lambda A, \tag{4.1}$$

where A is the amount of free-living biocontrol agent, and λ is the rate of decay. The initial amount of free-living biocontrol agent, A_s, was also included in the model fitting process as the winter wheat seeds were inoculated rather than the roots of already established plants. This meant that no recordings of the free-living biocontrol agent were taken in the first few days after planting, and it is impossible to establish how much free-living material

Table 4.3 Parameters included in each model variation of the SIXCA model.

	Parameters included in the model fitting													
Model variation	α_P	α_S	τ_I	τ_C	ω_P	ω_S	ϵ_P	ϵ_S	ψ_P	ψ_S	η	ϕ_η	ν	ϕ_ν
None	✓	✓	✓	✓	✘	✘	✘	✘	✘	✘	✘	✘	✘	✘
ω_P	✓	✓	✓	✓	✓	✘	✘	✘	✘	✘	✘	✘	✘	✘
ω_S	✓	✓	✓	✓	✘	✓	✘	✘	✘	✘	✘	✘	✘	✘
ϵ_P	✓	✓	✓	✓	✘	✘	✓	✘	✘	✘	✘	✘	✘	✘
ϵ_S	✓	✓	✓	✓	✘	✘	✘	✓	✘	✘	✘	✘	✘	✘
ψ_P	✓	✓	✓	✓	✘	✘	✘	✘	✓	✘	✘	✘	✘	✘
ψ_S	✓	✓	✓	✓	✘	✘	✘	✘	✘	✓	✘	✘	✘	✘
η	✓	✓	✓	✓	✘	✘	✘	✘	✘	✘	✓	✘	✘	✘
η and ϕ_η	✓	✓	✓	✓	✘	✘	✘	✘	✘	✘	✓	✓	✘	✘
ν	✓	✓	✓	✓	✘	✘	✘	✘	✘	✘	✘	✘	✓	✘
ν and ϕ_ν	✓	✓	✓	✓	✘	✘	✘	✘	✘	✘	✘	✘	✓	✓

material survived until the wheat plant roots began to grow. Time was converted from days to degree days $>0^\circ$C so that the obtained parameter values could be directly used in the subsequent model fitting. The data is visualised in Figure 4.4, with the parameters obtained through model fitting (Table 4.4) used to plot the two lines. The rate of decay for both data sets was determined to be very similar ($5.10 \times 10^{-3}\ t^{-1}$ for Elsas et al. (1986) and $5.16 \times 10^{-3}\ t^{-1}$ for Weller (1983)). The mean of these two values, $5.13 \times 10^{-3}\ t^{-1}$, is used as the fixed value for the rate of decay in all subsequent modelling work.

The initial amount of free-living biocontrol agent, A_s, to be used in subsequent model fitting is not taken from the values in Table 4.4. However, this initial amount is fixed for each model variations due to initial work finding strong collinearity between it and other parameters included in the model fitting process, as well as no data collected on this free-living material. Fixing the initial amount of free-living material was also required when fitting the SIX model to data from Werker et al. (1991), where the initial amount of free-living pathogen, X_s, was fixed at 0.1 (Section 3.5). The value for the initial amount of free-living biocontrol agent at the start of the first season was chosen so that the amount of free-living pathogen and biocontrol agent are scaled similarly. This value could be fixed

at different values across variations of the SIXCA model depending on which value scaled best to the amount of free-living pathogen.

Table 4.4 Values for the rate of decay and initial amount of free-living biocontrol agent *Pseudomonas fluorescens* when introduced into the rhizosphere of winter wheat plants. Data was obtained from Elsas et al. (1986) and Weller (1983), and an exponential decay function was fitted separately to the two data sets, where both the rate of decay and the starting amount of *Pseudomonas fluorescens* were included in the fitting.

	Value obtained through model fitting	
Parameter	Elsas et al. (1986)	Weller (1983)
λ	$5.16 \times 10^{-3}\ t^{-1}$	$5.10 \times 10^{-3}\ t^{-1}$
A_s	4.64×10^{7}	4.09×10^{6}

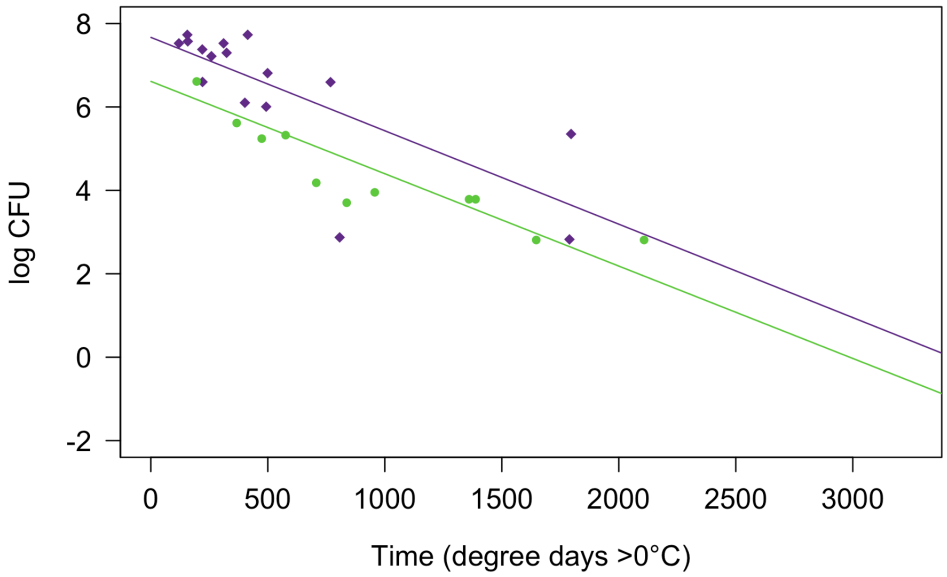

Fig. 4.4 Rate of decay of *Pseudomonas fluorescens* when introduced into the rhizosphere of winter wheat plants. Data shown by purple diamonds is from Elsas et al. (1986) and data shown by green circles is from Weller (1983). The two data sets are fitted separately to an exponential decay function, where both the rate of decay and the starting amount of *Pseudomonas fluorescens* are included in the fitting. The fitted parameter values can be found in Table 4.4.

Each of the biocontrol mechanisms is included in the model fitting separately, apart from 1) η and ϕ_η, and 2) ν and ϕ_ν. While a biocontrol mechanism is included in the

model, all other mechanisms are removed from the model (Table 4.3). It was assumed that this fitting problem would be more complex than for the SIX model, and therefore the model fitting process was performed 50,000 times for each variation of the SIXCA model, using different sets of initial parameter values each time. The biologically feasible values of these parameters were unknown and were therefore chosen from a significantly wider range of values than the hypothesised feasible parameter limits. These limits can be found in Table 4.5.

Table 4.5 Range of values that initial parameter values were chosen from when fitting different variations of the SIXCA model to the data in Werker et al. (1991). These different variations vary in the mechanisms included that the biocontrol agent can used to negatively affect the pathogen. All model variations include the parameters marked with ˆ.

Parameter	Lower bound	Upper bound
$\alpha_P\hat{}$	0	1
$\alpha_S\hat{}$	0	1
$\tau_I\hat{}$	0	100
$\tau_C\hat{}$	0	100
ω_P	0	100
ω_S	0	100
ϵ_P	0	1
ϵ_S	0	1
ψ_P	0	100
ψ_S	0	100
η	0	1
ϕ_η	0	100
ν	0	1
ϕ_ν	0	100

4.5.3 Which mechanisms cause take-all decline to occur?

There are multiple mechanisms that biocontrol agents can use to negatively affect a pathogen. However, biocontrol agents will often have a single main mode of suppression (Narayanasamy, 2013; Nega, 2014; Whipps, 2001; Xu et al., 2011; Xu and Jeger, 2013a).

Take-all decline is believed to be caused by the biocontrol agent 2,4-DAPG fluorescent *Pseudomonas* spp. If this is the case, it is likely that not all of the mechanisms included in the model variations will be effective at suppressing take-all disease, as they would not all be used by this biocontrol agent in the real-world. It may also be the case that the model with no additional mechanisms included is able to cause take-all decline through only competition for space on the crop roots. If this is so, the additional mechanism may become redundant and not help to suppress the pathogen, or they may work alongside competition to cause suppression.

Whether a model is able to cause take-all decline can be seen through how well the model is able to fit to the data (determined by how high the log likelihood value is), as well as visualisation of the model dynamics from a simulation of the model using the parameter values obtained through model fitting. However, it is more difficult to determine whether certain models fit to the data significantly better than others, and whether including an additional biocontrol mechanism improves the fit of the model over competition alone. In order to do this, the Aikake Information Criteria (AIC) was used, which allows models to be compared based on the number of parameters in the model and how well these models fit to the data (Akaike, 1973; Arnold, 2010; Bolker, 2008). Calculating an AIC value requires two pieces of information: 1) the number of parameters in the model, and 2) the log likelihood of the model fit to the data. The calculation is

$$\text{AIC} = -2(\text{log-likelihood}) + 2n_{par}, \tag{4.2}$$

where n_{par} is the number of parameters in the fitted model. A low AIC is desired, which is obtained through having as few parameters as possible and being able to fit the model closely to the data. If the AIC of a model with an additional parameter included does not have an AIC value of at least two lower than the model without this parameter included, this parameter is deemed to not significantly improve the ability of the model to fit to the

data (Burnham and Anderson, 2003). This will allow for all biocontrol mechanisms to be evaluated, and their ability to fit to the data analysed.

4.5.4 Analysing the model fitting output

The parameter values that were obtained from model fitting were used to simulate a trajectory of each model. This allowed for the number of susceptible, infected, and colonised roots, as well as the amount of free-living pathogen and biocontrol agent, to be visually seen. If there was no observable peak of disease followed by pathogen suppression over several consecutive years, the model variation was determined to not be able to cause take-all decline. Likewise, only model variations that had significantly lower (with a difference of >2) AIC values to the model with no additional biocontrol mechanisms included, were further analysed. The analysis carried out is the same as for the SIX model, which is described in Section 3.5.3. This includes examining collinearity values, obtaining 95% confidence intervals, and examining the model fitting landscape. As more than two parameters were included in the model fitting, the fitting landscape was calculated using principal component analysis in the *factoextra* (Kassambara and Mundt, 2020) and *FactoMine* (Le et al., 2008) packages. This allowed for an examination of the variation between all the parameter values on two axes, where PCA creates axes that show the highest variance in the data. The two axes that capture the most variance in the data are plotted on the x- and y-axes.

The PCA took into account all of the parameter values involved in the model fitting process, and each set of values can be plotted as a single point on a plot with the above PCA axes. Model fitting solutions that are closer together on the plot should have similar rate parameter values. By plotting all of these solutions, and relating them to their log likelihood values, the fitting landscape can be analysed. Any local optima can be identified, as well as how clustered or spread out the points are that compose the global optimum.

For these plots, the *x*- and *y*- coordinates were the results from the principal component analysis, and the individual points are coloured based on their log likelihood values.

4.6 Results

4.6.1 The SIX model

Most parameter values for the SIX model had been determined through previous model fitting work in Chapter 3. However, this work only focused on the dynamics during a single season where winter wheat infected by take-all was grown. The parameter τ_I, which is only involved in the dynamics between growing seasons, was therefore not estimated. This parameter was instead estimated during this later stage of model fitting, and has a different value for each of the model variations. A simulations of the SIX model, showing the range of trajectories that can be produced as τ_I is varied between the minimum and maximum values in Table 4.6 is produced (Figure 4.5). For each value of τ_I, the number of infected roots and the amount of free-living pathogen reaches a maximum value in the third growing season. After this, the model trajectory is the same for all consecutive years.

4.6.2 Model fitting

The model fitting process was performed 50,000 times for each of the 11 model variations, using randomly selected parameter values within the ranges found in Table 4.5. The fit that maximised the log likelihood for each model is shown in Table 4.6. The greatest log likelihood value was obtained was when both η and ϕ_η were included in the model (-224).

Using the parameter values from Table 4.6 to run simulations of the SIXCA model variations over 12 years produces the model trajectories seen in Figures 4.6, 4.7, 4.8, and 4.9. Each simulation is split into two plots – one that shows the crop roots and one that shows the free-living pathogen and biocontrol agent. The amount of free-living pathogen

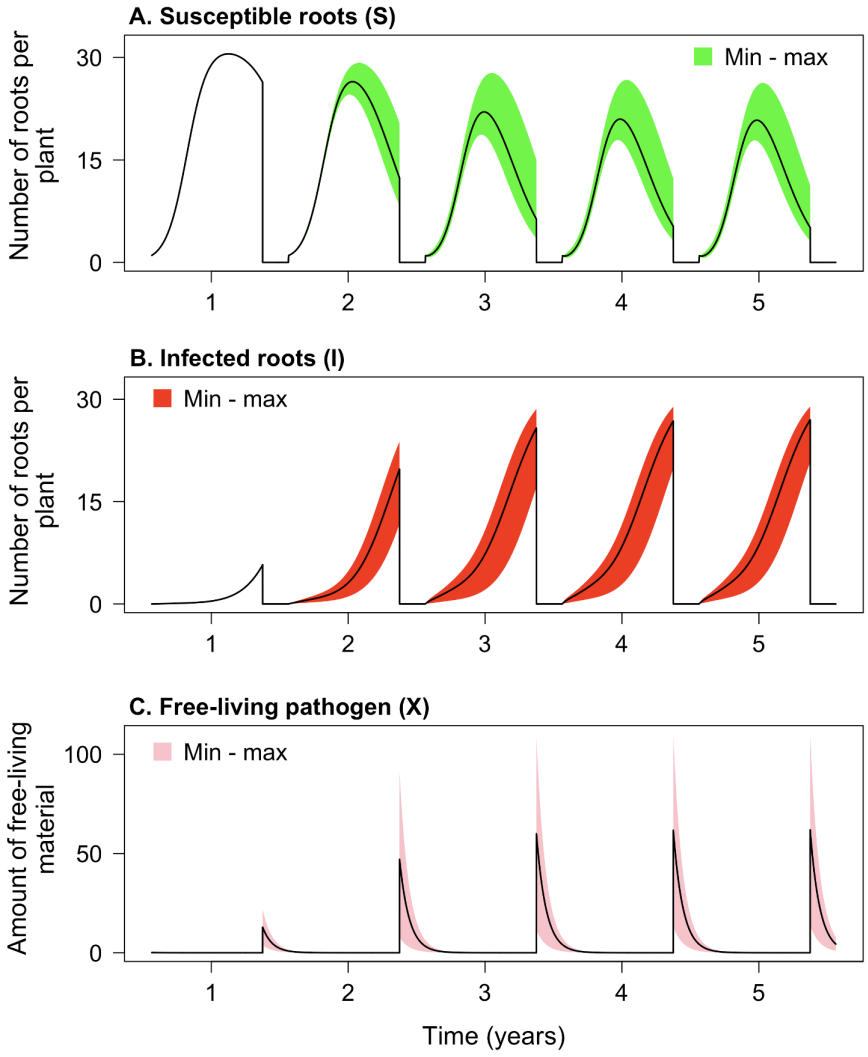

Fig. 4.5 Simulation of the SIX model over five years for values of τ_I between 0.663 - 3.80. This range of values represents the minimum and maximum values of τ_I when different variations of the SIXCA model was fitted to data from Werker et al. (1991). All the values for τ_I can be found in Table 4.6.

Table 4.6 Parameter values obtained through fitting variations of the SIXCA model to data over ten years of consecutively growing winter wheat infected by take-all disease. Maximum likelihood model fitting was used. The eleven models vary in the additional mechanism included that the biocontrol agent can use to negatively affect the pathogen, with all models including primary and secondary colonisation. Data was obtained from Werker et al. (1991). For each model, 50,000 fitting simulations were performed using random initial parameter values within the bounds found in Table 4.5. Out of these simulations, the one that produced the set of parameters that best fit to the data are given in this table. The value of the standard deviation (σ) calculated as part of the maximum likelihood model fitting process was 2.06 for the model with no additional mechanisms included or with ω_P, ω_S, ϵ_P, ϵ_S, η or ν included, 2.00 with ψ_P included, 1.99 with ψ_S included, 1.93 with η and ϕ_η included, and 1.94 with ν and ϕ_ν included.

Biocontrol	Parameters include in the model fitting							
mechanism	α_P (t^{-1})	α_S (t^{-1})	τ_I	τ_C	A_s	Mechanism 1	Mechanism 2	LL
None	5.39×10^{-2}	2.18×10^{-5}	3.16	3.14	2.5×10^{-2}	-	-	-232
ϵ_P	2.85×10^{-1}	2.67×10^{-5}	1.23	5.22×10^{-1}	1×10^{-3}	1.00 (ϵ_P)	-	-231
ϵ_S	5.38×10^{-2}	2.18×10^{-5}	3.15	3.15	2.5×10^{-2}	4.28×10^{-9} (ϵ_S)	-	-232
ω_P	5.55×10^{-2}	2.32×10^{-5}	3.52	2.57	2.5×10^{-2}	4.17 t^{-1} (ω_P)	-	-231
ω_S	5.30×10^{-2}	2.20×10^{-5}	3.11	3.14	2.5×10^{-2}	4.32×10^{-6} t^{-1} (ω_S)	-	-232
ψ_P	1.99×10^{-5}	1.01×10^{-4}	6.80×10^{-1}	5.42×10^{-1}	5×10^{-4}	3.59×10^{-2} t^{-1} (ψ_P)	-	-228
ψ_S	1.07×10^{-3}	5.42×10^{-5}	6.87×10^{-1}	1.56	4×10^{-3}	1.54×10^{-4} t^{-1} (ψ_S)	-	-227
η	5.87×10^{-2}	2.33×10^{-5}	3.80	2.42	2.5×10^{-2}	2.99×10^{-2} t^{-1} (η)	-	-231
η and ϕ_η	7.94×10^{-6}	2.47×10^{-4}	6.68×10^{-1}	5.68×10^{-9}	2.5×10^{-9}	4.39×10^{-9} t^{-1} (η)	3.38×10^{5} t^{-1} (ϕ_η)	-224
ν	5.43×10^{-2}	2.17×10^{-5}	3.18	3.16	2.5×10^{-5}	1.08×10^{-5} t^{-1} (ν)	-	-232
ν and ϕ_ν	2.98×10^{-6}	1.74×10^{-4}	6.63×10^{-1}	5.37×10^{-1}	8×10^{-10}	2.88×10^{-9} t^{-1} (ν)	7.48×10^{5} t^{-1} (ϕ_ν)	-225

before a subsequent decline and plateauing of disease severity at a lower level across several years. This is representative of take-all decline.

Across all model variations, the amount of free-living pathogen initially starts at a low level and gradually peaks after the season where disease severity is highest. This then reduces and remains at a lower level for all subsequent seasons. Between crop growing seasons, there is a sharp decay in free-living pathogen and free-living biocontrol agent, resulting in very little present in the soil by the end of each growing season. This was due to the fixed rates of decay for the free-living pathogen and biocontrol agent included into the models. However, the units of free-living pathogen produced from dead infected roots, and the units of free-living biocontrol agent produced from dead colonised roots, after harvest (determined by the rate parameters τ_I and τ_C, respectively) is high enough to result in a spike and reintroduction of new material each year.

For all but the models that include either η and ϕ_η (Figure 4.9A), or ν and ϕ_ν (Figure 4.9B), the only way that free-living biocontrol agent can be produced is through this end of growing season transition. However, these two models can also produce free-living biocontrol agent through interactions with the pathogen. For the model including η and ϕ_η, this can only happen within a growing season as the free-living biocontrol agent attacks infected roots and bulks up from this interaction. For the model including ν and ϕ_ν, this can happen both within and between growing seasons as the free living biocontrol agent attacks free-living pathogen and bulks up from this interaction. Unlike all other models, where the peak of free-living material is at the end of each growing season, the model that includes ν and ϕ_ν has a later peak occurring between harvesting and replanting. This is due to the bulk up of the biocontrol agent from interacting with the free-living pathogen during this period of time.

The amount of colonised roots is always low in the first season and gradually increases for each subsequent season, before plateauing at a higher level. The number of colonised

roots at the end of a growing season was always greater than the number of infected roots once this plateau has been reached, irregardless of model variation. The amount of free-living biocontrol agent is initially low for the first few seasons and gradually increases every season, before plateauing at a level that is often higher than that for the free-living pathogen. For most models (Figure 4.6A-C, 4.7A-B, and 4.8B-C), the amount of free-living biocontrol agent reaches its highest level once this plateau has been reached. However, for four of the models (Figure 4.7C, Figure 4.8A, and Figure 4.9A-B), the amount of free-living biocontrol agent peaks in an earlier year before plateauing at a lower level. This peak is especially prominent when the model includes either η and ϕ_η (Figure 4.9A), or ν and ϕ_ν (Figure 4.9B).

The area under the disease progress curves (AUDPC) for the same model simulations as seen in Figures 4.6, 4.7, 4.8 and 4.9 can be found in Figure 4.10. These are simulated over 100 growing seasons. All but the model that includes η and ϕ_η (Figure 4.10i) have reached a plateau within the first 50 years. The AUDPC values for the years after the plateau are higher than for the first year of the simulations, irregardless of model variation. This is reflective of previous work that has found that disease severity after take-all decline has occurred is similar or higher to levels of those seen in the first year of an epidemic (Cook, 2003).

4.6.3 Identification of the mechanisms that can cause take-all decline

Using the values from Table 4.6, all model variations had a visible pattern of take-all decline (Figures 4.6, 4.7, 4.8, and 4.9). It was therefore possible that the additional mechanism that the biocontrol agent can used to negatively affect the pathogen that was incorporated into each model variation was not required by the model to fit to the data and show a trend of take-all decline. There was therefore a need to determine how incorporating each

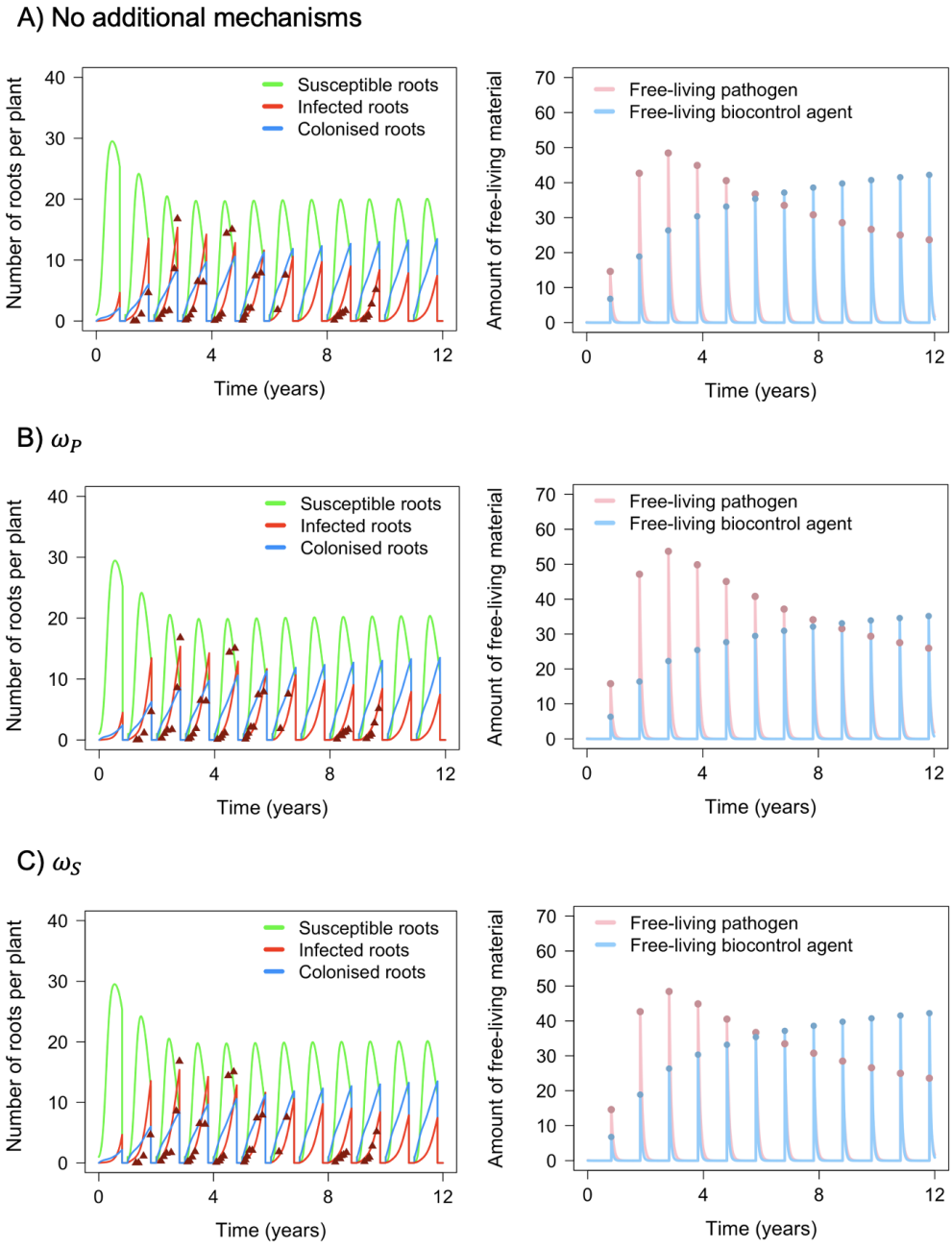

Fig. 4.6 Simulations of the SIXCA model with different biocontrol mechanisms included, run over 12 years using the parameter values found in Table 4.6. Data (red triangles) was obtained from field experiments carried out over 10 consecutive years, where winter wheat infected by take-all decline was grown (Werker et al., 1991). The left plots show the number of roots, whether susceptible (green line), infected by the pathogen (red line), or colonised by the biocontrol agent (blue line). The right plot shows the amount of free-living pathogen (pink) and biocontrol agent (light blue).

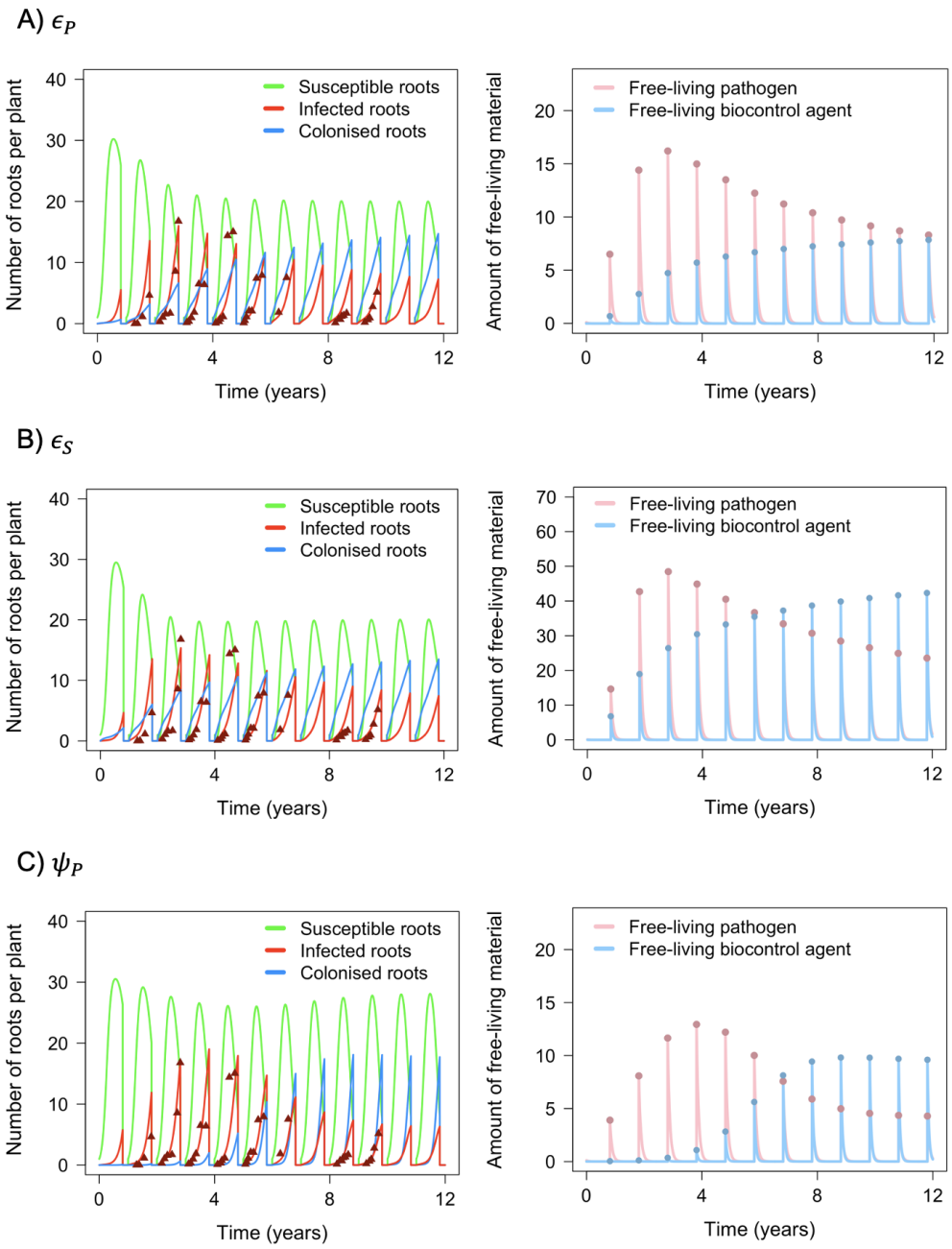

Fig. 4.7 Simulations of the SIXCA model with different biocontrol mechanisms included, run over 12 years using the parameter values found in Table 4.6. Data (red triangles) was obtained from field experiments carried out over 10 consecutive years, where winter wheat infected by take-all decline was grown (Werker et al., 1991). The left plots show the number of roots, whether susceptible (green line), infected by the pathogen (red line), or colonised by the biocontrol agent (blue line). The right plot shows the amount of free-living pathogen (pink) and biocontrol agent (light blue).

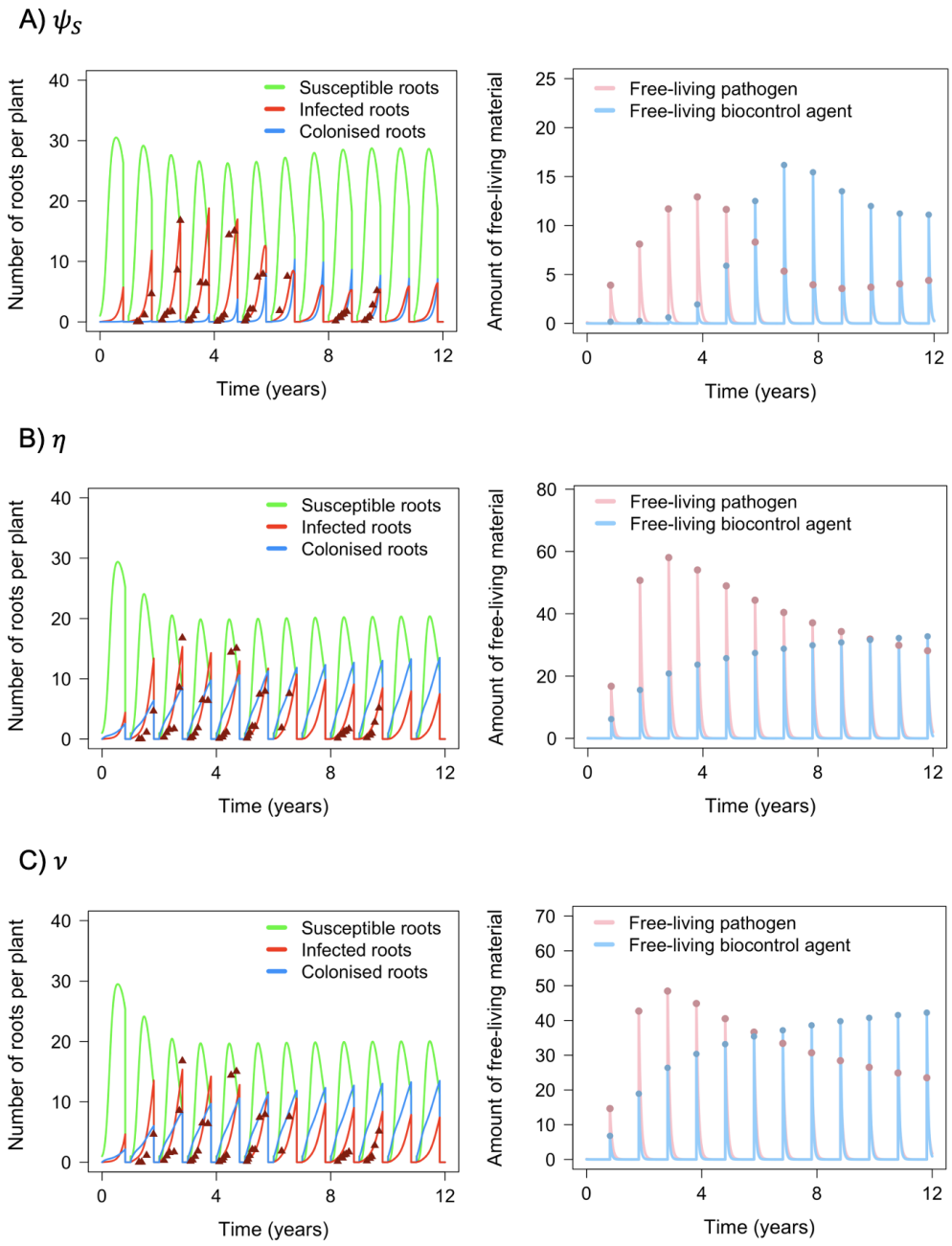

Fig. 4.8 Simulations of the SIXCA model with different biocontrol mechanisms included, run over 12 years using the parameter values found in Table 4.6. Data (red triangles) was obtained from field experiments carried out over 10 consecutive years, where winter wheat infected by take-all decline was grown (Werker et al., 1991). The left plots show the number of roots, whether susceptible (green line), infected by the pathogen (red line), or colonised by the biocontrol agent (blue line). The right plot shows the amount of free-living pathogen (pink) and biocontrol agent (light blue).

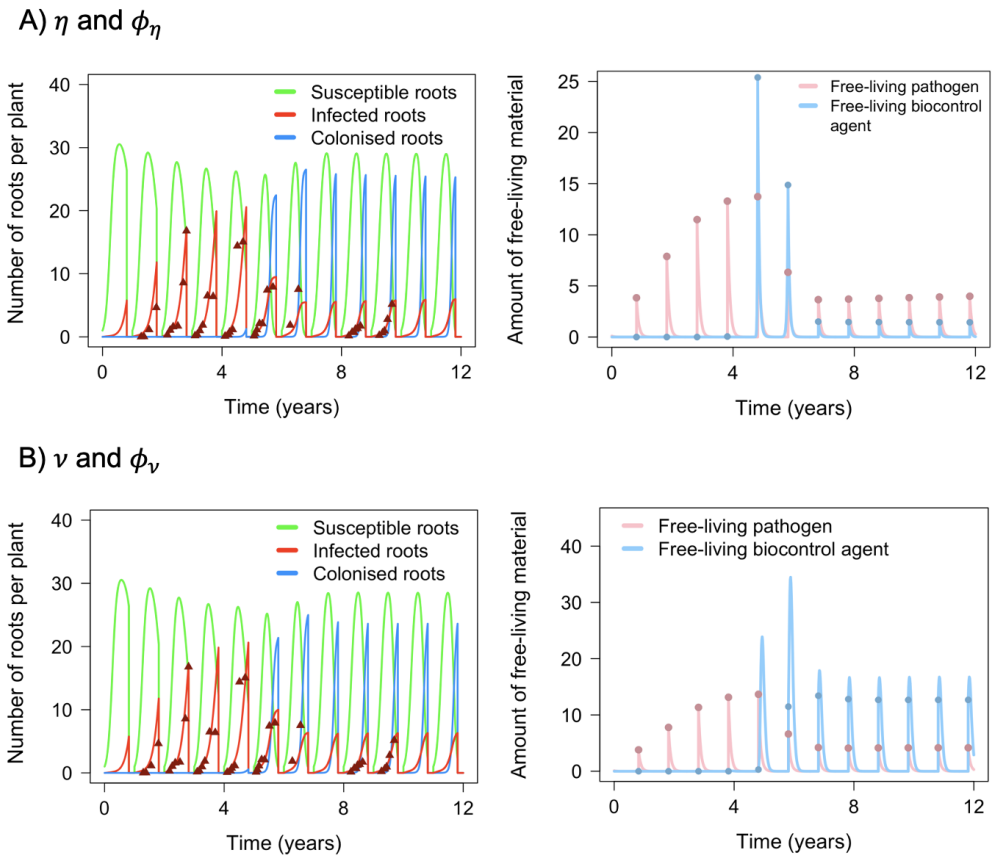

Fig. 4.9 Simulations of the SIXCA model with different biocontrol mechanisms included, run over 12 years using the parameter values found in Table 4.6. Data (red triangles) was obtained from field experiments carried out over 10 consecutive years, where winter wheat infected by take-all decline was grown (Werker et al., 1991). The left plots show the number of roots, whether susceptible (green line), infected by the pathogen (red line), or colonised by the biocontrol agent (blue line). The right plot shows the amount of free-living pathogen (pink) and biocontrol agent (light blue).

mechanism improved the fit of the model to the data, and whether the model could still fit well to the data without this additional mechanism. If the model could still fit well to the data without this mechanism, it could be discarded as one of the potential mechanisms involved in take-all decline, at least for this data set. It is possible to examine this to an extent by looking at the parameter values for each mechanism in Table 4.6. If a parameter value is close to 0, it is unlikely to have a significant impact on the model dynamics.

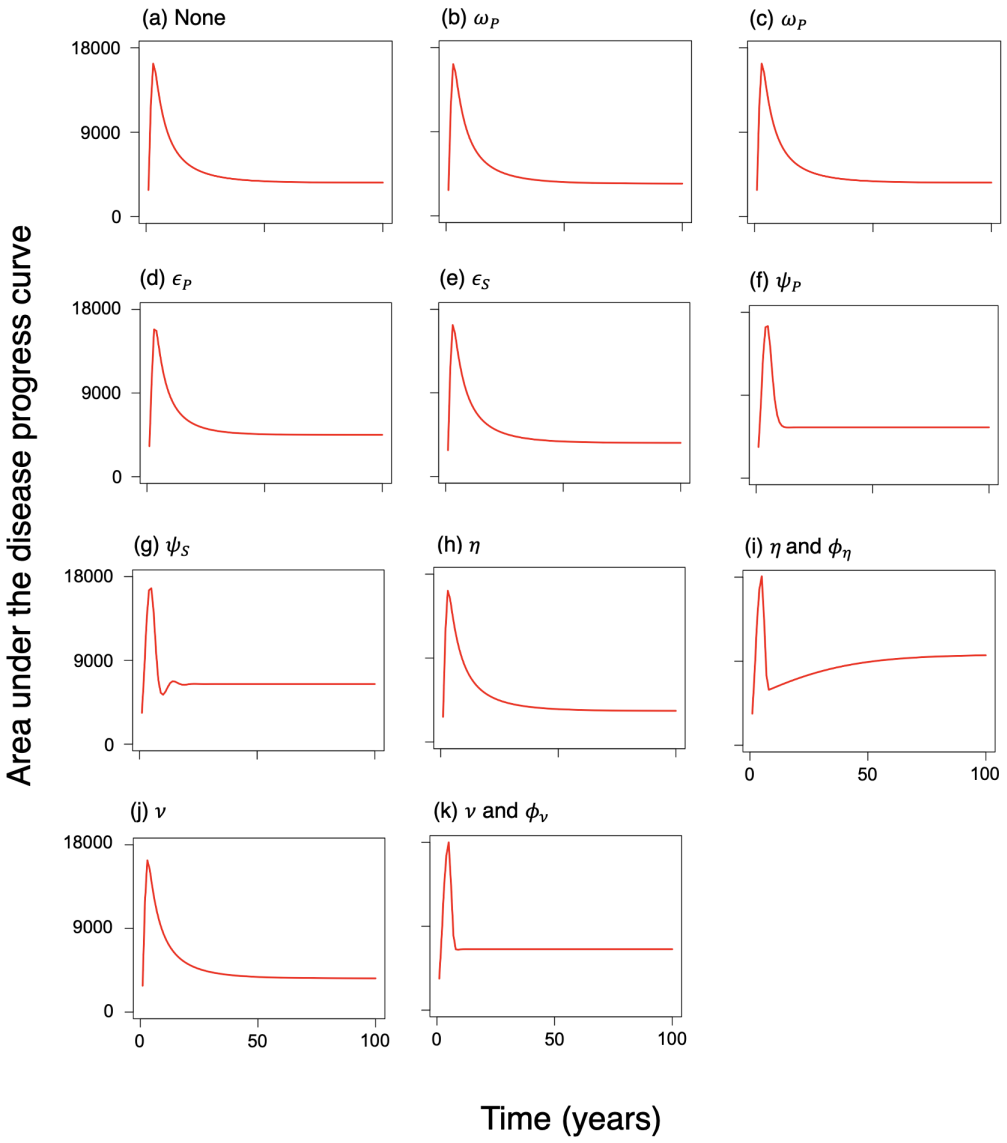

Fig. 4.10 Area under the disease progress curve for 100 growing seasons of a model simulation for each of the SIXCA model variations using the parameters values found in Table 4.6.

However, a more analytical way to do this is to compare the AIC values of each model. If a model variation has an AIC value at least two less than the model with no additional mechanisms included, it can be determined that there is a significant improvement of the model to fit to the data. Calculating the AIC values of each model variation found no significant improvement of the model fitting to the data when the mechanisms ω_P, ω_S, ϵ_P,

ϵ_S, η (without ϕ_η), or ν (without ϕ_ν) were included (Table 4.7). The models that included ψ_P, ψ_S, η and ϕ_η, or ν and ϕ_ν all had AIC values that were at least two less than the model with no additional mechanisms included, showing that including these mechanisms significantly improved the ability for the model to fit to the data. These model variations are shown in grey.

Table 4.7 Negative log likelihood (-LL) values and Akaike information criterion (AIC) for each of the SIXCA model variations using the parameters found in Tables 4.6. The model with no additional mechanisms included, as well as any model variations that have an AIC value at least 2 less than this model, are highlighted in grey.

Biocontrol mechanism	-LL	AIC
η and ϕ_η	-224.4	462.8
ν and ϕ_ν	-224.6	463.3
ψ_S	-227.4	466.9
ψ_P	-228.1	468.2
No additional mechanisms	-231.5	473.0
ϵ_P	-231.2	474.5
η	-231.4	474.8
ω_P	-231.5	474.9
ω_S	-231.5	475.0
ϵ_S	-231.5	475.0
ν	-231.5	475.0

4.6.4 Analysis of the mechanisms that can cause take-all decline

Five models were chosen to analyse further based on the previous research: 1) no additional biocontrol mechanisms included, 2) ψ_P included, 3) ψ_S included, 4) η and ϕ_η included, and 5) ν and ϕ_ν included. The collinearity values for each of these models can be found in Tables 4.8 and 4.9. For the model with no additional biocontrol mechanisms included (Table 4.8a), the collinearity value for the full model was 29.8. This is over the threshold value of

20, suggesting that the model may not be identifiable. Removal of a single parameter has minimal effect on the collinerity value, and it never drops below 20.

The four other models all have collinearity values of 102 or greater when all parameters are included in the model fitting. These are extremely high values and suggest that the models are not identifiable and that there may be multiple parameter values that can produce a similar fit to the data. This is especially the case for the model that includes η and ϕ_η (Table 4.9a), which has a collinearity value of 461 when all parameters are included in the model fitting. Dropping a single parameter was not able to reduce the collinearity value to less than 20 for any of the models apart from if ψ_P was dropped from its model. In this case, the collinearity value for the model dropped down to 18.0.

These results show that the amount of data in Werker et al. (1991) is not enough to easily fit to the SIXCA model. Additional data points, or information about the biocontrol agent either on the roots of a plant or free-living in the soil, would be likely to result in lower collinearity values. It would also be useful to know information about the potential bounds of these parameters, or be able to remove at least one parameter from the model fitting and fix it at a specific value.

Over the 50,000 simulations for each model variation, the log likelihood values were examined (Figure 4.11). Most of the simulations did not converge on a high log likelihood value, with the initial parameters causing the model to often not fit well to the data set. This problem could be reduced by having more knowledge about the parameter bounds so that tighter limits can be imposed. The model with no additional mechanisms included had the greatest number of solutions that converged on a high log likelihood value.

The variation in log likelihood values across the solutions is further visualised using principal components analysis (PCA), where similar sets of parameter values will be grouped more closely together. This can allow for any local optima to be detected. Only solutions with a log likelihood value of greater than -300 were examined so that there can be a focus

Table 4.8 Collinearity values for the SIXCA model with (a) no additional biocontrol mechanisms included, (b) mechanism ψ_P included, and (c) mechanism ψ_S included. The parameters used can be found in Table 4.6, and these were obtained through fitting to data from Werker et al. (1991). Data was obtained from field experiments carried out over ten consecutive years, where winter wheat infected by take-all decline was grown. The full model, and all variations of the model where one parameter value is excluded from the model fitting process, are shown.

(a) No additional biocontrol mechanisms included

α_P	α_S	τ_I	τ_C	Number of parameters	Collinearity value
✓	✓	✓	✓	4	29.8
✓	✓	✓	✘	3	27.7
✓	✓	✘	✓	3	28.3
✓	✘	✓	✓	3	28.7
✘	✓	✓	✓	3	28.9

(b) Mechanism ψ_P included

α_P	α_S	τ_I	τ_C	ψ_P	Number of parameters	Collinearity value
✓	✓	✓	✓	✓	5	154
✓	✓	✓	✓	✘	4	18.0
✓	✓	✓	✘	✓	4	42.2
✓	✓	✘	✓	✓	4	113
✓	✘	✓	✓	✓	4	27.0
✘	✓	✓	✓	✓	4	37.7

(c) Mechanism ψ_S included

α_P	α_S	τ_I	τ_C	ψ_S	Number of parameters	Collinearity value
✓	✓	✓	✓	✓	5	102
✓	✓	✓	✓	✘	4	32.2
✓	✓	✓	✘	✓	4	90.4
✓	✓	✘	✓	✓	4	92.0
✓	✘	✓	✓	✓	4	40.0
✘	✓	✓	✓	✓	4	29.6

Table 4.9 Collinearity values for the SIXCA model with (a) mechanisms η and ϕ_η included, and (b) mechanisms ν and ϕ_ν included. The parameters used can be found in Table 4.6, and these were obtained through fitting to data from Werker et al. (1991). Data was obtained from field experiments carried out over ten consecutive years, where winter wheat infected by take-all decline was grown. The full model, and all variations of the model where one parameter value is excluded from the model fitting process, are shown.

(a) Mechanisms η and ϕ_η included

α_P	α_S	τ_I	τ_C	η	ϕ_η	Number of parameters	Collinearity value
✓	✓	✓	✓	✓	✓	6	461
✓	✓	✓	✓	✓	✘	5	382
✓	✓	✓	✓	✘	✓	5	447
✓	✓	✓	✘	✓	✓	5	358
✓	✓	✘	✓	✓	✓	5	437
✓	✘	✓	✓	✓	✓	5	54.2
✘	✓	✓	✓	✓	✓	5	50.3

(b) Mechanisms ν and ϕ_ν included

α_P	α_S	τ_I	τ_C	ν	ϕ_ν	Number of parameters	Collinearity value
✓	✓	✓	✓	✓	✓	6	368
✓	✓	✓	✓	✓	✘	5	104
✓	✓	✓	✓	✘	✓	5	350
✓	✓	✓	✘	✓	✓	5	74.8
✓	✓	✘	✓	✓	✓	5	357
✓	✘	✓	✓	✓	✓	5	273
✘	✓	✓	✓	✓	✓	5	60.4

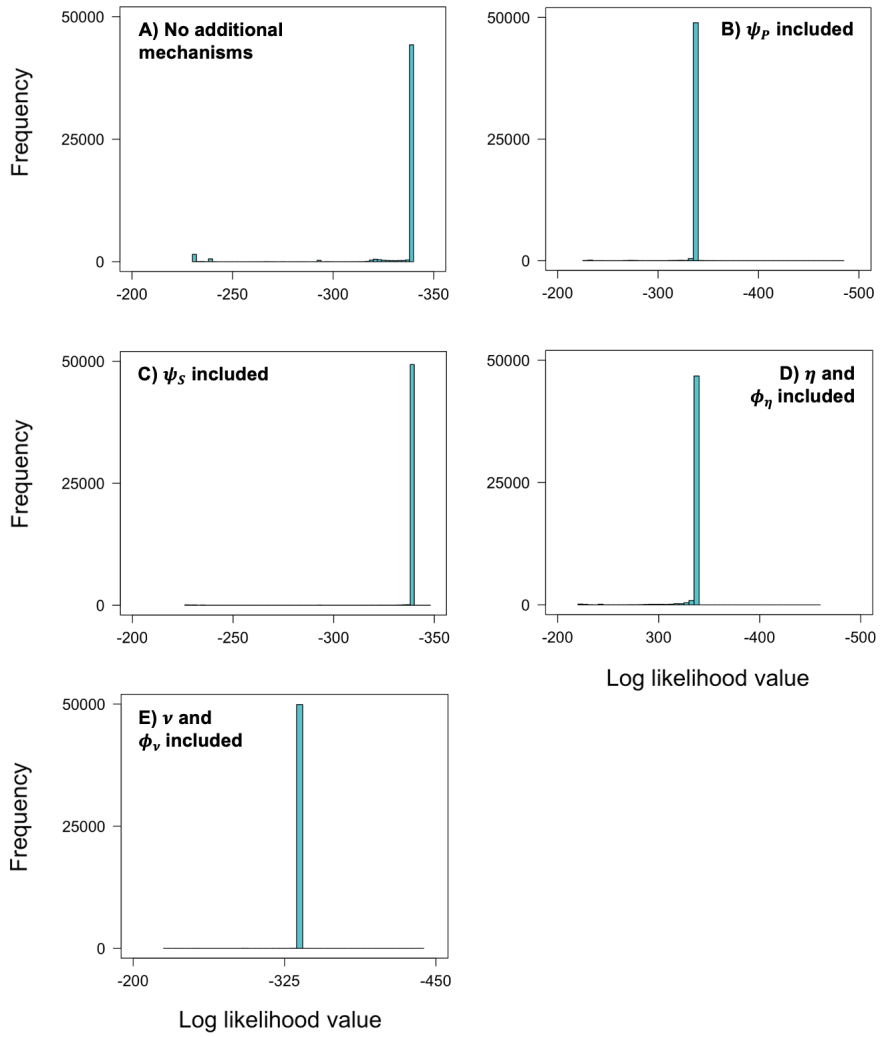

Fig. 4.11 Variation in the log likelihood values for 50,000 model fitting simulations and five model variations of the SIXCA model. Data was obtained from Werker et al. (1991) and focuses on the percentage of infected roots across ten growing seasons for winter wheat.

on local optima that fit reasonably well to the data, discarding any results with very low log likelihood values. All of the model variations have multiple local optima, with many peaks separated across the two PCA dimensions (Figures 4.12 and 4.13). This suggests that the identification of a definite global optimum will be difficult, and that there may be several sets of parameters that are able to fit reasonably well to the data.

Despite high collinearity values and multiple local optima, all parameters in the models where A) no additional biocontrol mechanisms are included, and B) mechanism ψ_S is included, had identifiable upper and lower confidence intervals (Table 4.10 and Figure 4.14). The model where mechanism ψ_P is included had identifiable upper and lower confidence intervals for all parameters but α_P, where it had an infinite lower bound. This suggests that α_P could be removed from the model and would not affect the ability for the model to fit to the data. This model has two ways to colonise roots through primary colonisation, where either susceptible roots (at rate α_P) or infected roots (at rate ψ_P) can be colonised by free-living biocontrol agent. This has made α_P redundant as primary colonisation now only occurs to already infected roots. The confidence intervals found here give a range of values that can produce a similar fit to the data, with the model with no additional mechanisms included having the narrowest range of values on average.

Confidence intervals could not be determined for the models that include either η and ϕ_η, or ν and ϕ_ν. This is likely due to the very high collinearity values between parameters (Table 4.9).

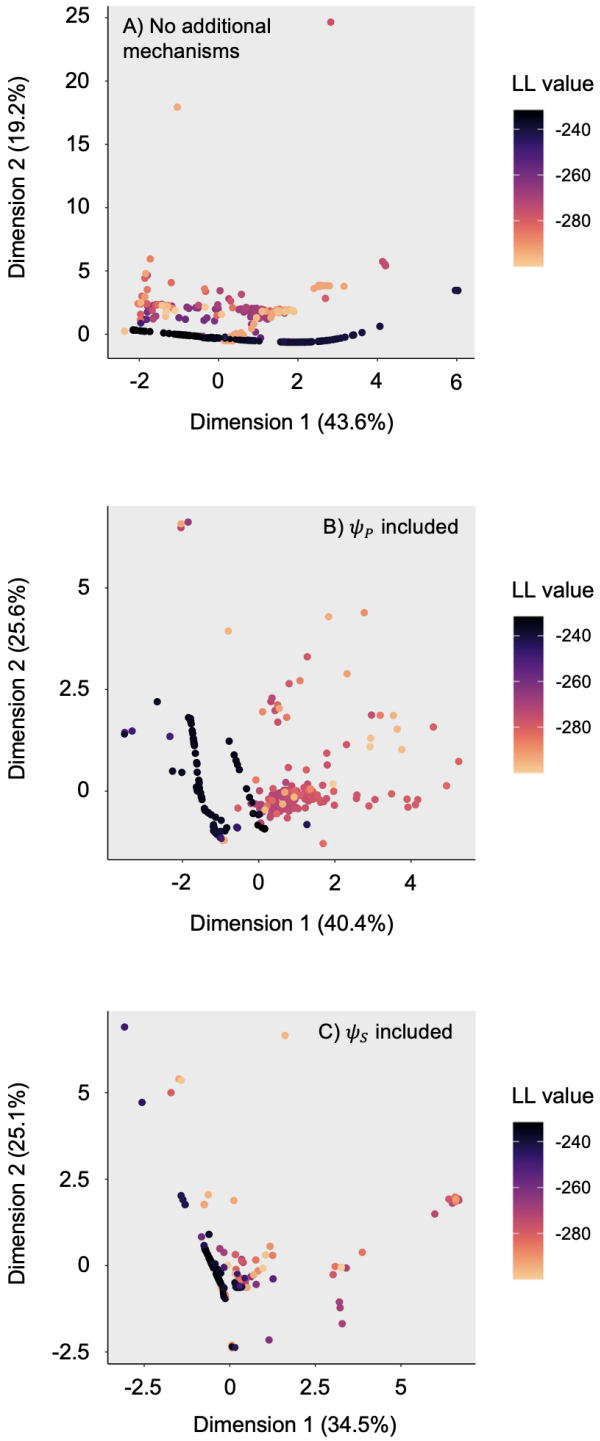

Fig. 4.12 Visualisation of all model fitting solutions with a log likelihood (LL) value of greater than -300 using principal component analysis for variations of the SIXCA model with A) no additional biocontrol mechanisms included, B) mechanism ψ_P included, and C) mechanism ψ_S included

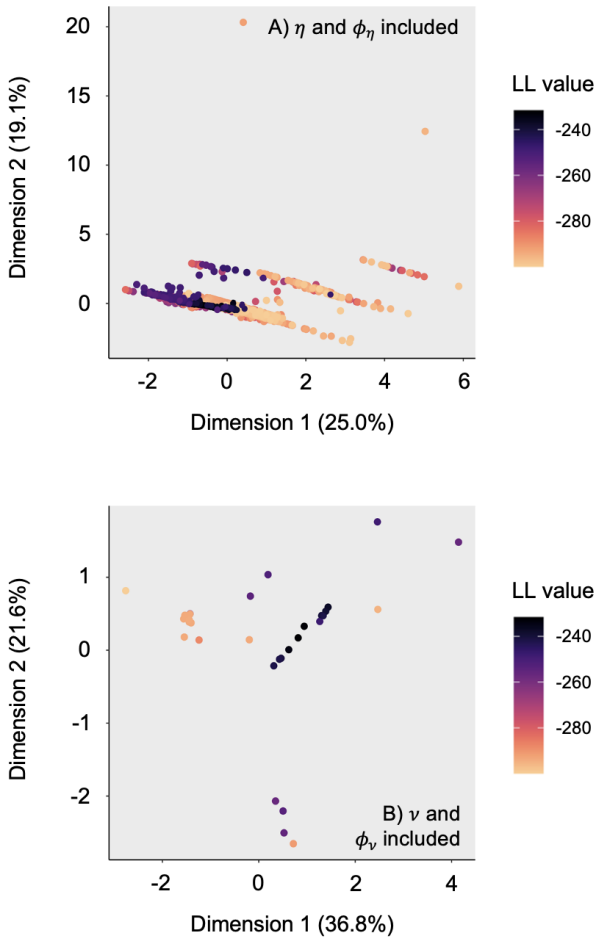

Fig. 4.13 Visualisation of all model fitting solutions with a log likelihood (LL) value of greater than -300 using principal component analysis for variations of the SIXCA model with A) mechanisms η and ϕ_η included, and B) mechanisms ν and ϕ_ν included

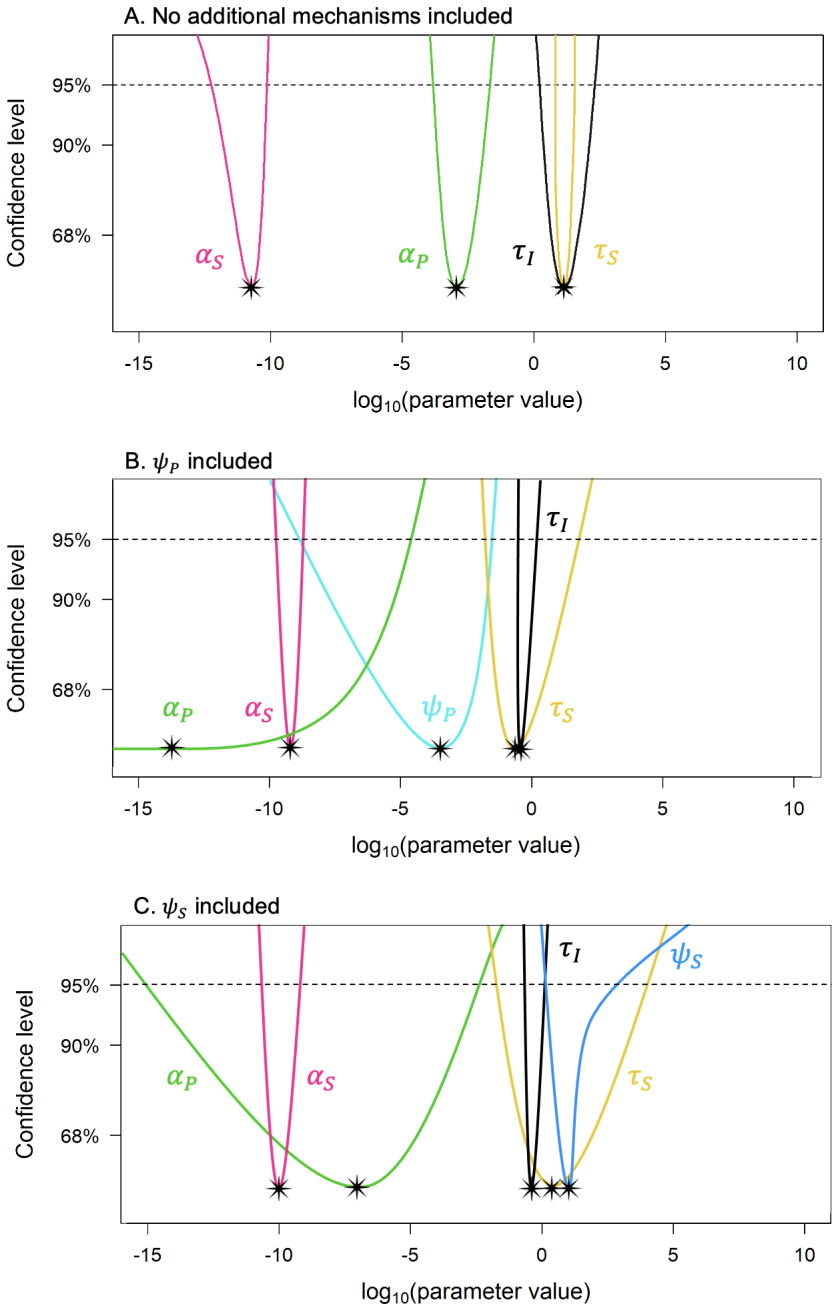

Fig. 4.14 Profile likelihood plots for variations of the SIXCA model where A) no additional mechanisms are included, and B) mechanism ψ_P is included, and C) mechanism ψ_S is included. All parameters are identifiable to the 95% confidence level apart from α_P when mechanism ψ_P is included in the model. The best fitting parameter values from Table 4.6 are marked on each profile likelihood curve by an asterisk. The 95% confidence intervals for σ are 1.82-2.38 when no additional mechanisms are included, 1.76-2.30 when mechanism ψ_P is included, and 1.40-2.45 when mechanism ψ_S is included.

Table 4.10 Parameter values and their 95% confidence intervals for variations of the SIXCA model where a) no additional mechanisms are included, and b) mechanism ψ_P is included, and c) mechanism ψ_S is included. Maximum likelihood model fitting was used, and the standard deviation (σ) that was calculated during this process is shown in the table. Data was obtained from Werker et al. (1991). Out of 50,000 model fitting simulations starting with different initial parameter values, these parameter values produced the highest log likelihood (LL) value. No lower confidence interval could be obtained for α_P in the model where mechanism ψ_P is included.

(a) No additional mechanisms included

		Confidence interval (95%)		
Parameter	Value	Lower	Upper	Units
α_P	5.39×10^{-2}	2.15×10^{-2}	1.89×10^{-1}	t^{-1}
α_S	2.18×10^{-5}	4.87×10^{-6}	3.86×10^{-5}	t^{-1}
τ_I	3.16	1.31	10.2	
τ_S	3.14	2.29	4.55	
σ	2.06	1.82	2.38	
LL	-232			

(b) Mechanism ψ_P included

		Confidence interval (95%)		
Parameter	Value	Lower	Upper	Units
α_P	1.99×10^{-5}	-	1.10×10^{-2}	t^{-1}
α_S	1.01×10^{-4}	6.15×10^{-5}	1.67×10^{-4}	t^{-1}
τ_I	6.80×10^{-1}	6.01×10^{-1}	7.81×10^{-1}	
τ_S	5.42×10^{-1}	1.72×10^{-1}	7.39	
ψ_P	3.59×10^{-2}	1.44×10^{-3}	1.35×10^{-1}	t^{-1}
σ	2.00	1.76	2.30	
LL	-228			

(c) Mechanism ψ_S included

		Confidence interval (95%)		
Parameter	Value	Lower	Upper	Units
α_P	1.07×10^{-3}	6.81×10^{-7}	1.22×10^{-1}	t^{-1}
α_S	5.42×10^{-5}	2.04×10^{-5}	8.27×10^{-5}	t^{-1}
τ_I	6.87×10^{-1}	4.36×10^{-1}	1.39	
τ_S	1.56	1.49×10^{-1}	6.68×10^{1}	
ψ_S	1.54×10^{-4}	1.50×10^{-5}	1.67×10^{1}	t^{-1}
σ	1.99	1.40	2.45	
LL	-227			

4.7 Discussion

4.7.1 Simulating take-all decline

The dynamics of the SIXCA model vary during the period of a year to account for the seasonal disturbances that crops such as winter wheat experience. Free-living material peaks when the crop is harvested, as infected roots die and are converted to free-living pathogen, and colonised roots die and are converted to free-living biocontrol agent. These dynamics can be further examined in Figure 4.15, where the proportion of primary and secondary roots change both across a single growing season, as well as between growing seasons. Both the pathogen and biocontrol agent exhibit two peaks in infection/colonisation throughout a growing season. The first is towards the start of the growing season, when there is a large amount of free-living pathogen and biocontrol agent in the soil that can cause high levels of primary infection and colonisation. However, the rapid decay of this free-living material means that primary infection and colonisation begins to drop and causes a reduction in the proportion of infected and colonised roots. As the season progresses, secondary infection and colonisation begin to dominate, and this causes the second peak in the proportion of infected and colonised roots.

As the seasons progress, this first peak in the percentage of colonised roots is higher due to greater population sizes of the free-living biocontrol agent in the soil. Likewise, this first peak is lower for the pathogen as it is suppressed and its population size declines. The biocontrol agent seems to suppress the first peak for the pathogen (caused by primary infection) more than the second (caused by secondary infection). Combining this biocontrol agent with one that targets the secondary infection peak more heavily may therefore result in much greater epidemic suppression.

Once the biocontrol agent has begun to establish in later years and competes for space on the crop's roots, this plateau in the proportion of infected roots during the middle of

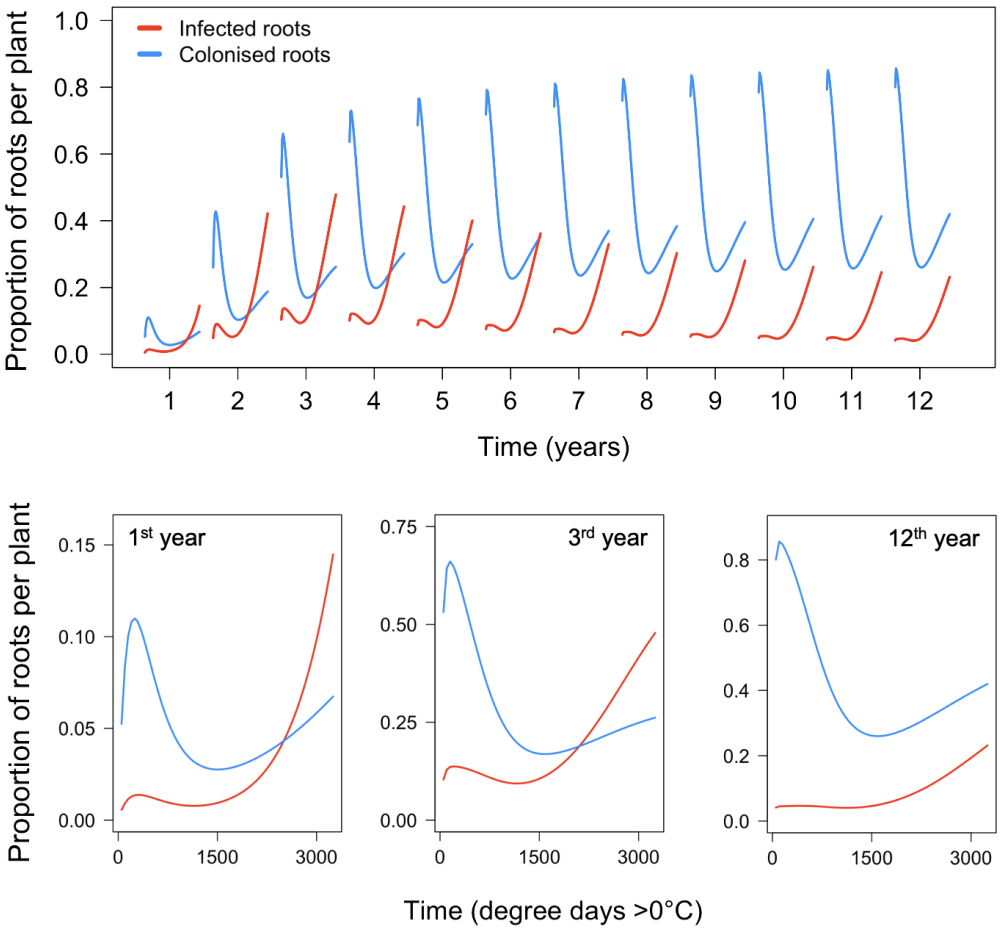

Fig. 4.15 Change in the proportion of infected and colonised roots in a field undergoing take-all decline. The same simulation over 12 years, but with a focus on the number of roots, can be found in Figure 4.6A. The SIXCA model can only negatively affect the pathogen through competition (primary and secondary colonisation). Three years are focused on in the bottom three plots: 1) the first growing season, when both the pathogen and biocontrol agent are present at low levels on a plant's roots, 2) the third growing season, where the number of infected roots reaches its peak value, and 3) the twelfth growing season, where take-all decline has occurred and the number of infected roots has been reduced due to biocontrol activity.

the growing season actually turns into a decline of the proportion of infected roots. The biocontrol agent therefore also delays the time at which secondary infection begins to dominate. Understanding such dynamics can improve the use of control strategies, such as planting later in the growing season to further reduce the amount of free-living pathogen,

or working out when is best to apply biocontrol agents to a field to act as a successful disease control strategy.

In order for the biocontrol agent 2,4-DAPG fluorescent *Pseudomonas* spp. to successfully suppress take-all and cause take-all decline, a threshold value of 10^5 CFU g^{-1} must be reached. This threshold value must then be maintained if suppression is to continue across subsequent years (Raaijmakers et al., 1999; Raaijmakers and Weller, 1998; Weller, 2007). During take-all decline, population sizes of 2,4-DAPG fluorescent *Pseudomonas* spp. are known to change from less than 10^4 CFU (colony forming units) g^{-1} of root to as many as 10^9 CFU g^{-1} (Weller, 2007). For the SIXCA model variations, the maximum value of free-living biocontrol agent always increased across successive years, and plateaus at a higher level once suppression of the pathogen has occurred (Figure 4.16). The largest increases in free-living material occur when either η and ϕ_η (1×10^{-6} - 1×10^{2}) or ν and ϕ_ν (1×10^{-8} - 1×10^{1}) are included in the model. The scale of the free-living material is smaller for the model than real-life populations as it was scaled to allow easier visualisation with the free-living pathogen. However, this high increase in free-living biocontrol agent over time suggests that 2,4-DAPG fluorescent *Pseudomonas* spp., or at least a biocontrol agent that rapidly expands its population size whilst causing pathogen suppression, caused the trend of take-all decline in Werker et al. (1991). *Pseudomonas* spp. are one of the only biocontrol agents where a link between population size and suppression has been found (Haas and Keel, 2003), and this is further supported by our findings.

All variations of the SIXCA model are successfully able to simulate take-all decline, with low levels of infection in the first year, rising to a peak in the third or fourth year, and then declining and plateauing at a lower level of infection for all subsequent seasons. A peak of infection in the third or fourth year of growing winter wheat is commonly seen in field conditions (Shipton, 1975; Weller et al., 2002), although the time of this peak is known to vary (Baker and Cook, 1982; Campbell and Madden, 1990; Gerlagh, 1968; Shipton, 1972;

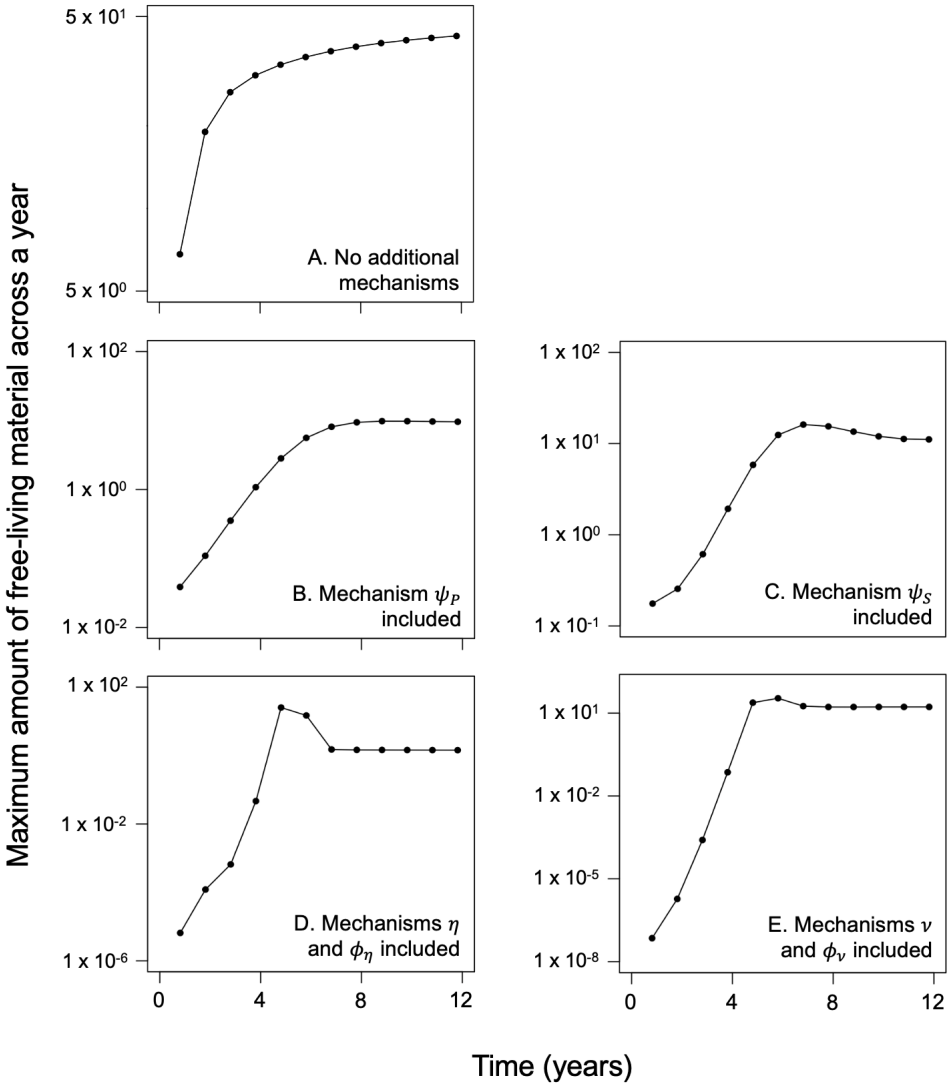

Fig. 4.16 Variation in the maximum amount of free-living biocontrol agent across each season for a 12-year simulation of the SIXCA model. The parameters used for this modelling can be found in Table 4.6. The amount of free-living biocontrol agent, shown on the y-axis, is represented by a log scale.

Walker, 1975). There was an abnormally low level of infection in the fourth year of the data obtained from Werker et al. (1991), presumably due to detrimental environmental conditions, which are known to have considerable effects on free-living material (Bossio et al., 1998; Smit et al., 2001; Weller, 1988). This may be one of the reasons why the peak of take-all decline can occur at different years in field trials, as detrimental environmental

conditions can reduce the ability for the biocontrol agent to persist and suppress the pathogen. However, the severe peaks in disease during the third and fifth years seem to have been enough to initiate take-all decline and cause successful suppression of the pathogen. It is promising to note that a single year of disruption to the pathogen and biocontrol agent can still result in take-all decline and pathogen suppression. One of the major reasons for a lack of uptake in using biocontrol agents as a control strategy is due to their variable effects in different environmental conditions. This experiment seems to show that they may be more resilient than often thought, at least once they have begun to establish and amplify in the soil in the presence of a host crop and pathogen.

Once take-all decline has occurred and the pathogen has been suppressed, the amount of colonised roots for all subsequent seasons remains high. This reflects the dynamics of real-life systems, where soils will often remain suppressive to the take-all pathogen for many years after take-all decline has occurred (Cook, 2003; Landa et al., 2006). The biocontrol agent remains at a high level in the soil once a peak of take-all has occurred, and then persists at this level long term. However, it should be noted that the biocontrol agent is never able to fully suppress the pathogen after take-all has occurred. It instead reduces infection severity to lower levels than in the peak years of infection (Hornby, 1998). It is therefore worth questioning whether this reduction in infection level results in enough disease suppression to obtain a suitable profit from the crop, or whether other control strategies that lead to much higher disease suppression would be required. Either way, it is worth noting that this suppression of take-all is often long term and free, which can be of considerable benefit to farmers with little money to spend on control methods.

4.7.2 Comparison of the potential mechanisms involved in take-all decline

The simplest variation of the SIXCA model, where the biocontrol agent can only affect the pathogen through competition for space on a crop's roots, was able to simulate take-all decline. The occupation of key sites on roots, known as niche exclusion, is a well-known mechanism of biocontrol agents (Kwak and Weller, 2013; Weller et al., 2002). The pathogen is prevented from establishing on these roots, reducing the total number of roots available to the pathogen.

However, biocontrol agents will often have at least one additional mechanism they can use that directly and negatively impacts pathogens (Jain and Das, 2016; Köhl et al., 2019b; Nega, 2014; Whipps, 2001). The biocontrol agent *Pseudomonas fluorescens* is known to have a rapid population increase whilst take-all decline is occurring, changing from less than 10^4 CFU g^{-1} of root to as many as 10^9 CFU g^{-1} (Weller, 2007). Even after this, it is believed to only make up 0.1-1% of the rhizobacterial populations surrounding a plant's roots (Haas and Défago, 2005), and occupies at most 0.1% of space on a plant's roots (Haas and Keel, 2003). This reduces the likely importance of competition in take-all decline, and suggests that at least one additional mechanism is involved.

Using AIC values, there were four mechanisms that were determined to improve the fit of the SIXCA model to the data compared to when just competition was included, accounting for a penalisation of the AIC value when additional parameter were included in a model. These models were: 1) colonisation of infected roots by free-living biocontrol agent (ψ_P), 2) colonisation of infected roots by already colonised roots (ψ_S), 3) death of the pathogen on infected roots and subsequent bulk of the biocontrol agent (η and ϕ_η), and 3) death of free-living pathogen and subsequent bulk up of the biocontrol agent (ν and ϕ_ν). All of these mechanisms involve the death of the pathogen. Although there is

still some discussion as to which and how many biocontrol agents are involved in take-all decline (Campbell, 1989; Kwak et al., 2012; Kwak and Weller, 2013; Weller et al., 2002), there is now substantial evidence that strains of *Pseudomonas fluorescens* that produce the broad-spectrum antibiotic 2,4- DAPG (phlD$^+$) are a vital part of this process. This antibiotic is known to be phytotoxic and can reduce the growth and continued prevalence of a variety of soil-borne pathogens. Many *Pseudomonas* species are also able to produce high-affinity iron chelating agents called siderophores (Calvente et al., 2001) which can further suppress the growth and persistence of pathogens. It therefore seems possible that multiple mechanisms of pathogen suppression are used by the biocontrol agent, although 2,4-DAPG production is believed to be the key player. As all four mechanisms that were found to improve the fit of the SIXCA model to the data from Werker et al. (1991) could be explained by antibiosis, it is impossible to distinguish whether one of these mechanisms is more important than others. However, it is reassuring that the mechanisms determined to be able to cause take-all decline by the model fitting process are supported by previous research.

4.7.3 The difficulty of model fitting

The model fitting process was a challenge due to multiple unknown parameter values and minimal data to fit the model to. A lack of data is a common problem with biological systems, where data collection can be time consuming and costly (Peck, 2004; Pullen and Morris, 2014). This is the case when collecting data on take-all decline, as it requires several consecutive years of data collection and suitable environmental conditions. Even if an experiment to analyse take-all across several consecutive years is performed, it is not always the case that take-all decline will be observed (Hornby et al., 1989). It is vital that such experiments continue to allow for this phenomenon to be explored in more detail. Take-all decline shows the successful use of a biocontrol agent to suppress a plant disease that is

difficult to control by other methods. Understanding more about this system may give further insights as to how we can successfully use biocontrol agents as control mechanisms against plant diseases.

For a system that is known to be so heavily influenced by the environment (Chng et al., 2015; Cook, 2003; Weller et al., 2002), using data from a single or from a small number of experiments is likely to not be completely representative of the system's dynamics. To fully understand take-all decline, and to identify how we can make biocontrol agents successful control strategies, will require multiple experiments to be performed under different environmental conditions. Until these are performed, biocontrol agents may always be seen as too variable and inconsistent to be used commercially.

The fitting process was further complicated by a lack of information on the potential bounds of the parameters included in the fitting, which can result in a cost surface that is large with many local optima (Transtrum and Qiu, 2012). This can make it impossible to determine the values of some parameters, or can lead to the selection of suboptimal parameter values (Abdullah et al., 2013a). The effect of these issues were explored in this chapter by beginning the fitting process at multiple initial parameter values, and through a visualisation of the cost surface and local optima using principle component analysis for the SIXCA model. This is similar to the analysis carried out in Fernández Slezak et al. (2010). If enough fitting attempts are performed, it is hoped that the cost surface can be fully explored and that local optima can be identified and ignored.

The SIXCA model variations had complex fitting landscapes, with multiple local optima that fit relatively well to the data. 95% confidence intervals could not be obtained for all of the parameters for three out of the five model variations that were explored in more detail. Very few model fitting attempts converged on a solution that fit well to the data, and high collinearity was also seen between parameters. Further experimentation to reduce

the bounds on at least some of the parameter values would reduce the cost surface and make the identification of the global optimum significantly easier.

Computational models are often known to be sloppy, where collinearity between parameters can cause them to be non-identifiable and have an infinite range of values that can produce a simular fit to the data. The collinearity between parameters was explored using the method from Omlin et al. (2001) and Brun et al. (2001), and the identifiability of parameters was explored using profile likelihood plots. Sloppiness was reduced in the SIXCA model by fitting the parameter values in different steps, through fixing the rates of decay for the free-living pathogen and biocontrol agent using previous experimental work, and through fixing the initial amount of free-living pathogen and biocontrol agent. However, there was still strong collinearity between parameter values, showing how complex the model fitting problem was.

There is often a difficulty in determining how much data needs to be collected. Collecting too little data may result in few conclusions that can be made, as well as a complex model fitting problem, whereas collecting too much data is a waste of time and resources. For model fitting, a suitable amount of data would allow for all unknown rate parameters to be determined during the model fitting process. All the rate parameters would have identifiable confidence intervals and a single global optimum. One way of helping to identify the optimal sample size for data collection is by using a power analysis. A power analysis is centered around specifying a specific power level, a significance level, and an effect size, which then allow for the optimal sample size for an experiment to be calculated. One important thing that needs to be considered is how noisy your data is likely to be. Microorganisms in the soil are known to have a patchy distribution, as well as being significantly affected by environmental conditions. If prior knowledge is known about factors that may add noise to any data collected, this can help to ensure that more data is collected to offset this. We

therefore suggest that the use of a power analysis, as well as a consideration about factors that may affect data collection, should always be an important part of experimental design.

4.7.4 Overfitting or underfitting

All parameters in the variation of the SIXCA model that can only negatively impact the pathogen through competition for space on a crop's roots (the model variation with the fewest parameters) were determined to be necessary for successfully modelling take-all decline. However, the addition of other mechanisms to the model often did not lead to a significantly better fit to the data. It is worth noting that the addition of a new parameter to a model will always improve the ability of the model to fit to a data set, and this often leads to unnecessarily complex and overfitted models (Gomez-Cabrero et al., 2011; Pullen and Morris, 2014). The use of AIC values allows for a judgement of whether any additional parameters improve the fit of the model to the data enough to justify including them (Abdullah et al., 2013b; Warne et al., 2019). Using AIC therefore allowed for an analysis as to which mechanisms might be involved in take-all decline, where mechanisms that are likely to be involved will result in lower AIC values than those that are unlikely to be involved. AIC should be seen as a vital step in model fitting to reduce the chance of overfitting and determine which parameter values, and therefore biological processes, are vital to a system. Although not possible here due to a lack of data, it would be interesting to see whether a combination of mechanisms produces an even better fit to the data (Köhl et al., 2019b; Xu et al., 2011; Xu and Jeger, 2013a,b).

4.7.5 Conclusions

The success of computational models to simulate biological systems depends on both the construction of a suitable model, as well as the ability to obtain suitable parameter values to use in simulations. This chapter has shown that, even for a complex model with noisy data,

it is still possible to obtain identifiable parameter values that reflect the dynamics between a crop, a pathogen, and a biocontrol agent. Certain assumptions had to be made due to a lack of data, especially because no data was collected for the biocontrol agent. However, the parameter values obtained allow for the model to have a biological standing and are a considerable improvement on randomly selected values. It is vital that large amounts of data are collected when researching soil-borne systems due to the significant impact of environmental conditions, as well as considerable temporal and spatial fluctuations.

Chapter 5: Optimising the use of biocontrol agents for disease suppression

5.1 Abstract

There is growing interest in the use of biocontrol agents as a control strategy against plant diseases. However, variable success across field trials has led to minimal commercial uptake. One area that requires significantly more research is determining how to apply a biocontrol agent to successfully reduce the severity of an epidemic. This includes determining the optimal amount to apply and the frequency of application, as well as how the mechanisms used by the biocontrol agent to suppress the pathogen may affect successful application.

A model was used to simulate the interactions between the roots of a plant, a soil-borne pathogen, and a soil-borne biocontrol agent. A range of application amounts were found to be able to cause complete or significant decreases to epidemic severity. However, more research that is specific to individual biocontrol agents must be carried out to prevent over- or under-application, resulting in wasted cost and reduction in profit.

The optimal frequency of application was often found to be once at the start of the first growing season, which gives the maximum time for the biocontrol agent to bulk up in the soil, resulting in faster epidemic suppression. This strategy also requires the least manual effort. However, significant fluctuations in the populations of biocontrol agents due to abiotic and biotic factors are well known, suggesting that more regular application may yield better results in field trials. There was no decrease in epidemic severity when the biocontrol agent was only applied in response to the disease reaching a certain threshold value rather than with regular application that did not take epidemic severity into account.

However, this responsive application often allowed for a reduced amount of biocontrol agent to be applied, decreasing the total cost of application and therefore increasing the overall profit obtained.

There was some difference in optimal application strategy depending on the mechanisms that the biocontrol agent could use to suppress the pathogen, as well as a difference in response to different amounts of application, and in the time taken until epidemic suppression caused by take-all decline occurs. A detailed understanding of the biological system is therefore needed before any biocontrol agent can successfully be applied, as well as considering external factors and the trade-off between application cost and the profit obtained from a healthy crop.

5.2 Introduction

5.2.1 Natural biocontrol agents and commercial use

The ability for certain types of soil to suppress soil-borne plant diseases has been well researched (Cook and Rovira, 1976; Mazzola, 2002; Schlatter et al., 2017; Weller et al., 2002), with the first suppressive soil reported in 1892 (Atkinson, 1892). Soil can either cause general suppression, where the activity of many microorganisms in the rhizosphere can result in pathogen suppression, or it can cause specific suppression, which is attributed to specific groups of microorganisms suppressing a pathogen. There have been many efforts to understand specific suppression for a wide range of soil-borne diseases, and the microorganisms linked to many of the soils that exhibit this suppressive behaviour have been identified (Cook and Rovira, 1976; Mazzola, 2002; Schlatter et al., 2017; Weller et al., 2002). It has long been hoped that some of these microorganisms can be used as successful disease control strategies by introducing them to non-suppressive soils.

However, although an extensive amount of research has been carried out on specific biological control agents and how they suppress pathogens, there has been very little commercial uptake for using them as control strategies (Deacon, 1988; Nega, 2014). This is due to variable success rates in field trials and often minimal suppression of disease (Fravel, 2005; Nega, 2014). This inconsistent performance is generally attributed to variations in environmental conditions, and multiple experiments have examined the large effects that factors such as temperature, water, and soil type can have on microbial populations (Huang et al., 2000; Larkin and Fravel, 2002; Whipps, 2001). Despite this, the potential advantages of an environmentally safe control strategy that can also enhance crop growth and yield (Alori and Babalola, 2018; Kumar and Verma, 2019; Welbaum et al., 2004) result in a growing amount of research on how biological control agents can be successfully used and applied to a field (Cook et al., 1996; Lewis and Papavizas, 1991; McIntyre and Press, 1991; Nega, 2014). A detailed understanding of biocontrol agents and how to optimise their application is necessary if we want to see them as viable control strategies.

5.2.2 Determining a successful application strategy

The application of chemical control methods is well researched, such as when to apply sprays and how much should be applied as a seed treatment (Beres et al., 2016; Cook et al., 1999; Sharma et al., 2015; Turkington et al., 2016). Significantly less is known about how to apply biocontrol agents successfully, and research that has been carried out often gives variable results. The first thing that should be established is whether the biocontrol agent is able to persist in the highly competitive rhizosphere of a plant. If it is only able to survive under very specific environmental conditions, it is not suitable to be used as a commercial control method (Nega, 2014). However, there are many biocontrol agents that are known to be effective across a range of environmental conditions. Examples of these

include *Pseudomonas* spp. (Weller, 2007), *Streptomyces* spp. (Vurukonda et al., 2018), *Trichoderma* spp. (Harman, 2006), and *Fusarium* spp. (Fravel et al., 2003).

Once a candidate biocontrol agent has been found, the next thing to think about is how the biocontrol agent can be applied to a field effectively. This will be explained in the following sections, which splits this topic into three categories: timing of application, the method of application, and the amount of application needed.

Timing of application

Biocontrol agents are often applied before, or at the time of planting a crop, through seed treatment or directly into the soil as dusts, granules or liquid suspensions (Deacon, 1988; Lewis and Papavizas, 1991). This allows the biocontrol agent to target the pathogen when it is most vulnerable. The pathogen has had to survive living in the soil without a host since the previous crop was harvested, often decaying rapidly in the soil during this period of time. Once the new crop is planted, any remaining energy will be used to locate and infect a plant's roots. A large application of biocontrol agent at the start of a growing season could lead to complete pathogen suppression if the biocontrol agent is able to negatively interact with the pathogen at this stage and prevent it from infecting a plant's roots.

It is more likely that a biocontrol agent cannot completely suppress a pathogen, but instead can limit its ability to infect a plant's roots. There is therefore a need for a successful biocontrol agent to persist in the soil for long enough to cause a significant negative impact on the pathogen's population (Weller, 1988). There are several examples of introduced biocontrol agents that have been found to persist across a growing season, or even across multiple growing seasons, from a single application (Adams and Ayers, 1982; Cooksey, 1982; Htay and Kerr, 1974; Moore and Cook, 1984; Sutton and Peng, 1993).

However, it is more common for an introduced biocontrol agent to decay rapidly once it has been introduced to the soil (Cook, 2003; Kim et al., 1997; Kimmey, 1969; Scherwinski

et al., 2007; Schippers et al., 1987; Steddom et al., 2002; Sundheim, 1982; Szczech and Shoda, 2006). This reduces the amount of time that a biocontrol agent that is applied once a year can act as a successful control mechanism, and suggests that regular application may be more effective. More frequent application of a biocontrol agent has been found to increase its population levels throughout a growing season, and lead to a longer period of disease suppression (Bahme, 1988; Fang, 1995; Martensson, 1990). Freeman et al. (2004) found that spraying strawberries with a mixture of *Trichoderma* strains at 7- and 10-day intervals reduced anthracnose disease severity, and Steddom and Menge (2001) found that ten applications of *Pseudomonas putida* through irrigation water resulted in population sizes similar to those from one application at a tenfold greater concentration. Huang et al. (2000) thought that inconsistent performance of biocontrol agents may be due to environmental conditions affecting their survival. They therefore suggest that it might be sensible to apply a biocontrol agent multiple times to reduce the impact of any external factors. Multiple applications at a lower dose can also reduce the potential problem of applying a biocontrol agent over its threshold level, which is a maximum application value after which there is no additional epidemic suppression (Heydari and Pessarakli, 2010), whilst also keeping it at a high enough level to have a considerable effect on the pathogen (Suslow, 1982; Xu and Gross, 1986).

It is often the case with plant diseases that a farmer will not proactively apply a control strategy at the start of a growing season, but will instead wait until disease severity exceeds a certain threshold. This allows farmers to keep their costs down as they do not have to pay for the control of diseases that are not present or will only occur at minimal levels. This method of responsive application works well for many foliar diseases (Wright et al., 2020). However, soil-borne diseases are often less visible and may only show above ground symptoms once the pathogen is very established (Werker et al., 1991). It therefore remains

to be seen whether responsive application could work for soil-borne diseases or whether predetermined application times are better.

Method of application

Many complex methods have been developed in laboratory experiments to successfully apply biocontrol agents to the soil (Nega, 2014; Tsegaye et al., 2018). In some cases, machinery has been developed that can apply a biocontrol agent across a whole field (Ardakani et al., 2009; Bahme, 1988). However, there will never be wide uptake of biocontrol agents as control strategies if growers need to use specialised and expensive machinery rather than being able to use machinery that they currently have (Mathre et al., 1999). Application methods for soil-borne biocontrol agents must also allow for the biocontrol agent to come into close contact with soil-borne diseases. For example, foliar sprays are frequently used for foliar diseases (Tsegaye et al., 2018), but they are unlikely to perform well for soilborne diseases as the foliage of a plant will block a large amount of the application to the soil and to a plant's roots. The application method must allow the pathogen and biocontrol agent to come into contact with each other in the rhizosphere (Cook et al., 1996; Fravel, 1992).

Two of the most common ways to apply a biocontrol agent are through seed treatments (Fravel, 1992; Kim et al., 1997; McIntyre and Press, 1991; Tsegaye et al., 2018; Weller et al., 1983; Weller, 1983) or applying at the time of planting (Ellis, 1986; Lumsden, 1983; Schüler et al., 1989, 1993; Workneh and van Bruggen, 1994). This results in a single application of the biocontrol agent at the start of each season. Application once at the start of a season can lead to a rapid decay of the biocontrol agent and reduction in disease suppression. However, the benefit of these strategies is that they are much easier and less time consuming than applying the biocontrol agent multiple times each season.

Bahme (1988) and Steddom and Menge (2001) found that multiple applications of a biocontrol agent in irrigation water were effective at root colonisation and disease

suppression. *Pseudomonads fluorescens* colonisation was also found to be much greater when applied as a drip delivery system compared to seed inoculation (Mathre et al., 1999). Using irrigation as the vector for transmission would allow for multiple applications per season and requires no new machinery, making it a possible way to repeatedly apply a biocontrol agent throughout a season.

Amount of application

There is always a trade off when using a control strategy between the cost of the strategy and the additional profit obtained from a less diseased crop (Steddom and Menge, 2001). The amount of application needed to suppress a pathogen will be less when there is minimal pathogen in a field, and higher when there is a greater amount of pathogen in a field. A high dose of biocontrol agent at the start of a season, before the pathogen has infected any hosts and multiplied, may be effective as it can suppress the pathogen before it has had time to establish and grow (Cook et al., 1996). However, it seems that there is a carrying capacity for some biocontrol agents where they reach a maximum population size that can be sustained in the rhizosphere (Deacon, 1988; Handelsman and Stabb, 1996; Newman, 1985). Application amounts greater than this would then be ineffective and wasteful.

If the application amount is too small, the biocontrol agent may not be able to establish in the rhizosphere or negatively affect the pathogen to any meaningful extent (Suslow, 1982; Xu and Gross, 1986). There is therefore a need to establish the minimum threshold of a biocontrol agent to effectively suppress a disease, and well as a maximum threshold where additional amounts of application will have no beneficial effect. It is important to determine how effective is it to apply a biocontrol agent once at a very high concentration (Cook et al., 1996) compared to multiple smaller applications (Steddom and Menge, 2001).

5.2.3 Epidemic control using break crops

The use of break crops, where a different crop is planted rather than growing the same each year, are often effective at suppressing soil-borne pathogens (Angus et al., 2015; Cook, 2003; Kirkegaard et al., 2008; McBeath et al., 2015). Between harvesting and planting a crop, the pathogen must survive in the soil on decaying plant matter. If the break crop that is planted in the next growing season cannot be infected by the pathogen, the pathogen must survive without a host for an entire growing season. This can often lead to the complete removal or high reduction of pathogen populations. Break crops are one of the only effective strategies against take-all disease on wheat, as the pathogen rapidly decays when it does not have a host plant (Cook, 1981; Gardner et al., 1998; Lawes et al., 2013).

Although break crops used in a rotation where winter wheat is the main crop are generally known to be unsuitable hosts for take-all infection (Cook, 1981; Lawes et al., 2013), they are often able to sustain the pathogen in other ways. This includes encouraging the growth of cereal volunteers that are hosts for take-all infection, or affecting the nutrients in the soil in a way that can benefit the pathogen (Jenkyn et al., 2014). It therefore may not always be as beneficial to plant a break crop for pathogen suppression as once thought, especially if the profit gained from a break crop is considerably less than the profit of the main crop.

The success of pathogen suppression often involves the combination of several control strategies together, referred to as integrated pest management (Deacon, 1988; Fravel, 2005; Lewis and Papavizas, 1991; Singh et al., 2012; Stenberg, 2017). It is worth considering what impact break crops may have on the success of a biocontrol agent, and how these strategies can be used together successfully. Crop rotation is known to affect the microorganisms present in the soil (Baker and Cook, 1982; Cook et al., 1996; Schippers et al., 1987). If both the pathogen and biocontrol agent depend on a specific host crop for survival, they will both decay considerably throughout the break crop period. This will affect systems

where biocontrol agents build up in the soil over time, as is seen with 2,4-DAPG fluorescent *Pseudomonas* spp. and take-all decline (Cook, 2003; Kwak and Weller, 2013). If the break crop causes significant decay of the biocontrol agent, any suppressive benefits may disappear. The use of break crops and biocontrol agents in combination is therefore a valuable area of future study, to ensure that one control method does not negatively affect the other.

5.2.4 Aims of this chapter

This chapter will focus on the following key questions:

- How does the application of a biocontrol agent affect disease severity, focusing both on the amount of biocontrol agent applied and how frequently it is applied?
- What effect does biocontrol application have on the presence of take-all decline and the time taken until epidemic suppression caused by take-all decline occurs?
- Is it beneficial to have responsive application, where the amount of biocontrol agent applied is dependent on the percentage of infected roots at the time of inspection, or is regular application, where the same amount of biocontrol agent is applied at regular time points, more beneficial?
- How can the application of biocontrol agents and the use of break crops be used together to effectively suppress the pathogen?
- How are the above points affected by the mechanisms that a biocontrol agent can use to affect the pathogen?

5.3 Methods

5.3.1 The SIXCA model

The SIXCA model is described in detail in Sections 2.3 and 2.4. It simulates the interactions between the roots of a plant and a soil-borne pathogen and biocontrol agent. A root begins as susceptible (S) and can become infected by the pathogen either through contact with an infected root (I), or through contact with free-living pathogen (X) in the surrounding soil. Likewise, a root can become colonised by the biocontrol agent through contact with a colonised root (C), or through contact with free-living biocontrol agent (A) in the surrounding soil. The model dynamics account for the temporal heterogeneity that occurs each year due to the planting and harvesting of seasonal crops. The plant's roots are only present for part of each year to represent the time in between planting and harvesting. Once the crop has been harvested, all roots die. The free-living pathogen (X) and biocontrol agent (A) are present throughout each year as they survive on decaying organic matter.

Five separate variations of the SIXCA model are explored. These vary in the mechanisms that the biocontrol agent can use to negatively affect the pathogen:

- Mechanism 1: through surrounding the plant's roots and protecting them from infection. This can either be through root-to-root colonisation (secondary colonisation) or through colonisation from free-living biocontrol agent in the surrounding soil (primary colonisation).
- Mechanism 2: the free-living biocontrol agent out-competes the pathogen on infected roots, causing them to transition to colonised roots
- Mechanism 3: colonised roots out-compete the pathogen on infected roots, causing them to transition to colonised roots

- Mechanism 4: through causing the death of pathogen living on the roots of a plant, and subsequent bulk up of the free-living biocontrol agent
- Mechanism 3: through causing the death of free-living pathogen, and subsequent bulk up of the free-living biocontrol agent

It is assumed that the biocontrol agent is always able to act through mechanism 1. The five models include 1) just mechanism 1, 2) mechanisms 1 and 2, 3) mechanisms 1 and 3, 4) mechanisms 1 and 4, and 5) mechanisms 1 and 5. This chapter will primarily focus on the model where only mechanism 1 is included, and then the four other models will be compared and contrasted to the results obtained from this initial analysis. These five models are referred to by their mechanisms throughout the chapter (Table 5.1), and the parameter values included in these model variations are listed in Table 5.2. Baseline parameters are obtained through fitting a model to data from Werker et al. (1991) (Chapters 3 and 4). This data represents take-all decline.

Table 5.1 Name for each variation of the SIXCA model, with any additional parameters compared to the baseline SIXCA model listed.

Mechanisms included	Additional parameters	Name
1	-	Competition only
1 and 2	ψ_P	Competition/out-competed by A
1 and 3	ψ_S	Competition/out-competed by C
1 and 4	η and ϕ_η	Competition/death of I
1 and 5	ν and ϕ_ν	Competition/death of X

Table 5.2 List of parameters and definitions for the SIXCA model. There are five different mechanisms listed that the biocontrol agent can use to negatively affect the pathogen. The values for all parameters included in this table can be found in Chapters 3 and 4.

Parameter	Definition	Units
S	Number of susceptible roots	
I	Number of roots infected by the pathogen	
C	Number of roots colonised by the biocontrol agent	
X	Density of free-living pathogen	
A	Density of free-living biocontrol agent	
t	Time (degree days $> 0^{\circ}$C)	
X_s	Initial amount of free-living pathogen present at the start of the first growing season	
A_s	Initial amount of free-living biocontrol agent present at the start of the first growing season	
ρ	Rate of root production	t^{-1}
κ	Carrying capacity of root production	
β_p	Rate of primary infection of roots by free-living pathogen	t^{-1}
β_s	Rate of secondary infection of roots	t^{-1}
λ_X	Rate of decay of pathogen inoculum	t^{-1}
τ_I	Units of pathogen present on an infected root. When the host crop is harvested at the end of a growing season, this parameter determines the amount of free-living pathogen released into the soil from an infected root	
λ_A	Rate of decay of free-living biocontrol agent	t^{-1}
τ_C	Units of biocontrol agent present on a colonised root. When the host crop is harvested at the end of a growing season, this parameter determines the amount of free-living biocontrol agent released into the soil from a colonised root	
Mechanism: Competition for space		
α_p	Rate of primary colonisation of roots by free-living biocontrol agent	t^{-1}
α_s	Rate of secondary colonisation of roots	t^{-1}
Mechanism: Out-competed by A		
ψ_P	Rate of primary colonisation of infected roots by free-living biocontrol agent	t^{-1}
Mechanism: Out-competed by C		
ψ_S	Rate of secondary colonisation of infected roots by colonised roots	t^{-1}
Mechanism: Death of I		
η	Death rate of the pathogen on infected roots by the free-living biocontrol agent	t^{-1}
ϕ_η	Production of free-living biocontrol agent through consumption of pathogen present on infected roots	t^{-1}
Mechanism: Death of X		
ν	Increased decay rate of the free-living pathogen by the free-living biocontrol agent	t^{-1}
ϕ_ν	Production of free-living biocontrol agent through consumption of free-living pathogen in the soil	t^{-1}

5.3.2 Calculating epidemic severity

The effect of take-all disease on a plant's roots was measured using the area under the epidemic progress curve for healthy roots (AUHC), which includes both susceptible and colonised roots. This is calculated in the same way as the area under the disease progress curve (AUDPC), which is commonly used to determine epidemic severity for plant diseases (Campbell and Madden, 1990; Jeger and Viljanen-Rollinson, 2001). Although the process of calculating the AUDPC can be difficult when using a small amount of experimental data (Jeger and Viljanen-Rollinson, 2001), the use of a model allows for a precise calculation due to the unlimited amount of data that can be generated using it. Using AUHC allows for a comparison between the number of healthy roots in a simulation when a pathogen is present compared to when it is not present (Elderfield, 2018). The AUHC is calculated using

$$\text{AUHC}_{\text{normalised}} = \frac{\text{AUHC\_I}}{\text{AUHC\_S}}, \tag{5.1}$$

where AUHC_I is the AUHC for a simulation where a pathogen is present, and AUHC_S is the AUHC for the same simulation if no pathogen was present. This will calculate a number between 0 and 1, where 0 corresponds to a simulation where all roots are diseased, and 1 corresponds to a simulation where all roots are healthy. The epidemic severity can then be calculated by

$$\text{Epidemic severity} = 1 - \text{AUHC}_{\text{normalised}}, \tag{5.2}$$

where a higher value represents a greater proportion of infected roots.

5.3.3 Regular application of a biocontrol agent

Free-living biocontrol agents are known to suppress a variety of plant diseases (Baker and Cook, 1982; Campbell, 1989; Weller et al., 2002). One example of this is take-all decline, where 2,4-DAPG fluorescent *Pseudomonas* spp. is able to suppress take-all after several years of consecutively growing winter wheat. However, this suppression requires at least one, and often multiple, years of high epidemic severity before the population size of the biocontrol agent has increased enough to successfully suppress the pathogen. The potential to increase disease suppression through additional applications of the biocontrol agent is explored during this chapter, either through one application at the start of the first growing season, or through more regular applications, across a 20 year growing period. This period of time was chosen to represent a period over which epidemic suppression, such as that seen with take-all decline, could occur. In Werker et al. (1991), data is collected across 10 years, and Durán et al. (2017) examines soil for suppression after at least 10 years of growing wheat consecutively. The simulation duration of 20 years should provide enough time to allow for take-all decline or any other form of epidemic suppression to occur, as well as still being within a sensible time frame to make suggestions to real world growers.

Varying the initial amount of biocontrol agent present

In a field, naturally occurring biocontrol agents can be present in the soil before a crop is planted. This is the case for take-all decline, where naturally occurring populations of 2,4-DAPG fluorescent *Pseudomonas* spp. slowly build up over successive years of planting winter wheat without any external application needed. This can be simulated with the SIXCA model by starting the first year of the simulation with a small amount of free-living biocontrol agent (A), acting as a naturally occurring population. A simulation can run for multiple years, carrying over the biocontrol agent from the previous season rather than adding any more into the system. The baseline amount of free-living biocontrol agent,

determined during the model fitting process in Chapter 4, varies between different variations of the SIXCA model. This variation is done to ensure that the population sizes of the free-living pathogen and biocontrol agent are scaled similarly for each model variation, allowing for improved visualisation of model simulations (Figures 4.6 - 4.9). These values can be found in Table 4.6 but are all referred to as A_S in this chapter. In order to assess the effect of the initial amount of free-living biocontrol agent on epidemic severity, this initial amount is varied between $A_S \times 10^{-4}$ and $A_S \times 10^4$. The natural population size of 2,4-DAPG fluorescent *Pseudomonas* spp. during take-all decline can vary by a factor of 10^8 (Mavrodi et al., 2007; Raaijmakers and Weller, 2001). We will look at varying the initial amount of biocontrol agent present, where this initial amount could be seen as a single application of a biocontrol agent, as well as variation in the size of a naturally occurring biocontrol agent population in the first year that winter wheat is planted. If it is seen as a single application, this amount will vary between a relatively large application to a very small or unsuccessful application. The latter could be due to failure for the biocontrol agent to persist in the rhizosphere directly after application. The epidemic severity (Equation 5.2) is calculated separately for each year across 20 years of successive winter wheat planting.

Optimal timing of biocontrol application

Repeated application of a biocontrol agent may be more beneficial for disease suppression than a single application, as is the case with chemical sprays where multiple applications are needed per season (Carmona et al., 2020; Christ and Maczuga, 1989; Kim et al., 2013; Van Den Berg et al., 2013). The effect of four different application strategies on epidemic severity are compared over 20 consecutive growing seasons. These strategies are:

1. The biocontrol agent is all applied at the start of the first growing season, as soon as the crop is planted

2. The biocontrol agent is applied once at the start of each growing season

3. The biocontrol agent is applied once at the start of each growing season, and once in the middle of each growing season (0 and 1625 degree days >0°C)

4. The biocontrol agent is applied four times each growing season, with application timing spread evenly apart (0, 813, 1625, and 2438 degree days >0°C)

Each of these is simulated using a total budget of between $A_S \times 10^{-4}$ - $A_S \times 10^4$ units of biocontrol agent. For each budget, a separate simulation was performed that ranged between 1 and 20 years consecutive years, calculating the cumulative AUHC across all included years. This meant that the normalised AUHC for each group of years was calculated using

$$\text{AUHC}_{\text{normalised}} = \left(\frac{\sum_i^{n_y} \text{AUHC\_I}_i}{\sum_i^{n_y} \text{AUHC\_S}_i} \right), \tag{5.3}$$

where n_y is the number of years that a simulation is run for, AUHC_I is the AUHC for a simulation where a pathogen is present, and AUHC_S is the AUHC for the same simulation if no pathogen was present. Epidemic severity can then be calculated in the same way as Equation 5.2, where

$$\text{Epidemic severity} = 1 - \text{AUHC}_{\text{normalised}}. \tag{5.4}$$

An epidemic severity value closer to 1 reflects a more severe epidemic. The total budget was split across the number of years that the simulation was run for, resulting in a bigger budget per application when the simulation is run for fewer years. An example of this can be seen in Table 5.3. The total budget also remained the same regardless of application strategy. This results in the application amount per season being four times less when the biocontrol agent is applied four times per season compared to once per season. An example of this can also be seen in Table 5.3. Maintaining a fixed total budget despite the number of years or the frequency of application ensures that a comparison between

application amount and strategy can be made without bias due to simulation length and number of applications per year.

Table 5.3 Variation in the amount of biocontrol agent applied per application when the total budget available is 10 units. The 10 units are split evenly across each application, resulting in smaller application amounts when simulations are run for longer or when there are more applications per year.

	Biocontrol agent units applied per application			
Application strategy	1 year simulation	5 year simulation	10 year simulation	20 year simulation
Once at the start of season one	10	10	10	10
Once per season	10	2	1	0.5
Twice per season	10	1	0.5	0.25
Four times per season	10	0.5	0.25	0.125

Most and least successful application strategies

The epidemic severity (Equation 5.4) for each application strategy was compared to determine whether any strategies were more or less successful at disease suppression. An application strategy was deemed to be the most successful strategy if it increased the AUHC by greater than 1% (>0.01 reduction in epidemic severity) over all other strategies. Increasing this threshold value to 5% (>0.05 reduction in epidemic severity) was also examined. These thresholds were used to ensure that there was a significant difference in the benefit of using a single strategy compared to all other strategies. Without these, incredibly minor changes to the epidemic severity value would change the calculated optimal strategy. However, the 1% and 5% thresholds were still low enough to allow for minor improvements in epidemic severity to be detected. The least successful application strategy was calculated in the same way, where a strategy was deemed to be the least successful it if decreased the AUHC by 1% over all other strategies, with a 5% increase also examined.

Calculating the number of years before epidemic suppression occurs due to take-all decline

The baseline parameters used in this model are able to simulate take-all decline. There can be considerable variation in the number of years before epidemic severity peaks and then begins to decline with take-all decline (Baker and Cook, 1982; Cook, 1988; Shipton, 1975, 1972; Walker, 1975). This variation in time before suppression occurred was examined as 1) the total budget of biocontrol application, and 2) the frequency of biocontrol application, varied. The number of years from the time winter wheat infected by take-all is planted (always the first year of a simulation), to the first time a threshold level of suppression is reached, is referred to as TAD_{sup}. The total duration required before TAD_{sup} occurred was calculated using the criteria:

1. There must be at least one year where the percentage of infected roots exceeds 35%. This ensures that there is a significant peak in epidemic severity. The percentage of infected roots regularly reaches 35% or greater during the peak year of a take-all epidemic (Bailey and Gilligan, 1999; Bailey et al., 2005; Hornby, 1979; Werker et al., 1991).

2. The first year must have a percentage of infected roots less than 20%. This ensures that the peak of disease does not happen in the first season, and that there is an increase in take-all severity across at least two years.

3. After the peak of disease, disease severity must drop to less than 25% in the successive years. This represents at least a 10% decrease in epidemic severity, which is typical for take-all decline.

These criteria can be observed in Figure 5.1 and are commonly stated as necessary conditions to assess whether take-all decline has occurred or not (Cook, 2003; Hornby,

1998; Walker, 1975). The duration of TAD_{sup} (calculated in years) is recorded from the first year of the simulation to the first year where take-all severity drops to less than 25% after a peak of disease greater than 35%. For Figure 5.1, the duration of TAD_{sup} would be 9 years. This is the amount of time from when the first susceptible crop is planted to the time until infection drops to below 25%.

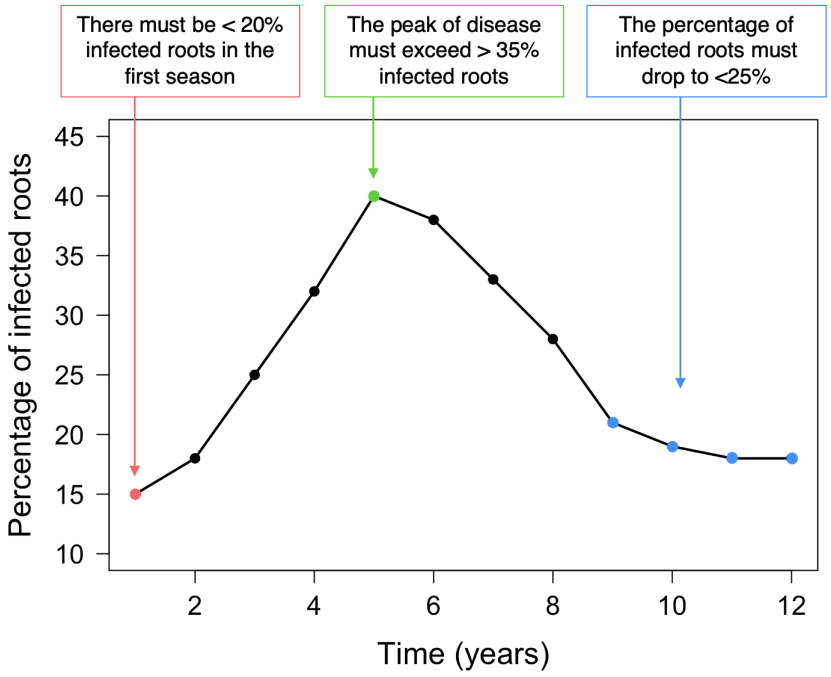

Fig. 5.1 Conditions required to determine whether take-all decline has occurred in the roots of a crop grown over several successive years, and how many years is takes until suppression, TAD_{sup}, begins. In the example shown here, TAD_{sup} takes nine years to occur.

5.3.4 Responsive application of a biocontrol agent

As is often the case with plant diseases, control methods may only be implemented once a field has been scouted for disease, and only if this examination finds a disease that exceeds a certain threshold value (Homan and Clausen, 1996; Mumford and Norton, 1984; Schillhorn van Veen et al., 1998; Tang et al., 2010). This responsive form of application is most common for foliar diseases due easy visualisation of symptoms. However, the

development of methods such as flow cytometry and real-time PCR allow easy detection of soil-borne pathogens and an examination of how prevalent they are in the soil (Fang and Ramasamy, 2015; Fox, 1990, 1997; Lievens et al., 2006; Porter et al., 1997). The effect of only applying the biocontrol agent once a threshold value is reached is examined, with the following factors that could be varied:

- How often the field is checked each season for disease
- What threshold value of disease results in biocontrol application
- How long after checking for disease should the biocontrol agent be applied
- How large should the total budget of biocontrol application be

The default values for these can be found in Table 5.4.

Table 5.4 Default values for the responsive application of a biocontrol agent.

Description	Value
Frequency that a field is inspected for disease	1-20 times per season
Threshold disease severity needed to initiate an application	5% infected roots
Time between checking for disease severity and application	0 days
Total budget of biocontrol application	$A_S \times 10^{-4}$ - $A_S \times 10^4$ units

With regular application of a biocontrol agent (Section 5.3.3), and in the case where the biocontrol agent is applied at least once per season, the first application time each season is always at 0 degree days >0°C. This is not the case for responsive application as there is no point in checking a field for disease at 0 degree days >0°C. This is because the crop has not yet been planted and is therefore incapable of having diseased roots. Like with regular application, a field is checked for disease at a predetermined number of times that are equally spaced out over the season. However, the responsive application strategy will ensure that the dates that a field is checked for disease are evenly spread out, excluding any application at 0 degree days >0°C. This results in a difference in the dates that the

biocontrol agent is applied (regular application) or the frequency that a field is checked for disease (responsive application) even when the number of applications/frequency of inspection are identical. For example, regular application of a biocontrol agent once a year would mean applying the biocontrol agent at 0 degree days >0°C. However, if the field is inspected once a year for responsive application, this would take place at the middle of the season (1625 degree days >0°C). More examples of this are given in Table 5.5.

Table 5.5 Difference in application timing when applying a biocontrol agent regularly, compared to responsively. The amount of biocontrol agent applied remains constant at each application period for regular application, whereas the amount varies for the responsive model depending on the number of infected roots found in the field when it is inspected for disease. The total number of degree days >0°C in a growing season is 3250, and it is assumed here that inspection and application happen at the same time for responsive application. If this was not the case, the times here would reflect the time of inspection rather than application.

Application/inspection frequency	Application/inspection timing (degree days >0°C)	
	Regular application	Responsive application
Once per season	0	1625
Twice per season	0, 1625	1083, 2167
Four times per season	0, 813, 1625, 2438	650, 1300, 1950, 2600

The total possible budget of biocontrol that can be applied varies between $A_S \times 10^{-4}$ and $A_S \times 10^4$. The amount per application is calculated by,

$$\text{Application amount} = \left(\frac{B_t}{n_y \zeta}\right) \text{TAI}, \tag{5.5}$$

where B_t is the total initial budget for the biocontrol agent, n_y is the number of years included in the simulation, and ζ is the number of times that a field is checked for disease each year. The take-all index (TAI) was designed to score the severity of take-all disease within a field (Beale et al., 1998; Schoeny and Lucas, 1999). This was modified to create a scale to calculate the amount of biocontrol agent that should be applied in a single application depending on the percentage of infected roots present. Each value for the

TAI can be found in Table 5.6. A greater percentage of infected roots results in a larger application of the biocontrol agent. At low levels of disease (<5% infected roots), no biocontrol agent is applied.

Table 5.6 Take-all index (TAI) value assigned to a plant depending on the percentage of roots found to be infected. Values based on the TAI from Schoeny and Lucas (1999) and Beale et al. (1998).

Percentage of infected roots	TAI value
<5%	0
5-10%	1
10-30%	2
30-60%	3
>60%	4

If there is not enough biocontrol agent left in the budget for the calculated full application amount, the remaining amount is used. After this, there will be nothing remaining in the budget and therefore no subsequent application of the biocontrol agent will occur. This strategy allows for a greater application of the biocontrol agent when disease severity is higher.

Comparing regular application with responsive application

Regular application of the biocontrol agent (Section 5.3.3) can be compared against responsive application (Section 5.3.4) to examine whether there is any benefit to adjusting application amount depending on disease severity rather than just applying the same amount at regular time periods. These two strategies were compared through regular application four times each year compared to the responsive model where the plant's roots are inspected for disease four times each year. Unlike in Table 5.5, where the timings for regular application and responsive application four times a year are different, they now both occur at the same times for a direct comparison (650, 1300, 1950, 2600 degree days >0°C).

The difference between epidemic severity when using either regular or responsive application is examined first. The epidemic severity is calculated for the two strategies over the specified number of years, using Equations 5.3 and 5.4 . An application strategy is deemed to be significantly better at reducing epidemic severity if the epidemic severity is lower than the other strategy by more than 1% (>0.01 reduction in epidemic severity). This is also compared to when the difference must be more than 5% (>0.05 reduction in epidemic severity).

One of the benefits of responsive application compared to regular application is that responsive application may not use the whole budget of biocontrol agent. If the entire budget is not used, less cost will have been spent on application compared to regular application where the total budget is always used. This was therefore factored into a calculation to determine the total profit obtained, with a high proportion of healthy roots across the simulation increasing the total profit, and a low application amount also increasing the total profit. This can be represented by

$$\text{Total profit} = \text{Proportion of healthy roots} - \text{Cost of application}, \tag{5.6}$$

where the proportion of healthy roots is determined by normalised the area under the epidemic progress curve for healthy roots ($AUHC_{normalised}$). This value includes both susceptible and colonised roots, and the calculation of $AUHC_{normalised}$ over the 20-year growing season can be found in Equations 5.3 and 5.4. This calculates a number between 0 and 1, where 0 corresponds to a simulation where all roots are diseased, and 1 corresponds to a simulation where all roots are healthy. The cost of application is calculated as

$$\text{Cost of application} = \text{Cost of total budget } x \text{ Proportion of budget used}, \tag{5.7}$$

where the cost of total budget is varied between 0-1. The proportion of budget used can range between 0-1, where 0 represents no application of the biocontrol agent, and 1

represents application of the whole budget of the biocontrol agent. For regular application, the proportion of budget used is always 1 as a fixed amount is applied each application time. For responsive application, the proportion of budget used can range between 0-1. The cost of application can vary between 0-1.

The total profit can therefore range between -1 and 1. A value of -1 represents a simulation with no healthy roots (proportion of healthy roots = 0), where the cost of total budget is at a maximum value of 1, and where the proportion of budget used is 1. A value of 1 represents a simulation where all roots are healthy (proportion of healthy roots = 1), and where either the cost of budget is at a minimum value of 0, or where the proportion of budget used is 0. The difference in profit obtained between responsive and regular application as 1) the total application budget available, and 2) the cost of this application budget compared to the profit obtained from an entirely healthy winter wheat crop vary, is examined.

5.3.5 Using a break crop to effectively suppress an epidemic

Over ten consecutive growing years, five different strategies for planting a break crop were analysed:

1. Plant a year of break crop after every year of planting winter wheat (WW, B)
2. Plant a year of break crop after every two years of planting winter wheat (WW, WW, B)
3. Plant two years of break crop after every year of planting winter wheat (WW, B, B)
4. Plant two years of break crop after every two years of planting winter wheat (WW, WW, B, B)
5. Plant winter wheat every year with no break crops (WW continuously)

Any infection or colonisation will occur from a single introduction of free-living pathogen and biocontrol agent at the start of the first growing season. The amount of each is the same as calculated during the model fitting process (Table 4.6). Two parameters are allowed to vary to examine how planting specific break crops (e.g. oats, oilseed rape, beans) may affect the profitability and effectiveness of the different strategies:

1. **Ability for the break crop to maintain the free-living pathogen population.** The value for this ranges between 0, where the break crop creates a completely unsuitable environment for the free-living pathogen to bulk-up and 1, where the break crop provides an environment that allows the production of free-living pathogen to bulk up at the same level as on winter wheat. Although break crops of winter wheat are generally known to be unsuitable hosts for take-all infection, they are able to sustain the pathogen in other ways, such as encouraging the growth of cereal volunteers that are hosts for take-all infection, or affecting the nutrients in the soil which benefits the pathogen (Jenkyn et al., 2014). The amount of free-living pathogen at the end of a season of growing a break crop is calculated by

$$X_B = \upsilon X_{-1}, \tag{5.8}$$

where X_B represents the the amount of free-living pathogen at the end of the current growing season, and X_{-1} represents the amount of free-living pathogen during the previous crop growing season. The parameter υ represents the ability for the break crop to maintain the free-living pathogen population. If $\upsilon = 0$, the break crop was not able to sustain the free-living pathogen at all, whereas if $\upsilon = 1$, the population size of the free-living pathogen is the same as it was when the previous crop was harvested. However, there is a lower threshold value for X_B, which is the same as the amount of free-living pathogen that would be present if it was only able to decay

for an entire season and not bulk up at all. This prevents the pathogen from ever fully being eliminated from the model.

2. **Profit of the break crop relative to winter wheat.** This value can vary between 0, where the break crop is entirely non-profitable, and 1, where the break crop yields the same profit as a completely healthy winter wheat crop.

The effectiveness of a specific break crop strategy is calculated by determining the profit of both the winter wheat crops as well as the break crops. The profit of the winter wheat crop was measured using the area under the epidemic progress curve for healthy roots (AUHC). The AUHC is calculated the same way as in Figure 5.1,

$$\text{AUHC} = \left(\frac{\text{AUHC\_I}}{\text{AUHC\_S}}\right), \tag{5.9}$$

where AUHC_I is the AUHC for a simulation where a pathogen is present, and AUHC_S is the AUHC for the same simulation if no pathogen was present. This will calculate a number between 0 and 1, where 0 results from a simulation where all roots are diseased, and 1 results from a simulation where all roots are healthy.

It is assumed that any infection during the growth of a break crop does not affect its yield. The overall profit obtained over ten consecutive growing years is therefore

$$\text{Profit} = \left(\sum_{W=1}^{W=W_F} \text{AUSC}_W\right) + B_F P, \tag{5.10}$$

where W is a season where winter wheat is grown, W_F is the total number of seasons when winter wheat is grown, and B_F is the total number of seasons where a break crop is grown. This calculation produces a maximum score of 10 over 10 seasons. A strategy is determined to be optimal if its profit is $\geq 1\%$ compared to all other strategies. If two or more strategies have maximal profits that lie within 1% of the maximum profit, no strategy is deemed to be optimal.

If the biocontrol agent is present in the simulation, the ability for the break crop to maintain its free-living population is calculated in the same way as Equation 5.8, where the amount of free-living biocontrol agent at the end of a season of growing a break crop is calculated by

$$A_B = \delta A_{-1}, \tag{5.11}$$

where A_B represents the the amount of free-living biocontrol agent at the end of the current growing season, and A_{-1} represents the amount of free-living biocontrol agent during the previous crop growing season. The parameter δ represents the ability for the break crop to maintain the free-living biocontrol agent population. This allows for an examination of how the choice of break crop can impact the population size of the biocontrol agent, and how it might influence its ability to suppress the pathogen in subsequent seasons. A break crop may be able to provide an environment that allows the free-living biocontrol agent to bulk up at the same level as on winter wheat ($\delta = 1$) or it may provide a completely unsuitable environment where the biocontrol agent can only decay ($\delta = 1$), as well as anything between these values.

5.4 Results

The results in Sections 5.4.1 - 5.4.4 focus on the variation of the SIXCA model that can only affect the pathogen through competition for space on a plant's roots. This is referred to as the "Competition only" model throughout this chapter. Four other variations of the SIXCA model, all including an additional way that the biocontrol agent can negatively affect the pathogen, are then compared with these results in Section 5.4.5. These five models are explained in detail within Section 5.3.1.

5.4.1 Variation in the initial amount of biocontrol agent present

The amount of biocontrol agent present at the start of a 20 year simulation was allowed to vary between $A_S \times 10^{-4}$ and $A_S \times 10^4$, where A_S was the initial amount of free-living biocontrol agent present during the process of fitting the SIXCA model to data representing take-all decline (Table 4.6). This amount results in the occurrence of take-all decline and can be assumed to be the amount of free-living biocontrol agent that was present at the start of the first year of the experiment that the data used for model fitting was obtained from. For each initial amount of biocontrol agent, the epidemic severity was calculated for each year of the simulation (Figure 5.2), with application amounts of $A_S \times 10^{-4}$, A_S, and $A_S \times 10^4$ examined in more detail (Figure 5.3). Epidemic severity remained at less than 0.1 throughout the first year, regardless of application amount. For higher application amounts, the pathogen was completely suppressed by the biocontrol agent and no roots became infected over the 20 year simulation. Lower application amounts resulted in more severe epidemic severity values, both through individual years having a greater number of infected roots, and through needing a greater number of years before disease suppression began to occur. For the lowest application amounts, epidemic severity still remained high by the 20^{th} year. However, for intermediate application amounts, there was an initial peak in epidemic severity before it declined in later years. This is representative of take-all decline.

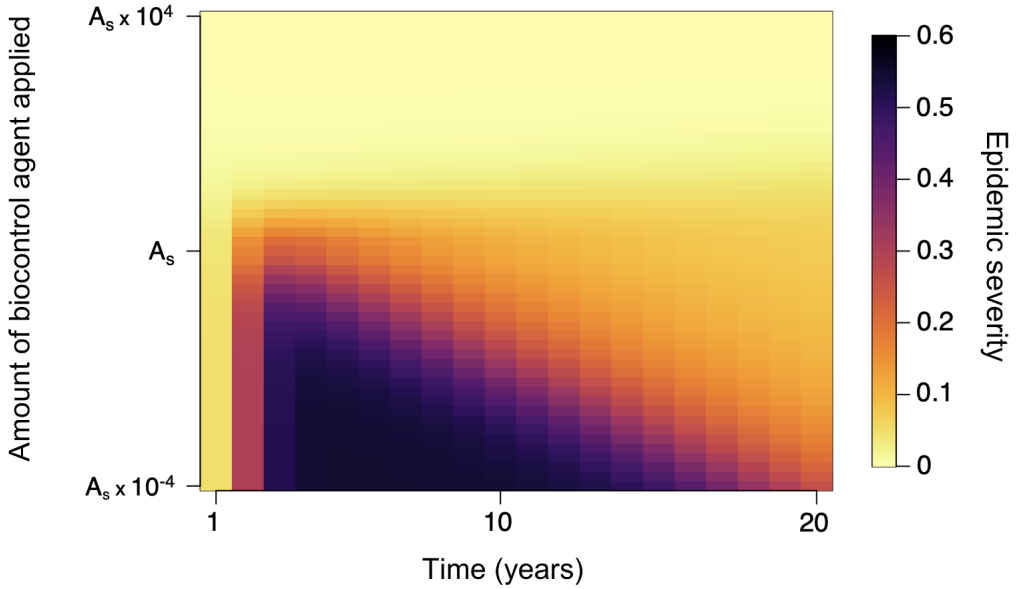

Fig. 5.2 Change in epidemic severity across a 20 year simulation as the amount of biocontrol agent at the start of the simulation is varied between $A_S \times 10^{-4}$ - $A_S \times 10^4$. The amount of biocontrol agent applied, shown on the y-axis, is represented by a log scale (Model: "competition only").

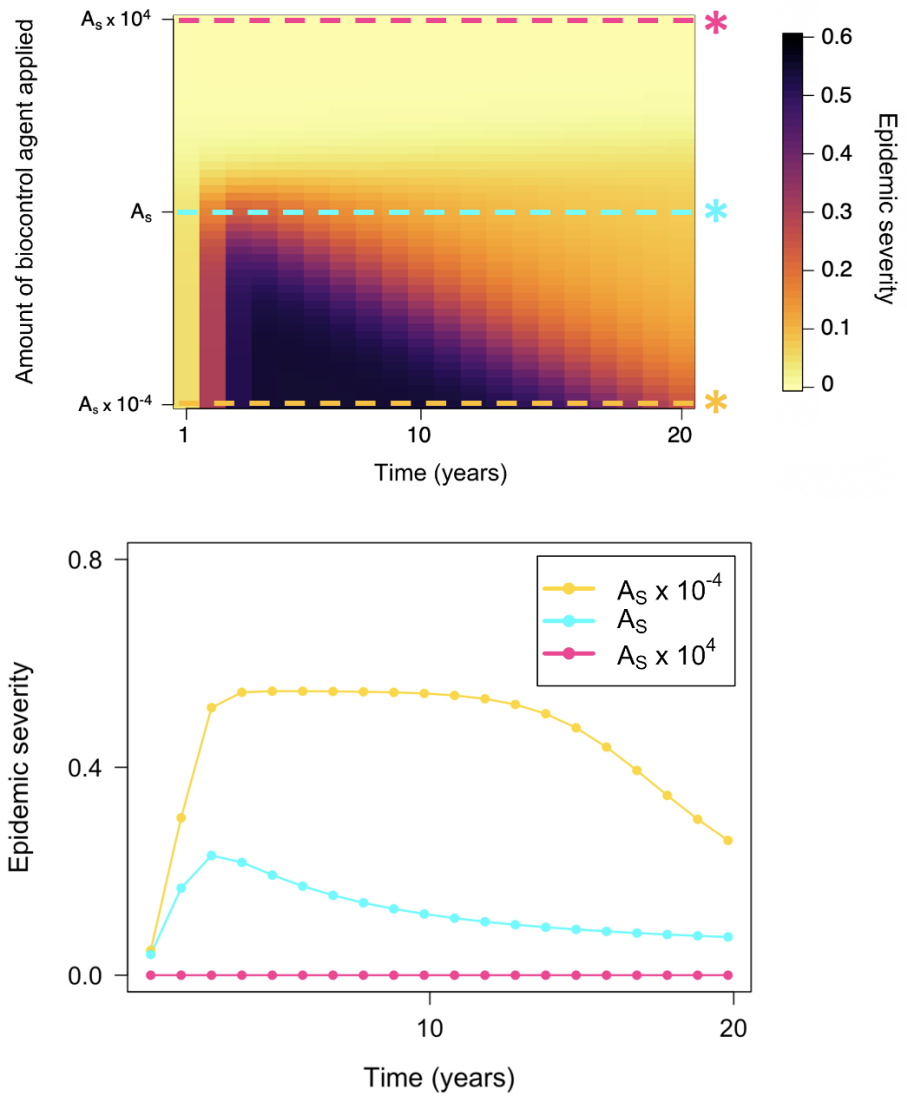

Fig. 5.3 Change in the epidemic severity across 20 year simulations when the initial amount of biocontrol agent is either $A_S \times 10^{-4}$, A_S, or $A_S \times 10^4$. The amount of biocontrol agent applied, shown on the y-axis, is represented by a log scale (Model: "competition only").

5.4.2 Regular application of a biocontrol agent

The mean epidemic severity was examined for simulations that were performed between 1-20 years over four different application strategies (Figure 5.4). The general trend in epidemic severity was the same for each strategy, although there was slight variation depending on application amount and number of years included in the simulation. Applying all of the biocontrol agent at the start of the first season resulted in overall slightly lower mean epidemic severity values. However, there was no considerable difference between application strategies.

A quantitative analysis of these results found that there was commonly no single strategy that out-performed the others by reducing the mean epidemic severity by greater than 1% or 5% (Figure 5.5). This was always the case for high application amounts, or when the simulation was performed for fewer than 8 years. However, at low to moderate application amounts and for simulations performed for longer than 8 years, applying all of the biocontrol agent at the start of the first season was often determined to be the most successful strategy. This is because applying all of the biocontrol agent at the start of the first season gives the biocontrol agent maximum time to bulk up and increase to a greater population size.

There was commonly no least successful application strategy at extreme application amounts. However, a high proportion of moderate application amounts and simulation duration's found that applying once at the start of each season was the least successful strategy at reducing epidemic severity. A detailed examination of the performance of the four different strategies when a simulation is performed for 1 year, 5 years, and 20 years is given in Figure 5.6. Very little difference in epidemic severity can be seen when the simulation is only performed for a year, or at very high or low application amounts. At moderate application amounts across 5 and 20 years, there is a noticeable increase in epidemic severity when the biocontrol agent is applied once per season. For the 20 year

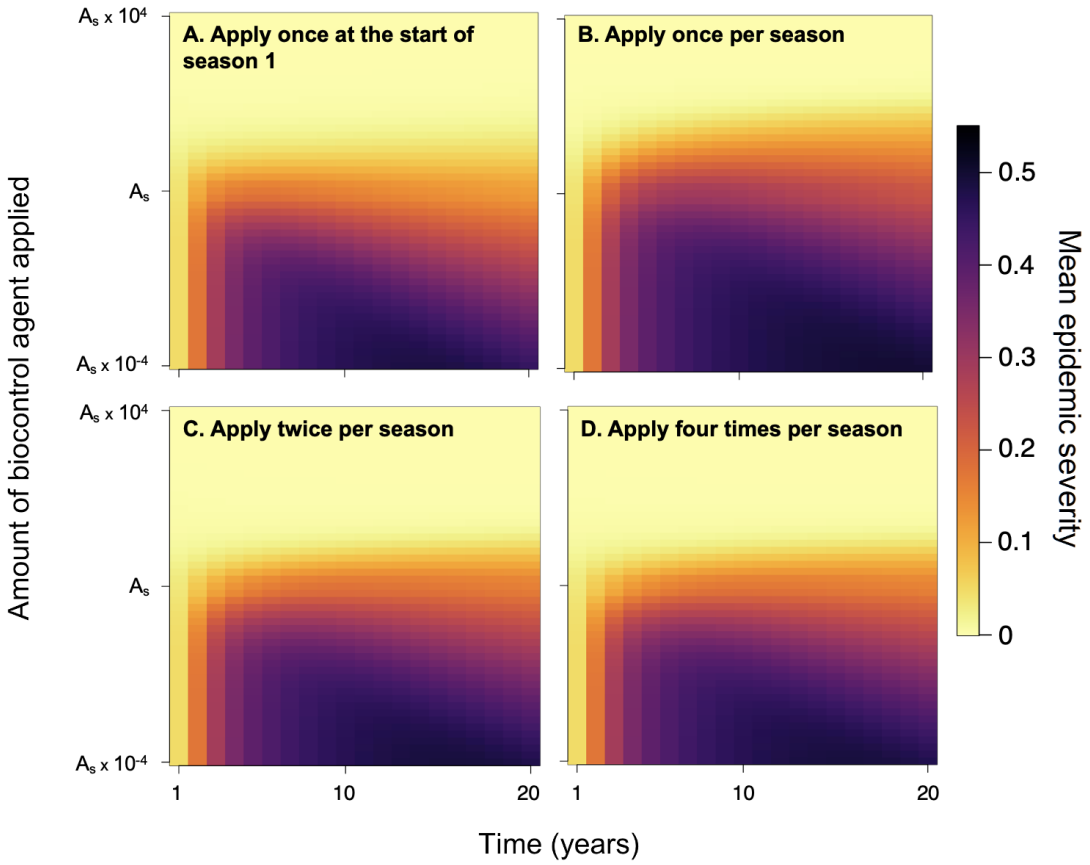

Fig. 5.4 Mean epidemic severity for simulations that were performed between 1-20 years, with varying total budgets of biocontrol agent over four different application strategies: A) applying all of the biocontrol agent at the start of the first season, B) applying the biocontrol agent at the start of each season, C) applying the biocontrol agent twice per season, and D) applying the biocontrol agent four times per season. The mean epidemic severity is calculated from all previous years of the simulation. For example, the mean epidemic severity at the tenth year is the mean value of the epidemic severity from seasons 1-10. The total amount of biocontrol agent that is applied throughout a simulation is the same regardless of the number of years that the simulation is run for or the amount of application times per season. This means that there is a greater amount of biocontrol agent applied per application when the simulation is run for fewer years or when there are fewer application times, with examples given in Table 5.3. The amount of biocontrol agent applied, shown on the y-axis, is represented by a log scale (Model: "competition only").

simulation, applying the biocontrol agent once at the start of season one has a visible decrease in epidemic severity compared to the other strategies. Applying the biocontrol

agent once or twice per year had very similar epidemic severity values, irregardless of simulation duration or application amount.

The least successful application strategy was often found to be application once at the start of each year. This is because it does not give maximum time for the biocontrol agent to bulk up like with only one application, but also occurs too early in the season to have a significant impact on the pathogen. As the biocontrol agent decays rapidly in the soil, applying the biocontrol agent later on in the growing season can result in a significant peak in free-living biocontrol agent that can increase epidemic suppression compared to a single application at the start of each season. This means that multiple application times per seasons was more successful than a single application at the start of each season.

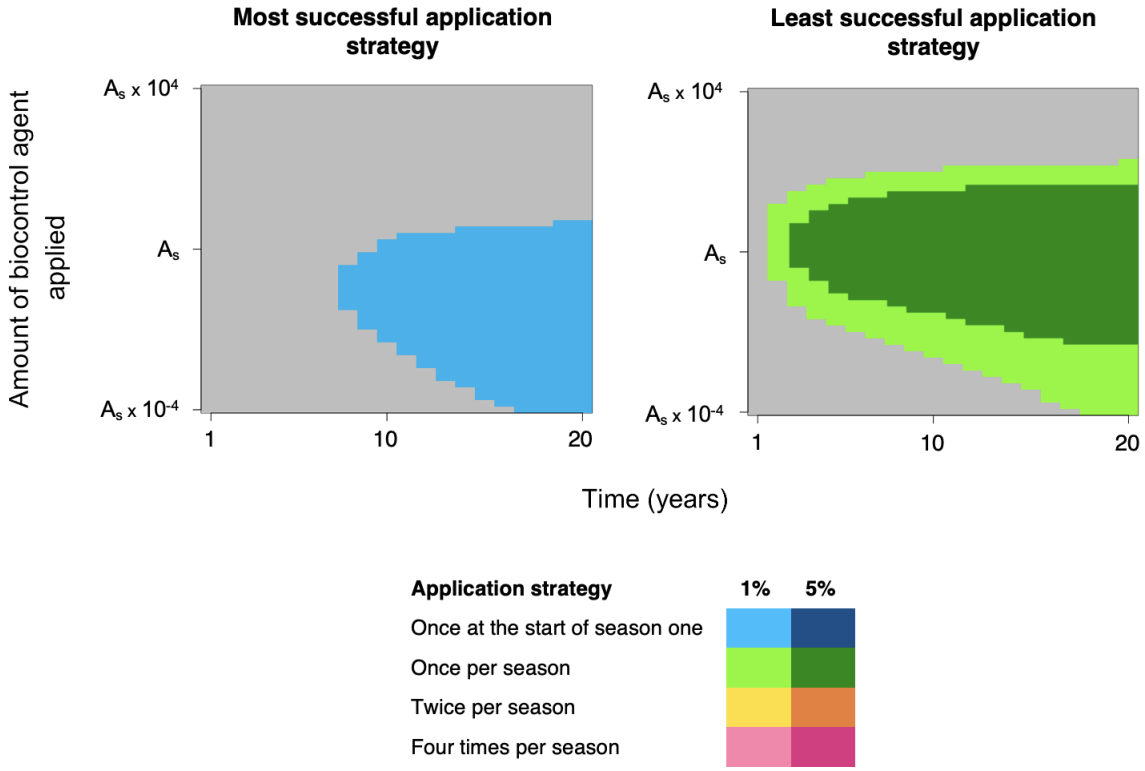

Fig. 5.5 Most and least successful strategies for the application of a biocontrol agent to suppress epidemic severity. A strategy was determined to be the most successful if it reduced the mean epidemic severity by >1% or >5% compared to any other strategy. A strategy was determined to be the least successful if it increased the epidemic severity by >1% or >5% compared to any other strategy. The amount of biocontrol agent applied, shown on the y-axis, is represented by a log scale (Model: "competition only").

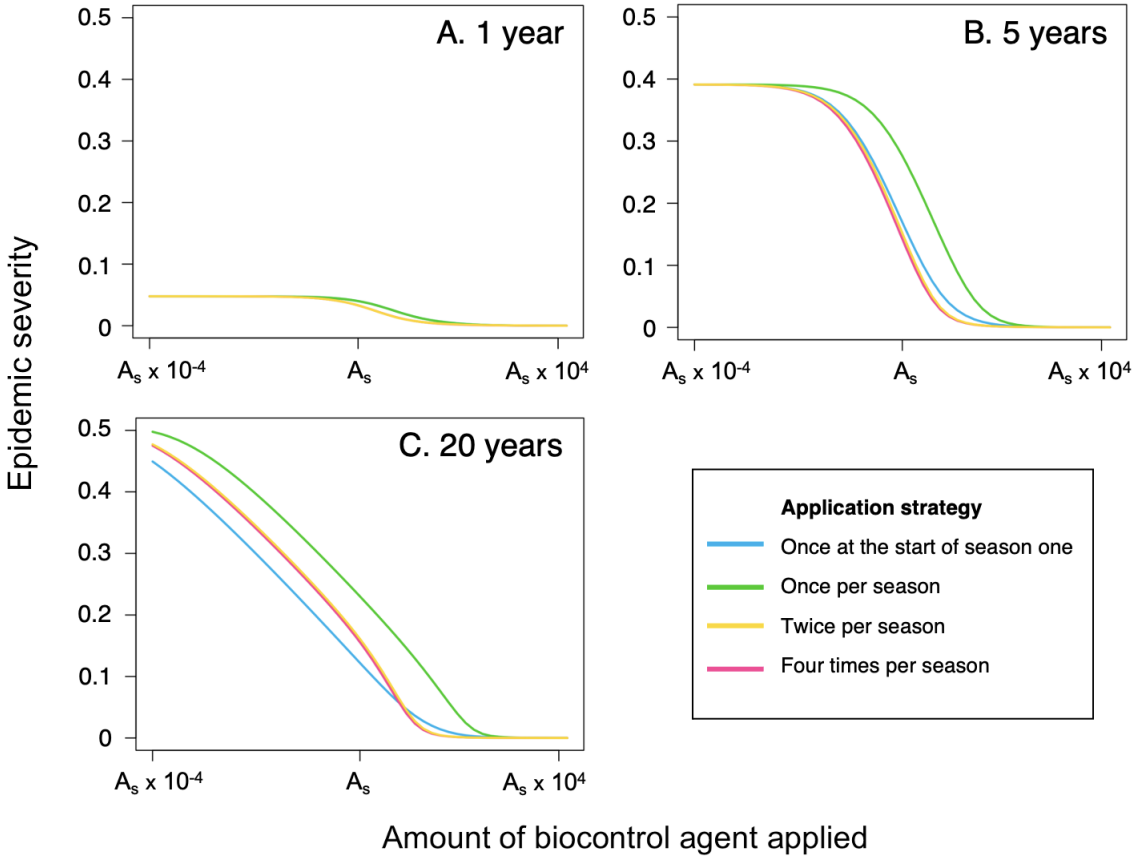

Fig. 5.6 Changes in epidemic severity for four different application strategies across A) 1 year, B) 5 years, and C) 20 years. The amount of biocontrol agent applied, shown on the x-axis, is represented by a log scale (Model: "competition only").

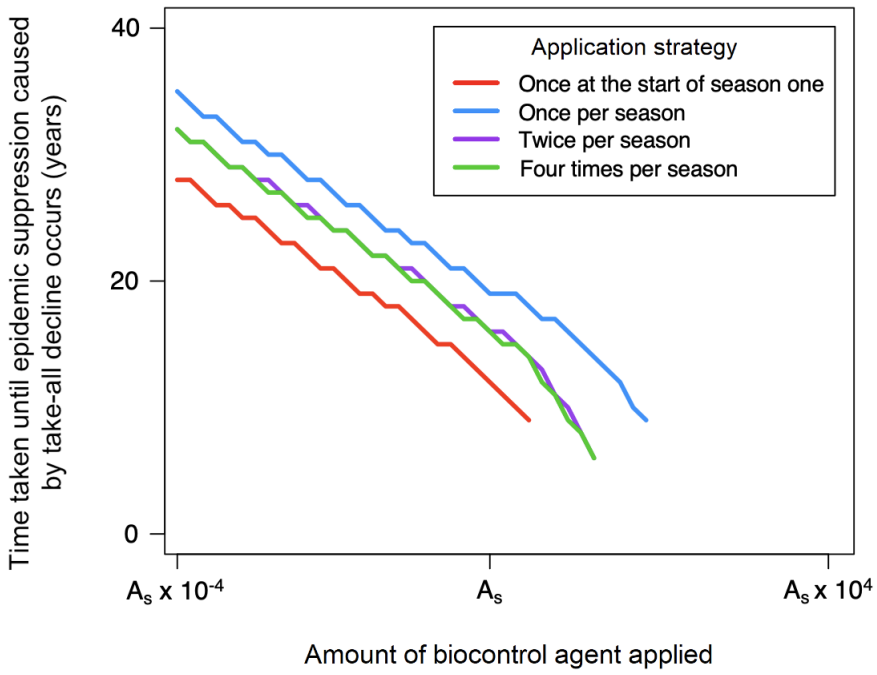

Fig. 5.7 Variation in the duration of time taken until take-all suppression (TAD_{sup}) occurs under different application strategies and different application amounts of a biocontrol agent. If the conditions necessary for establishing that TAD_{sup} has occurred were not met (Section 5.3.3), no data is plotted. The amount of biocontrol agent applied, shown on the x-axis, is represented by a log scale (Model: "competition only").

Both the application strategy and the total budget of biocontrol agent applied were found to affect the time taken until epidemic suppression caused by take-all decline (TAD_{sup}) occurred (Figure 5.7). Applying all of the biocontrol agent at the start of the first season consistently lowered the duration of TAD_{sup} compared to the three other strategies. Likewise, applying the biocontrol agent once at the start of each season consistently raised the duration of TAD_{sup} compared to the other strategies. Once the total budget for biocontrol application is high enough, the epidemic does not become severe enough to allow for the conditions of TAD_{sup} to be met (Section 5.3.3). This lack of TAD_{sup} occurs at a lower application amount when the biocontrol agent is applied once at the start of the first season, and at a higher application amount when the biocontrol agent is applied once at the start of each season. TAD_{sup} takes a long time to occur at low application amounts

as the biocontrol agent requires multiple years of wheat monoculture before it can increase to a population size that is high enough to suppress the pathogen.

5.4.3 Using a responsive model to determine application timing

When the biocontrol agent is only applied in response to searching for and finding a certain percentage of infected infected roots, the mean epidemic severity across 1 year, 5 years, 10 years, and 20 years was examined as 1) the total budget of biocontrol agent available varied between $A_S \times 10^{-4}$ and $A_S \times 10^4$, and 2) the number of times that a plant was inspected for infected roots varied between 1 - 20 times a season (Figure 5.8). There was minimal change in epidemic severity for the first year of the simulation, regardless of inspection frequency or application budget (Figure 5.8A). For 5 years, 10 years, and 20 years (Figure 5.8B-D) there was minimal effect of increasing the inspection frequency on epidemic severity. Compared to regular application, where a single application time occurs at the start of the season, for regular application it occurs in the middle. These results therefore show that even a single application in the middle of the season can suppress the pathogen as well as multiple applications. The amount of free-living biocontrol agent will be very low in the middle of the crop growing season due to it having a rapid decay rate. Introducing the biocontrol agent whilst the current population level is low can therefore result in successful epidemic suppression, regardless of how many times the field is inspected. There was also a strong effect of total budget of biocontrol agent, with a decrease in epidemic severity as the total budget increases. The minimal effect of inspection frequency on epidemic severity is further explored in Figure 5.9, where the total budget of biocontrol application is fixed at A_S. The lowest epidemic severity is recorded when the inspection frequency is once a season, but there is little fluctuation across any of the inspection frequencies.

Regular application of the biocontrol agent four times a year, and responsive application, where a field is inspected for disease four times each year and application amount determined

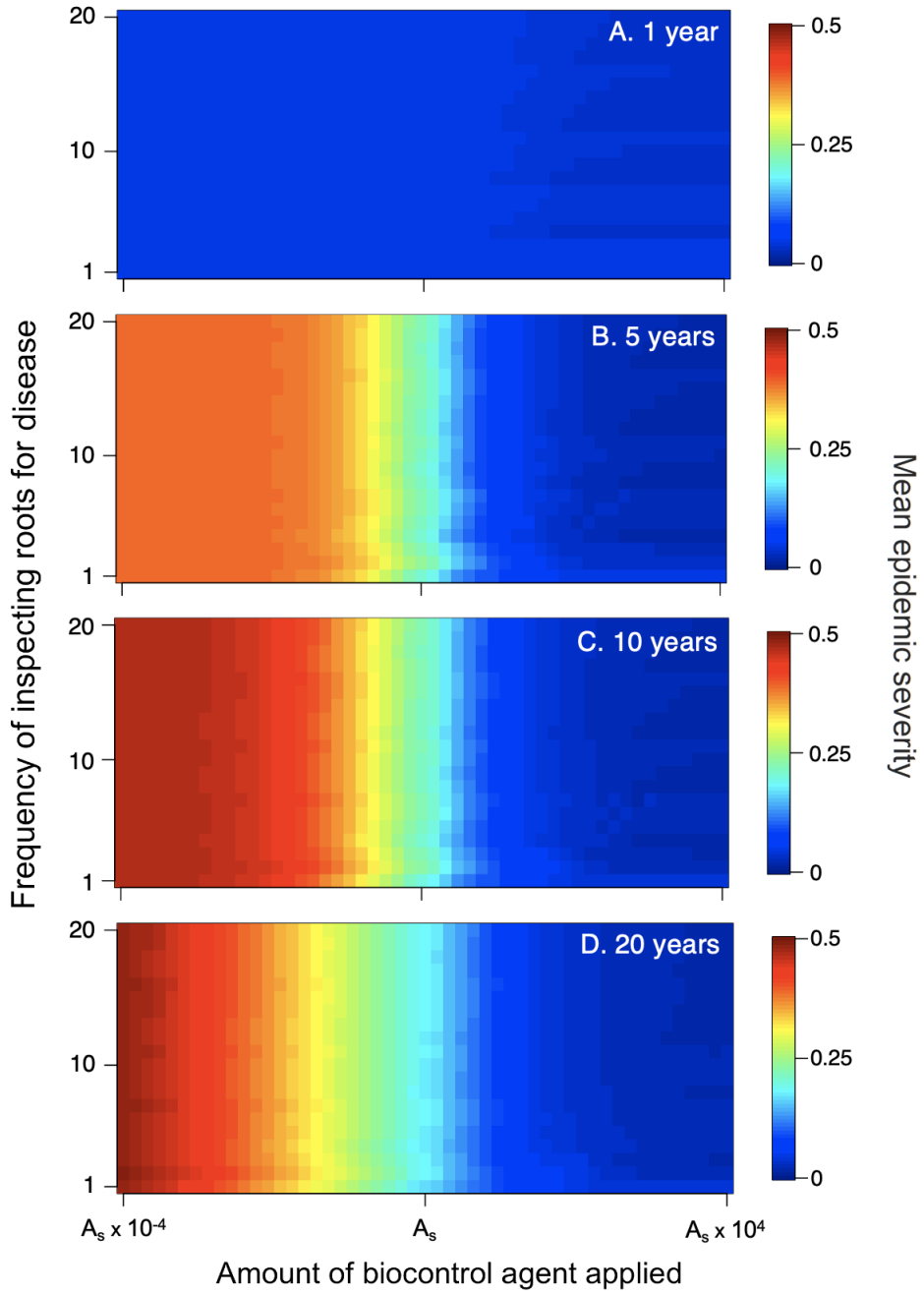

Fig. 5.8 Variation in the mean epidemic severity of the roots of a winter wheat plant infected by take-all disease when the biocontrol agent is applied responsively, varying the total budget of biocontrol available and the frequency that a plant's roots are inspected for disease. Results are obtained for simulations performed over A) 1 years, B) 5 years, C) 10 years, and D) 20 years. The amount of biocontrol agent applied, shown on the x-axis, is represented by a log scale. (Model: "competition only").

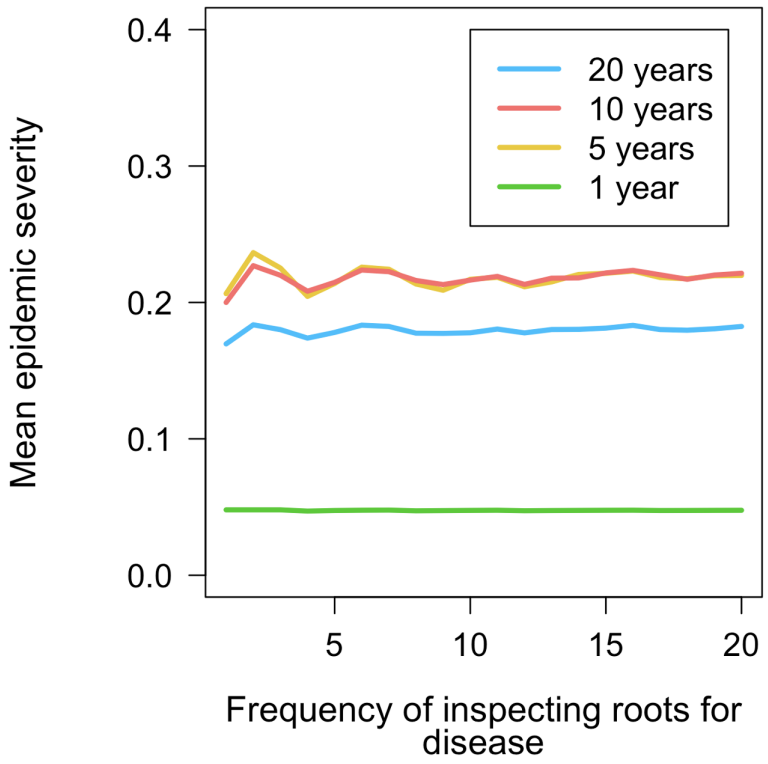

Fig. 5.9 Variation in the mean epidemic severity for responsive application as the frequency that a plant's roots are inspected for disease each season varies, with the total budget of biocontrol agent fixed at A_S. Results are obtained for simulations performed over A) 1 years, B) 5 years, C) 10 years, and D) 20 years (Model: "competition only").

by Equation 5.5, were compared to examine their effects on epidemic severity (Figure 5.10). The application time for regular application, and the inspection time and possible subsequent application time for responsive application, were the same for both strategies. At high application amounts, regular application was found to be the optimal strategy. Responsive application was never found to be the optimal strategy. However, there is never a drastic difference in epidemic severity depending on whether responsive or regular application is used. When the threshold for determining which model performs best increases requires a strategy to have a 5% reduction in epidemic severity compared to the other strategy, there is almost always no difference between the two application strategies (Appendix Figure B.1). Responsive application never reduces the epidemic severity by greater than 5% compared

to regular application, whereas regular application only does this compared to responsive application for moderate application amounts.

Regular application of a biocontrol agent requires a fixed amount of application, regardless of the disease severity present at each application time. This means that the total budget for a biocontrol agent is evenly distributed throughout a simulation and will always be used up by the end. Responsive application allows the application amount to vary depending on the percentage of roots that are infected at the time of inspection. A large percentage of infected roots at the time of inspection increases the application amount, whereas fewer than 5% infected roots results in no application (Section 5.3.4). This means that it is possible for the total budget to run out before the end of an epidemic simulation, as well as the possibility that not all of the budget is used by the end.

In a simulation run for 20 years with the same application dynamics for the regular and responsive models as seen in Figure 5.10, and the cost of the total budget of application fixed at 0.2, the total profit is higher for responsive application than regular application when the total application budget available is greater than A_S (Figure 5.11). This is because the responsive application does not apply all of the budget of biocontrol agent available when there is a large budget available. The profit obtained from the crop, calculated as the proportion of healthy roots, has no noticeable difference between the two application strategies. However, the reduction in budget used by the responsive application means that the total profit is higher than for regular application, where the entire budget has to be used.

The difference between the success of regular and responsive application can be examined further in Figure 5.12. There is no noticable difference between application strategies when the total application budget is low. This is because the total budget will be used up by both strategies. However, the responsive application strategy does not use up the entire

budget when it is higher than A_S, resulting in a greater total profit. This difference in profit is greater as the cost of the application budget increases.

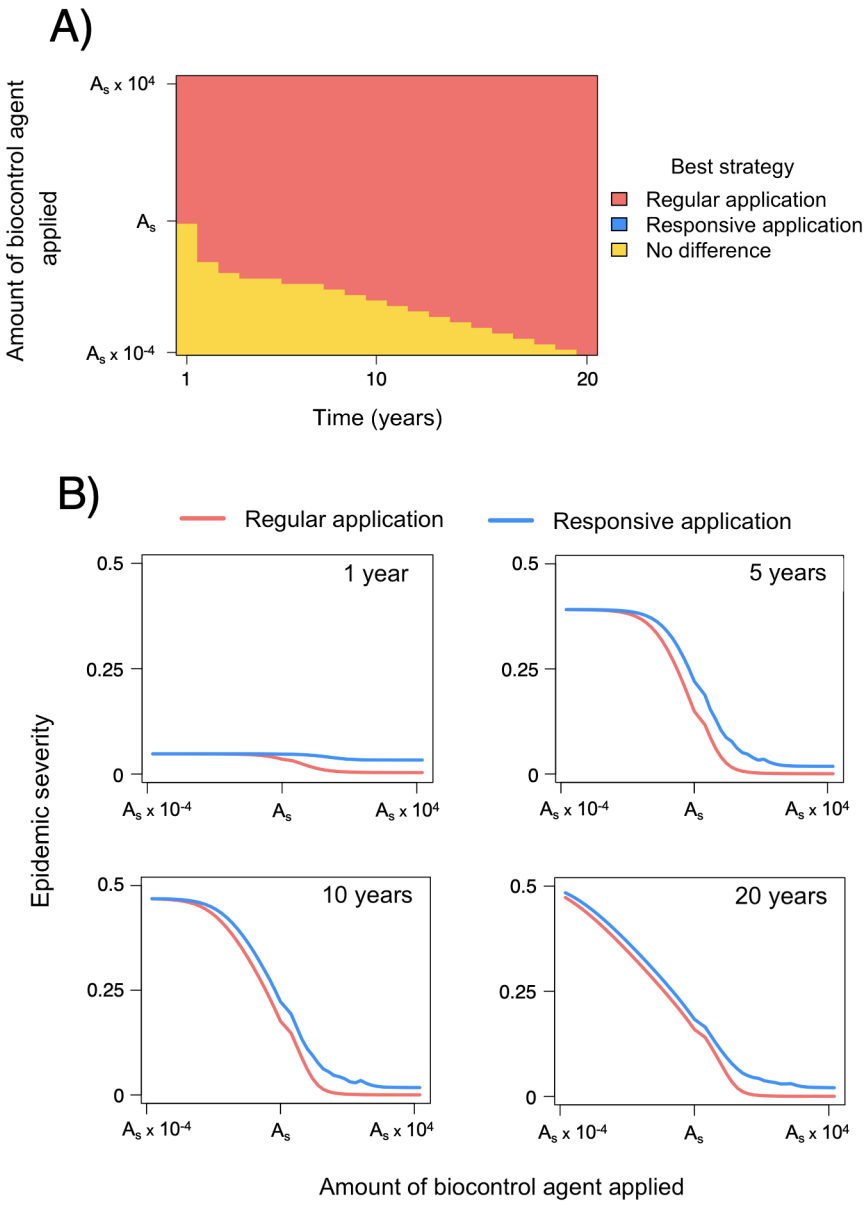

Fig. 5.10 Comparison of regular application and responsive application of a biocontrol agent on epidemic severity. Both application strategies require visiting the crop four times a year, with regular application applying the same amount of biocontrol agent each time, whereas responsive application varies the amount dependent on the percentage of infected roots present. A) Determining whether regular or responsive application is the most successful at disease suppression. A strategy is determined to be more successful than the other if it is able to reduce the epidemic severity by >1%. B) Differences in epidemic severity between regular application and responsive application over 1 year, 5 years, 10 years, and 20 year simulations. The amount of biocontrol agent applied, shown on A) the y-axis and B) the x-axis, is represented by a log scale (Model: "competition only").

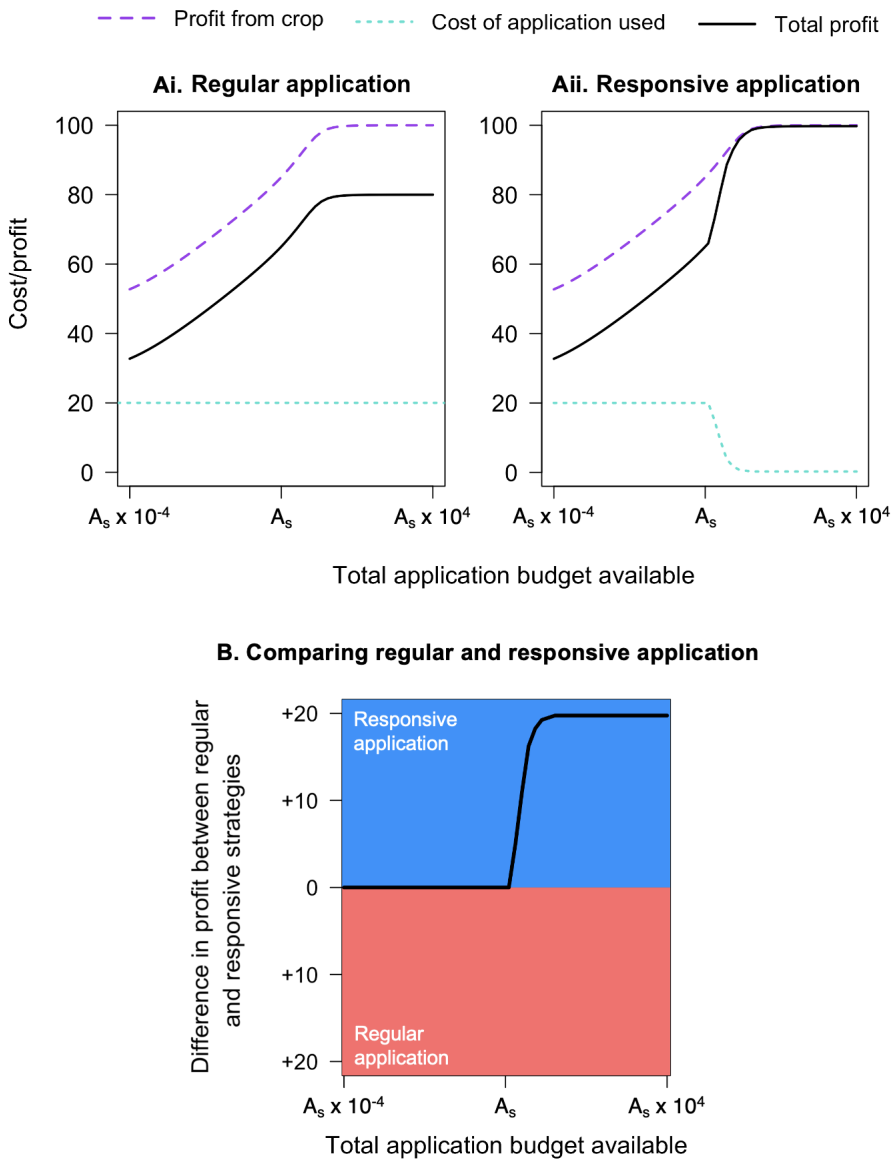

Fig. 5.11 Difference in the total cost of application and the profit obtained from a healthy crop for responsive and regular application. Both application strategies require visiting the crop four times a year, with regular application applying the same amount of biocontrol agent each time, whereas responsive application varies the amount dependent on the percentage of infected roots present. The cost of the total budget of application is 0.2. The proportion of healthy roots equals the profit obtained from a plant and can therefore vary between 0-1. A) The total profit for regular and responsive application strategies. Regular application will always use the entire budget, whereas responsive application will only apply the biocontrol agent is a threshold level of disease is reached. B) Comparison of the difference in profit between regular and responsive strategies (Model: "competition only").

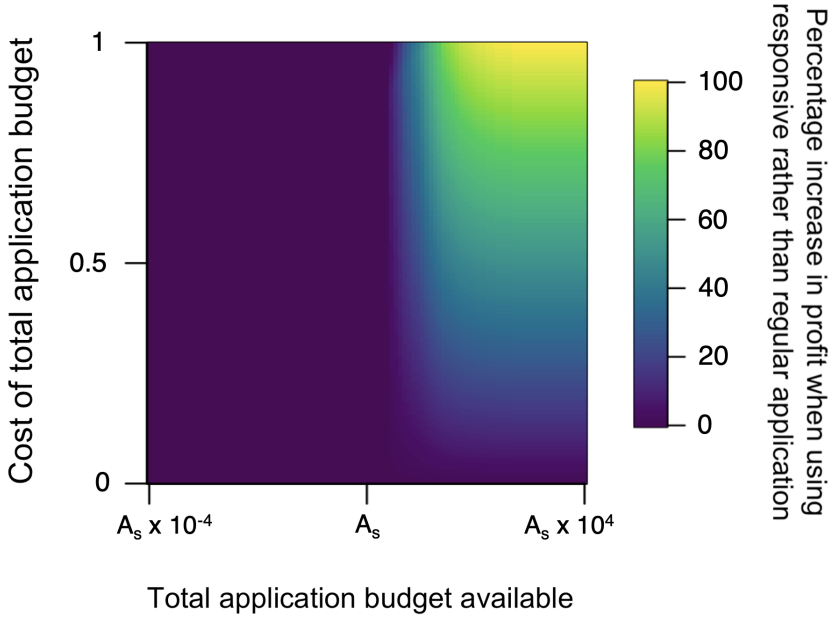

Fig. 5.12 Identifying whether regular or responsive application results in the greatest profit when both yield loss due to infection, and the cost of application, are considered. Both application strategies require visiting the crop four times a year, with regular application applying the same amount of biocontrol agent each time, whereas responsive application varies the amount dependent on the percentage of infected roots present. The regular application never results in a higher profit compared to responsive application. The plot therefore examines the percentage increase in profit when using responsive application rather than regular application as both the cost of the total application budget, and the total application budget available, vary (Model: "competition only").

5.4.4 Using a break crop to effectively suppress an epidemic

Four different ways that a break crop can be incorporated into a ten-year simulation are visualised in Figure 5.13Ai-v. The biocontrol agent is not included in these simulations, instead focusing on the plant's roots and the pathogen. Irregardless of strategy, there is a decline in the number of healthy roots in the second year that a winter wheat crop is grown consecutively. When the break crop is grown for a single year (Figure 5.13Ai and Aii), the number of healthy roots is lower for the season after this break compared to when the break crop is grown for two consecutive years (Figure 5.13Aiii and Aiv). The number of healthy roots when winter wheat is grown continuously without a break crop drops down to its lowest value in the third crop, and then remains at this level for the rest of the simulation (Figure 5.13Av).

When the profit of the break crop is fixed at 0.5, the amount that the break crop maintains the free-living pathogen population relative to winter wheat is fixed at 0.5, and the profit of the winter wheat crop can vary between 0-1 depending on the percentage of healthy roots, the yearly profit for each break crop strategy can be seen in Figure 5.13B. All crops have the same profit in the first year, and this is a relatively high profit due to minimal infected roots. If winter wheat is grown again in the subsequent year, there is a reduction in the number of healthy roots. There is always a high peak in profit for the first year that winter wheat is grown after a two year break due to a high number of healthy roots.

Calculating the cumulative profit from the profit obtained from each year of the simulation produced the values seen in Figure 5.13C. There is very little difference in the cumulative profit of each strategy for the first few seasons. However, towards the final year, there is a slight benefit of the strategy where two break crops are grown consecutively after each year of growing winter wheat (Figure 5.13Aiii), and a slight disadvantage of growing winter wheat continuously.

Figure 5.13 illustrates the profit of five strategies of growing a break crop when 1) the amount that the break crop maintains the free-living pathogen population relative to winter wheat is fixed at 0.5, and 2) the profit of the break crop is fixed at 0.5. As the amount that the break crop maintains the free-living pathogen population relative to winter wheat is varied between 0-1, and the profit of the break crop is varied between 0-1, the strategy that produces the highest overall profit can be seen in Figure 5.14. As the profit of the break crop increases, the optimal strategy is often determined to be growing winter wheat for a year, followed by growing a break crop for two years. When the amount that the break crop is able to maintain the free-living pathogen population relative to winter wheat is very low, the optimal strategy is either growing two consecutive years of winter wheat followed by growing two consecutive years of a break crop, or growing two consecutive years of winter wheat followed by growing a single year of the break crop. When the profit of the break crop is low, and the amount that the break crop maintains the free-living pathogen population relative to winter wheat is high, the best strategy is to grow winter wheat continuously. Growing a single year of winter wheat followed by a single year of the break crop was never found to be the best strategy.

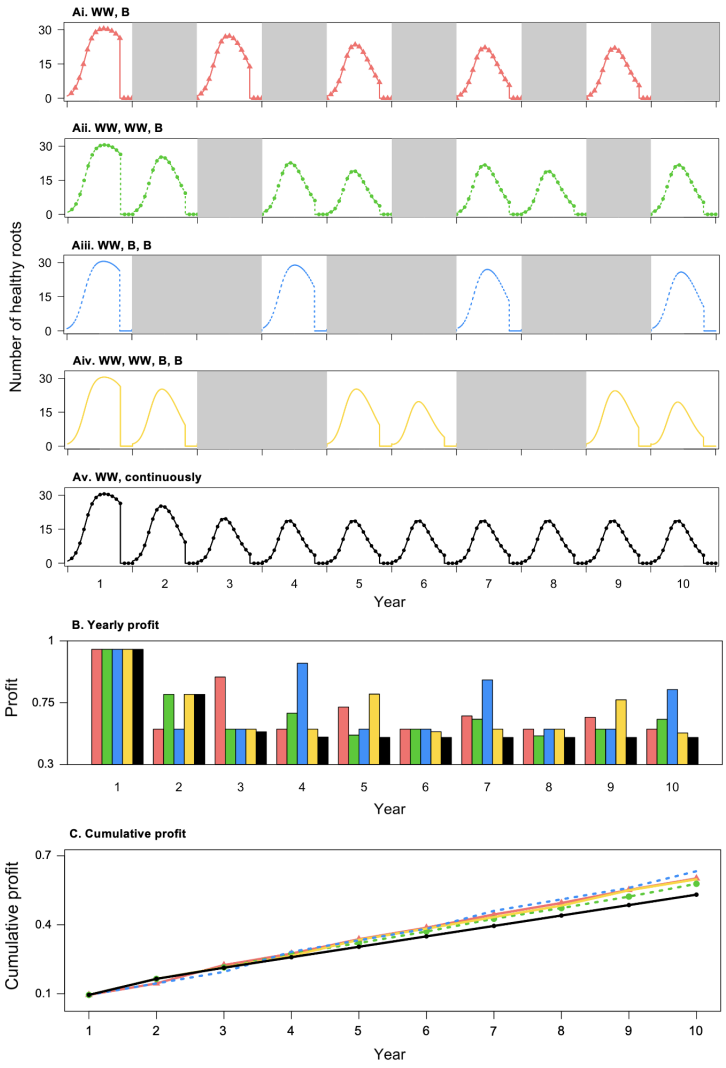

Fig. 5.13 Variation in the profit of an infected field across a ten-year simulation as the strategy of planting a break crop varies. A) Five strategies are compared: growing winter wheat every year (red), incorporating a break crop every other year of growing winter wheat (purple), incorporating a break crop every second year of growing winter wheat (blue), incorporating two years of break crop for every year of growing winter wheat (green), and incorporating two years of break crop for every two years of growing winter wheat (yellow). The number of healthy roots is shown for every year that winter wheat is planted, whereas each year that a break crop is planted is coloured grey. The amount that the break crop maintains the free-living pathogen population relative to winter wheat is fixed at 0.5. B) The profit for each year is calculated, where the profit for years in which winter wheat is grown depends on the proportion of healthy roots (Section 5.3.5), and the profit for years in which the break crop is planted are given a fixed value. In this plot, the profit of a break crop is fixed at 0.5. C) The cumulative profit across the ten-year simulation allows for a comparison between each strategy and identification of the optimal strategy. Determining whether a single strategy is optimal is explained in Section 5.3.5 (Model: "competition only").

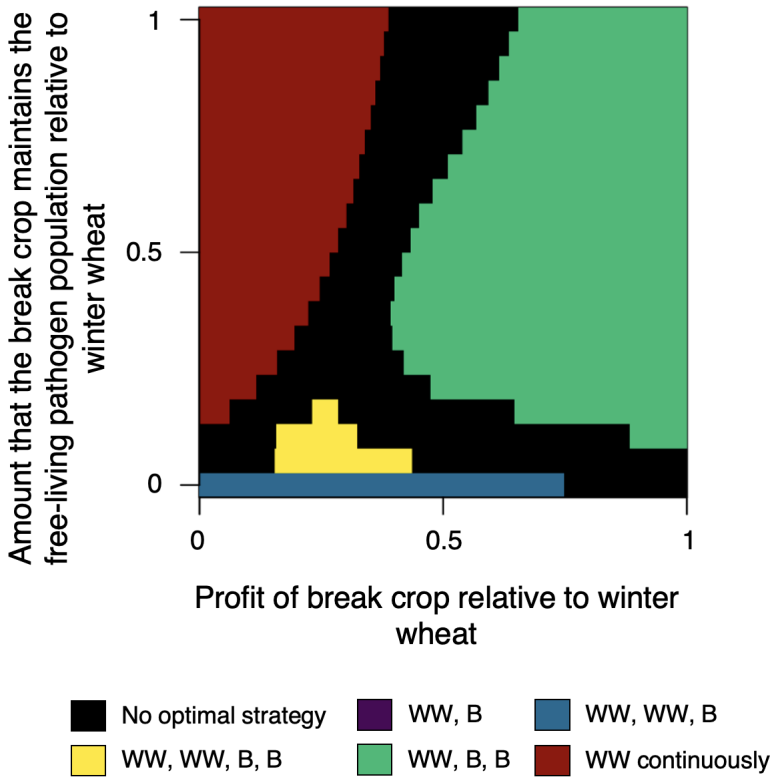

Fig. 5.14 Impact of incorporating a break crop on epidemic severity for winter wheat grown over a consecutive ten-year period, and identification of the most successful strategy. Five strategies are compared: growing winter wheat every year (red), incorporating a break crop every other year of growing winter wheat (purple), incorporating a break crop every second year of growing winter wheat (blue), incorporating two years of break crop for every year of growing winter wheat (green), and incorporating two years of break crop for every two years of growing winter wheat (yellow). Determining whether a single strategy is optimal is explained in Section 5.3.5. The biocontrol agent is not present in the model (Model: "competition only").

5.4.5 Comparison of models

Variation in the initial amount of biocontrol agent present

When the initial amount of biocontrol agent present at the start of a 20 year simulation is allowed to vary between $A_S \times 10^{-4}$ and $A_S \times 10^4$, and there is no additional application after this, the epidemic severity never exceeds 0.4 across the four model variations (Figure 5.15). This is different to the "competition only" model (Figure 5.2) where lower application amounts result in an epidemic severity of close to 0.6. The biocontrol agent is still able to suppress the pathogen to an extent when application is low for these models, whereas for the "competition only" model, a low application results in minimal biocontrol activity whilst it is at a low level in the soil.

As with the "competition only" model, epidemic severity was less than 0.1 during the first season regardless of application amount across all model variations. For all model variations, lower application amounts than A_S resulted in an increase in epidemic severity for the first years of the simulation, followed by a decrease and plateau of infection at a lower level in later years that is consistent with take-all decline. As the application amount decreased, the duration of the peak in epidemic severity for the models including "competition/out-competed by A" (Figure 5.15A) or "competition/out-competed by C" (Figure 5.15B) increased for a similar number of years to that seen in the "competition only" model (Figure 5.2). However, for the models that included "competition/death of I" (Figure 5.15C), or "competition/death of X" (Figure 5.15D), the peak in epidemic severity never lasted longer than 11 years before plateauing at a lower level.

Regular application of a biocontrol agent

Across the four model variations and four application strategies, the only application strategy determined to be the most successful at reducing epidemic severity is when all

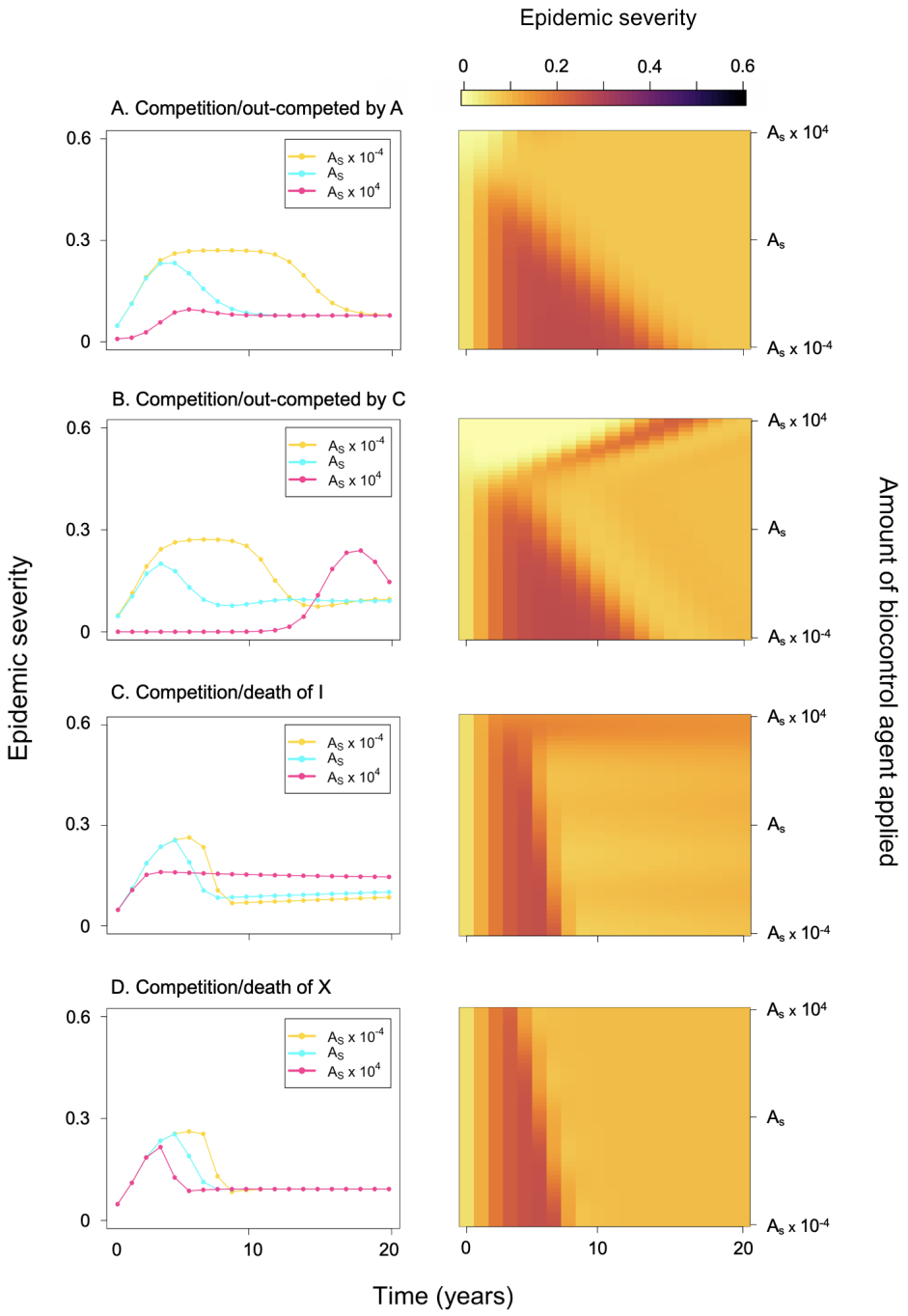

Fig. 5.15 Change in epidemic severity across a 20 year simulation for four variations of the SIXCA model as the amount of biocontrol agent present at the start of the simulation is varied between $A_S \times 10^{-4}$ - $A_S \times 10^{4}$. The amount of biocontrol agent applied, shown on the y-axis for the four plots on the right hand side, is represented by a log scale (Models: four model variations).

of the biocontrol agent is applied at the start of the first season (Figure 5.16A). This is most frequently determined to be the most successful application strategy for the "competition/out-competed by A" model. This success can be attributed to providing maximum time for the pathogen to bulk up in the soil. Likewise the least successful application is often identified when the biocontrol agent is applied once per season, due to providing less time for the pathogen to bulk up, as well as a rapid decay of free-living material resulting in minimal epidemic suppression later on in each season. However, for the "competition/out-competed by A", "competition/out-competed by C", and "competition/death of I models", the least successful strategy is sometimes determined to be application once at the start of the first season. This occurs at very high application amounts and for simulations that are run for a multiple years (Figure B.2). The additional mechanisms included into these models that the biocontrol agent can use to affect the pathogen require the presence of the pathogen. As the pathogen is completely suppressed at high application amounts, the biocontrol agent cannot bulk up from this interaction, and therefore steadily declines over successive years. It eventually reaches a low enough level that the pathogen can begin to infect the plant, therefore reducing the success of this strategy. This is explored more in Figures B.3 and B.4.

The duration of time taken before suppression caused by take-all decline (TAD_{sup}) occurred varied depending on the model variation and the application strategy (Figure 5.17). The "competition only" model has a greater range of years over which TAD_{sup} occurred, and the "competition/death of I" and competition/death of X" models has the lowest range. There was minimal impact of application strategy on the range of years that TAD_{sup} could take to occur across the five models. This suggests that the pathogen is able to increase to a similar population size across all application strategies within the first few years of a simulation.

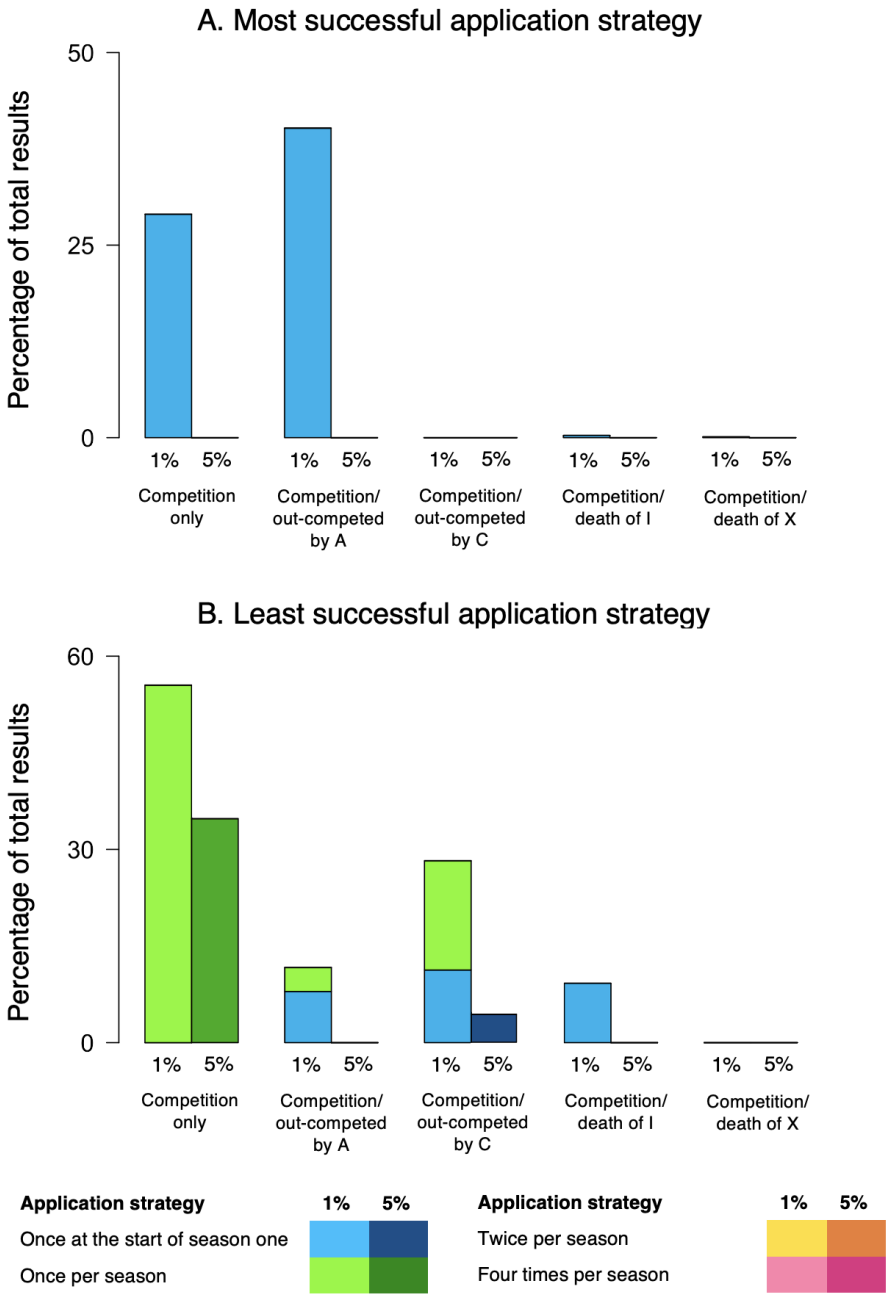

Fig. 5.16 Most and least successful strategies for the application of a biocontrol agent to suppress disease severity across five variations of the SIXCA model. A strategy was determined to be the most successful if it reduced the epidemic severity by >1% or >5% more than any other strategy. A strategy was determined to be the least successful if it increased the epidemic severity by >1% or >5% more than any other strategy (Models: all models).

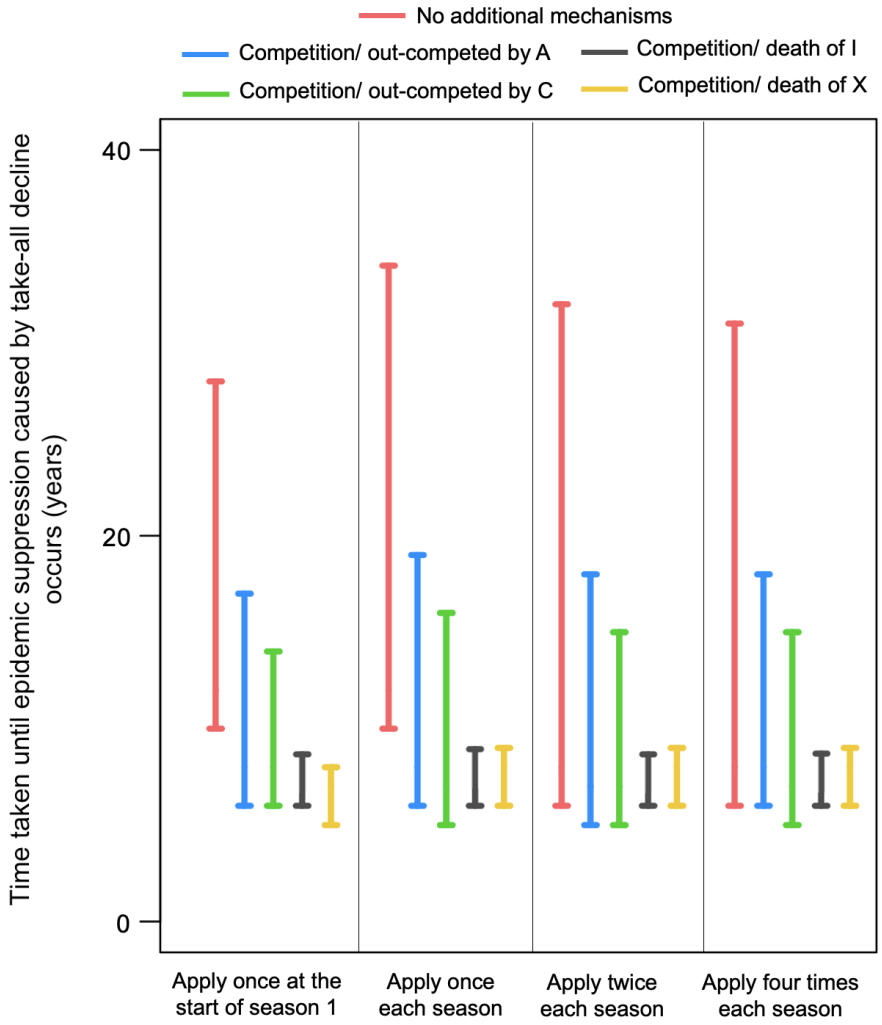

Fig. 5.17 Variation in the duration of time taken before suppression of take-all (TAD_{sup}) occurs for different application strategies, with a total application budget between $A_S \times 10^{-4}$ - $A_S \times 10^{4}$ (Models: all models).

Using a responsive model to determine application timing

As seen for the "competition only" model (Figure 5.9), there is minimal effect of inspection frequency on epidemic severity when looking at the four other variations of the SIXCA model (Figure 5.18). Regular application of the biocontrol agent four times a year, and responsive application, where a field is inspected for disease four times each year and application amount determined by Equation 5.5, were compared to examine their effects

on epidemic severity (Figure 5.19). Across the models, there was never an increase in profit when regular application was used. However, there was also rarely an improvement of responsive application. The entire application is almost always used up for responsive application, even when the total application budget is high. These models are not able to suppress the pathogen to levels as low as for the "competition only" model (Figure 5.12), and therefore the threshold for biocontrol application is more regularly met.

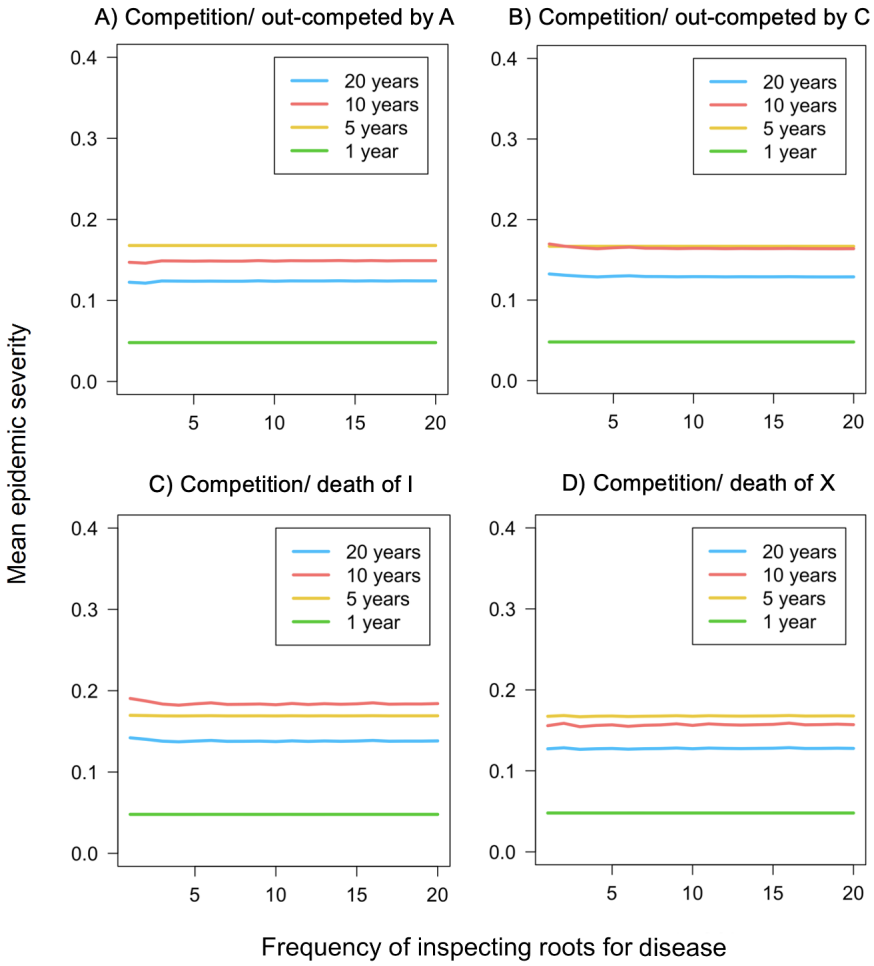

Fig. 5.18 Variation in the mean epidemic severity for responsive application as the frequency that a plant's roots are inspected for disease each season varies, with the total budget of biocontrol agent fixed at A_S. Results are obtained for simulations performed over A) 1 years, B) 5 years, C) 10 years, and D) 20 years (Models: four model variations).

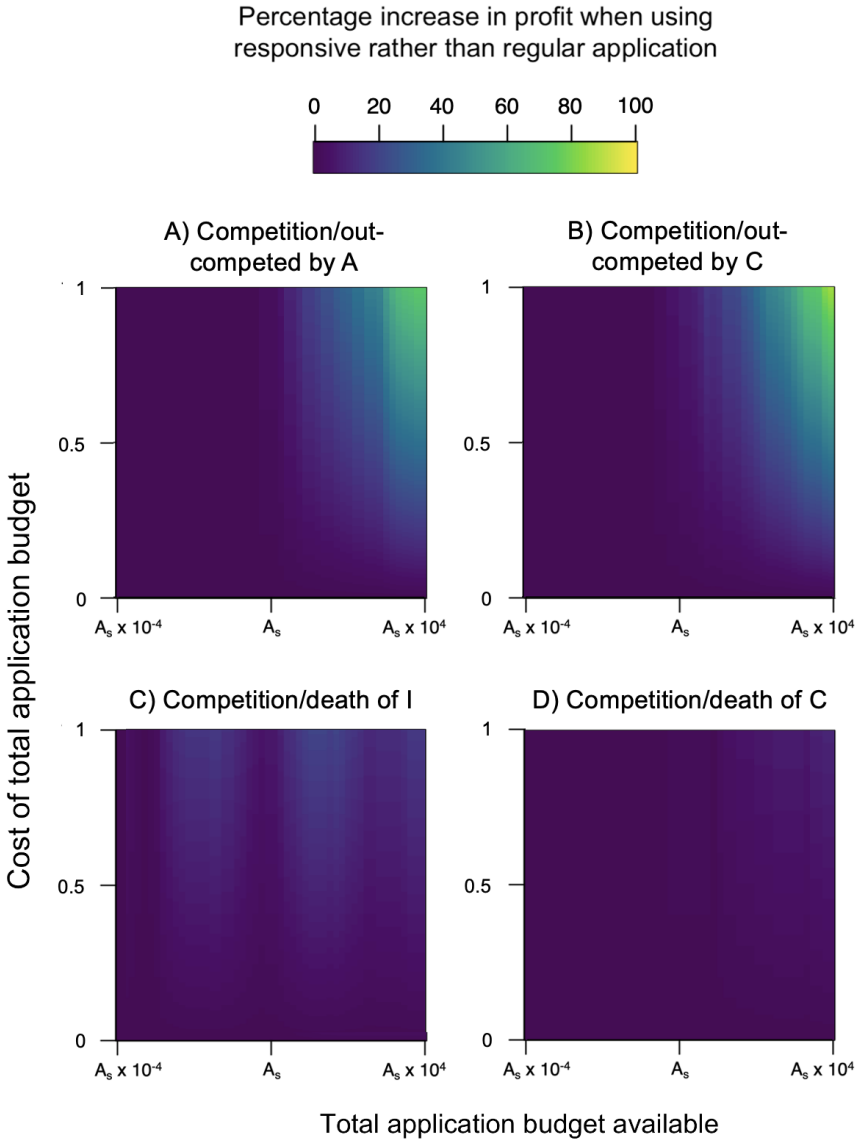

Fig. 5.19 Identifying whether regular or responsive application results in the greatest profit across four variations of the SIXCA model, when both yield loss due to infection, and the cost of application, are considered. Both application strategies require visiting the crop four times a year, with regular application applying the same amount of biocontrol agent each time, whereas responsive application varies the amount dependent on the percentage of infected roots present. The regular application never results in a higher profit compared to responsive application. The plot therefore examines the percentage increase in profit when using responsive application rather than regular application as both the cost of the total application budget, and the total application budget available, vary (Models: four model variations).

Using a break crop to effectively suppress an epidemic

Comparing five different break crop strategies for a 10 year simulation produced very similar results for all five model variations (Figure 5.20). When the biocontrol agent was not included in the model, and the profit of the break crop strategy was low, the optimal strategy was found to be growing winter wheat continuously. However as the profit of the break crop increased, there was either no optimal strategy determined, or the optimal strategy was either to grow two years of winter wheat followed by a year of the break crop, or growing one year of winter wheat followed by two years of the break crop. When the biocontrol agent was included in the model simulations, growing winter wheat continuously was found to be the optimal strategy more regularly. Continuous winter wheat was often found to be the optimal strategy as it provides a host for the biocontrol agent and allows it to remain at high population sizes in the soil. As a break crop can reduce the size of a biocontrol agent population by not being a suitable host, it reduces the ability of the biocontrol agent to suppress the pathogen.

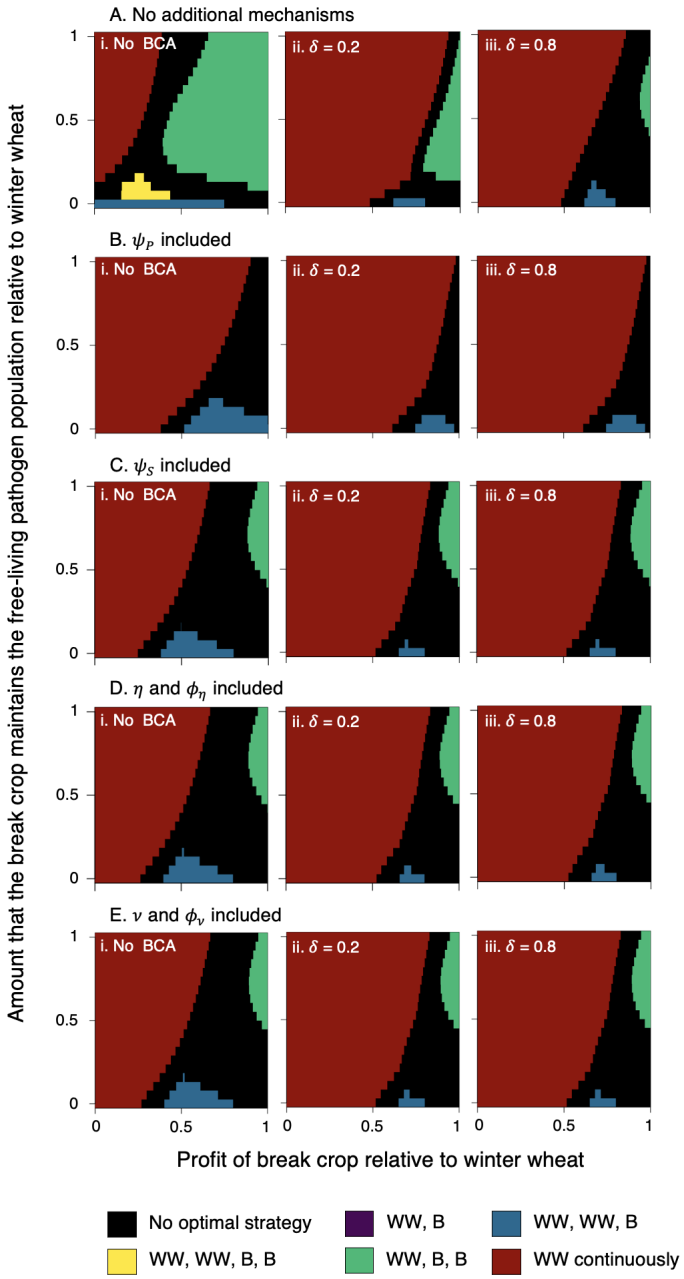

Fig. 5.20 Impact of incorporating a break crop and biocontrol agent on epidemic severity for winter wheat grown over a consecutive ten-year period, and identification of the most successful strategy. Five strategies are compared: growing winter wheat every year (red), incorporating a break crop every other year of growing winter wheat (purple), incorporating a break crop every second year of growing winter wheat (blue), incorporating two years of break crop for every year of growing winter wheat (green), and incorporating two years of break crop for every two years of growing winter wheat (yellow). Determining whether a single strategy is optimal is explained in Section 5.3.5. The biocontrol agent is either (i) not present in the model, or the ability for the free-living biocontrol agent to survive on the break crop relative to winter wheat (δ) is set at (ii) 0.2 or (iii) 0.8 (Models: all models).

5.5 Discussion

5.5.1 Single application of a biocontrol agent

Simulating the application of a biocontrol agent at the start of the first season when winter wheat is grown continuously can represent a naturally occurring population. The value A_S represents this amount and therefore varying this amount can give us an idea of how low or high naturally occurring biocontrol agent populations can affect epidemic severity across multiple years. Lowering the amount of biocontrol agent at the start of the first season resulted in a higher mean epidemic severity across the 20-year simulation for the "competition only" model. This was both due to a higher epidemic severity in the seasons where epidemic severity peaked, and due to a greater number of seasons where the epidemic was at this peak value.

Some farmers grow wheat continuously, either due to a high demand for cereal crops, or environmental conditions reducing the profitability of alternative crops (Andrade et al., 2011; Chng et al., 2015; Durán et al., 2017; Li et al., 2002; Lithourgidis et al., 2006). One of the reasons for expecting a high profit for wheat will be due to the hope of a decrease in epidemic severity after around two to three years of planting due to take-all decline. These results suggest that take-all decline may take considerably longer than this if there is an initial low population of free-living biocontrol agent in the soil. These results may also help to explain the difference in duration of take-all decline across different experimental work, ranging from 2-3 years (Baker and Cook, 1982; Shipton, 1972; Walker, 1975) to 12-15 years (Cook, 1988; Raaijmakers et al., 1997), to never occurring (Durán et al., 2017; Hornby, 1998). For farmers who do not have the money available to add biocontrol agents to the soil, they must ensure that the conditions are met to keep naturally occurring populations high enough to provide adequate disease suppression. This could be through ensuring that any previously planted crops, as well as the continuous wheat crop,

enhance rhizosphere competence and make the biocontrol agent more effectively colonise the crop's roots. This can be through choosing cultivars that are strongly able to support DAPG-producing pseudomonads, as well as adding fertiliser and other soil treatments to stimulate their growth (Kwak et al., 2012; Meyer et al., 2010; Okubara et al., 2004).

High application of the biocontrol agent at the start of the first growing season for the "competition only" model can result in complete disease suppression. This suggests that it may be advantageous to apply a large amount of biocontrol agent once at the start of the first season, and that the biocontrol agent can maintain its population size and continue to suppress the disease for many years after this application. However, a plant's roots are thought to have a carrying capacity for microbial relationships and are only able to support a specific number of microorganisms (Handelsman and Stabb, 1996; Newman, 1985). This suggests that, over a certain limit, any additional biocontrol agent would be a waste and would have no increased impact on epidemic suppression. This seems to be the case with this chapter's research too, where complete disease suppression occurs for application amounts lower than the maximum. There may also be a negative impact of introducing too much biocontrol agent. For example, *Pseudomonas fluorescens* introduced to the rhizosphere of wheat crops can become phytotoxic at high concentrations and cause damage to a plant's roots (Bull et al., 1991).

Although take-all decline is now believed to be caused by 2,4-DAPG fluorescent *Pseudomonas* spp. (Kwak et al., 2012; Kwak and Weller, 2013; Raaijmakers and Weller, 1998; Raaijmakers et al., 1997; Weller, 2015), multiple other microorganisms in the soil are thought to enhance and sustain this beneficial relationship (Campbell, 1989; Schlatter et al., 2017; Weller et al., 2002). Applying an excessive amount of a biocontrol agent may lead to a highly competitive rhizosphere and may lead to the death of other microorganisms, resulting in a lower overall suppression of take-all.

The other four models that were analysed responded differently to variation in application dose. For all of the models, decreasing the application amount resulted in higher epidemic severity through increasing the number of years where epidemic severity was high. However, the maximum duration of this peak was shorter for the "competition/death of I" and "competition/death of X" models. The mechanisms of disease suppression by the biocontrol agent therefore seems to have an impact on the duration of take-all decline and the overall severity of the disease. At maximum application levels for the "competition/death of X" model, and at close to maximum levels for the "competition/death of I" model, there is no significant reduction in epidemic severity. Unlike with the "competition only" model, there is still a peak in disease before suppression to a lower level. Higher application isn't as advantageous in this case as there is only a small difference in mean epidemic severity across different application amounts.

For high application amounts with the "competition/out-compete with C" and the "competition/out-compete with A" models, complete disease suppression is achieved for the first few years of the epidemic. However, gradual decay of the free-living biocontrol agent over time results in a late peak of epidemic severity, before take-all decline occurs and the epidemic severity is suppressed to a lower level. Successful epidemic suppression requires the establishment and maintenance of a certain population size for the biocontrol agent, and dropping to below this may eliminate or reduce epidemic suppression (Suslow, 1982; Xu and Gross, 1986).

All of these models can help to explain why take-all decline occurs over different periods of time in the real world. Both the initial amount of biocontrol agent, as well as the strategies used by the biocontrol agent to suppress the pathogen, can have a considerable impact on epidemic severity. Long amounts of time before suppression caused by take-all decline occurs could be due to very small starting amounts of the biocontrol agent, or reasons for increased decay of the biocontrol agent. These reasons include certain environmental

conditions, competition from other soil-borne biocontrol agents, lack of nutrients, soil type, or cultivar of crop grown. Short amounts of time before suppression occurs suggests that a large amount of initial biocontrol agent is present in the soil, or that there are conditions that allow the biocontrol agent to bulk up quickly and easily. A lack of take-all decline but constant high disease severity could just be because a field trial hasn't run for long enough and the biocontrol agent was initially present at a very low level (and take-all decline will eventually happen if left long enough), or it could mean that the necessary biocontrol agent isn't present (or decays too quickly due to a variety of conditions). Likewise, a lack of take-all decline and very low disease severity could be due to very high amounts of the biocontrol agent present in the soil – it is able to successfully suppress take-all without the need for take-all decline to occur. The peak of an epidemic may also be delayed, as with the "competition/out-compete with C" and "competition/out-compete with A" models, but this peak may then happen several years later.

Although there are problems associated with applying too much biocontrol agent, it should be noted that application amount should often be higher than the amount determined to be optimal in controlled experiments. Adams et al. (1984) suggested from laboratory experiments that the lowest amount of biocontrol agent that could be applied to the soil to suppress *Sclerotinia minor* was 22kg/ha. However Deacon (1988) notes that the experiment involved thoroughly mixing spores into the soil, which could not be done to the same extent across a field. Xu and Hu (2020) found that spatial aggregation of the biocontrol agent, which will be higher without thoroughly mixing the biocontrol agent into the soil, reduced its ability to suppress a pathogen. A suitable amount of biocontrol application determined from a laboratory experiment should therefore be thought of as an absolute minimum application amount for use in a field, and that it would be beneficial to apply more to account for a reduced amount of mixing in the field's soil. Biocontrol agent applied to the seeds of a crop may also not survive for long enough to colonise the plant's roots, or some

of the biocontrol agent may be out-competed by other microorganisms in the rhizosphere. A careful look at application amount and biocontrol survival in field trials should be done to ensure that application occurs at an optimal amount for epidemic suppression.

5.5.2 Regular application of a biocontrol agent

There is minimal difference in epidemic severity across application strategies, regardless of the mechanisms used by the biocontrol agent. However, there is a often slight decrease in epidemic severity when applying all of the biocontrol agent at the start of the first season, and a slight increase when applying once at the start of every season. Applying all the biocontrol agent at the start of the first season allows it to suppress the pathogen whilst the pathogen exists at low levels. Proactively applying the biocontrol agent before the pathogen has had time to multiply has been found to be an effective strategy across multiple systems (Adams and Ayers, 1982; Htay and Kerr, 1974; Kerr, 1980; Moore, 1979; Sutton and Peng, 1993). This application method also requires the least effort, applying as a seed coating or at the time of planting (Mathre et al., 1999). However, this is a risky strategy as it requires the biocontrol agent to be highly competitive and persist in the rhizosphere long term. The rhizosphere is an incredibly competitive place, and biocontrol agents are known to rapidly decay after introduction (Cook, 2003, 1988). Environmental conditions can also severely affect microorganisms, and a single application would be at risk of being completely eliminated due to unsuitable conditions (Fravel, 2005; Steddom and Menge, 2001). It would be impossible to grow a break crop in between wheat crops too, as an unsuitable host will lead to rapid decay of the free-living material, and a reduction in epidemic suppression in the next season. Finally, it is more likely that the incorrect amount of biocontrol agent would be applied with a single application, either applying too much and wasting money, or applying too little and still having high epidemic severity.

Applying at the start of every season is sometimes unsuccessful due to the rapid decay of the biocontrol agent, coupled with the fact that it doesn't have a maximal amount of time to bulk up in the soil compared to the single application method. By the time the pathogen has established and begun to infect the roots of a plant, the biocontrol agent will have decayed to levels that are too low to effectively suppress it. Applying the biocontrol agent multiple times per season allows it to be applied whilst the pathogen is present and infecting the plant. As the biocontrol agent decays rapidly, the introduction of more biocontrol agent throughout a season can result in a large increase in population size relative to current levels. Repetitive application has been seen as a successful strategy across multiple experiments (Bahme, 1988; Freeman et al., 2004; Hoy, 1992; Martensson, 1990; Steddom et al., 2002; Steddom and Menge, 2001). Although repeated application requires more manual effort, it benefits from being less affected by environmental conditions and maintains populations at a level that is neither too low or high. It also reduces the impact of competition in the rhizosphere with other microorganisms. There may therefore be more benefits to repeated application if certain environmental factors were included in the model.

The application strategy did not have a significant impact on the duration of take-all decline across the five models. However, there was a considerable difference in the number of years that take-all decline took to occur depending on the application amount and the model variation chosen. This may also help to explain some of the variability in the amount of time taken before suppression caused by take-all decline occurs in the real world.

5.5.3 Applying the biocontrol agent responsively

There was minimal improvement in the suppression of an epidemic when applying a biocontrol agent in response to specific infection levels compared to regular application regardless of epidemic severity. However, only applying a control strategy in response

to detecting a specific amount of disease is common in farming, including for soil-borne diseases (Fang and Ramasamy, 2015; Fox, 1990, 1997; Homan and Clausen, 1996; Lievens et al., 2006; Mumford and Norton, 1984; Porter et al., 1997; Schillhorn van Veen et al., 1998; Tang et al., 2010). It allows for the control strategy to only be bought and used if required, reducing the amount spent trying to suppress multiple diseases that may have no or minimal impact on the crop. A higher overall profit can therefore be obtained using responsive application through minimal application costs and high epidemic suppression.

The total budget available for application was fixed within this chapter to allow for an easier comparison between different application strategies. However, in an agricultural setting, a crop grower is not likely to have a fixed budget for their control strategy, instead applying what they determine to be the optimal application amount as and when required. There therefore needs to be a careful consideration as to how high the budget of application can be, taking into consideration factors such as the size of a field, the expected profit of the crop, and the cost of the application. These factors will vary between locations and years, and a cost-benefit analysis of application amount therefore needs to be regularly performed.

The use of responsive application requires additional manual effort compared to regular application, as a field must be examined for disease prior to any application taking place. This manual effort is increased further for soil-borne plant pathogens as they often have no or minimal above-ground symptoms, and therefore more complex examinations of a crop's roots must take place. Any benefit from the use of responsive application should therefore be weighed against the increased manual labour and the time taken to thoroughly inspect a field for disease.

We found no benefit of increasing the frequency of inspecting a field for disease more than once a season. Although this allows for successful application with minimal manual labour, the benefit of more repeated application due to a smaller impact of environmental

conditions should be considered. There must therefore always be a careful analysis as to the reduced manual effort from fewer inspections per season compared to the decreased risk from more applications per season.

5.5.4 Using a break crop to effectively suppress an epidemic

Break crops are commonly used to reduce the epidemic severity of take-all and other soil-borne diseases of wheat. The rate of pathogen decay for take-all is known to be rapid, significantly reducing the inoculum available after a break crop. The decay is so rapid that even a year's break, or planting winter wheat later in the season than is typical, can reduce epidemic severity (Cook, 1993; Schippers et al., 1987; Yarham, 1986). However, take-all is known to still remain in the soil after a break crop, albeit at lower levels. This is seen with our results, where the pathogen is able to persist in the soil after a break and cause infection in the next season that winter wheat is grown. Regardless of how a break crop is used, epidemic severity was still relatively high the next year that winter wheat was grown. Combining a break crop with other control methods may therefore be necessary to successfully suppress the pathogen.

Across the break crop strategies when the biocontrol agent was not present, the highest number of healthy roots are obtained in the first season of winter wheat after a break crop, as well as after two years of growing the break crop. However, although the use of break crops results in a greater number of healthy roots, they are likely to have a lower profit compared to winter wheat. The use of a break crop is therefore only beneficial if it is able to suppress the pathogen enough to increase crop yield in the seasons where winter wheat is grown, as well as providing enough profit from winter wheat to offset the lower profit of the break crop.

Although the profit of the break crop is varied between 0-1 in these results, it is likely to be between 0.7-1 for real break crops (Angus et al., 2015; de la Pasture and Allen-Stevens,

2017). Within these bounds, the results show that two strategies produce a higher overall profit than the others. These are 1) growing two years of winter wheat followed by a year of a break crop, and 2) growing one year of winter wheat followed by two years of a break crop. The former strategy is optimal when the amount that the break crop maintains the free-living pathogen relative to winter wheat is low, and the latter strategy is optimal when this is high. Choosing the best timing for break crops is therefore dependent on the break crop chosen and how it interacts with the pathogen. Unless information is known about this, incorporating a break crop may not reduce epidemic severity as much as expected.

Combining control strategies together is often suggested to increase effectiveness and lead to greater suppression of the pathogen. However, little work has been done on what impact combining these strategies together can have on their success. This research found that using both a biocontrol agent and break crop together often led to an ineffective control strategy. As the biocontrol agent needs a host crop to sustain its population size and allow it to bulk up in the soil, a break crop can result in a reduction in this population size and therefore a reduction in the ability for the biocontrol agent to suppress the pathogen (Baker and Cook, 1982; Cook and Rovira, 1976). Fluorescent *Pseudomonas* spp. are well known to vary in population size depending on the crop planted as well as which crop cultivar is used (Bergsma-Vlami et al., 2005; Botelho and Mendonça-Hagler, 2006; Ganeshan and Kumar, 2005; Rotenberg et al., 2007). When the biocontrol agent was included in the simulation, the optimal strategy was often found to be growing winter wheat consecutively without any breaks due to the decrease of free-living biocontrol agent when a break crop was grown. This was the case apart from when the break crop has a very high profit. Unlike often thought, combining control strategies is seen here to actually decrease epidemic suppression and not be beneficial.

5.5.5 Conclusions

The use of biocontrol agents as viable control strategies is often rejected due to variable effects over field trials and different environmental conditions. It is worth reminding ourselves that these are living organisms, and that effective use of them will require a strong understanding of them and how they interact within the rhizosphere. One of the important factors to consider must be application amount and timing. The research in this chapter has shown how epidemic severity is affected by frequency of application, amount of application, and the mechanisms that the biocontrol agent uses to suppress the pathogen. Application of a biocontrol agent multiple times during a season would be suggested to reduce the impacts of environmental factors and competition within the rhizosphere. Determining the correct amount to apply will involve experimentation, with both too much and too little producing detrimental results.

The combined use of control strategies, or even the combined use of different biocontrol agents, is often suggested to increase epidemic suppression (Cook, 2003; Deacon, 1988; Fravel, 2005; Pal and McSpadden Gardener, 2006; Ruano-Rosa and Mercado-Blanco, 2015; Singh et al., 2012; Whipps and Davies, 2000). However, this research found that combining two control strategies can have a negative impact on epidemic suppression. It is vital that the crop, pathogen, and biocontrol agent, as well as the interactions between these three, are extensively researched through both field and experimental work, as well as through modelling. Biocontrol agents can not only suppress pathogens but can also promote crop growth (Alori and Babalola, 2018; Antoun and Prévost, 2006; Kumar and Verma, 2019; Welbaum et al., 2004), making them invaluable components of maximising crop yield and profit. Optimising the application of them, and ensuring that they are not negatively impacted by other control strategies, should therefore be a main focus of future research on crop control strategies.

Chapter 6: Small-scale spatial modelling of take-all disease on winter wheat

6.1 Abstract

Soil-borne plant pathogens will often produce patches of infected plants. Inoculum in the soil will infect the roots of a single plant, and the pathogen can then spread out radially from this point by moving between the roots of neighbouring plants that are in close contact. Due to this, the spatial arrangement of crops can have a significant impact on epidemic severity. Spatial modelling of a plant disease can allow for a detailed examination of pathogen spread and how the spatial arrangement of plants can be optimised to reduce this spread. There was a focus on the take-all pathogen, *Gaeumannomyces graminis* var. *tritici*, on the roots of winter wheat plants throughout this analysis.

Dispersal kernels for primary and secondary infection were incorporated into the SIX model, which examines the interactions between the roots of a host plant and a soil-borne pathogen. Plants were spatially modelled and equally spaced apart. Starting from a single central source of inoculum, epidemic spread was examined over a season as both the scale of dispersal and the space between crops was varied. Parameter values were identified for the dispersal kernels that produced patches of infected plants between 15-35cm. This spread was identified in the literature as being typical for *Gaeumannomyces graminis* var. *tritici*.

Host growth was incorporated into the model to allow for the rate of secondary infection to vary depending on how far apart the plants were spaced from each other, as well as how this distance between-plants reduces as the roots of both plants grow closer to each other.

The rapid lateral growth of wheat roots, coupled with the close planting of crops in an agricultural setting, resulted in fast contact between the roots of different plants. There was therefore minimal effect of host growth on epidemic severity.

The effect of crop spatial arrangement on epidemic severity was examined across a two-year simulation. Between-season dispersal was incorporated into the model to represent the dispersal of pathogen inoculum by agricultural machinery between harvesting and replanting. Four spatial arrangements were examined: evenly spaced, and rows with 12.5cm, 25cm, or 50cm space between them. Each arrangement had the same density of plants. During the first season there was a reduction in epidemic severity when the crops were planted in 12.5cm rows or were evenly spaced. Between-season dispersal removed any benefit of spatial arrangement and therefore all spatial arrangements had similar epidemic severity values in the second season. The impact of these results on optimising crop planting are discussed.

6.2 Introduction

6.2.1 Spatial modelling of soil-borne plant diseases

Incorporating spatial dynamics into a model allows us to examine the spread of a disease and how pathogen dispersal can affect an epidemic. Short-distance pathogen dispersal that results in small clusters of infected hosts needs to be spatially modelled on a different scale compared to long-distance pathogen dispersal with infected hosts sparsely spread out over a larger area (Esker et al., 2008; Thrall and Burdon, 1999). Examining spatial heterogeneity of infection across host plants can help identify which control methods may be effective, predicting where the epidemic is going to spread and how wide the area of control should be (Bailey et al., 2004; Cunniffe et al., 2016; Gilligan et al., 2007; Meentemeyer et al., 2011; Stacey et al., 2004).

The scale of pathogen dispersal, as well as how widely distributed a pathogen is across a specific area, can impact observable patterns of disease. For example, a wind-borne pathogen may easily spread across a field and cause infection across a wide area. Even if it was initially present at a single location, it may soon spread across an entire field or further. A more informative spatial scale may therefore be across multiple fields rather than across individual plants. However, a pathogen with a shorter range of dispersal may form easily observable clusters of infection across a small area of plants, and therefore looking at a spatial scale across a small section of a field may be more beneficial.

If a pathogen is located at multiple points in a field or is dispersed across the field within a short period of time, it can be difficult to examine epidemic spread and determine where the epidemic began. A common approach to this is to ignore spatial dynamics and instead focus on the mean level of infection across a large area (Li et al., 2012; Perry, 1995). However, this ignores the often patchy distribution of plant pathogens and is likely to result in over- or under-estimating the pathogen prevalence and epidemic severity. SADIE (Spatial Analysis by Distance Indices) is one method that has been created to analyse spatial patterns between individuals, and can be used for plant epidemics to identify patches of disease and epidemic spread (Winder et al., 2019; Xu and Madden, 2003, 2004).

The use of computational simulations can also examine epidemic spread through incorporating spatial dynamics into a model. Incorporating spatial dynamics can be especially important for soil-borne plant diseases as pathogen dispersal within a crop growing season is often very restricted. This can result in small clusters of infected plants due to slow spread of the pathogen through the soil and the ability to only infect nearby hosts (Bailey et al., 2000; Campbell and Noe, 1985; Chellemi et al., 1988; Cook, 2003; Ettema and Wardle, 2002; Gilligan, 1995). Restricted movement of pathogen inoculum means that most spread of infection within a growing season can only occur due to contact between the roots of nearby neighbouring plants (Brain and Marshall, 1999; Cotterill and Sivasithamparam,

1988; Gilligan, 1980; Grundy et al., 1999; Marshall and Brain, 1999; Truscott and Gilligan, 2001). Focusing on the mean level of infection across an experimental plot, and assuming spatial homogeneity of the pathogen, may therefore not give an accurate representation of the landscape of infected hosts. This may reduce the ability to understand the pathogen dynamics and identify successful control strategies for suppressing the pathogen.

6.2.2 Spatial heterogeneity of take-all disease

Take-all disease is commonly known to occur in patches under wet conditions (Clarkson and Polley, 1981; Cook, 2003; Gosme et al., 2007; Hornby, 1998; Hornby et al., 1989; Kwak and Weller, 2013; Prew, 1980b). Pathogen inoculum can only grow several millimetres through the soil, relying on the nearby roots of a plant to grow close to any inoculum before infection can occur (Brown and Hornby, 1971; Garrett, 1936; Gilligan, 1980; Pope and Jackson, 1973; Warcup, 1957; Wildermuth et al., 1984). Patches of infected plants are formed by root-to-root contact between the infected and susceptible roots of neighbouring plants (Cook, 2003; Paulitz et al., 2002), resulting in a progressive spread of disease outwards from a source of inoculum (Gosme and Lucas, 2011; Prew, 1980a).

The lateral growth of wheat roots are capable of reaching up to 75cm under optimal conditions and with no other plants present in the surrounding soil (Manschadi et al., 2006). However, wheat plants are often spaced less than 5cm apart (Abichou et al., 2019; Kemp et al., 1983; Koscelny et al., 1990; Robertson et al., 2004; Salgado et al., 2017; Teich et al., 1993). This results in significant overlap between the roots of different plants, and therefore a high likelihood of infection spreading between-plants, producing the characteristic patches of disease.

Although most studies focus on the mean level of take-all infection across an experimental plot (Bailey et al., 2009; Moore and Cook, 1984; Polley and Clarkson, 1980; Schoeny et al., 2001; Werker et al., 1991), there is some research into cluster sizes and epidemic spread.

From a single infected plant or source of inoculum over one growing season, infection spreads slowly outwards though root-to-root contact between-plants. Disease intensification within a crop growing season is thought to occur more within a cluster than through spread across many plants (Gosme and Lucas, 2011; Gosme et al., 2007), with concentrated clusters of highly infected plants common. Experimental studies that recorded this spread from a central location of inoculum can be found in Table 6.1. The distance of epidemic spread within a growing season varies between studies, from no spread (Gosme et al., 2007) to a maximum of 75cm spread (Wehrle and Ogilvie, 1956). All research apart from Prew (1980a) and Gosme and Lucas (2011) only recorded a maximum distance of pathogen spread rather than a mean or average. This is likely to give an overestimate of the typical spread within a season and can be heavily influenced by any outliers. Gosme and Lucas (2011) did not state an exact distance of spread but mentioned that the effect of pathogen inoculum was reduced by 95% at a distance of 15cm away from the location of pathogen incoulum. This means that there is a 95% reduction in the chance of a plant becoming infected during a single growing season once it is 15cm away from the source of pathogen inoculum, suggesting that within-season spread was unlikely to be seen further away than this distance. Prew (1980a) recorded an average spread of 10cm. Although Gosme et al. (2007) recorded no within season-spread, their quadrat size of 0.5x0.5m will have reduced their ability to look at small scale plant-to-plant spread, with the values from Gosme and Lucas (2011), Prew (1980b) and Willocquet et al. (2008) all estimating that cluster size is less than or equal to 0.5x0.5m. The most accurate recordings of cluster size are likely to be from Gosme and Lucas (2011) and Prew (1980b), as they record the average spread of infection as well as examining spread between individual plants or small areas of plants rather than using large quadrats.

Although within-season spread of many soil-borne pathogens is minimal, there is often greater pathogen dispersal between growing seasons due to mechanical cultivation. Methods

Table 6.1 Spread of take-all disease across plants from one source of pathogen inoculum at the end of a single growing season. Seed density was converted from kg/ha to seeds/m^2 in Prew (1980b) for an easier comparison with the other experiments.

Author	Within-season spread of infection from a source of inoculum	Crop spatial arrangement	Additional information
Gosme and Lucas (2011)	Around 15cm	Rows (14cm apart), broadcast sowing, and hill sowing (19 cm between hills across sowing rows, 50 cm between hills within rows). All had a seed density of 300 seeds/m^2	The effect of pathogen inoculum was reduced by 95% at a distance of 15cm away from the point of infestation. There was no effect of crop spatial arrangement on within-season spread of infection
Prew (1980b)	Average 10cm, maximum 18cm	Rows (18cm apart) with a seed density of 400 seeds/m^2	
Willocquet et al. (2008)	Maximum 20cm (line-sowing), maximum 25cm (broadcast sowing)	Rows (14cm apart) and broadcast sowing. Both had a seed density of 300 seeds/m^2	
Gosme et al. (2007)	No spread	Rows and broadcast sowing. Both had a seed density of 300 seeds/m^2	Data was from the second year of an experiment, when infected clusters were between 0.5m x 0.5m and 2.5m x 2.5m
Adam and Colquhoun (1936)*	Maximum 51cm (plants 5cm apart), 41cm (plants 10cm apart), and 20cm (plants 20cm apart)	Evenly spaced in both directions	Garrett (1936) believed that soil conditions were favourable for pathogen spread
Suzuki et al. (1957)*	Maximum 12cm, 30cm, and 45cm		Garrett (1936) believed that soil conditions were favourable for pathogen spread
Wehrle and Ogilvie (1956)	Maximum 75cm	Rows (7 inches and 10 inches apart)	Prew (1980b) assumed that high spread was either due to environmental conditions or because the pathogen was already distributed throughout the field

* Paper could not be directly accessed; information obtained from Prew (1980b)

such as ploughing, harrowing, and seed drilling can move material in the soil over several metres from its original location (Brain and Marshall, 1999; Grundy et al., 1999; Marshall and Brain, 1999; Truscott and Gilligan, 2001). This increased between-season dispersal results in larger clusters in the second or third year of consecutively growing wheat infected by take-all disease (Hornby et al., 1989). The size of second year clusters from a single source of inoculum introduced at the start of the first season can be found in Table 6.2. Prew (1980b) found that, for wheat grown for the first time in an experimental plot, mechanical dispersal of the pathogen before the crop was planted resulted in cluster sizes up to 2.5m x 2.5m. This further suggests that most epidemic spread occurs due to mechanical dispersal between crop growing seasons.

There are considerable differences between the cluster sizes shown in Table 6.2, from 0.5m x 0.5m to uniform incidence across a field. Prew (1980a) assumed that the uniform incidence found in their experiment was due to prior dispersal of the pathogen throughout the field before their experiment began. If an experiment begins the year after wheat infected by take-all was grown, the pathogen will still be present and could therefore impact the study. Certain break crops and weeds can also sustain the take-all pathogen and increase the time taken for it to decay. It is therefore vital that experiments involving take-all have at least a year between the last winter wheat crop grown and the experiment beginning, as well as ensuring that any break crop grown does not allow the pathogen to persist and be able to infect the next crop. The cluster size in Oliver et al. (2003) is large, but this will be significantly affected by only collecting data at 24m intervals. The values of 0.5m x 0.5m - 2.5m x 2.5m from Gosme et al. (2007) and 2m x 2m from Cotterill and Sivasithamparam (1988) are therefore likely to be the most accurate recordings of cluster size in the second growing season.

Table 6.2 Size of area occupied by plants infected by take-all disease in the second year of consecutively growing winter wheat that has been infected by the pathogen. The pathogen was introduced at the start of the first growing season at a single location. Seed density was converted from kg/ha to seeds/m^2 in Prew (1980a) and Cook et al. (2002) for an easier comparison with the other experiments.

Author	Second year size of infected plant cluster	Crop spatial arrangement	Additional information
Gosme et al (2007)	0.5m x 0.5m - 2.5m x 2.5m	Rows and broadcast sowing. Both had a seed density of 300 seeds/m^2	
Oliver et al. (2003)	Up to 72m x 75m	Rows	Data only recorded at 24m intervals
Cotterill and Sivasithamparam (1989)	Average 2m x 2m		Cluster size calculated by Gosme et al. (2007) using data from this paper
Prew (1980a)	Uniform incidence, no clusters	Rows (18cm apart) with a seed density of 240 seeds/m^2	Author assumed that pathogen was already distributed throughout the soil at the start of the experiment
Cook et al. (2002)	Uniform incidence, no clusters	Rows (18-19cm apart) with a seed density of 156 seeds/m^2	Author assumed that conditions were too dry to allow take-all to spread through root-to-root contact

6.2.3 Spatial arrangement of crops

Patches of infection due to take-all disease are dependent on close contact between the roots of neighbouring plants, allowing runner hyphae to grow between-plants. Although dispersal of pathogen inoculum through mycelial growth is on the scale of millimetres (Brown and Hornby, 1971; Garrett, 1936; Gilligan, 1980; Pope and Jackson, 1973; Wildermuth et al., 1984), lateral growth of roots can reach up to 75cm (Manschadi et al., 2006), allowing overlap between even sparsely planted crops. The chance of the roots of two plants coming into contact with each other will decrease as the distance between-planting locations increases. However, close contact between-plants is necessary to allow for sufficient profit to be obtained. Optimising crop location to reduce epidemic spread and severity therefore needs to work under the constrains that plants will be in close contact and that some will get infected, but that this should be minimised as much as possible.

Many crops, including wheat, are planted in rows to enhance yield, reduce competition for resources, and allow for mechanical weed control (Abichou et al., 2019; GRDC, 2011; Kolb et al., 2012; Mertens and Jansen, 2002). Between row spacing can vary between approximately 5cm and 40cm (Abichou et al., 2019; Kemp et al., 1983; Koscelny et al., 1990; McLeod et al., 1997; Nagelkirk and Pennington, 2019; Robertson et al., 2004; Salgado et al., 2017). There is always a difficulty when planting crops on determining the optimal number that should be planted to maximise profit. Planting at a high density with narrow rows and tightly packed plants maximises the number of plants that can be harvested. However, plants that are too close to each other will compete for resources and light, and are likely to produce a lower yield per plant than crops spaced further apart. Even if the optimal number of seeds to plant can be determined, experimental work has found significant conflicts in whether narrow or wide row spacing is optimal for crop yield. The most accepted view is that narrow row spacing optimises crop yield due to an increase in productive tillers, and the optimisation of light and nutrients (Ali et al., 1999; Hussain et al., 2012; Kirkland, 1993;

Lee and Herbek, 2010; Sandler et al., 2015). However, narrow rows will increase interrow competition and have been found to decrease yields compared to wider rows in some field experiments (Lafond et al., 1999; Pandey et al., 2013). There is also conflicting research when trying to obtain the optimal row spacing for disease suppression. Cook (2001) states that wide rows may be advantageous for the suppression of soil-borne diseases due to a greater soil surface exposed, as well as an increase in distance between-plants from different rows. This allows for increased warming and drying of the soil which are unfavourable conditions for the spread of diseases such as take-all. Glynne (1951) and Salt (1957) found that there was a reduced incidence of eyespot disease in wheat when wider rows were used, and Legard et al. (2000) found the same for Botrytis fruit rot in strawberries. Wider rows have also been found to reduce disease severity for Sclerotinia blight on peanuts (Maas et al., 2006), *Cercospora apii* blight on celery (Berger, 1975) and *Cercospora beticola* on groundnut (Muhammad and Bdliya, 2015). However, other research has found no effect on the width of row spacing on the epidemic severity of soil-borne wheat (Bailey et al., 1998; Lafond, 1994) and barley (Piening, 1983) diseases.

Other crop planting patterns have been found to have an effect on the epidemic severity of soil-borne plant diseases, including paired-row spacing (two rows very close together with wider spaces in between these pairs) (Cook, 2001), planting parallel to a previous year's rows (Garrett et al., 2004), and using broadcast or hill sowing (Gosme and Lucas, 2011). It is possible that previous experimental work has been affected by environmental conditions, soil type, and cultivars used, causing such disparity in the results of how crop spacing affects epidemic severity. A computational examination of epidemic spread across different spatial planting patterns may therefore allow for less variable results to be obtained.

6.2.4 Incorporating host growth

The term pathozone represents the volume of soil surrounding a host plant in which a pathogen must occur if it has a chance of causing infection (Gilligan, 1985). For wheat roots, which can have a lateral spread of up to 75cm (Manschadi et al., 2006) and reach a depth of over 2 metres (Fan et al., 2016; Rasmussen and Thorup-Kristensen, 2016; Weaver, 1926), the pathozone can cover a large volume of soil for root-to-root spread of infection. Although the chance of a pathogen causing infection towards the edges of the pathozone are minimal, the likelihood will increase as a crop's roots grow and come into closer contact with neighbouring plants over time.

It is uncommon for epidemiological models between either a plant and a pathogen, or a plant, pathogen, and biocontrol agent, to incorporate spatial dynamics (Gubbins and Gilligan, 1997c; Park et al., 2001; White and Gilligan, 1998; Xu and Jeger, 2013a). Any spatial variation in infection rate is usually ignored, instead assuming that the chance of infection between two neighbouring plants remains constant over time. However, Leclerc et al. (2013) determined that incorporating host growth into a model for the fungus *Rhizoctonia solani* on sugar beet could change an epidemic from non-invasive to invasive due to a reduced spacing between host plants during a growing season. If the roots of two plants were too far away from each other, there would be no between-plant secondary infection. Likewise, once the roots of two plants have grown enough to be touching, the rate of between-plant secondary infection would reach a maximum value.

Incorporating host growth into Leclerc et al. (2013) is relatively simple to define due to most of the growth of the host crop, sugar beet, occurring at a large central taproot. This has a well determined circumference that varies over time, with a decrease in the space between the taproots of different plants throughout the season. Incorporating host growth of wheat roots is more difficult as the roots can spread at multiple angles and different roots will grow at different rates. Even if the roots of two plants grow enough to be capable

of touching, they may not have grown at the same angle or depth in the soil to allow them to come into close contact with each other. However, incorporating growth into a model may still give invaluable insights into optimal crop spacing and pattern. Examining how host growth affects an epidemic may suggest how spatial distribution of host plants can be optimised to reduce contact between-plants and minimise the spread of disease through a population.

6.2.5 Key questions

This chapter will focus on the following key questions:

1. Can parameter values for primary and secondary infection dispersal kernels be determined, producing cluster sizes similar to those mentioned in the literature?
2. Can the variation between within-season and between-season spread be determined, examining the importance of both of these on epidemic spread and severity over two growing seasons?
3. How does adjusting the spatial arrangement of plants affect disease severity within a field?
4. Does host growth, and the subsequent variation in the rate of between-plant secondary infection throughout a growing season, have an effect on epidemic severity and cluster size of infected plants?

There will be a focus on small-scale dynamics, covering a maximum area of 2.5m x 2.5m. This area size was chosen as it was a compromise between 1) having a large enough area to simulate epidemic spread and pathogen dispersal, and 2) reducing simulation times and computational effort. This allows for a detailed analysis about how clusters of take-all spread across individual plants in the first two years of an epidemic, and how the spatial arrangement of crops can affect this spread.

6.3 Methods

6.3.1 The SIX model

The SIX model is described in detail in Section 2.2. It is extended within this chapter to spatially model the spread of a soil-borne disease across multiple host plants, each of which has its own root system. Each plant is located at a particular spatial position in the model, whereas the roots within a single plant are individually modelled but do not have further spatial structure. Infection by the pathogen can occur through free-living pathogen in the surrounding soil, through root-to-root spread within a single plant, and between root-to-root contact of different plants. The model is seasonal to account for the removal of crops each year due to harvesting, as well as the dispersal of free-living inoculum between growing seasons. Crops are planted at the same spatial locations each year. Between growing seasons when the crop is no longer present, only the free-living pathogen is present within the model.

Spatial distribution of the crop

Each host plant is given a set of Cartesian (x,y) coordinates to represent the centre of the plant's location. Although the individual roots of a plant are not spatially represented, it is assumed that they grow outwards from this point and can interact with the roots of neighbouring plants through a dispersal kernel. The average density of pathogen inoculum in the region surrounding each plant is also modelled. Plants are thought to be either evenly spaced or in rows, as would be typically found in an agricultural field. Examples of crop spatial arrangements are shown in Figure 6.1, where each green dot represents a single plant's location.

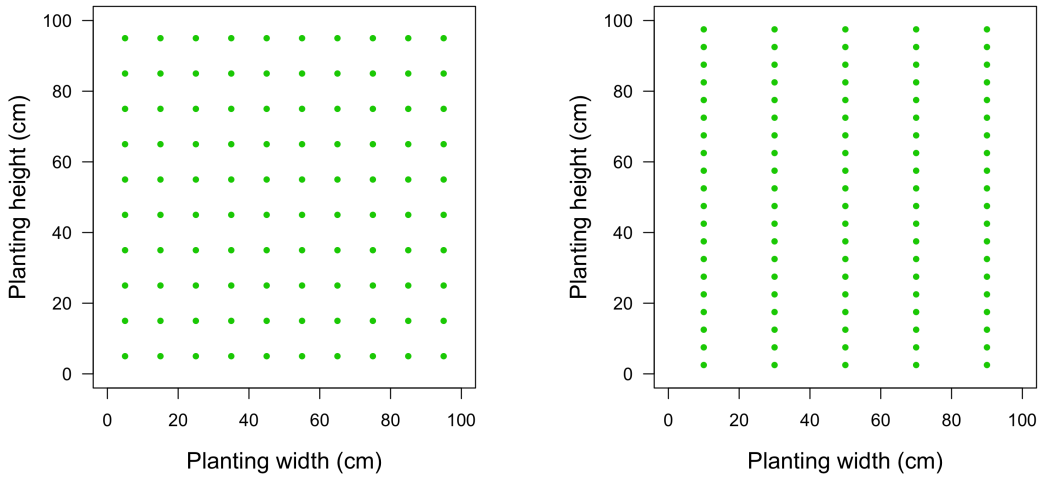

Fig. 6.1 Examples of the possible spatial distributions of plants included in the spatial SIX model. The location of each plant is represented by a green dot, and both plots contain 100 plants. Each plant in the left plot is spaced equally apart whereas the plants on the right are grouped into five rows.

Within-season dynamics for each plant

Once a host plant has been planted and is present in the field, any roots that grow can be either susceptible (S) or infected by the pathogen (I). Free-living pathogen (X) is also present in the surrounding soil. The rate equations for a single plant are

$$\frac{dS}{dt} = \rho(S+I)\left(\frac{\kappa-(S+I)}{\kappa}\right) - \beta_p S \sum_{k=0}^{4} X_k \frac{1}{2\pi\gamma_X^2}\exp\left(-\frac{d_k}{\gamma_X}\right) \tag{6.1}$$
$$-\beta_s S \sum_{k=0}^{4} I_k \frac{1}{2\pi\gamma_I^2}\exp\left(-\frac{d_k}{\gamma_I}\right),$$

$$\frac{dI}{dt} = \beta_p S \sum_{k=0}^{4} X_k \frac{1}{2\pi\gamma_X^2}\exp\left(-\frac{d_k}{\gamma_X}\right) + \beta_s S \sum_{k=0}^{4} I_k \frac{1}{2\pi\gamma_I^2}\exp\left(-\frac{d_k}{\gamma_I}\right) - \mu I, \tag{6.2}$$

$$\frac{dX}{dt} = -\lambda_X X, \tag{6.3}$$

with a summary of the parameters used and definitions for each included in Table 6.3, and a more detailed explanation of the dispersal kernel in Equations 6.4 - 6.10 and Figure 6.2.

This model is an extension of that found in Chapters (Need to include model fitting and application timing chapters) and all corresponding modelling decisions are identical.

Susceptible roots can become infected by the pathogen through primary (β_p) or secondary (β_s) infection. As well as roots within a specific host plant able to infect each other, the four nearest neighbour plants (north, south, east, and west of a host plant) can also cause infection. The rate of infection within a host plant and between nearest neighbour plants is determined by an exponential dispersal kernel for both primary and secondary infection. The scale parameter (γ_X for primary infection and γ_I for secondary infection) determines the effect of the distance between-plants on the force of infection. If the rate of between-plant infection (both primary and secondary) goes up due to a change in the kernel parameter, then the corresponding rate of within-plant infection goes down. This occurs due to the normalisation constant and is done under the assumption that the pathogen has many roots that it can reach and has the chance to infect, but has limited resources to infect them all. Some of the infection that would have spread between the roots of a single plant will now spread between the roots of different plants.

The distance between a specific host plant at location $[i, j]$ and its neighbours is denoted by d_k, where

- k = 0 at location [i,j] (within-plant infection)
- k = 1 at location [i,j+1] (infection by nearest neighbour from the north)
- k = 2 at [i+1,j] (infection by nearest neighbour from the east)
- k = 3 at [i,j-1] (infection by neighbour from the south)
- k = 4 at [i-1,j] (infection by neighbour from the west)

Table 6.3 List of parameters and definitions for the spatial and seasonal SIX model.

Parameter	Definition	Default value	Source
S	Number of susceptible roots	-	-
I	Number of roots infected by the pathogen	-	-
X	Density of free-living pathogen	-	-
X_s	Initial amount of free-living pathogen present at the start of the first growing season	25	Fixed
t	Time (degree days $> 0°C$)	-	-
ρ	Rate of root production	$3.31 \times 10^{-3}\ t^{-1}$	Chapter 3
κ	Carrying capacity of root production	32.1	Chapter 3
β_p	Rate of primary infection of roots by free-living pathogen	$1.35 \times 10^{-3}\ t^{-1}$	Chapter 3
β_s	Rate of secondary infection of roots	$5.92 \times 10^{-5}\ t^{-1}$	Chapter 3
λ_X	Rate of decay of pathogen inoculum	$3.53 \times 10^{-3}\ t^{-1}$	Bailey and Gilligan (1999); Bailey et al. (1995)
τ_I	Number of root fragments produced from a dead infected root when the host crop is harvested	3.16	Chapter 4
γ_I	Scale parameter for the dispersal kernel between susceptible roots and infected roots from different plants	0-4cm	-
γ_X	Scale parameter for the dispersal kernel between susceptible roots from one plant and free-living pathogen associated with a different plant	0-4cm	-
γ_B	Scale parameter for the mechanical dispersal of free-living pathogen between growing seasons	0-20cm	-

Between growing seasons - mechanical dispersal

During the between growing season period, free-living material can be picked up by agricultural machinery and dispersed over large distances due to mechanical processes such as ploughing and harrowing (Marshall and Brain, 1999). This dispersal can pick up any free-living pathogen and move it over a greater distance than it would be able to spread to through root-to-root infection during a crop growing season. This results in a larger area of soil that contains the pathogen compared to if there was no mechanical dispersal, and therefore can lead to more plants becoming infected during the next growing season. This between season dispersal has a large impact on cluster size and epidemic severity, and is therefore included in this research.

The chance of a piece of inoculum travelling a certain distance from its original location is assumed to decline exponentially as the distance increases, following a similar approach to that found in Truscott and Gilligan (2001), Grundy et al. (1999), Marshall and Brain (1999), and Stacey et al. (2004). Pathogen inoculum can be associated with the location of any host plant, and each of these locations is assumed to experience the same dispersal. Dispersal was modelled stochastically to incorporate an element of variation in the dispersal distance of material in the soil, as would be seen with agricultural machinery.

Plane polars are used due to the ease of calculating dispersal of inoculum from a central origin, with a schematic of dispersal from a central origin shown in Figure 6.2. The dispersal kernel is

$$K(R) = N \exp\left(-\frac{R}{\gamma_B}\right), \tag{6.4}$$

where N is the normalisation constant, R is the dispersal distance, and γ_B is the scale parameter. The area of a sector of an annulus between radii R and $R + dR$, and angles between θ and $\theta + d\theta$ is

$$dA = R\, dR\, d\theta, \tag{6.5}$$

and the probability of landing in this area is

$$P(R, \theta) = K(R)\, dA. \tag{6.6}$$

Obtaining the normalisation constant for the dispersal kernel requires solving

$$\int_R \int_\theta N \exp\left(-\frac{R}{\gamma_B}\right) R dR d\theta = 1, \tag{6.7}$$

and results in

$$N = \frac{1}{2\pi a^2}, \tag{6.8}$$

where a is the scale parameter that determines the mean dispersal distance. The chance of going anywhere at all within an annulus between radius R and radius R + dR will be equal to the area of the annulus ($2\pi R\,dR$) multiplied by the normalised dispersal kernel,

$$\text{PDF} = \frac{R}{a^2}\exp\left(-\frac{R}{\gamma_B}\right), \tag{6.9}$$

where PDF is the probability density function. This needs to be integrated to obtain the cumulative distribution function, CDF,

$$\text{CDF} = -\frac{R}{\gamma_B}\exp\left(-\frac{R}{\gamma_B}\right) + 1 - \exp\left(-\frac{R}{\gamma_B}\right), \tag{6.10}$$

which can then be used to determine the distance that each piece of inoculum can travel from its original location. The angle of travel must also be determined, and the steps needed for each dispersal event are:

1. Use inverse transform sampling on CDF to calculate the distance that the inoculum travels from the origin (D)

2. Generate a random deviate of the uniform distribution on $[0, 2\pi)$ to calculate the angle of travel (θ)

3. Calculate the cartesian coordinates of the newly dispersed inoculum, where $x = D\cos(\theta)$ and $y = D\sin(\theta)$

4. Determine which crop location this piece of inoculum falls closest to, and assign this as its new location

If inoculum falls outside of the crop planting area, is it discarded as available inoculum and removed from the model. This corresponds to the area being surrounded by completely uninfected plants, as there is no flow of infection from outside this area. This represents a single cluster of infected plants with no infected plants nearby. Clusters of infection are typical for take-all and other soil-borne pathogens (Cook, 2003; Weller et al., 2002). Dispersal occurs from a central location of pathogen inoculum for all computational simulations within this chapter, and scale parameters for within-season and between-season dispersal are low enough to negate the effects of any dispersal of free-living pathogen outside of the focus area. It is assumed that mechanical dispersal occurs only once each season, and that this is in the middle of the between-season period.

6.3.2 Obtaining suitable parameter values for within-season epidemic spread

The literature on within-season epidemic spread for take-all suggests that a cluster diameter of infected plants should be close to 15-35cm (Table 6.1). Obtaining a similar within-season spread of infection to the values found in Table 6.1 required suitable values for the scale parameters γ_X and γ_I to be determined. Values for γ_X and γ_I were varied between 0-4cm across separate simulations, and each simulation was run for a single growing season. This value was initially varied between 0-20cm, before further analysis reduced this down to focus on a smaller range of values. At the end of the growing season, the number of plants that had at least one infected root were counted. The maximum diameter of the cluster of infected plants, calculated as the greatest number of plants infected across a horizontal direction, was calculated to determine the maximum spread of infection within a season. Although the horizontal distance of pathogen spread was chosen to focus on, the same results would be obtained by focusing on the vertical distance. The desired cluster diameter

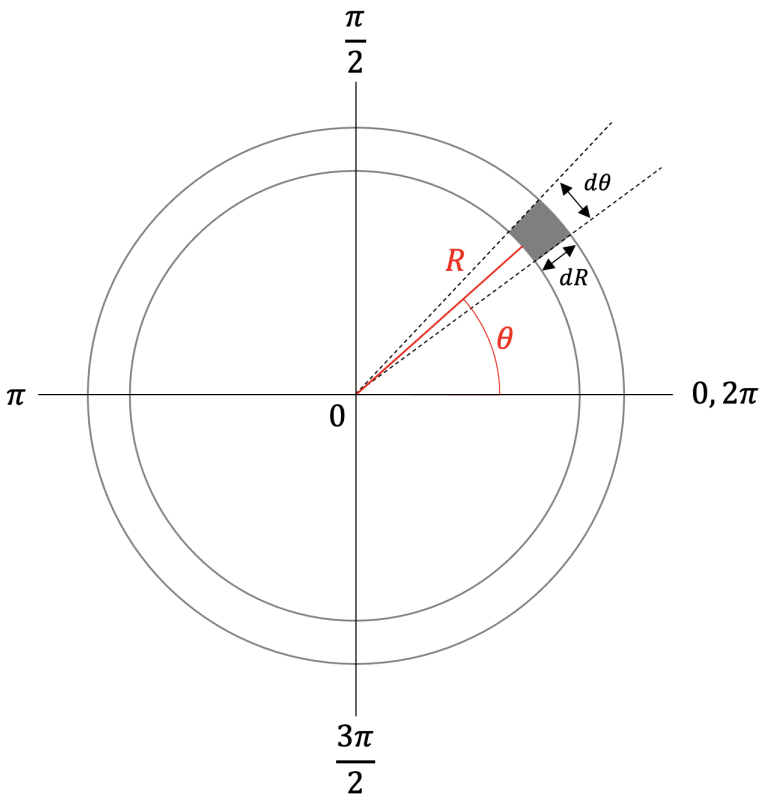

Fig. 6.2 Schematic of a dispersal event from origin 0 by kernel $K(R)$ to the area marked in grey using polar coordinates. The area is located between two circles with radii R and $R + dR$, intersected by lines at angles θ and $\theta + d\theta$. $K(R)\, dR\, d\theta$ is the probability of dispersal to an area between distance R and $R + dR$ from the origin, at a direction between θ and $\theta + d\theta$. Diagram is an edited version of Figure 15.3 from Nathan et al. (2012).

was between 15-35cm, which is a similar value to those found in the literature (Kabbage and Bockus, 2002; Prew, 1980a; Willocquet and Lebreton, 2005; Willocquet et al., 2008).

This analysis was carried out for crops evenly spaced between 1cm and 20cm apart. A visual representation of a 40x40cm area of crops is shown in Figure 6.3, showing how greater crop spacing results in fewer plants in a specific area. There is a large difference in the area occupied by 169 evenly spaced plants at different crop spacing values; crops spaced 1cm apart would take up a 13x13cm area, whereas crops spaced 20cm apart would take up a 260x260cm area. To allow for easier visualisation of the same number of crops but over different areas, each crop is assigned a grid square, with the plant at the centre of the grid.

This can be further visualised in Figure 6.4. Figure 6.4A represents a 60x60cm area where all crops present in the area are represented by a 1x1cm square, and any space in between crops is represented by grey. At 1cm crop spacing there are 3600 plants present, whereas at 10cm crop spacing there are only 9 plants. Removing this grey space and representing each plant as equally sized grid squares produces the plots shown in Figure 6.4B, where 169 plants are represented as occupying an identical amount of space regardless of the spacing between crops. This allows for an easier visualisation of epidemic spread, and is used throughout this chapter when looking at epidemic spread across evenly spaced plants.

Each simulation started with 25 units of pathogen inoculum placed at the same location as the central plant. This was to represent the introduction of a moderate amount of inoculum to a field that is capable of initiating an epidemic. Variation in the number of infected plants (plants with at least one infected root at the end of a growing season) as this initial amount of inoculum changes can be seen in Figure 6.5, where the maximum number of infected plants can reach 25 as the amount of inoculum increases. The number of infected plants varied between 0 and 25 as the initial amount of pathogen inoculum changed, and the chosen value of 25 units of pathogen inoculum resulted in 21 infected plants.

Although the desired cluster diameter was determined to be between 15-35cm, the number of infected plants that would be included in a cluster of this size will vary depending on the space between them. As the space between crops is varied between 1-20cm, more infected plants will be needed to form a cluster with a diameter between 15-35cm when the space between-plants is small, and fewer infected plants will be needed when the space between-plants is large. For example, a cluster diameter of 30cm could be achieved by 6 plants in a row that are spaced 5cm apart, or 3 plants in a row that are spaced 10cm apart.

Rather than focus on the total number of plants needed to produce a cluster with a diameter between 15-35cm, this research focuses on the horizontal spread of infection from

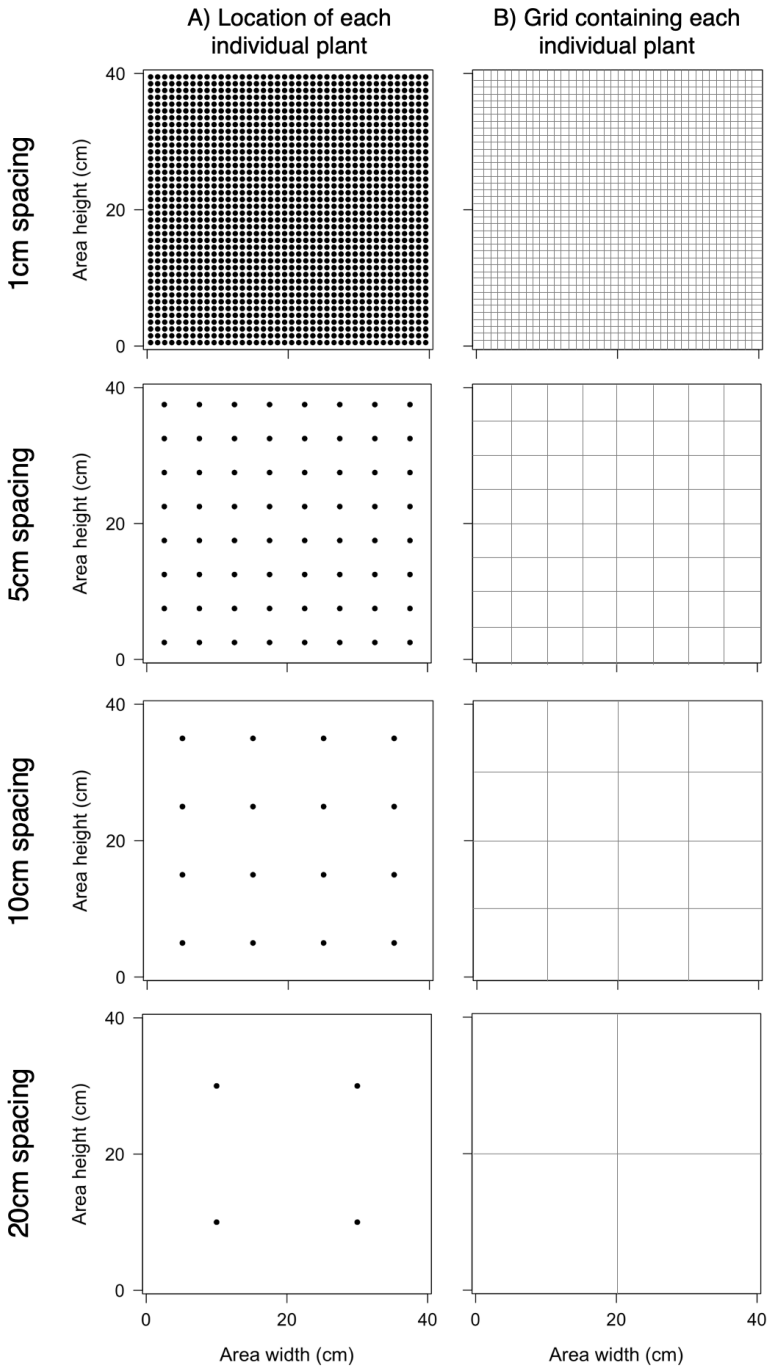

Fig. 6.3 Visualisation of an area of plants, where each plant is represented by A) a point, or B) a grid square. The total area is a 40x40cm square, and there are either 1cm, 5cm, 10cm, or 20cm spaces between-plants. When plants are represented by grid squares, each plant is placed in the centre of a grid square, with only one plant per square.

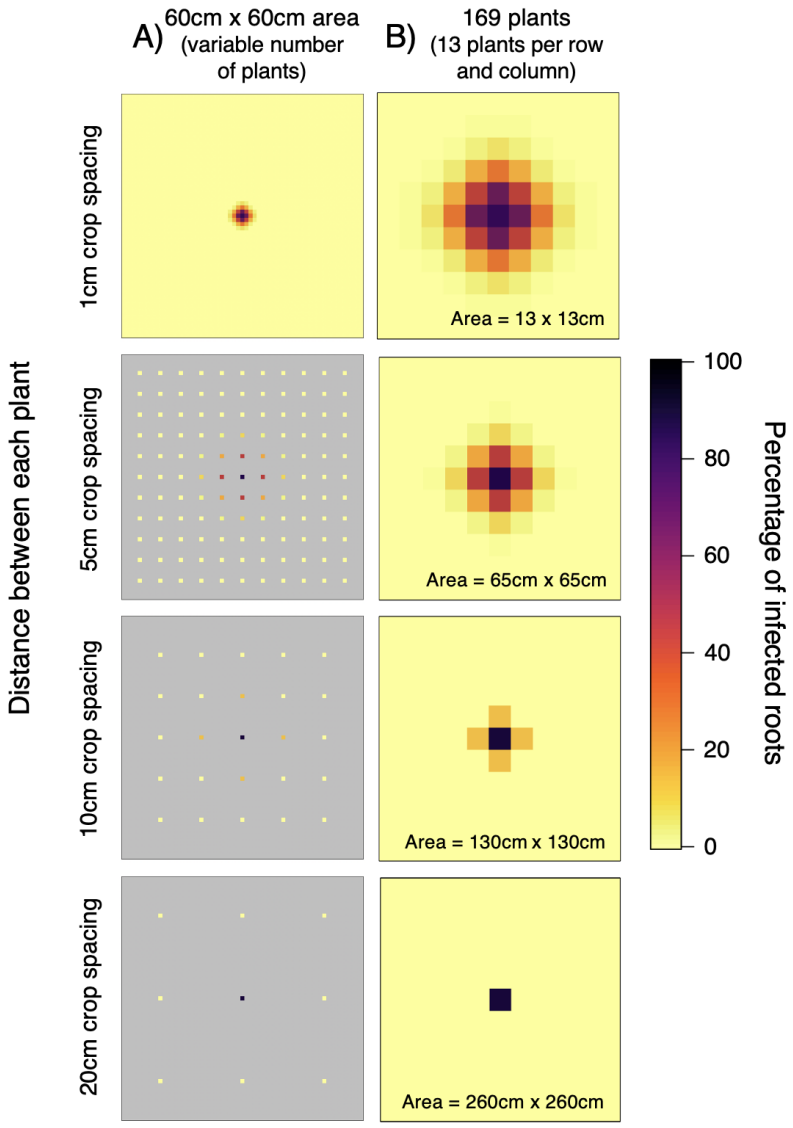

Fig. 6.4 Visualisation of evenly spaced plants at the end of a single growing season with 1cm, 5cm, 10cm, and 20cm between each plant across A) a 60cm x 60cm area, and B) a grid of 169 plants. Pathogen inoculum is placed in the central location of each plot at the start of a growing season, and can spread to surrounding plants by primary and secondary infection. A) Each plant is represented by a 1x1cm square, with the colour of this square dependent on the percentage of infected roots that the plant has at the end of a growing season. Any space between-plants is represented by grey. B) Each plant is represented by a square, which represents a 1x1cm area for 1cm crop spacing, a 5x5cm area for 5cm crop spacing, a 10x10cm area for 10cm crop spacing, and a 20x20cm area for 20cm crop spacing. The colour of each square is dependent on the percentage of infected roots that each plant has at the end of a growing season.

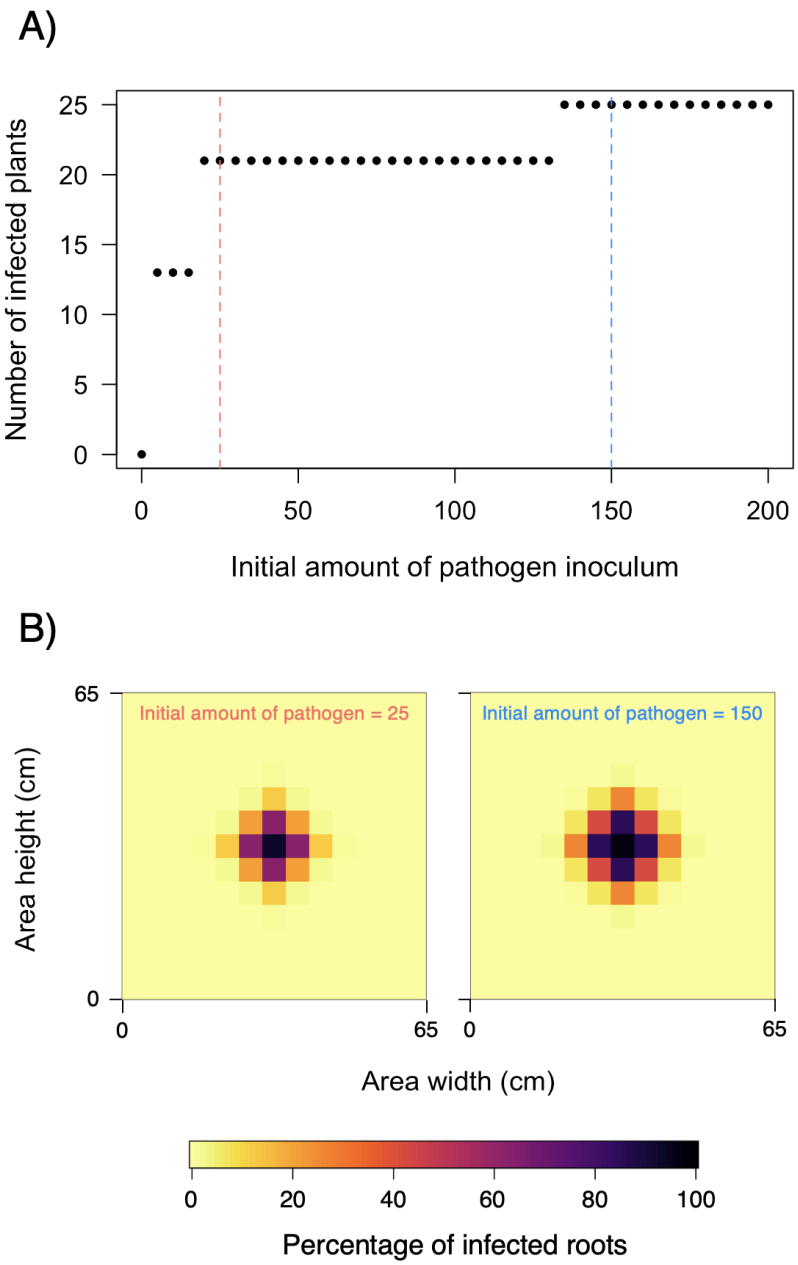

Fig. 6.5 Number of infected plants at the end of a single growing season when there is a variable amount of pathogen inoculum placed at the centre of 169 plants spaced evenly across a grid with 5cm between-plants. A) The amount of inoculum varied between 0-200 units, with a red dashed line representing 25 units and a blue dashed line representing 150 units. B) Epidemic spread across 169 plants when either 25 units or 150 units of inoculum are placed at the same location as the central plant at the start of the simulation.

a central plant that can be infected by free-living pathogen. The number of plants that are infected on the left and right side of this central plant represents the maximum diameter of the infected cluster. The horizontal distance occupied by infected plants will always be an odd number, as infection spreads outwards from a single plant and at the same speed across all sides from this plant. There will always be at least one infected plant, as the model parameters will always result in the central plant becoming infected. An initial analysis showed that the maximum horizontal amount of plants that infection could spread across was nine, regardless of crop spacing or the values of γ_X or γ_I. This is because the fixed rates of primary (β_P) and secondary (β_S) infection, obtained through prior model fitting (Chapter 3), restrict both the amount of infection that could occur within a single plant, as well as how much could spread between-plants in a single growing season. Although it was not analysed in this research, Figure 6.6 shows how varying these two rate parameters can affect the cluster size at the end of a single growing season.

The horizontal width of infection can therefore be across 1, 3, 5, 7, or 9 plants. The horizontal width taken up by this many plants at crop spacing values between 1-20cm can be seen in Table 6.4. The number of plants that produced a spread of infection closest to the desired value of 15-35cm are highlighted. For crop spacing values of between 3-7cm and 12-14cm, the optimal horizontal distance occupied by plants can have more than one value. For 1cm crop spacing, the horizontal distance of spread is always lower than the desired amount due to the limit of horizontal spread across nine plants. For some crop spacing values, there is no value that produced between 15-35cm of spread. In these cases, the number of plants that produces a horizontal distance closest to the optimal spread is selected.

Values of γ_X and γ_I are varied between 0-4cm for each crop spacing, and the horizontal distance of spread is recorded. The optimal values of γ_X and γ_I will be when they can produce the horizontal spread marked in grey in Table 6.4 for each crop spacing.

Table 6.4 The horizontal distance occupied by 1, 3, 5, 7, and 9 plants with a distance of 1-20cm between each plant. Within a growing season, where all infection spreads from a single source of inoculum, the maximum horizontal spread of infection is across 9 plants. The horizontal distance of spread that is most similar to the optimal cluster diameter (between 15-35cm) is marked in grey.

	Horizontal distance occupied by plants (cm)				
Crop spacing (cm)	1 plant	3 plants	5 plants	7 plants	9 plants
1	1	3	5	7	9
2	2	6	10	14	18
3	3	9	15	21	27
4	4	12	20	28	36
5	5	15	25	35	45
6	6	18	30	42	54
7	7	21	35	49	64
8	8	24	40	56	72
9	9	27	45	63	81
10	10	30	50	70	90
11	11	33	55	77	99
12	12	36	60	84	108
13	13	39	65	91	117
14	14	42	70	98	126
15	15	45	75	105	135
16	16	48	80	112	144
17	17	51	85	119	153
18	18	54	90	126	162
19	19	57	95	133	171
20	20	60	100	140	180

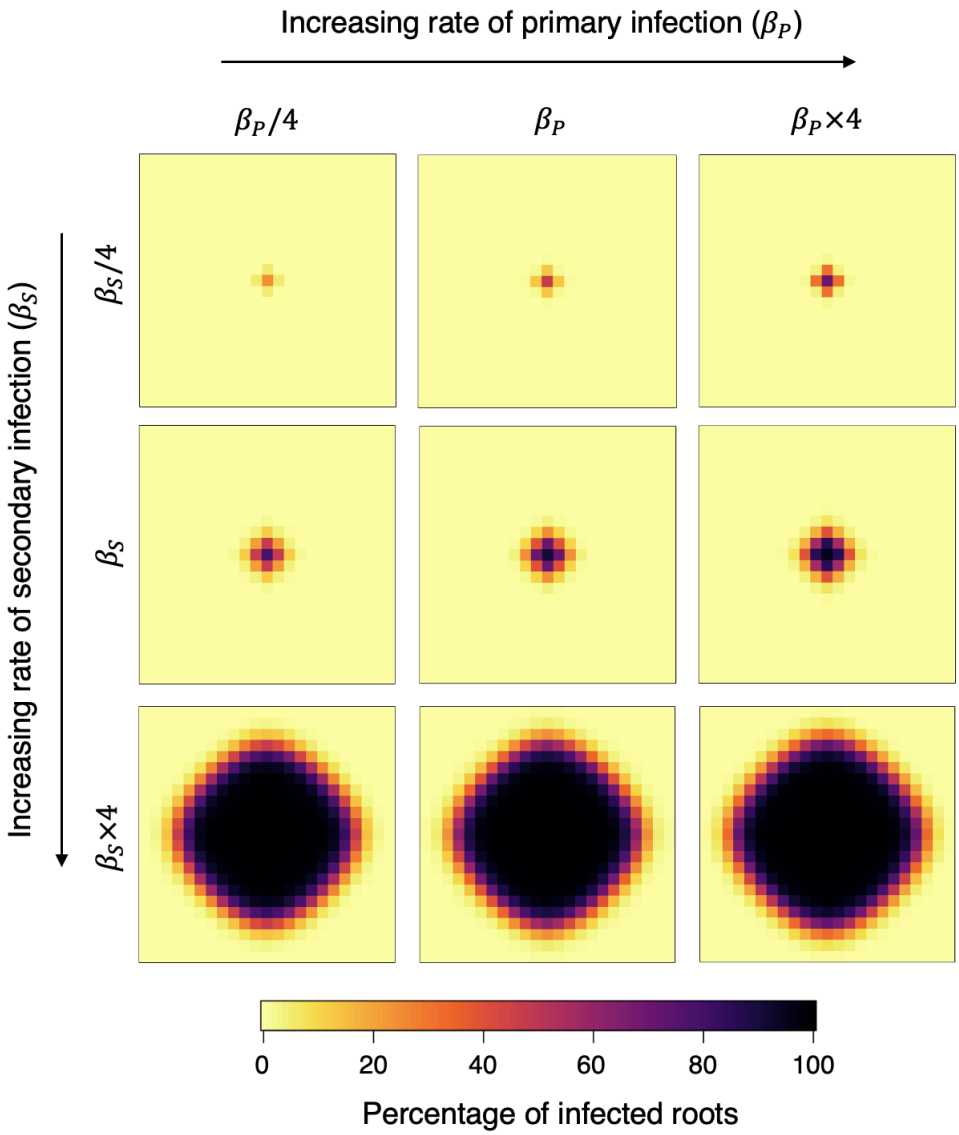

Fig. 6.6 Variation in the spread of infection across plants from a single source of central pathogen inoculum at the end of a single growing season as the rates of primary (β_p) and secondary (β_s) vary. The default values for primary and secondary infection were obtained through model fitting to data in Chapter 3. Each square represents a single plant with its individual set of roots.

6.3.3 Host growth

The horizontal spread of wheat roots has been reported to reach up to 25cm (Weaver et al., 1924), between 15-30cm (Weaver, 1926), and between 45-75cm (Manschadi et al., 2006)

either side of winter wheat plants, and approximately 46cm (Hays and Boss, 1899), nearly 23cm (Ten Eyck, 1899), and a maximum of 30cm (Weaver, 1926) either side of spring wheat plants. Apart from Manschadi et al. (2006), all of these measurements involved collecting soil samples from field experiments and detecting any roots present within them. These measurements are likely to be less accurate than those in Manschadi et al. (2006), where wheat plants were grown in large root-observation chambers. This allowed root growth to be viewed through Perspex surfaces and did not require disruption of the roots during sampling. However, Manschadi et al. (2006) does state that such controlled growing conditions with no competition from other plants is likely to promote root growth and increase it to that seen in field conditions.

Weaver et al. (1924) was the only research found that recorded horizontal root growth at multiple time points throughout a growing season rather than just providing a maximum value at the end of a season. Data, shown in Figure 6.7, was recorded from planting on 20th September to 14th December, where it was then stated that minimal growth occurred until harvest the following year. This is contradictory to Manschadi et al. (2006), who observed horizontal growth of roots until the end of the growing season.

A monomolecular growth curve

$$\frac{dG}{dt} = \rho(\kappa_G - G), \tag{6.11}$$

was fitted to the data using maximum likelihood model fitting, where errors and normally distributed, and where κ_G represents the maximum lateral distance that a root can grow from a plant. Initial analysis determined that fitting the data to a monomolecular growth curve produced the best fit out of several other growth curves. The process of model fitting used the *optim* function in the *stats* package (Soetaert and Petzoldt, 2010).

Incorporating root growth into the model allows for variation in the rate of between-plant secondary infection as the distance between the roots of two adjacent plants varies. At the

start of a growing season, adjacent plants may be too far apart to be able to cause infection through root-to-root contact. However, as the season progresses and the roots of adjacent plants grow closer together, the rate of between-plant secondary infection will increase as the likelihood of the roots of these plants touching will be greater. Calculating the rate of secondary infection as the distance between roots changed required calculating D,

$$D = \kappa_G - d, \tag{6.12}$$

where the maximum lateral growth of roots is the same as the carrying capacity for monomolecular growth (κ_G), and d is the point that is equidistant between two neighbouring plants (the distance that a plant's roots have to grow before they are touching their neighbours, if both plants are assumed to have the same rate of root growth). The rate of secondary infection can then be calculated by

$$\begin{aligned} \beta_s(t) = \beta_s\left(\frac{G(t)}{\kappa_G}\right) \text{ when } 0 < G(t) + D < \kappa_G, \\ \beta_s(t) = \beta_s \text{ when } G(t) + D \geq \kappa_G, \\ \beta_s(t) = 0 \text{ when } G(t) + D \leq 0, \end{aligned} \tag{6.13}$$

where $G(t)$ is the lateral growth of a root at time t.

Obtaining parameter values for lateral root growth required data from both Manschadi et al. (2006) and Weaver et al. (1924). As no data was collected for over half of the growing season in Weaver et al. (1924), and as Manschadi et al. (2006) reported much higher growth rates at the end of a growing season, two different growth curves were produced:

1. **Low lateral root spread:** Only using the data from Weaver et al. (1924)

2. **High lateral root spread:** The data from Weaver et al. (1924) was used, with an additional data point added at the end of the growing season representing similar growth to that seen in Manschadi et al. (2006) (55cm at 1750 degree days $> 0°C$)

These two growth curves are represented in Figure 6.7A, with the parameter values obtained during the model fitting process found in Table 6.5. The two growth rates are included separately into model simulations with crop spacing between 1-20cm to analyse the effect of root growth on epidemic spread and severity. Root growth only affects the rate of secondary infection (root-to-root infection) between different plants. Within a single plant, the rate of secondary infection remains constant throughout a growing season. between-plants, the rate of secondary infection is the same as within the roots of a single plant when the roots are touching. If the roots are not yet touching, the rate of secondary infection is reduced relative to the distance between-plants. This can be visualised in Figure 6.7B. For crops that are planted close together, the rate of secondary infection will have a narrower range of possible values and will reach a fixed value faster than when crops are planted further apart.

Table 6.5 Parameter values obtained for low and high monomolecular lateral spread of a crop's roots. ρ is the rate of root growth and κ_G is the maximum distance that roots can horizontally spread.

	Lateral root growth rate	
Parameter	Low	High
ρ	$2.96 \times 10^{-3}\ t^{-1}$	$7.72 \times 10^{-4}\ t^{-1}$
κ_G	25.9	59.6

For both growth rates, as well as for a model with no lateral root growth (a fixed value of β_S), a simulation was run over a single growing season with a grid of 13x13 plants evenly spaced. Pathogen inoculum (25 units) was placed at the location of the central plant at the start of the season. These simulations were repeated for crops spaced between 1-20cm apart.

The severity of the epidemics were measured using the area under the epidemic progress curve for healthy roots (AUHC), which includes both susceptible and colonised roots. This is calculated in the same way as the area under the disease progress curve (AUDPC), which is commonly used to determine epidemic severity for plant diseases (Campbell and Madden, 1990; Jeger and Viljanen-Rollinson, 2001). Although the process of calculating the AUDPC can be difficult when using a small amount of experimental data (Jeger and Viljanen-Rollinson, 2001), the use of a model allows for a precise calculation due to the unlimited amount of data that can be generated using it. Using AUHC allows for a comparison between the number of healthy roots in a simulation when a pathogen is present compared to when it is not present (Elderfield, 2018). The AUHC is calculated using

$$\text{AUHC}_{\text{normalised}} = \frac{\text{AUHC\_I}}{\text{AUHC\_S}}, \tag{6.14}$$

where AUHC_I is the AUHC for a simulation where a pathogen is present, and AUHC_S is the AUHC for the same simulation if no pathogen was present. This will calculate a number between 0 and 1, where 0 corresponds to a simulation where all roots are diseased, and 1 corresponds to a simulation where all roots are healthy. The epidemic severity can then be calculated by

$$\text{Epidemic severity} = 1 - \text{AUHC}_{\text{normalised}}, \tag{6.15}$$

where a higher value represents a greater proportion of infected roots.

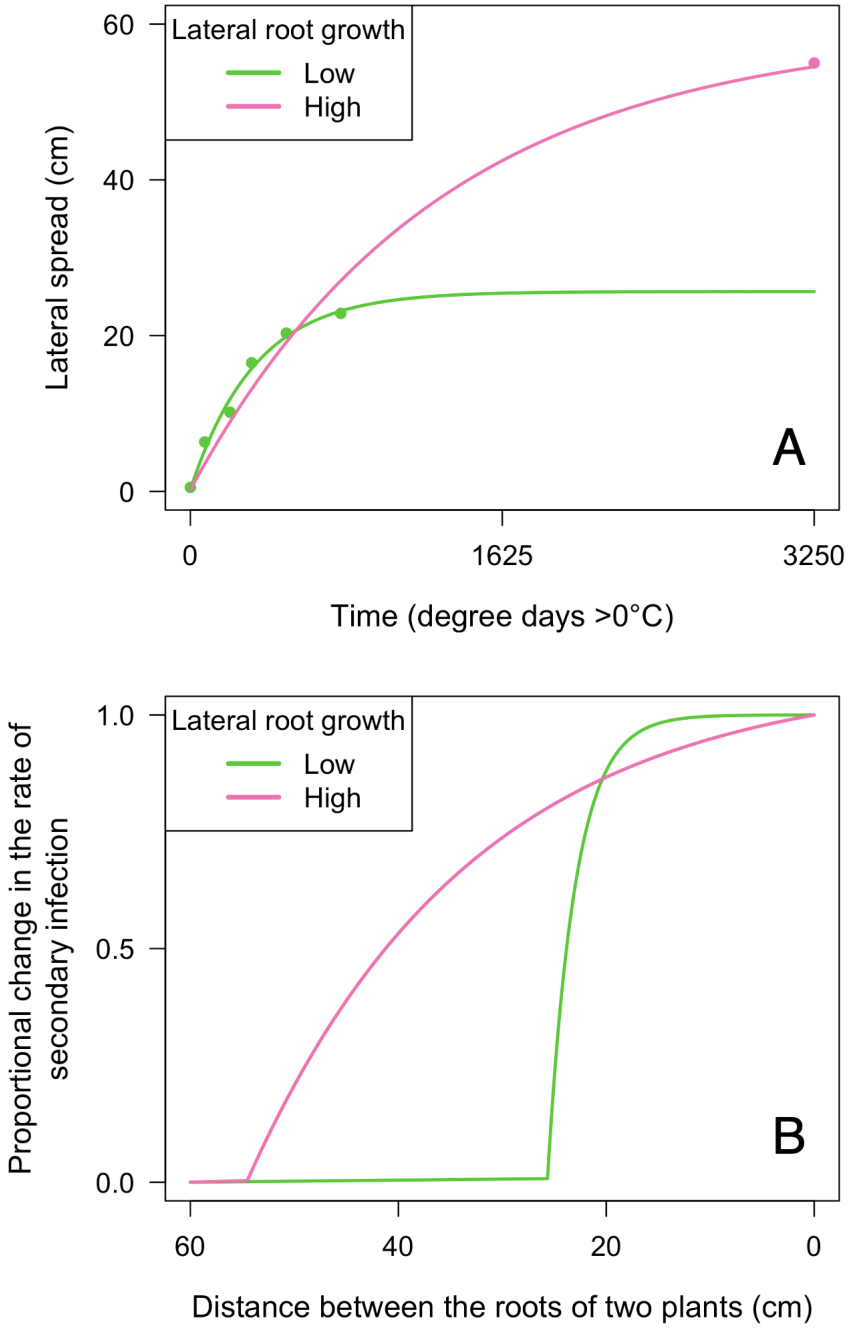

Fig. 6.7 Representation of A) the lateral spread of a crop's roots across a single growing season, and B) the proportional decrease in the rate of secondary infection between two plants as the distance between them varies. A) Data from Weaver et al. (1924) is shown as green points. The calclulated lateral spread at the end of a growing season from Manschadi et al. (2006) is shown as a pink point. B) The rate of secondary infection decreases to 0 when the distance between-plants exceeds the maximum predicted range of infection. When the roots of two plants are touching, the rate of secondary infection stays fixed at its maximum value.

6.3.4 Spatial arrangement of crops

Plants were ordered in four different spatial arrangements to examine how planting in rows can affect epidemic spread and severity. These arrangements were even spacing between-plants (no rows) or in rows spaced 12.5cm, 25cm, or 50cm apart. These row spacing values were chosen based on common row spacing values within agricultural fields (Abichou et al., 2019; Koscelny et al., 1990; McLeod et al., 1997; Salgado et al., 2017; Teich et al., 1993). The planting area was 2.5m x 2.5m and contained 2025 plants, with a planting density of 324 plants/m^2. This resulted in the spatial arrangements of:

- **Evenly spaced:** 45 rows with 45 plants per row
- **12.5cm row spacing:** 20 rows with 101 plants for 15 of these rows and 102 plants for 5 of these rows.
- **25cm row spacing:** 10 rows with 202 plants for 5 of these rows and 203 plants for 5 of these rows.
- **50cm row spacing:** 5 rows with 405 plants per row.

A visual representation of these over a smaller area size of 150x50cm area can be seen in Figure 6.8. For 12.5cm and 25cm row spacing where the number of plants per row differs, the shorter rows are found to the left of the planting area and the empty planting spaces are directly at the bottom of the area. This will minimise the impact of any difference in crop row size on epidemic spread.

As these simulations were performed over two years, there was stochastic dispersal of the free-living pathogen between the first and second growing seasons. Due to variation in the simulation results from this stochastic event, each simulation was performed 10 times, and the mean value for the number of infected roots for each plant was used.

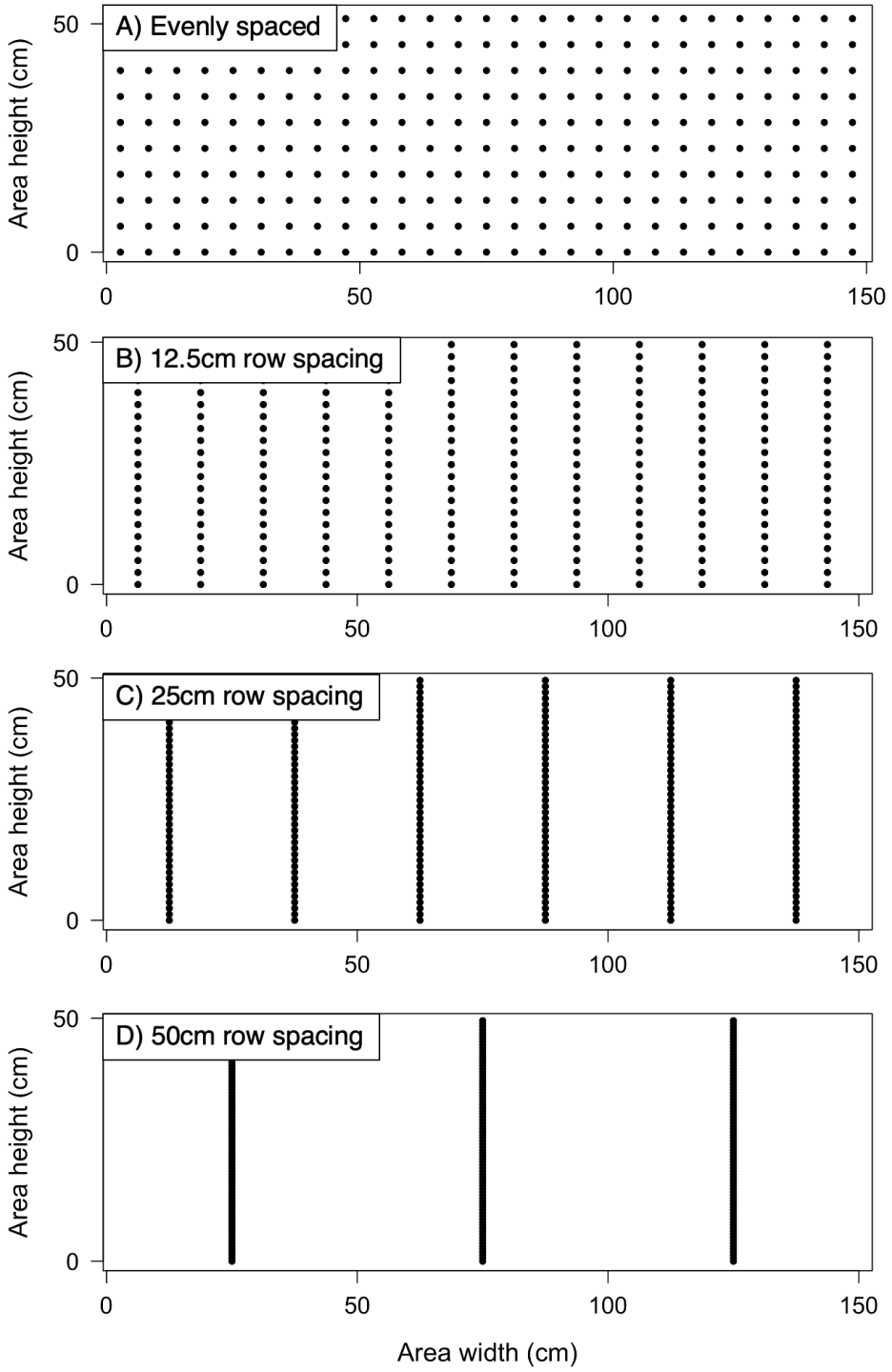

Fig. 6.8 Visualisation of crops planted A) evenly spaced, B) in rows 12.5cm apart, C) in rows 25cm apart, and D) in rows 50cm apart. Each plant is represented by a black dot, and all crops have a planting density of 324 plants/m^2.

Each epidemic begins with all units of inoculum grouped together at a central plant's location, representing a field where a single point of infection occurs. If the number of rows is an odd number, this plant is located in the middle row. If the number of rows is an even number, this plant is located in the row to the left of the centre. Within a row, if the number of plants is an odd number, this plant is located in the middle plant of this row. If the number of plant within a row is even, this plant is located at the position to the top of the centre.

Epidemics are simulated across two years so that between-season dispersal, and its effects on epidemic spread and severity, can also be analysed. The value for the scale parameter for between-season dispersal (γ_B) was initially varied between 0-50cm, examining how the total number of infected plants and the cluster size were affected. The desired cluster width and height was approximately 2m x 2m - 2.5m x 2.5m, which is similar to the size of a take-all cluster after the second year of growing winter wheat (Cotterill and Sivasithamparam, 1988; Gosme et al., 2007; Wehrle and Ogilvie, 1956). A value of 15cm for γ_B was then chosen after initial modelling work showed that it produced a cluster size similar to that found in the literature but that did not exceed the spatial area. Examples of cluster size in the second year of an epidemic when γ_B is set to 2cm, 10cm, and 20cm are shown in Figure 6.9. Although take-all epidemics have been thought to spread greater distances than this (Oliver et al., 2003), a constraint on planting area due to computational power meant that larger scale parameter values were not selected.

The severity of the epidemics across each year were measured using the area under the epidemic progress curve for healthy roots (AUHC), which is explained in Section 6.3.3.

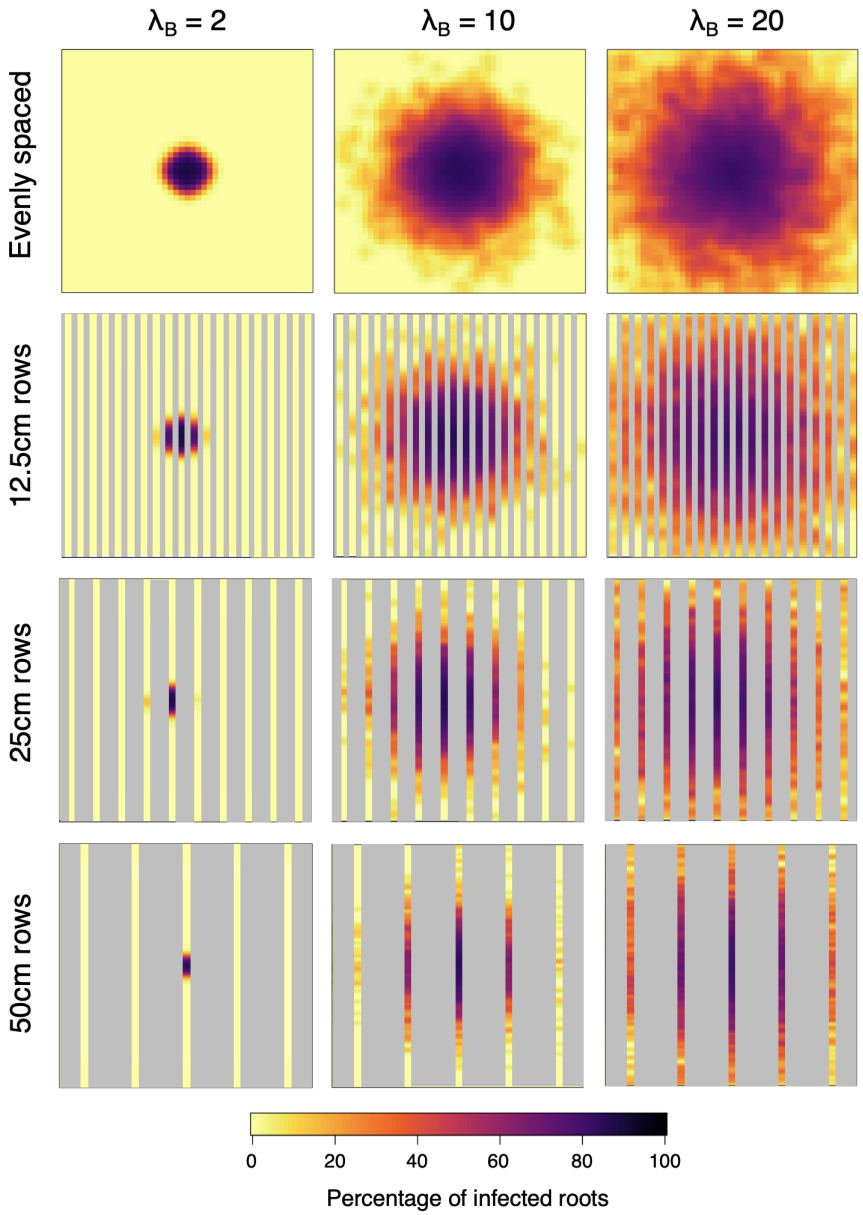

Fig. 6.9 Variation in cluster size at the end of the second year of two consecutive growing seasons across four different crop spatial arrangements. Each area is a 2.5m x 2.5m grid and contains 2025 plants. Each plant has its own individual roots, which can either be infected or not. The scale parameters for dispersal kernels are set at 1.2cm for primary infection (γ_P), 2.1cm for secondary infection (γ_S), and vary between 2cm, 10cm, and 20cm for between-season inoculum dispersal (γ_B). Spaces between rows are marked in grey. Although the space between-plants within a row varies across the crop spatial arrangements, all plants are represented as occupying the same amount of space in the figure due to easier visualisation.

6.4 Results

6.4.1 Obtaining suitable parameter values for within-season epidemic spread

Pathogen inoculum was placed in the centre of a 13x13 grid of 169 plants that were evenly spaced apart to examine the spread of disease across a single growing season. In Figure 6.10, plants were evenly spaced either 1cm, 5cm, 10cm or 20cm apart, and the scale parameters for primary (γ_P) and secondary (γ_S) dispersal kernels varied between 1cm, 5cm, and 20cm. These were chosen was so that a wide range of values could be visualised. There was greater epidemic spread when the distance between crops was smaller and the scale parameters were larger. For plants with 10cm and 20cm spaces between each other, with values for γ_P and γ_S of 1cm, there was no detectable spread of infection to surrounding plants. This is because the scale parameter values were too low compared to the distance between each plant to allow infection between-plants to occur. Likewise, the spread of infection between-plants was similar regardless of the distance between them when the scale parameter values were high. High scale parameter values for the dispersal kernels cause a greater spread of infection between-plants.

For any distance between-plants and all scale parameter values, the maximum number of infected plants ($\geq$ 1 root infected) along the longest width of a cluster never exceeded nine. A closer examination of the number of infected plants along the largest width of a cluster when scale parameter values varied between 0-4cm can be seen in Figure 6.11A. This restriction was due to a limitation on epidemic spread because of the time that a simulation was run for, as well as the fact that infection was only able to spread to nearest neighbours. Plants that are spaced closer together require smaller scale parameter values to spread across a width of nine plants. Plants that are spaced further apart need larger

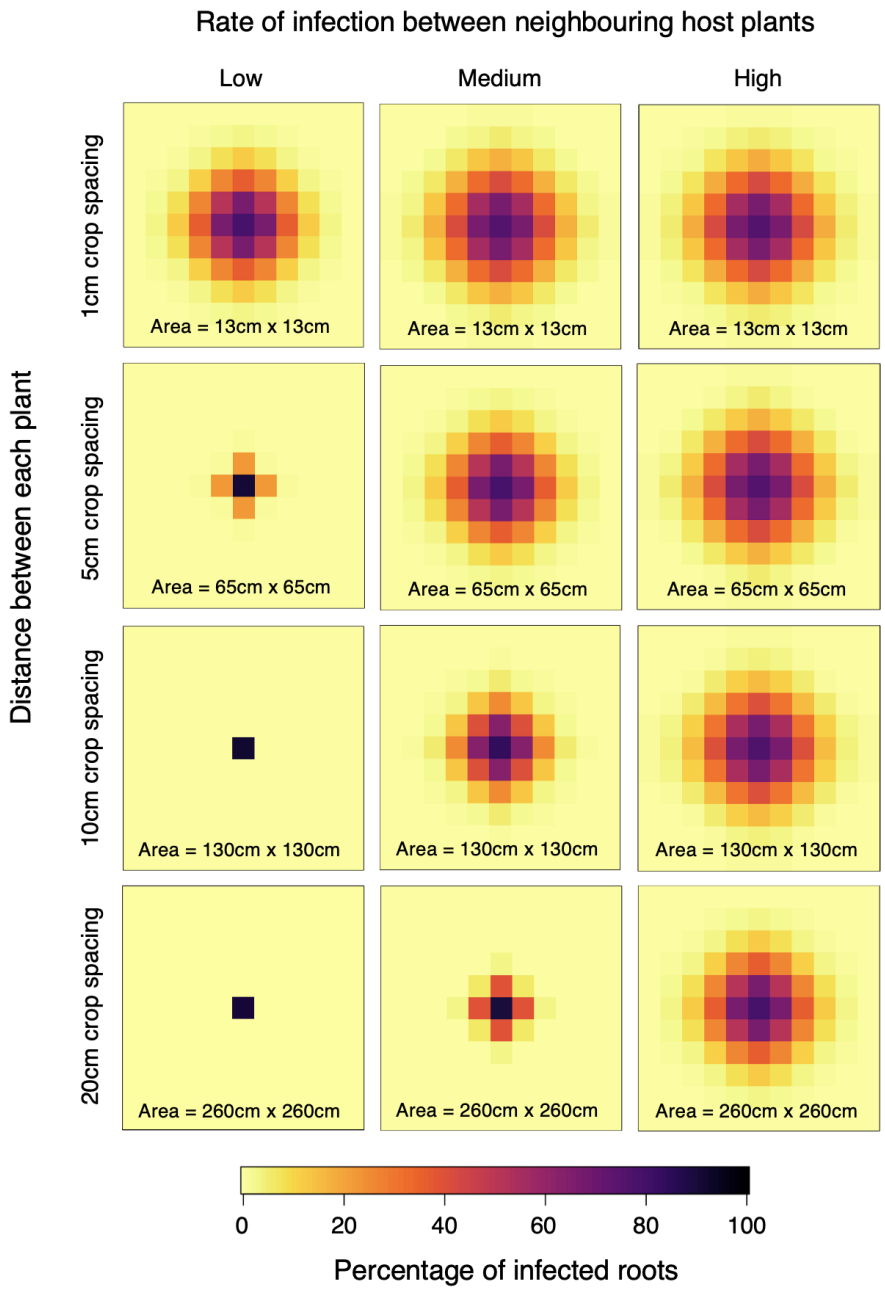

Fig. 6.10 Spread of infection from a central source of inoculum as the space between crops and the within-season dispersal scale parameters for primary and secondary infection vary. Each square represents a single plant with its individual set of roots. Crops are evenly spaced with either 1cm, 5cm, 10cm, and 20cm between crops. The scale parameters for primary (γ_P) and secondary (γ_S) infection vary between 1cm (low), 5cm (medium), and 20cm (high).

scale parameter values before infection can spread as far. This means that plants spaced closer together are more susceptible to getting infected by their neighbours compared to plants that are spaced further apart, especially when the scale parameters for the dispersal kernels are small.

Due to differences in crop spacing, the area taken up by the same number of plants varied considerably. For example, the space taken up by 49 infected plants in a square grid will be 7cm x 7cm for 1cm crop spacing, whereas it will be 140cm x 140cm for 20cm crop spacing (Figure 6.11B). A significantly greater number of plants can be planted within an area if they are spaced closer together. Although planting far apart is beneficial as it reduced epidemic spread, it is unlikely to be an economically feasible strategy for most growers.

A cluster size between 15-35cm was desired as it was similar to the spread found to occur within a single growing season (Table 6.1). However, the desired spread of infection to surrounding plants will vary depending on the amount of space between-plants. A greater spread of infection was desired when crops were spaced closer together, whereas no spread was desired for crops spaced very far apart. For crop spacing values between 1-20cm, Table 6.4 provides the optimal spread of infection to produce clusters with diameters similar to 15-35cm. For each crop spacing value between 1-20cm, both the scale parameters for primary (γ_P) and secondary (γ_S) infection were varied between 0-4cm in steps of 0.1cm. At the end of a growing season, if the cluster size was between 15-35cm, with the corresponding amount of plants required to be infected to produce this spread found in Table 6.4, the values for γ_P and γ_S are deemed as producing a suitable cluster size. These values are combined together over all crop spacing values between 1-20cm to produce a range of suitable kernel scale parameter values (Figure 6.12). Only a small range of values for γ_P and γ_S produced the optimal cluster size over all crop spacing values. As the spread of secondary infection is thought to be greater than that of primary infection (Garrett, 1936;

Leclerc et al., 2013; Otten et al., 2003; Wildermuth, 1977), any values that had a greater primary infection scale parameter than secondary infection scale parameter were discarded (Figure 6.13). The selected values for γ_P and γ_S were those that maximised the difference between γ_P and γ_S within the suitable parameter space. This resulted in selecting a value of 1.2cm for γ_P and 2.1cm for γ_S for all future analysis. However, additional analysis using other values that are marked as suitable in Figure 6.13 did not significantly impact any of the obtained results within this chapter.

Using these values to simulate epidemics when crops have 1cm, 5cm, 10cm, and 20cm spaces between each other, the cluster size varied between 9cm x 9cm (for 1cm crop spacing) to 30cm x 30cm (for 10cm crop spacing) (Figure 6.14). Although a greater number of plants are infected when crops are planted closer together, the reduction in space between crops can still result in smaller cluster sizes. Although the optimal cluster width is between 15-35cm, this is not possible for the lower crop spacing values. There is some variation in cluster diameter as the distance between crops varied, but these values consistently fluctuate around the desired diameter (Figure 6.15).

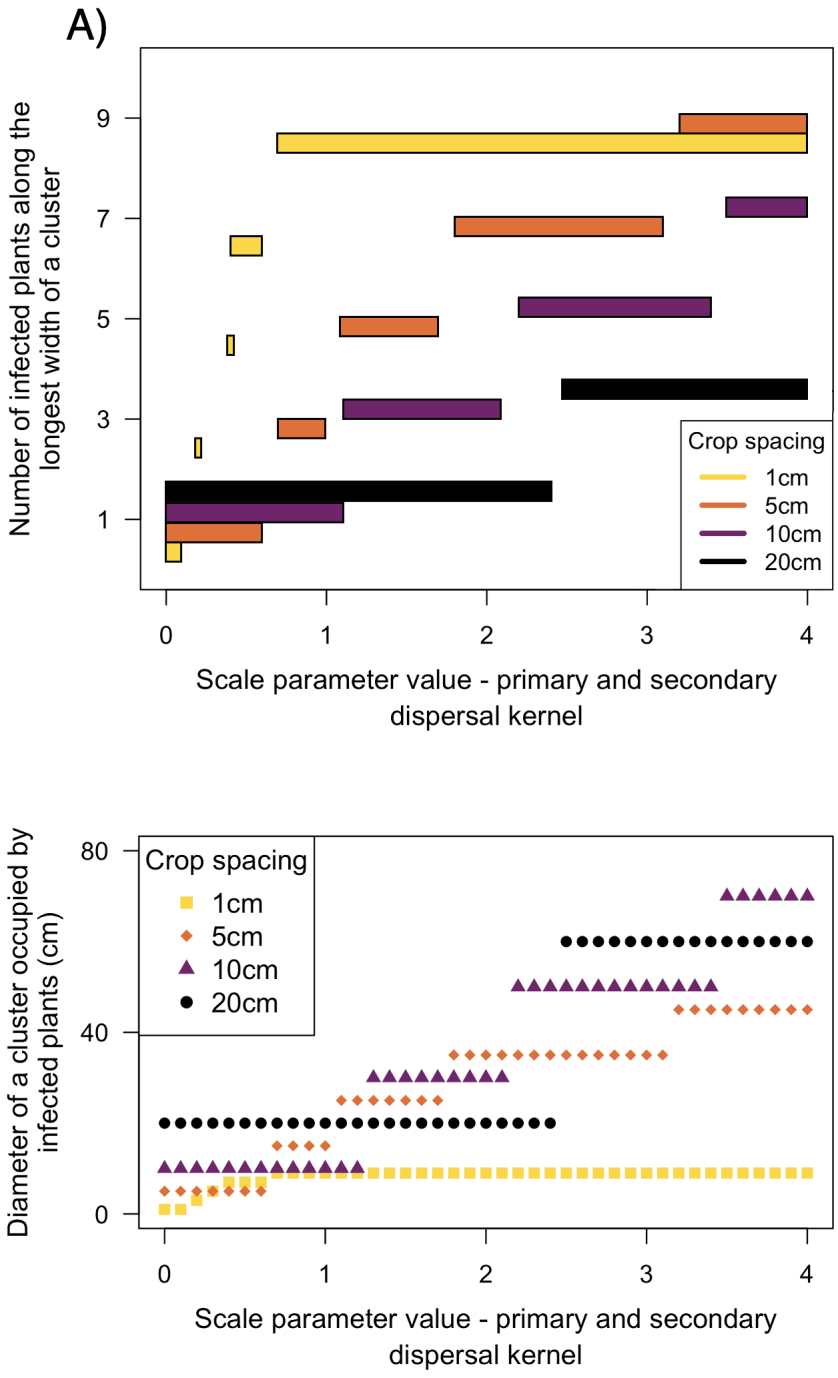

Fig. 6.11 A) Number of infected plants along the longest width of a cluster, and B) Diameter of a cluster occupied by infected plants (cm), as both the scale parameters for primary (γ_P) and secondary (γ_S) infection kernels, and the spacing between crops, varies. Crops are evenly spaced across rows and columns, with either 1cm, 5cm, 10cm, or 20cm spaces between-planting locations. The scale parameters for the primary and secondary infection kernels vary between 0-4 in steps of 0.1.

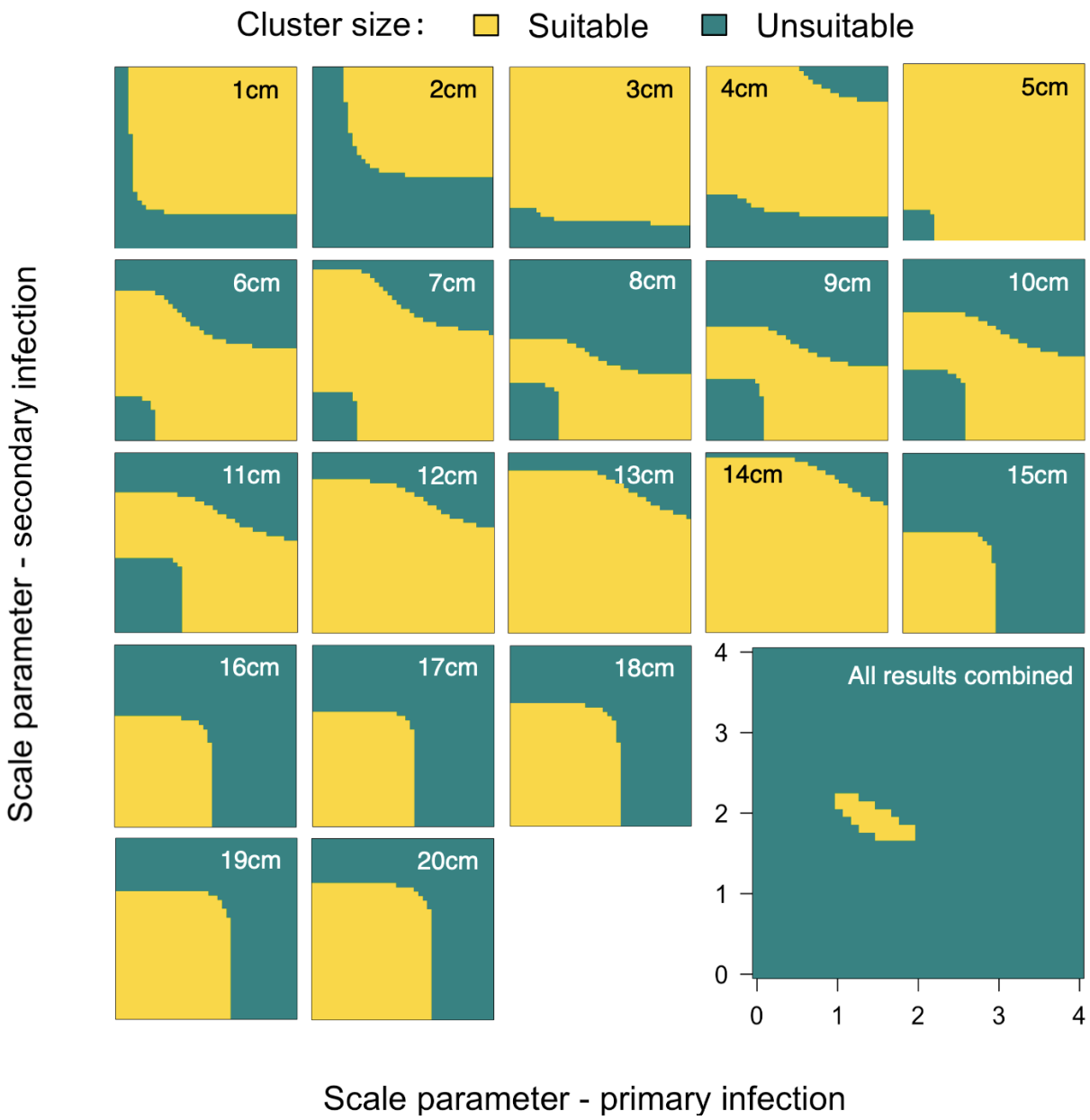

Fig. 6.12 Range of values for primary (γ_P) and secondary (γ_S) infection scale parameters over evenly spaced crops between 1-20cm apart that produce a suitable cluster size. Although the optimal cluster size is between 15-35cm, a suitable cluster size may deviate slightly from this at different crop spacing values, with all suitable values found in Table 6.4. Values for primary and secondary infection scale parameters are varied between 0-4cm in increments of 0.1cm.

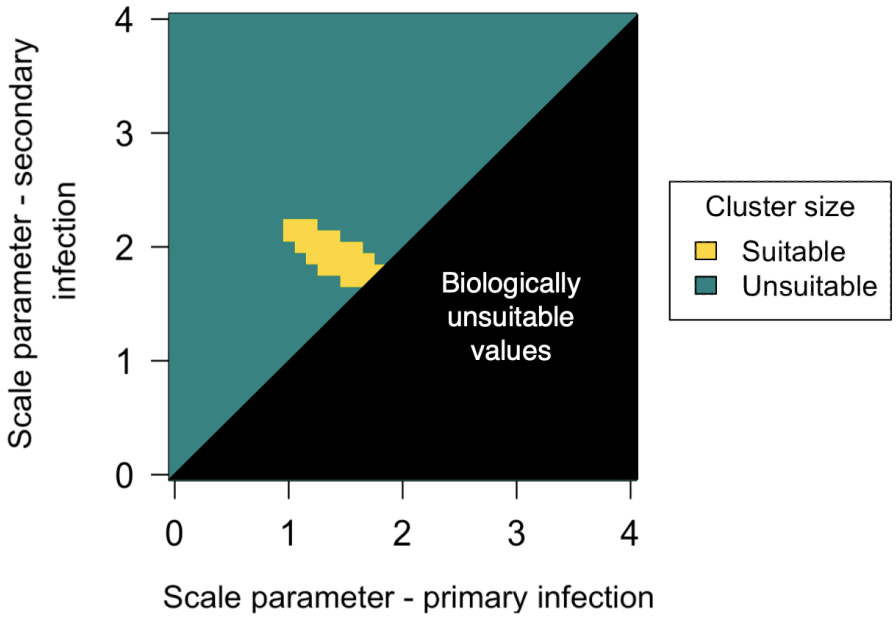

Fig. 6.13 Range of values for primary (γ_P) and secondary (γ_S) infection scale parameters over evenly spaced crops between 1-20cm apart that produce a suitable cluster size. Although the optimal cluster size is between 15-35cm, a suitable cluster size may deviate slightly from this at different crop spacing values, with all suitable values found in Table 6.4. Values for primary and secondary infection scale parameters are varied between 0-4 in increments of 0.1. Secondary infection is known to have a greater spread than primary infection, and therefore any values where the scale parameter for primary infection is greater than the scale parameter for secondary infection are ignored.

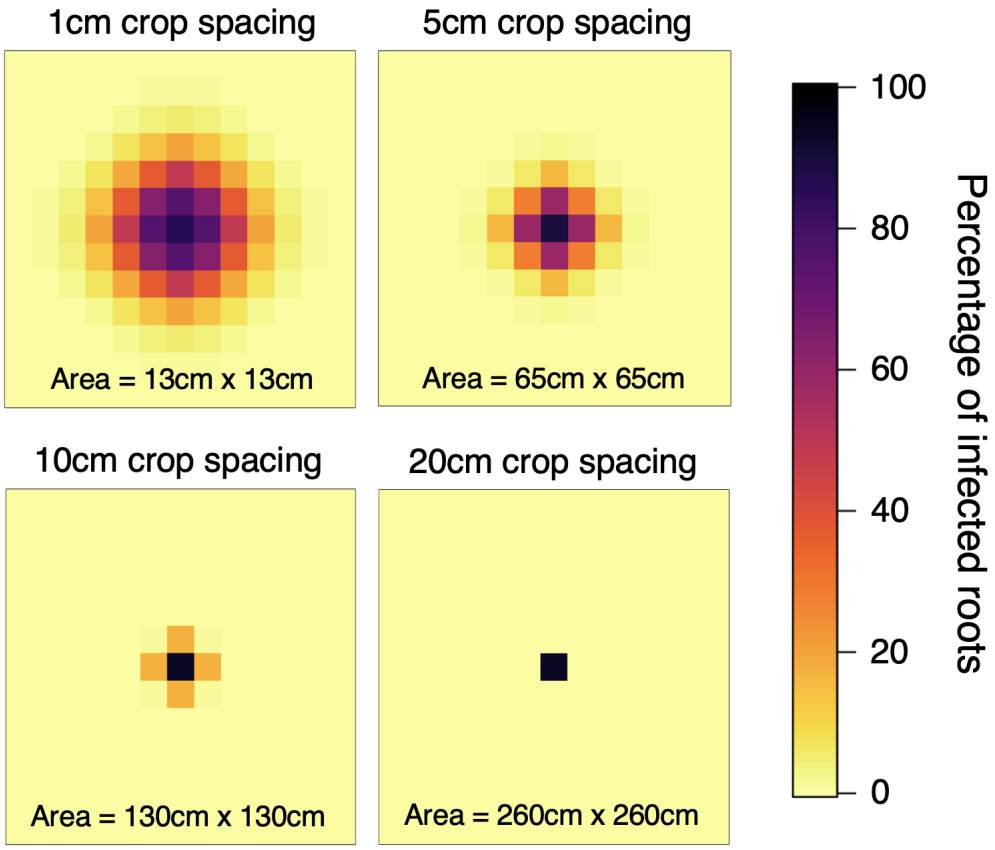

Fig. 6.14 Variation in epidemic spread and cluster diameter at the end of a single growing season as the scale parameter for primary (γ_P) infection is fixed at 1.2cm, the scale parameter for secondary (γ_S) infection is fixed at 2.1cm, and the spacing between evenly spaced crops is either 1cm, 5cm, 10cm, and 20cm. Each square represents a single plant with its individual set of roots.

Fig. 6.15 Variation in cluster diameter at the end of a single growing season as the scale parameters for primary (γ_P) infection is fixed at 1.2cm, the scale parameters for secondary (γ_S) infection is fixed at 2.1cm, and the spacing between evenly spaced crops varies between 1-20cm. The green area represents the optimal cluster diameter, which is between 15-35cm, representing between 7.5-17.5cm of spread in one direction from a source of pathogen inoculum.

6.4.2 Host growth

Host growth was included in the model to allow for a decrease in the rate of between-plant secondary infection as the distance between the roots of two adjacent plants increases. Including host growth into a simulation where disease spreads between-plants from a single starting cluster of inoculum had no noticeable change on the mean epidemic severity, regardless of the space between crops or the growth rate (Figure 6.16). The reason for this lack of effect was further explored in Figures C.1 and C.2.

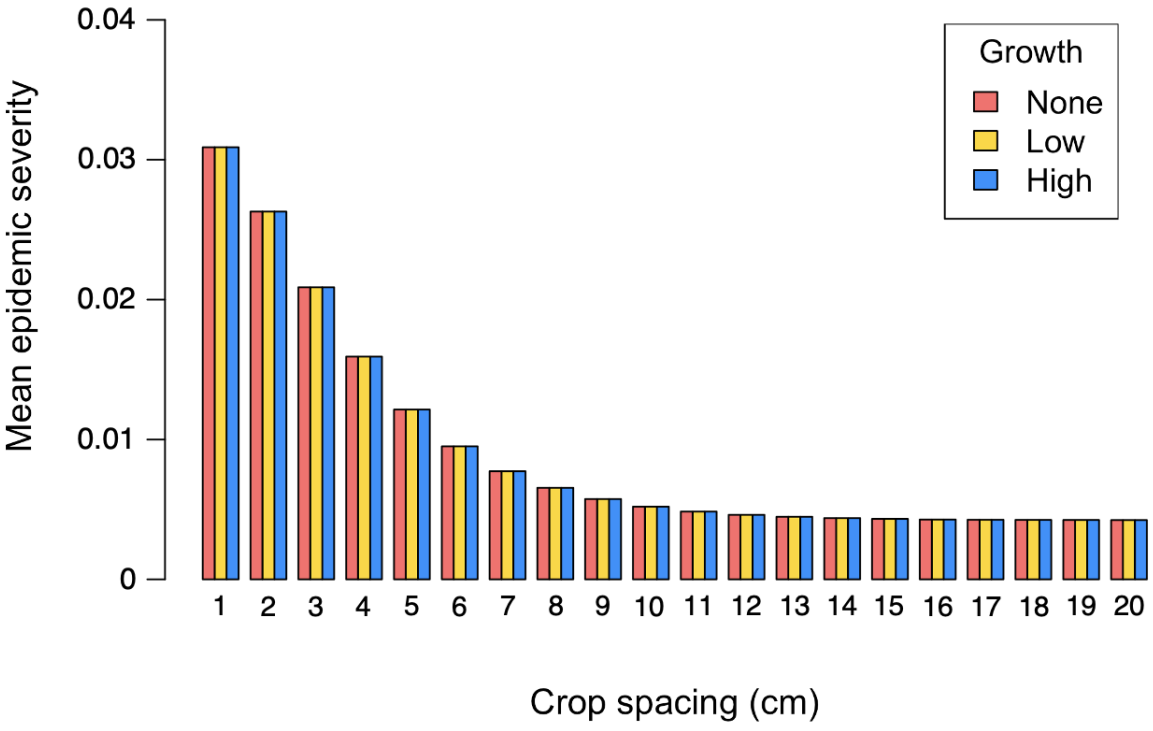

Fig. 6.16 Variation in the mean epidemic severity when low or high lateral root growth are included in a simulation of disease spreading across equally spaced plants over a single growing season. The parameters for host growth can be found in Section 6.3.3.

6.4.3 Spatial arrangement of crops

In the first year of a simulation where crops are evenly spaced within a field and pathogen inoculum is placed in the centre of the field, there is both horizontal and vertical spread of the pathogen, creating a circular cluster (Figure 6.17). When crops are planted in rows that are 12.5cm, 25cm or 50cm apart, there is no noticeable spread of infection to adjacent rows and instead only spread within a single row is seen. In the second year of the epidemic, between-season dispersal of the pathogen due to mechanical agricultural processes resulted in a greater spread of the pathogen. Infected plants are found in multiple rows for all three row spatial arrangements, with visually similar cluster shapes for all crop spatial arrangements.

The mean percentage of infected roots for the first growing season is below 0.4% regardless of spatial arrangement (Figure 6.18A). This reflects what is seen in Figure 6.17, where most plants are not infected during the first season. Evenly spaced plants have a lower mean percentage of infected plants throughout most of the season, and only increase slightly more than when plants are in 12.5cm rows at the end of the season. The mean percentage of infected roots is highest when plants are in 25cm or 50cm rows. Infection spreads fastest within rows rather than between rows, with low scale parameter values for primary and secondary dispersal kernels causing a significant reduction in the spread of infection to plants that are further away. As wider spaces between rows result in reduced interrow space between plants, a greater number of plants will come into contact with the pathogen and become infected as between-row spacing increases.

For the second season (Figure 6.18B), there is minimal difference of the different spatial arrangements on the mean percentage of infected roots. This suggests that between-season dispersal negates any impact of within-season spread of infection. For both season one and two, there is a drop in the mean percentage of infected roots towards the middle of the growing season, before it begins to increase again. This pattern is well studied and

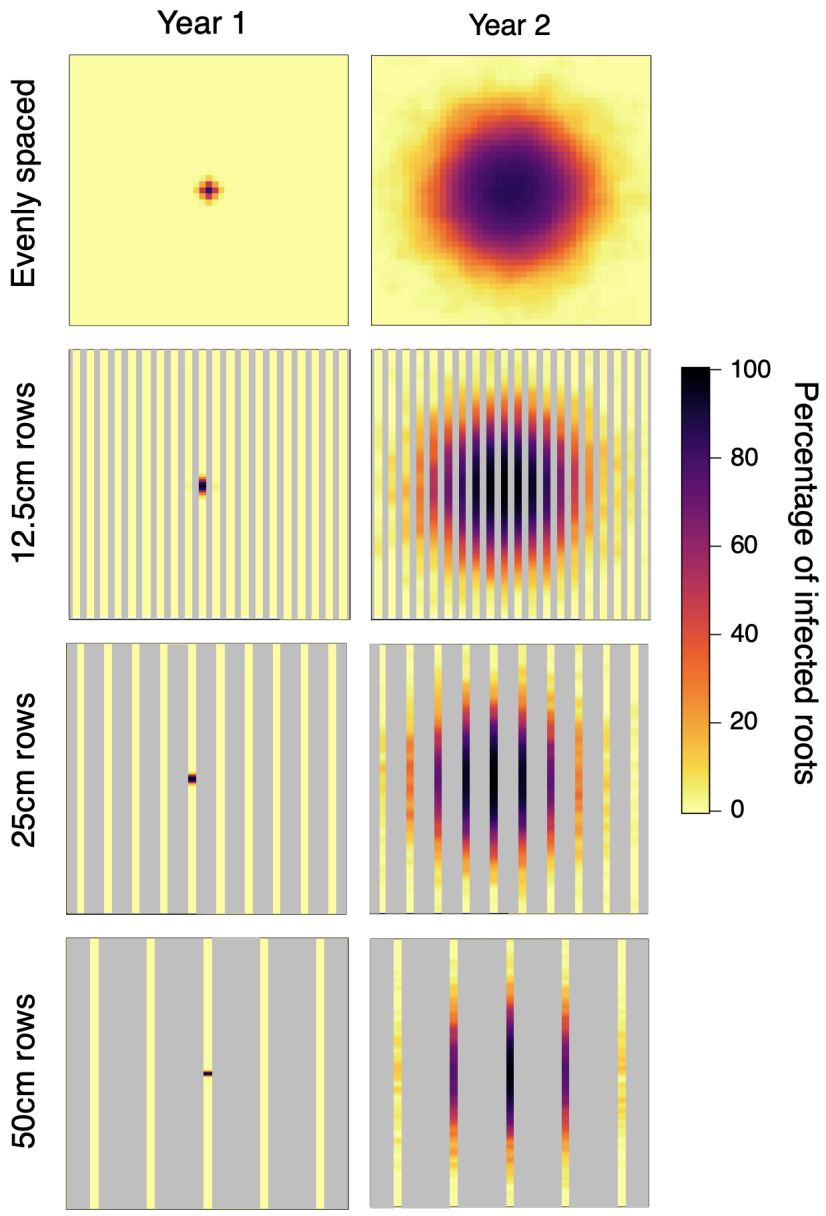

Fig. 6.17 Variation in cluster size at the end of two consecutive growing seasons across four different crop spatial arrangements. Each area is a 2.5m x 2.5m grid and contains 2025 plants. Each plant has its own individual roots, which can either be infected or not. The scale parameters for dispersal kernels are set at 1.2cm for primary infection (γ_P), 2.1cm for secondary infection (γ_S), and 10cm for between-season inoculum dispersal (γ_B). Spaces between rows are marked in grey. Although the space between-plants within a row varies across the crop spatial arrangements, all plants are represented as occupying the same amount of space in the figures due to easier visualisation.

represents the period of time between the dominance of primary and secondary infection. Primary infection is high at the start of the growing season whilst there is still a significant amount of free-living pathogen living in the soil. However, this decays rapidly and creates the dip in infection. Secondary infection then begins to take over as infection spreads between the roots of plants, causing the second peak of infection.

The effect of spatial arrangement on epidemic severity is further explored in Figure 6.19, which examines the mean epidemic severity at the end of the first and second growing seasons. Epidemic severity can vary between 0, where no roots are infected, and 1 where all roots are infected. As in Figure 6.18A, the mean epidemic severity is very low in the first season due to the amount of plants that have no infected roots (Figure 6.19A). Evenly spaced plants have the lowest mean epidemic severity, followed by plants in 12.5cm rows, 25cm rows, and 50cm rows. The use of wide rows prevents the pathogen from infecting plants in adjacent rows, but increases the number of plants that get infected in the same row. There is no detectable infection to the rows either side of the infected row when they are spaced 12.5cm apart, suggesting that this is far enough to prevent significant spread of the pathogen. If the pathogen was able to spread further through increasing the scale parameters for primary or secondary infection, there is likely to be more of a benefit of wider rows.

There is minimal difference between the mean epidemic severity values in the second growing season (Figure 6.19B). Plants in 12.5cm and 50cm rows have slightly lower values. However, this could be due to the random dispersal of the free-living pathogen between seasons, causing this to be higher by chance.

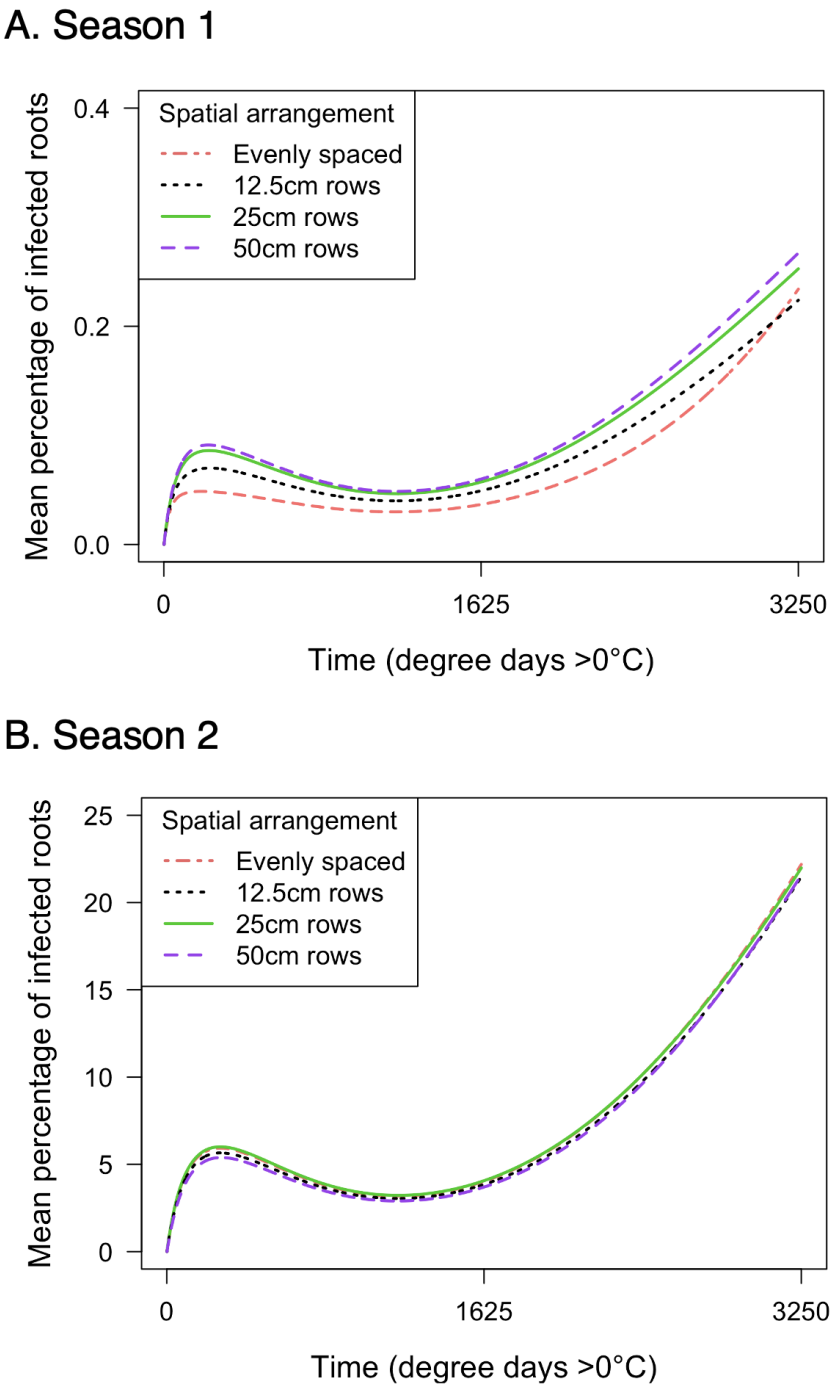

Fig. 6.18 Variation in the mean percentage of infected roots over four different spatial arrangements for an epidemic starting with a central source of pathogen inoculum over the A) first and B) second years of the simulation. Planting occurs at 0 degree days $> 0°C$ and the crops are harvested and removed at 3250 degree days $> 0°C$.

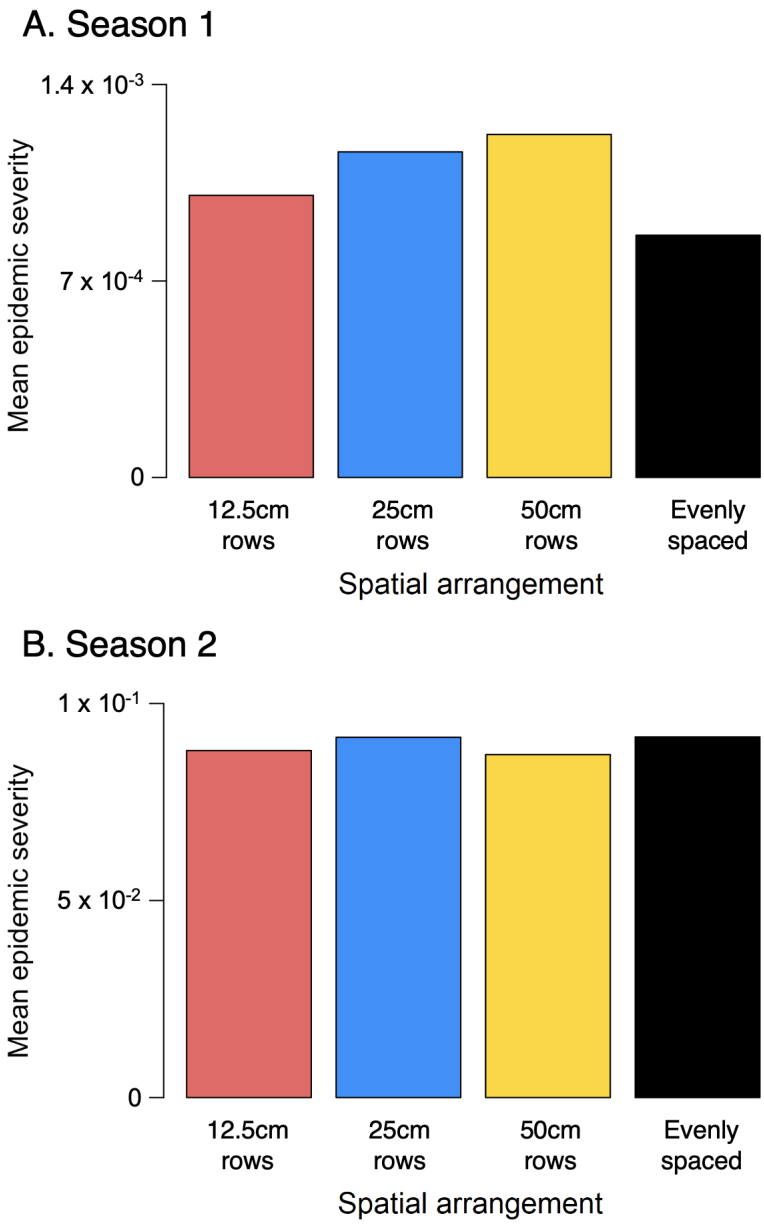

Fig. 6.19 Variation in the mean epidemic severity for four different crop spatial arrangements at the end of the A) first year and B) second year of planting.

6.5 Discussion

6.5.1 Within-season spread of a pathogen

The spatial SIX model was able to simulate the clusters of infected plants that are commonly seen from take-all disease. Infection initially occurs from free-living material, infecting the roots of any nearby plants, before spreading out radially from this location through contact between the roots of different plants (Cook, 2003). The spread of infection between-plants was severely limited when crops were spaced further apart due to the small values of the scale parameters for the primary and secondary dispersal kernels. The inability for soil-borne pathogens to spread over large distances means that slightly increasing the space between-plants can have a considerable effect on epidemic severity and spread within a growing season. There is therefore an important trade-off between epidemic severity and the number of crops to plant when trying to maximise profit. Although increasing the number of plants across a field will increase the maximum profit that can be obtained if there is no disease, this will also increase the spread of soil-borne diseases and may lead to an overall decrease in profit.

Our results were able to find a small number of values for the scale parameters for primary and secondary dispersal kernels that were able to produce cluster sizes with the desired 15-35cm diameter across almost all crop spacing values between 0-20cm. The mean distances of dispersal were similar to those found in the literature for primary and secondary infection (Gosme and Lucas, 2011; Gosme et al., 2007; Prew, 1980b). However, some of these values had a greater scale parameter for primary infection than secondary infection, which does not fit previous research (Brown and Hornby, 1971; Garrett, 1936; Gilligan, 1980; Pope and Jackson, 1973; Warcup, 1957; Wildermuth et al., 1984). It is important with all modelling work to understand any results and examine how they fit with prior knowledge about the biological system. A result that is computationally possible is

not necessarily biologically possible (Fernández Slezak et al., 2010), and therefore there is a need to combine knowledge on both of these topics when examining any results.

The cluster size and epidemic spread were limited due to the rates of primary and secondary infection. These were determined in Chapter 3 and are specific to take-all disease. A potential extension of this research could be through varying these infection rates to examine what impact they have on cluster size and epidemic severity. This could also make the results more applicable to other plant-pathogen systems. Soil-borne pathogens are often known to spread minimal distances, with contact between the roots of different plants required to spread the disease (Raaijmakers et al., 2009; Weller et al., 2002). However, above-ground pathogens may be spread by insects or the wind and could lead to significantly greater spread (Aylor, 1990). Allowing the rates of primary and secondary infection, as well as the scale parameters for dispersal, to vary would allow for an examination of epidemic severity across a wide range of biological systems.

The small-scale dispersal of take-all demonstrates the potential inaccuracy of determining the epidemic severity within a field by sampling a small number of plants and calculating the mean severity value across these samples. Clusters of infected plants could easily be missed, calculating a much lower epidemic severity value than is actually present. Similarly, an examination of cluster size requires the use of small quadrats or even the examination of individual plants. Oliver et al. (2003) only recorded data at 24m intervals which is significantly too far apart and has the potential to span multiple clusters of take-all infection. The distance of pathogen spread within a season should therefore play a key role in determining which sampling methods are required to examine epidemic severity across a field. For pathogens like *Gaeumannomyces graminis* var. *tritici* that have very low epidemic spread, a more detailed approach of examining individual clusters, or taking many samples across a field, may be required to provide an accurate representation of epidemic severity.

6.5.2 The impact of root growth on epidemic severity

There was minimal impact on epidemic severity when root growth was included in the spatial SIX model. This is in contrast to Leclerc et al. (2013) who found that incorporating root growth into their model could change an epidemic from invasive to non-invasive. Their research focused on sugar beet, which has a single main taproot and only minimal smaller root growth off this central root. This is in contrast to wheat which has no primary root, and the root system is instead composed of many seminal and adventitious roots that spread out in multiple directions from the base of a plant (Bailey and Gilligan, 1999; Bailey et al., 2005). The growth of a taproot is easy to spatially model, with radial spread from a central location, and accurate information about the maximum and mean distance of root growth easy to obtain. As most root growth occurs from this taproot, and as the roots of different plant may still not be touching by the end of a growing season, it can easily be seen how taproot growth could have a significant impact on the spread of a soil-borne disease.

However, wheat roots grow rapidly and have a significantly wider lateral spread than the distance between-plants in a field (Manschadi et al., 2006; Weaver et al., 1924). This will result in the possible contact between roots towards the start of the growing season, especially when the space between-plants is low. For both the low and high root growth incorporated into the SIX model, there was a significant amount of time where roots had grown enough to be touching and therefore where there was no change to the rate of secondary infection. The rapid growth of wheat roots therefore reduces the effect of root growth on epidemic severity compared to any crops that have a central taproot.

Most root growth occurred at the start of the season, with roots in very close contact or touching as the season progressed. The infection of wheat roots by take-all is known to occur primarily through primary infection at the start of the growing season, before secondary infection dominates for the second half of the season (Bailey and Gilligan, 1999;

Bailey et al., 2005; Brassett and Gilligan, 1988; Schoeny and Lucas, 1999). The growth of roots was modelled to only have an impact on secondary infection, as it requires the close contact between the roots of different plants. Primary infection is more likely to be due to close contact between a single plant and piece of free-living pathogen. However, as the root growth mainly occurred towards the start of the growing season, and secondary infection mainly occurs towards the end of the growing season, the lack of effect of root growth on epidemic severity becomes apparent. The roots of different wheat plants will likely already be touching by the time secondary infection dominates, so incorporating root growth into the model has minimal effect on epidemic severity.

It is therefore a suitable modelling decision to not include root growth in this model. This is likely to be the case for other agricultural systems where root growth is fast, where the distance between crops is significantly smaller than the maximum lateral spread of the crop's root system, and where primary infection by a pathogen is the main source of infection at the start of a growing season. However, incorporating root growth into models where radial spread of roots is much smaller, or when crops are more spaced out, may have more of a significant impact on epidemic severity.

6.5.3 Optimising the spatial arrangement of a crop

During the first growing season, the lowest mean epidemic severity value was obtained when crops were evenly spaced rather than in rows. This is similar to the research in Gosme and Lucas (2011), who found that epidemic severity was reduced with broadcast sowing compared to line sowing. Evenly spaced crops allow for each plant to be as far away from all other plants as possible. For pathogens such as *Gaeumannomyces graminis* var. *tritici* that are known to have minimal spread within a season, maximising the space between-plants will have a significant impact on the total number of plants that can get infected.

When plants were spatially arranged in rows, epidemic severity increased as the distance between rows increased. This was due to an increased spread of infection between the closely spaced plants within each row. Although the use of rows can limit or prevent the spread of a pathogen between rows, too much space between rows will result in tightly spaced plants within rows that the pathogen can easily spread between. The importance of row spacing is likely to be dependent on the pathogen and its ability to move between-plants. The low spread of *Gaeumannomyces graminis* var. *tritici* means that even 12.5cm rows provided enough space between-plants to remove any noticeable infection between rows. The use of 25cm or 50cm rows therefore have no additional advantage compared to the 12.5cm rows, instead increasing the mean epidemic severity by increasing inter-row infection. These results are similar to Willocquet et al. (2008), who found that there was minimal epidemic spread between the rows of plants with 14cm between them. They instead found that most epidemic spread occurred within a row.

There was minimal impact of the spatial arrangement of a crop on epidemic severity for the second growing season. Mechanical dispersal resulted in high pathogen movement between rows for all three row spacing values. As this dispersal is much greater than the dispersal that occurs within a growing season, it reduces the benefit of any particular spatial arrangement. It may therefore be more beneficial for growers to implement agricultural procedures that limit the dispersal of material between growing seasons rather than selecting a specific spatial arrangement for planting. Marshall and Brain (1999) found that ploughing and seed drilling moved seeds much shorter distances in the soil than tine cultivations and harrowing. Disrupting the free-living pathogen as little as possible will lead to fewer overall infected plants, as well as smaller clusters of infected plants.

6.5.4 Conclusion

The small-scale spread of soil-borne pathogens like *Gaeumannomyces graminis* var. *tritici* provide interesting systems to spatially model, with small variations in crop spacing and dispersal kernels having significant impacts on epidemic severity. They highlight the problems associated with using large quadrats or small sample sizes to examine the impact of a pathogen across a field. They also show how agricultural machinery can cause significant increases to pathogen dispersal and can result in greater epidemic severity. If initial clusters of a pathogen can be targeted early, there is a chance for a significant reduction in epidemic spread and severity. There should therefore be a focus on examining the spread of pathogens, both within a season and between seasons, to identify how they can most effectively be targeted and suppressed.

Chapter 7: The effect of aggregation of a pathogen and biocontrol agent on epidemic severity

7.1 Abstract

The ability for a biocontrol agent to suppress a pathogen is dependent on contact between the two. However, as with other microorganisms within the soil, soil-borne pathogens will often have a patchy distribution across a field. Likewise, naturally occurring biocontrol agents may have the same patchy distribution. Current application methods are unlikely to result in homogeneous dispersal of a biocontrol agent. This coupled with the often-minimal distances that microorganisms can travel over is likely to result in populations of the biocontrol agent that cannot reach the pathogen.

Although there is often minimal within-season spread of microorganisms, mechanical dispersal from agricultural process between harvesting and replanting can transport soil over larger distances. This can result in initially small clusters of a pathogen expanding and moving across a field over several consecutive growing seasons. This chapter begins by examining the effect of aggregation of a pathogen on epidemic spread and severity across a five-year simulation. The scale of between-season dispersal is varied between low, medium, and high levels of dispersal. Epidemic severity increased as the pathogen became

less aggregated. A larger kernel scale parameter resulted in greater epidemic severity across successive years as the pathogen was able to spread across the host landscape more quickly.

The effect of aggregation of both a pathogen and a biocontrol agent on epidemic spread and severity was then examined. The selected model only allowed the biocontrol agent to negatively affect the pathogen through competition for space on a plant's roots. Epidemic severity was lower when the pathogen was more aggregated and when the biocontrol agent was less aggregated. If the biocontrol agent was highly aggregated at the start of the first season, high between-season dispersal allowed it to spread across the host landscape faster and therefore led to greater epidemic suppression. To the extent that it is possible, biocontrol application methods should focus on ensuring close to homogeneous dispersal whilst minimising disruption to the soil to ensure that the pathogen remains aggregated.

7.2 Introduction

7.2.1 Spatial aggregation of soil-borne plant diseases

Soil-borne pathogens often result in clusters of infected plants due to minimal movement of the pathogen within a growing season (Boland and Hall, 1988; Cook, 2003; Ferrin and Mitchell, 1984). Infection initially occurs from contact between the roots of a plant and free-living pathogen in the soil, before further spread can occur through transmission of the pathogen by root-to-root contact between different plants (Gosme and Lucas, 2011; Paulitz et al., 2002; Prew, 1980a). The number of clusters in a field of plants will depend on the distribution of free-living pathogen at the time that the crop is planted.

There is often a much greater spread of a pathogen between harvesting a crop and planting the next due to the movement of soil by agricultural processes such as harrowing or ploughing. Marshall and Brain (1999) examined the use of crop-harvesting machinery and soil cultivations on the movement of beads in the soil. The mean distances of dispersal were

between 0.26-1.58m, dependent on the agricultural process used. The take-all pathogen, *Gaeumannomyces graminis* var *tritici*, is known to often travel less than 20cm throughout a crop growing season. Initial infection occurs from pathogen inoculum in the soil, which can only grow several millimetres and therefore relies on the nearby roots of a plant to grow close to any inoculum (Brown and Hornby, 1971; Garrett, 1936; Gilligan, 1980; Pope and Jackson, 1973; Warcup, 1957; Wildermuth et al., 1984). The pathogen can then spread further by root-to-root contact between the infected and susceptible roots of neighbouring plants (Cook, 2003; Paulitz et al., 2002), resulting in a progressive spread of disease outwards from a source of inoculum (Gosme and Lucas, 2011; Prew, 1980a). However, the free-living pathogen can be dispersed over an area greater than 2m x 2m from the mechanical dispersal between growing seasons due to agricultural processes (Cotterill and Sivasithamparam, 1988; Gosme et al., 2007).

This mechanical spread is therefore highly influential on the incidence of a pathogen across growing seasons. A pathogen that was initially clustered may end up with a uniform incidence across a field after multiple large dispersal events. Ferrin and Mitchell (1986) hypothesised that the aggregation of a pathogen can create an upper limit on epidemic severity. If a pathogen that spreads minimally during a growing season is aggregated in one place or a small number of places, there will be a limit on the number of plants that the pathogen can access and have the opportunity to infect. A reduction in dispersal of the pathogen can therefore result in smaller clusters of infection which may lead to lower epidemic severity. However, the clustering of a pathogen will also lead to higher epidemic severity within these areas. There may therefore be a trade-off between the total number of infected plants and disease severity within these infected plants.

7.2.2 Successful application of a biocontrol agent

The use of biocontrol agents as control strategies against plant pathogens are often found to be successful in controlled laboratory experiments. However, there is minimal commercial uptake due to high variability in their success across different field trials (Fravel, 2005). Some of this variability is believed to be due to ineffective application, resulting in minimal transfer of the biocontrol agent to areas that contain the target pathogen (Mathre et al., 1999). One reason for this is due to application methods that result in heterogeneous dispersal of the biocontrol agent (Xu and Hu, 2020). A biocontrol agent must come into close contact with a pathogen to affect it. The aggregation of a biocontrol agent may therefore reduce its ability to suppress a pathogen. If the pathogen and biocontrol agent are both in different spatial locations, there will be little or no interaction between the two and therefore the biocontrol agent will not be able to effectively suppress the pathogen.

Soil-borne biocontrol agents are likely to be highly affected by aggregation due to them often being able to move minimal distances through the soil. Deacon (1988) suggested that the success of the mycoparasite, *Sporidesmium sclerotivorum*, in laboratory experiments against *Sclerotinia minor* was dependent on thorough mixing of it through the soil. This cannot be done to the same extent across an entire field, resulting in greater aggregation of the biocontrol agent and therefore less ability for it to suppress the pathogen. Liu et al. (2000) also demonstrated that virus transmission of a hypovirus which can act as a biocontrol agent against chestnut blight fungus, *Cryphonectria parasitica*, was overestimated if spatial heterogeneity was ignored. This further suggests that the spatial aggregation of a biocontrol agent can impact its effectiveness as a control method against pathogens.

Research has previously been carried out that has examined the effect of aggregation of a biocontrol agent on its ability to suppress a pathogen. Kessel et al. (2005) demonstrated that a uniform cover of *Ulocladium atrum* conidia on dead cyclamen leaf tissue was better able to suppress *Botrytis cinerea* than when it was aggregated. Xu and Hu (2020) used a

model to examine the aggregation between a biocontrol agent and a pathogen and found that greater aggregation of the biocontrol agent resulted in reduced biocontrol potential. Increased aggregation also resulted in increased variability in the success of the biocontrol agent. Bae and Knudsen (2007) found that high aggregation of the soil-borne pathogen *Sclerotinia sclerotiorum* resulted in a higher rate of colonisation by the biocontrol agent *Trichoderma harzianum* than if the pathogen was randomly distributed. Jeger et al. (2004) determined that the random distribution of propagules of a mycoparasite, acting as a biocontrol agent against soil-borne plant diseases, resulted in a slower rate of epidemic suppression than if the propagules were uniformly distributed.

There is often a focus on small-scale spatial interactions when examining aggregation of a pathogen and biocontrol agent, such as infection over the surface a leaf (Kessel et al., 2005). Although Bae and Knudsen (2007) examined the effect of spatial aggregation over two years, a single year with no temporal heterogeneity is often the limit of experimental work too. However, Gubbins and Gilligan (1997a) found that both temporal and spatial heterogeneity had an impact on the persistence of a biocontrol agent. It is therefore possible that both spatial aggregation, as well as temporal disturbances due to the harvesting and replanting of annual crops each year, may have a significant impact on the distribution of a biocontrol agent and therefore affect its ability to suppress a pathogen.

7.2.3 The effect of aggregation of both a pathogen and a biocontrol agent across a large-scale spatial model

This chapter focuses on the use of a mathematical model to simulate the effect of the aggregation of a pathogen and biocontrol agent across five growing seasons. There will be an initial examination of the effect of aggregation on epidemic spread and severity in the absence of a biocontrol agent. The analysis will then incorporate a biocontrol agent to see how the aggregation of both the pathogen and the biocontrol agent can affect each other.

The examination of spatial heterogeneity across multiple seasons allows for an analysis into the long-term success of a biocontrol agent. Although the population size of many biocontrol agents declines rapidly after application (Cook, 2003; Kim et al., 1997; Kimmey, 1969; Scherwinski et al., 2007; Schippers et al., 1987; Steddom et al., 2002; Sundheim, 1982; Szczech and Shoda, 2006), some biocontrol agents are known to persist in the soil for several years afterwards (Adams and Ayers, 1982; Cooksey, 1982; Htay and Kerr, 1974; Moore and Cook, 1984; Sutton and Peng, 1993). One example of this is with take-all decline, where the population of 2,4-DAPG fluorescent *Pseudomonas* spp. build up gradually in the soil over several years of growing winter wheat consecutively, and eventually results in long-term epidemic suppression as long as wheat continues to be grown each season (Cook, 2003; Raaijmakers and Weller, 1998). As the take all pathogen, *Gaeumannomyces graminis* var. *tritici*, is known to cause clusters of infected plants, the success of 2,4-DAPG fluorescent *Pseudomonas* spp. will be heavily dependent on close contact to these clusters.

7.2.4 Key questions

This chapter will focus on the following key questions:

1. How does aggregation of a pathogen affect epidemic spread and severity across a five year simulation?

2. How does aggregation of a biocontrol agent affect its ability to suppress a pathogen?

3. What effect does the scale of between-season dispersal of the pathogen and biocontrol agent have on epidemic severity and pathogen suppression?

There will be a focus on large-scale dynamics, covering an area of 16m x 16m . This area size was chosen as it was a compromise between 1) having a large enough area to simulate dispersal of the pathogen and biocontrol agent across multiple years, and 2) reducing the simulation time and computational effort required.

7.3 Methods

7.3.1 The SIX and SIXCA models

The SIX and SIXCA models are described in detail in Chapter 2. The SIX model simulates the interactions between the roots of a plant and a soil-borne pathogen. A root begins as susceptible (S) and can become infected by the pathogen either through contact with an infected root (I), or through contact with free-living pathogen (X) in the surrounding soil. The SIXCA model is an expansion of this model where roots can also become colonised by the biocontrol agent through contact with a colonised root (C), or through contact with free-living biocontrol agent (A) in the surrounding soil.

The SIX and SIXCA model dynamics account for the temporal heterogeneity that occurs each year due to the planting and harvesting of seasonal crops. The plant's roots are only present for part of each year to represent the time in between planting and harvesting. Once the crop has been harvested, all roots die. The free-living pathogen (SIX and SIXCA models) and biocontrol agent (only the SIXCA model) are present throughout each year as they survive this between-season period using decaying organic matter in the soil as a host. A summary of the parameters used in the SIXCA model can be found in Table 7.1, where the SIX model includes all of these parameters apart from these related to the biocontrol agent.

7.3.2 Spatial distribution of the crop

The crop is spread over an area measuring 16m x 16m. Each 50x50cm square is spatially modelled and is given a set of Cartesian (x,y) coordinates to represent the centre of the area's location. This results in 1024 sets of coordinates. The average level of infection

Table 7.1 List of parameters and definitions for the spatial and seasonal SIXCA model, where the biocontrol agent can only negatively affect the pathogen through competition for space on a plant's roots by primary (α_P) and secondary (α_S) colonisation.

Parameter	Definition	Default value	Source
S	Number of susceptible roots	-	-
I	Number of roots infected by the pathogen	-	-
C	Number of roots colonised by the biocontrol agent	-	-
X	Density of free-living pathogen	-	-
A	Density of free-living biocontrol agent	-	-
X_s	Initial amount of free-living pathogen present at the start of the first growing season	25	Fixed
A_s	Initial amount of free-living biocontrol agent present at the start of the first growing season	25	Fixed
t	Time (degree days $> 0^{\circ}$C)	-	-
ρ	Rate of root production	$3.31 \times 10^{-3}\ t^{-1}$	Chapter 3
κ	Carrying capacity of root production	32.1	Chapter 3
β_p	Rate of primary infection of roots by free-living pathogen	$1.35 \times 10^{-3}\ t^{-1}$	Chapter 3
β_s	Rate of secondary infection of roots	$5.92 \times 10^{-5}\ t^{-1}$	Chapter 3
λ_X	Rate of decay of pathogen inoculum	$3.53 \times 10^{-3}\ t^{-1}$	Bailey and Gilligan (1999); Bailey et al. (1995)
τ_I	Number of root fragments produced from a dead infected root when the host crop is harvested	3.16	Chapter 4
α_p	Rate of primary colonisation of roots by free-living biocontrol agent	$5.39 \times 10^{-2}\ t^{-1}$	Chapter 4
α_s	Rate of secondary colonisation of roots	$2.18 \times 10^{-5}\ t^{-1}$	Chapter 4
λ_A	Rate of decay of free-living biocontrol agent	$5.13 \times 10^{-3}\ t^{-1}$	Elsas et al. (1986); Weller (1983)
τ_C	Number of root fragments produced from a dead colonised root when the host crop is harvested	3.14	Chapter 4
γ_B	Scale parameter for the mechanical dispersal of free-living pathogen and biocontrol agent between growing seasons	5cm, 15cm, or 30cm	-

and colonisation within each 50x50cm square, as well as the average density of free-living pathogen and biocontrol agent in the region surrounding these plants, is modelled.

The dispersal of soil-borne microorganisms within a growing season is often low, relying on root-to-root contact between neighbouring plants. Take-all disease commonly results in patches of infected plants, where initial infection occurs from pathogen inoculum in the soil, and the pathogen then spreads radially outwards between the interconnected roots of different plants. Dispersal of take-all is known to be low, rarely spreading further than a

50x50m square within a growing season (Section 6.2.2). Infection or colonisation between plants during a growing season is therefore not spatially modelled, instead assuming that each area of plants can only infect or colonise other plants within this area.

The use of 50x50cm grid squares within this research was was chosen as it was a compromise between 1) allowing for a large enough area to be simulated to examine between-season dispersal of the pathogen and biocontrol agent, and 2) reducing simulation times and computational effort. A smaller grid size would also have to take into account the potential for infection and colonisation to spread between clusters during a growing season, which would have further increased the computational effort required.

7.3.3 Between growing seasons - mechanical dispersal

Within a growing season, there are no spatial dynamics between the plants in each 50x50cm area. During the between growing season period, free-living material can be picked up by agricultural machinery and dispersed over large distances due to mechanical processes such as ploughing and harrowing (Marshall and Brain, 1999). Between-season dispersal can result in the movement of the free-living pathogen and biocontrol agent over a much larger distance than they would be able to travel on their own. This results in a larger area of soil that contains the pathogen and biocontrol agent compared to if there was no mechanical dispersal, and can therefore lead to more plants becoming infected or colonised during the next growing season. Between-season dispersal is spatially modelled to examine how dispersal distance and aggregation of the pathogen and biocontrol agent affect epidemic severity and disease suppression. It is also a stochastic process to allow for an element of variation in the dispersal distance of material in the soil to be incorporated, as would be seen with agricultural machinery.

The chance of a piece of free-living material travelling a certain distance from its original location is assumed to decline exponentially as the distance increases, following a similar

approach to that found in Truscott and Gilligan (2001), Grundy et al. (1999), Marshall and Brain (1999), and Stacey et al. (2004). Information about the dispersal kernel used to calculate the movement of free-living material can be found in Section 6.3.1. It contains a normalisation constant and has a mean dispersal dispersal of 2γ, where γ is the scale parameter used in the dispersal kernel. Although Section 6.3.1 focuses on the dispersal of a pathogen, it is assumed that this between-season dispersal is identical for the pathogen and the biocontrol agent.

7.3.4 Analysing the effect of pathogen and biocontrol agent aggregation on epidemic severity

Measuring epidemic severity

The severity of the epidemic across each year was measured using the area under the epidemic progress curve for healthy roots (AUHC), which includes both susceptible and colonised roots. This is calculated in the same way as the area under the disease progress curve (AUDPC), which is commonly used to determine epidemic severity for plant diseases (Campbell and Madden, 1990; Jeger and Viljanen-Rollinson, 2001). Although the process of calculating the AUDPC can be difficult when using a small amount of experimental data (Jeger and Viljanen-Rollinson, 2001), the use of a mathematical model allows for a precise calculation due to the unlimited amount of data that can be generated using it. Using AUHC allows for a comparison between the number of healthy roots in a simulation when a pathogen is present compared to when it is not present (Elderfield, 2018). The AUHC is calculated using

$$\mathrm{AUHC}_{\mathrm{normalised}} = \frac{\mathrm{AUHC\_I}}{\mathrm{AUHC\_S}}, \tag{7.1}$$

where AUHC_I is the AUHC for a simulation where a pathogen is present, and AUHC_S is the AUHC for the same simulation if no pathogen was present. Equation 7.1 will calculate a number between 0 and 1, where 0 corresponds to a simulation where all roots are diseased, and 1 corresponds to a simulation where all roots are healthy. The epidemic severity can then be calculated by

$$\text{Epidemic severity} = 1 - \text{AUHC}_{\text{normalised}}, \tag{7.2}$$

where a higher value represents a greater proportion of infected roots.

Effect of pathogen aggregation and between-season dispersal on epidemic severity

There is initially a focus on the SIX model, which simulates the interactions between a pathogen and host plant. An epidemic begins with 25 units of free-living pathogen, which was determined in Section 6.3.2 to represent the introduction of a moderate amount of free-living pathogen into a field. The effect of pathogen aggregation on epidemic severity was examined by dividing this amount of free-living material over a certain number of locations. This varied between a single cluster of inoculum to evenly spread inoculum across all 1024 grid locations. Each cluster had an equal amount of pathogen inoculum. The location of each cluster was chosen randomly, and the mean epidemic severity across 20 simulations was used to reduce any impact of the initial cluster locations. Each simulation was performed for 5 years to examine how the pathogen spread over this time. A visualisation of epidemic spread with one cluster, 50 clusters, or when the pathogen is evenly spread can be seen in Figure 7.1.

In Figure 7.1, the scale parameter for between-season mechanical dispersal of the pathogen, γ, is fixed at 15cm. This represents a mean dispersal distance of 30cm, and is the value used within Chapter 6. This distance is similar to the mean distance that free-living

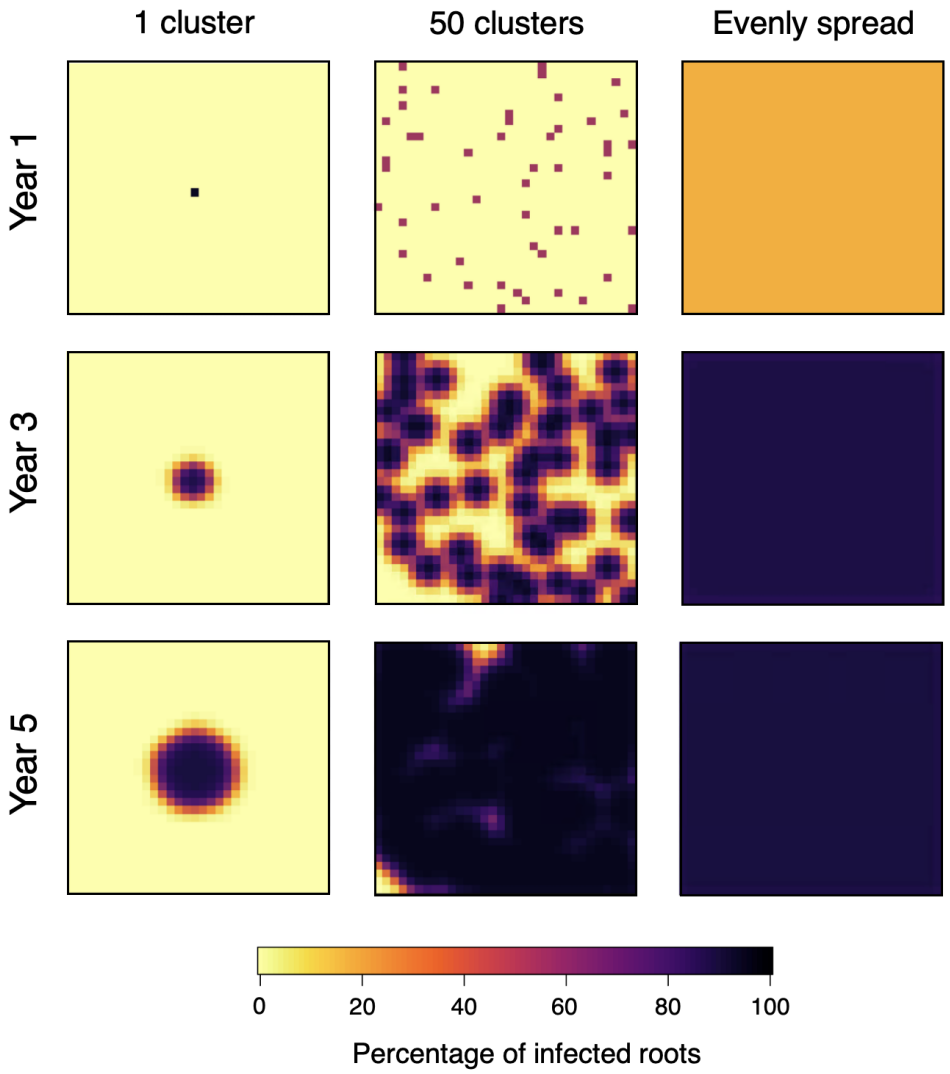

Fig. 7.1 Dispersal of a pathogen across a 16m x 16m area where the free-living pathogen is either all grouped together in one cluster, is spread across 50 clusters, or is evenly spread across the area at the start of the first season. Dispersal of the pathogen occurs between harvesting the previous crop and planting the next, using an exponential dispersal kernel with a scale parameter value of 15. The percentage of infected roots at the end of the growing season after the first, third, and fifth years of consecutive planting are shown. The initial cluster locations are chosen at random.

material was found to move due to ploughing or seed drilling (Marshall and Brain, 1999). The effect of varying γ to 5cm or 30cm on epidemic severity is examined. A value of 5cm can be seen as low dispersal, 15cm as moderate dispersal, and 30cm as high dispersal. An example of the effect of γ on epidemic spread across a five year simulation can be seen in

Figure 7.2, where γ is varied between 5cm, 15cm, and 30cm whilst the initial number of clusters remains fixed at 50.

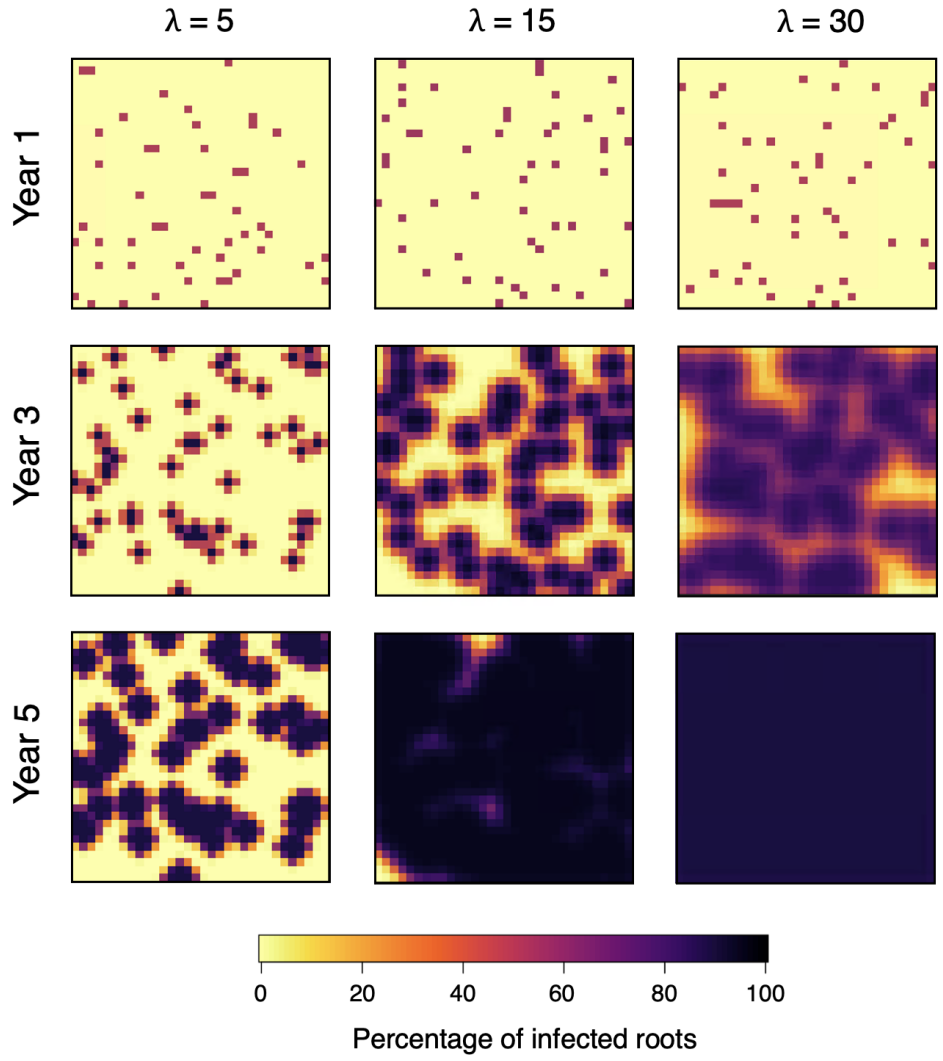

Fig. 7.2 Dispersal of a pathogen across a 16m x 16m area where the free-living pathogen is split into 50 clusters at the start of the first season. Dispersal of the pathogen occurs between harvesting the previous crop and planting the next, using an exponential dispersal kernel with a scale parameter value of 5cm, 15cm, or 30cm. The percentage of infected roots at the end of the growing season after the first, third, and fifth years of consecutive planting are shown.The initial cluster locations are chosen at random.

Addition of a biocontrol agent

The effect of aggregation of both the pathogen and the biocontrol agent on epidemic severity was examined. This used the SIXCA model and required between-season dispersal of both the free-living pathogen and biocontrol agent. As in Section 7.3.4, the initial starting locations of the pathogen and biocontrol agent were chosen randomly between all the 50x50cm areas. The mean epidemic severity across 20 simulations was used to reduce the impact of the initial cluster locations, with initial analysis suggesting that this number of repetitions was enough to significantly reduce the impact of these initial locations.

Two variations in the spatial aggregation of the pathogen and biocontrol agent were examined:

1. The aggregation of the pathogen and biocontrol agent are the same. Both the free-living pathogen and biocontrol agent vary between being present in a single cluster, to being evenly spread across all 1024 locations. An example of this can be seen in Figure 7.3, where there are 50 clusters of the pathogen and 50 clusters of the biocontrol agent

2. The aggregation of the pathogen and biocontrol agent are opposite to each other. As the pathogen increases the number of clusters that it is initially present across (decreased spatial aggregation), the biocontrol agent decreases the number of clusters that it is initially present across (increased spatial aggregation). Examples of this can be seen in Figures 7.4 and 7.5. Figure 7.4 examines the number of infected and colonised roots when the free-living pathogen is initially split across 50 clusters, and when the free-living biocontrol agent is initially split across 1000 clusters. Figure 7.5 examines the number of infected and colonised roots when the free-living pathogen is initially split across 1000 clusters, and when the free-living biocontrol agent is initially split across 50 clusters

The initial locations of the pathogen and biocontrol agents were allowed to occur within the same area. The effect of the scale parameter for the dispersal kernel on epidemic severity was examined by comparing the results when it is varied between 5cm, 15cm, and 30cm. The dispersal kernel is always fixed at the same value for both the pathogen and biocontrol agent.

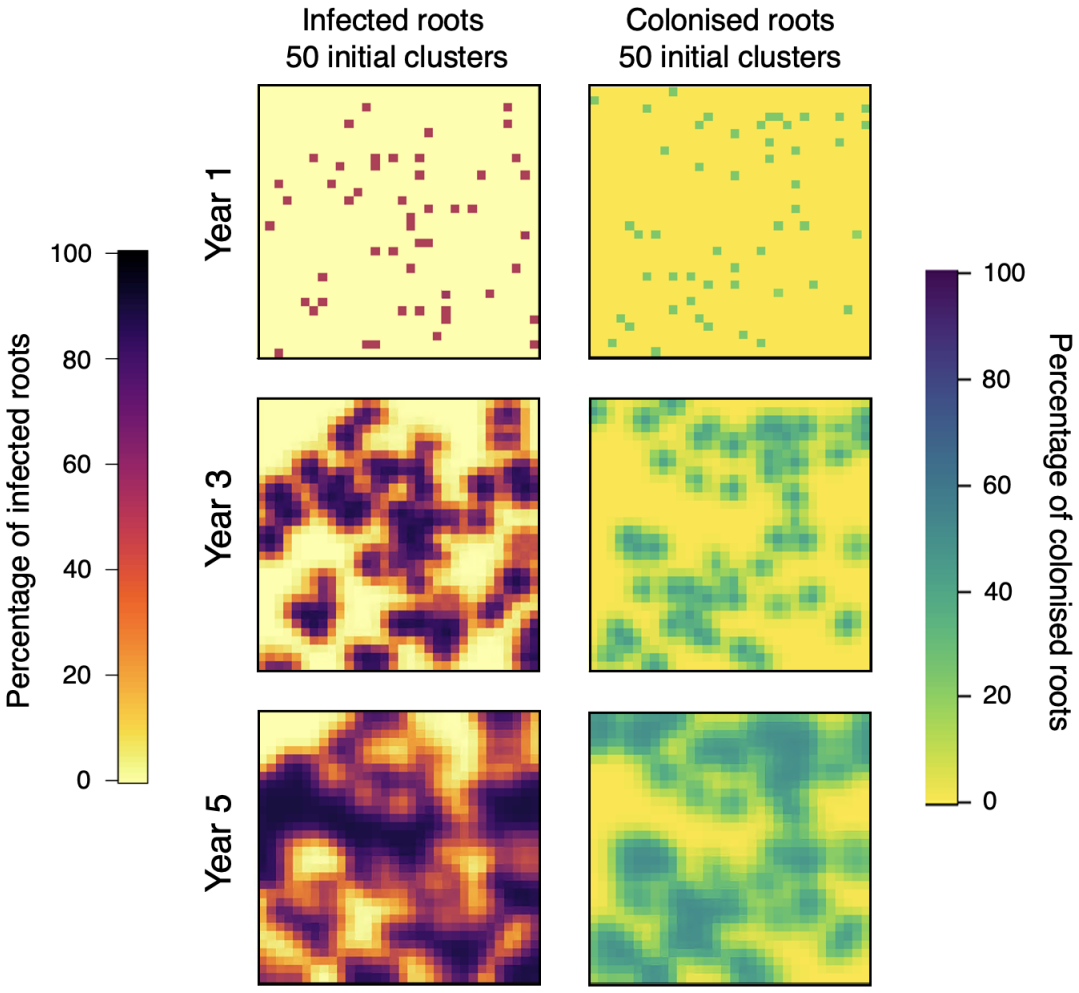

Fig. 7.3 Dispersal of a pathogen and biocontrol agent across a 16m x 16m area where the free-living pathogen and biocontrol agent are divided into 50 clusters at the start of the first season. Dispersal of the pathogen and biocontrol agent occurs between harvesting the previous crop and planting the next, using an exponential dispersal kernel with a scale parameter value of 15cm. The plots represent the percentage of infected roots and the percentage of colonised roots at the end of the growing season after the first, third, and fifth years of consecutive planting. The initial cluster locations are chosen at random.

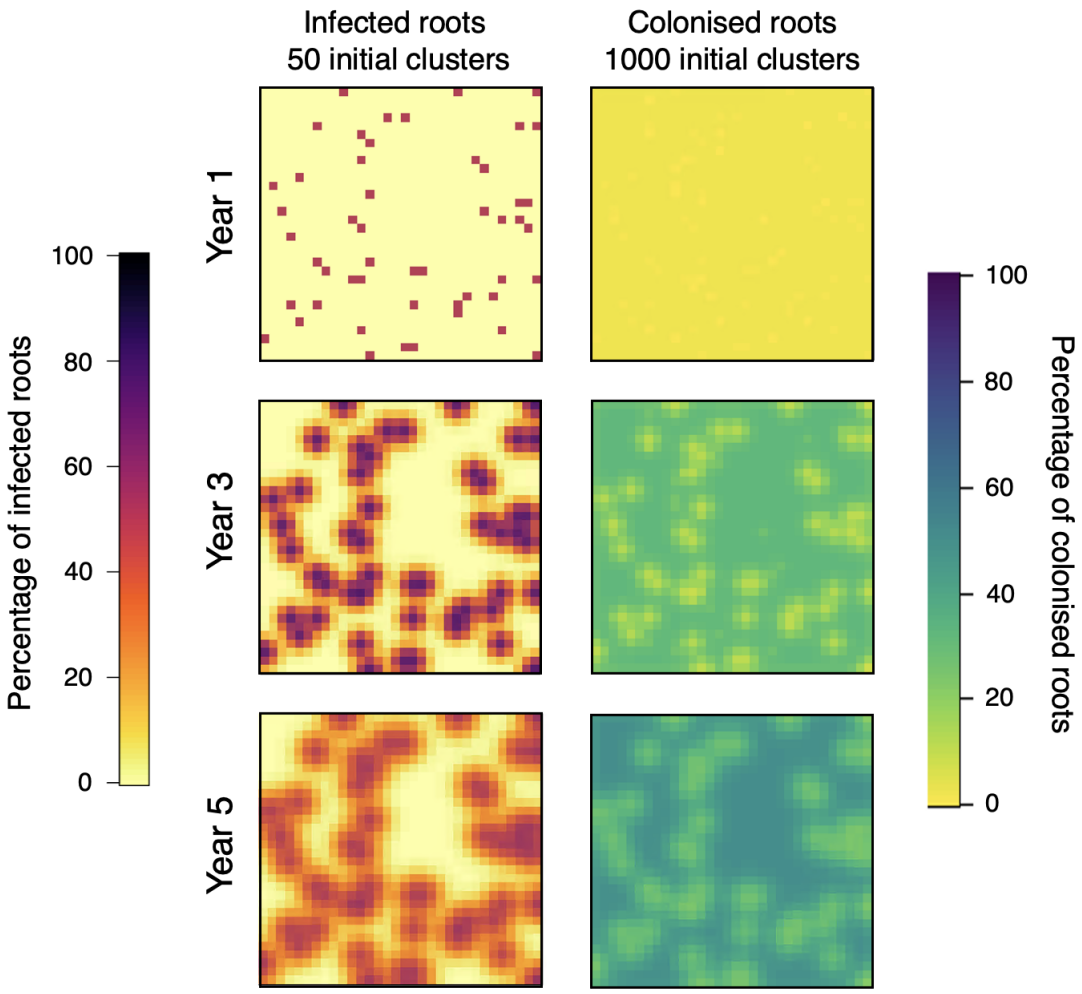

Fig. 7.4 Dispersal of a pathogen and biocontrol agent across a 16m x 16m area where the free-living pathogen is divided into 50 clusters and the free-living biocontrol agent is divided into 1000 clusters at the start of the first season. Dispersal of the pathogen and biocontrol agent occurs between harvesting the previous crop and planting the next, using an exponential dispersal kernel with a scale parameter value of 15cm. The plots represent the percentage of infected roots and the percentage of colonised roots at the end of the growing season after the first, third, and fifth years of consecutive planting. The initial cluster locations are chosen at random.

Identifying the optimal spatial aggregation of the pathogen and biocontrol agent

The epidemic severity is examined when

1. The biocontrol agent is present or absent

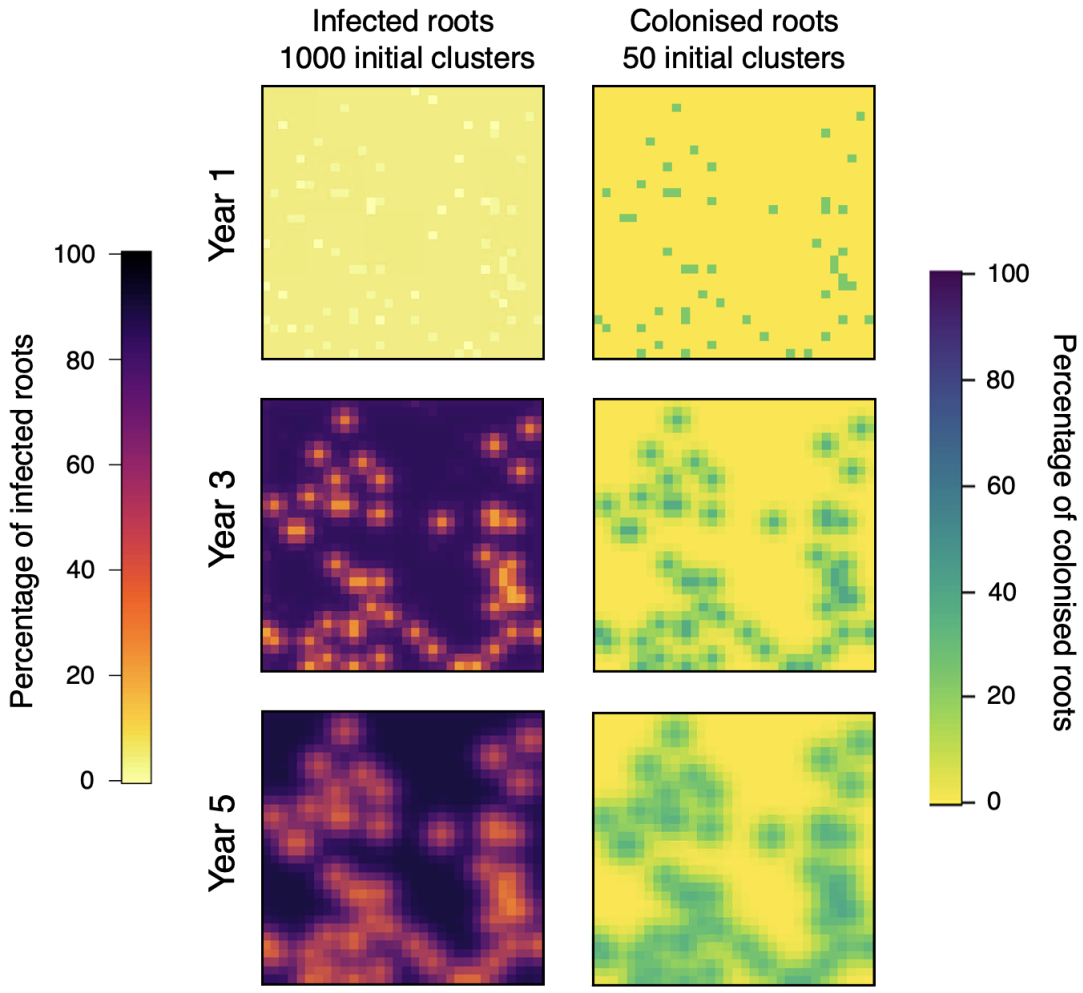

Fig. 7.5 Dispersal of a pathogen and biocontrol agent across a 16m x 16m area where the free-living pathogen is divided into 1000 clusters and the free-living biocontrol agent is divided into 50 clusters at the start of the first season. Dispersal of the pathogen and biocontrol agent occurs between harvesting the previous crop and planting the next, using an exponential dispersal kernel with a scale parameter value of 15cm. The plots represent the percentage of infected roots and the percentage of colonised roots at the end of the growing season after the first, third, and fifth years of consecutive planting. The initial cluster locations are chosen at random.

2. The scale parameter for the dispersal kernel is varied between 5cm, 15cm, and 30cm

3. The initial aggregation of the pathogen and biocontrol agent vary between all being located at a single cluster to being evenly spread.

This allows for an examination as to which factors may have a significant impact on epidemic severity and disease suppression.

7.4 Results

7.4.1 Aggregation of the pathogen with no biocontrol agent present

Across the first year of the simulation, there was low epidemic severity regardless of how aggregated the pathogen was (Figure 7.6). The pathogen is unable to spread during this first season and is therefore confined to the locations it was placed at the start of the simulation. As can be seen in Figure 7.1, low clustering will result in a few areas that have high epidemic severity, whereas high clustering or evenly spaced pathogen will result in a large area that has low epidemic severity. These two spatial arrangements will therefore result in similar overall epidemic severity levels.

For the third year of the simulation, a decrease in aggregation of the pathogen results in an almost linear increase in epidemic severity. Two between-season dispersal events have allowed the pathogen to spread out from its initial locations. However, the highly aggregated pathogen is limited by the scale parameter for between-season dispersal and will still not be able to reach all the plants. As the pathogen becomes less aggregated, there is a greater area that is reached by it. Areas that were infected by the pathogen in the first and second year will have produced pathogen inoculum that is dispersed in the successive seasons, resulting in an even greater epidemic severity as aggregation decreases.

For the fifth year of the simulation, the entire cropping area is infected by the pathogen for all but the simulations that had the highest initial aggregation of the pathogen. Between-season dispersal has resulted in the maximum spread of pathogen inoculum across the spatial landscape, as well as a maximum level of infection for each plant.

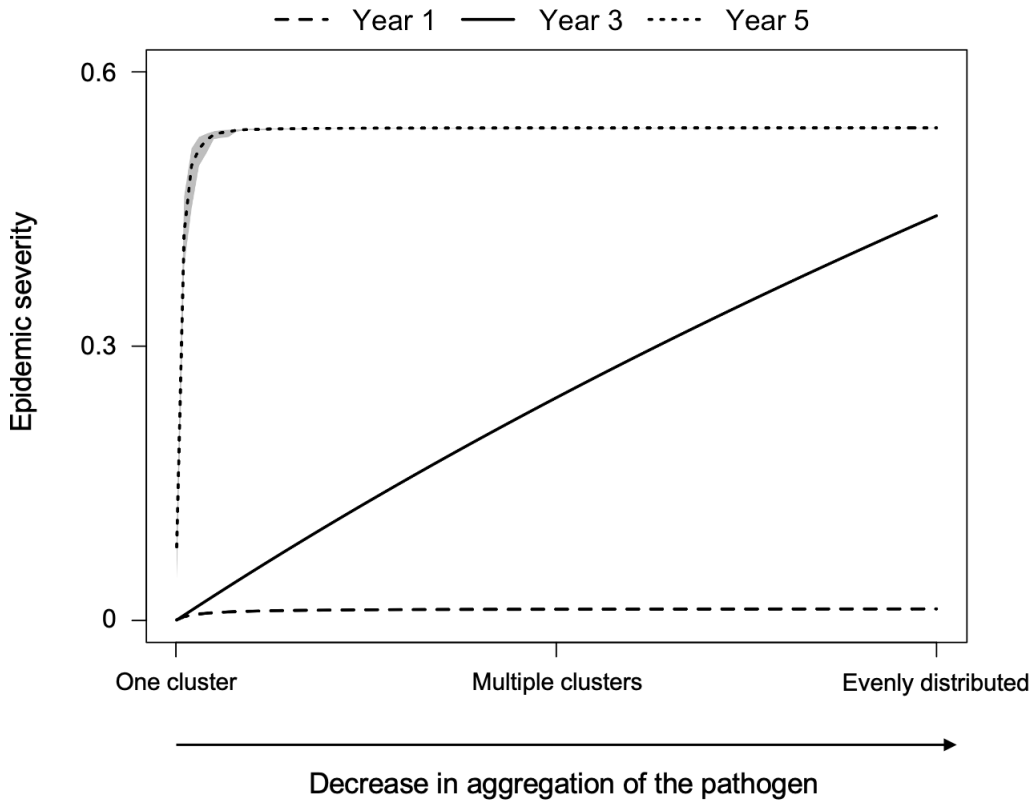

Fig. 7.6 Change in epidemic severity in the first, third, and fifth year of an epidemic as the aggregation of a pathogen varies. The epidemic severity represents the mean value of epidemic severity across all plants included in a simulation. The scale parameter for between-season dispersal is fixed at 15cm.

Across a five year simulation, there was an increase in epidemic severity as the aggregation of the pathogen decreased for scale parameter values of the between-season dispersal kernel fixed at 5cm, 15cm, or 30cm (Figure 7.7). There was a steeper increase in epidemic severity as aggregation of the pathogen decreased when the scale parameter was higher. Dispersal of the pathogen across a greater area is able to transport it to new locations faster than when dispersal occurs across a smaller area. Lower dispersal of the pathogen reduces the mean epidemic severity across the five year simulation when the pathogen is initially aggregated, but has no difference when the pathogen is evenly distributed.

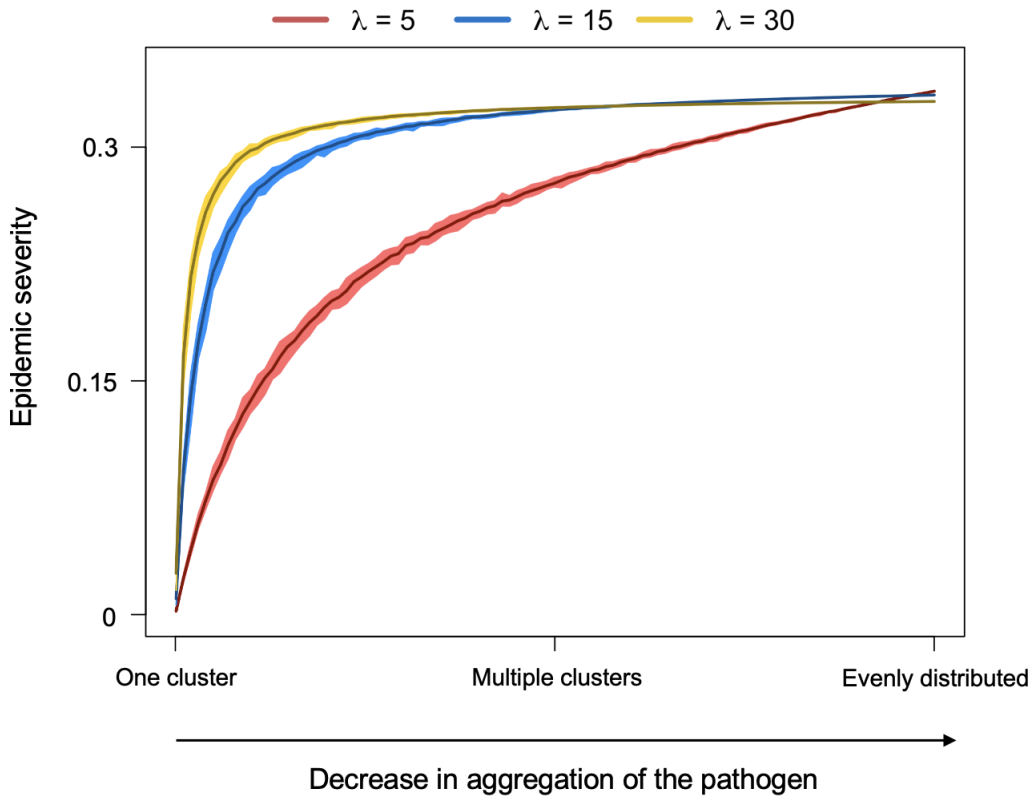

Fig. 7.7 Change in epidemic severity for a five year simulation as pathogen aggregation and the scale of between-season dispersal varies. The epidemic severity represents the mean value of epidemic severity across all plants included in a simulation. Between-season dispersal occurs through an exponential dispersal kernel with the scale parameter fixed at either 5cm, 15cm, or 30cm. The mean value across 20 simulations is plotted as a darker line, with the range of values across these simulations shown by a lighter area behind this line. The amount of clusters varies between one, with all pathogen in this cluster, and 1024, where the pathogen is evenly spread across the area.

7.4.2 Aggregation of the pathogen and the biocontrol agent

Epidemic severity was examined across a five year simulation as the aggregation of the pathogen and the biocontrol agent varied (Figure 7.8). A decrease in aggregation of the pathogen and the biocontrol agent resulted in an increase in epidemic severity. Compared to when when the biocontrol agent was not included in the model (Figure 7.7), there is a lower

maximum value for epidemic severity. This maximum value is reached for simulations with a higher level of aggregation when the scale parameter for the dispersal kernel is higher.

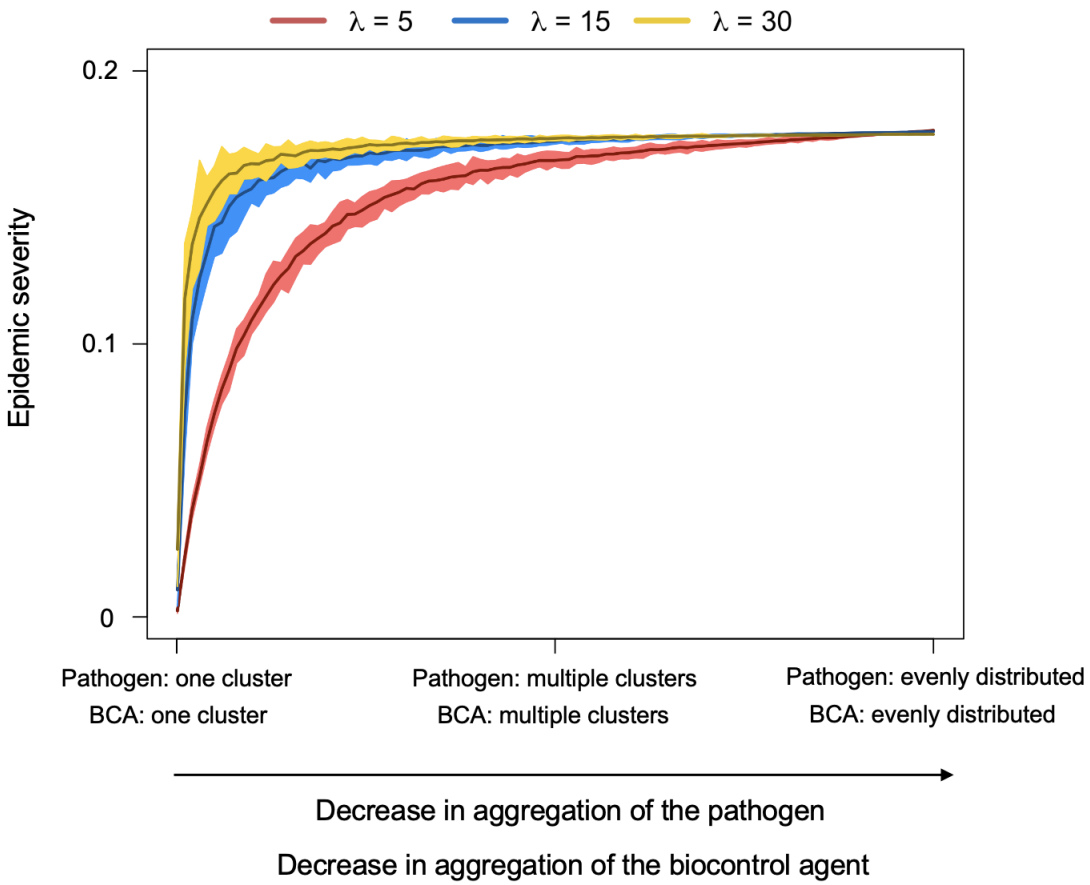

Fig. 7.8 Change in epidemic severity for a five year simulation as aggregation of the pathogen and biocontrol agent (BCA), as well as the scale of between-season dispersal, varies. The pathogen and biocontrol agent both have the same amount of aggregation, where the number of initial clusters of the pathogen is always the same as the number of initial clusters of the biocontrol agent. The epidemic severity represents the mean value of epidemic severity across all plants included in a simulation. Between-season dispersal occurs through an exponential dispersal kernel with the scale parameter fixed at either 5cm, 15cm, or 30cm. The mean value across 20 simulations is plotted as a darker line, with the range of values across these simulations shown by a lighter area behind this line. For both the pathogen and the biocontrol agent, the amount of clusters varies between one, with all pathogen or biocontrol agent in this cluster, and 1024, where the pathogen or biocontrol agent is evenly spread across the area.

The effect of opposite levels of aggregation between the pathogen and biocontrol agent across a five year simulation is explored in Figure 7.9. As the aggregation of the pathogen increases across different simulations, the aggregation of the biocontrol agent decreases. Likewise, as the aggregation of the pathogen decreases across different simulations, the aggregation of the biocontrol agent increases. There was an increase in epidemic severity as the aggregation of the pathogen decreased and the aggregation of the biocontrol agent increased. When the biocontrol agent is aggregated across fewer locations, it is not always in close contact with the pathogen and is therefore limited in its ability to suppress the pathogen.

When there is high aggregation of the pathogen and low aggregation of the biocontrol agent, epidemic severity is higher when between-season dispersal is higher. When there is low aggregation of the pathogen and high aggregation of the biocontrol agent, epidemic severity is lower when between-season dispersal is higher. Successful application of a biocontrol agent therefore requires either low aggregation of the biocontrol agent and a low dispersal kernel, or high aggregation of the biocontrol agent and a high dispersal kernel. Both of these allow the biocontrol agent to spread as much as possible across the simulation area, maximising its contact with the pathogen across a field. Increased between-season dispersal of the biocontrol agent reduces the effect of initial aggregation due to greater movement of the biocontrol agent, allowing it to spread over a larger area more quickly. If initial aggregation is low for the biocontrol agent but high for the pathogen, it is beneficial to have a low dispersal kernel to limit the movement of the pathogen.

7.4.3 Examining the effect of aggregation of a pathogen and biocontrol agent on epidemic severity

For the first year of a growing season, there is minimal effect of biocontrol presence or biocontrol aggregation on epidemic severity (Figure 7.10). There has been no between-

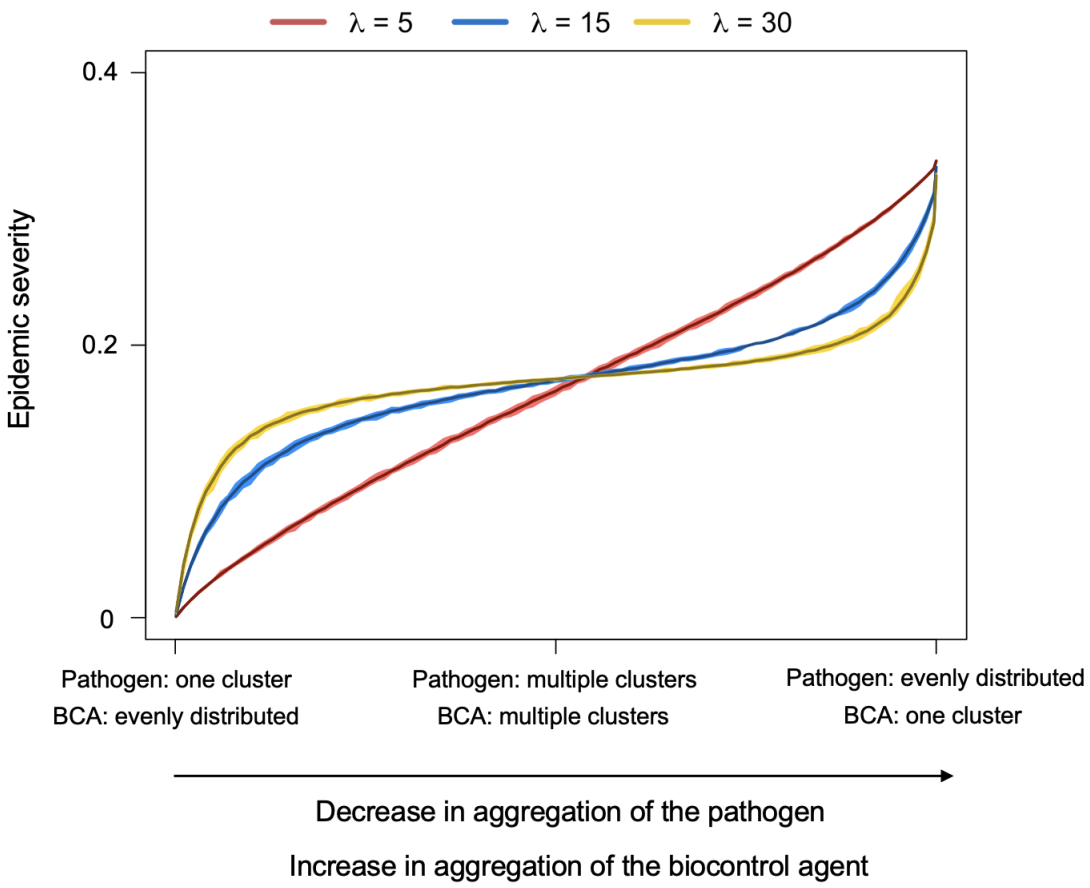

Fig. 7.9 Change in epidemic severity for a five year simulation as aggregation of the pathogen and biocontrol agent (BCA) vary, as well as the scale of between-season dispersal, varies. As the pathogen becomes more aggregated, the biocontrol agent becomes less aggregated. Similarly, as the pathogen becomes less aggregated, the biocontrol agent becomes more aggregated. The epidemic severity represents the mean value of epidemic severity across all plants included in a simulation. Between-season dispersal occurs through an exponential dispersal kernel with the scale parameter fixed at either 5cm, 15cm, or 30cm. The mean value across 20 simulations is plotted as a darker line, with the range of values across these simulations shown by a lighter area behind this line. For both the pathogen and the biocontrol agent, the amount of clusters varies between one, with all pathogen or biocontrol agent in this cluster, and 1024, where the pathogen or biocontrol agent is evenly spread across the area.

season dispersal of the pathogen and biocontrol agent at this point, and therefore they are both only able to infect/colonise within the area that they were placed at the start of the simulation. There is a slight increase in epidemic severity as the pathogen aggregation

decreases, and a slight decrease in epidemic severity when the biocontrol agent is included in the simulation. However, clustering of the biocontrol agent had minimal impact on epidemic severity during this first season.

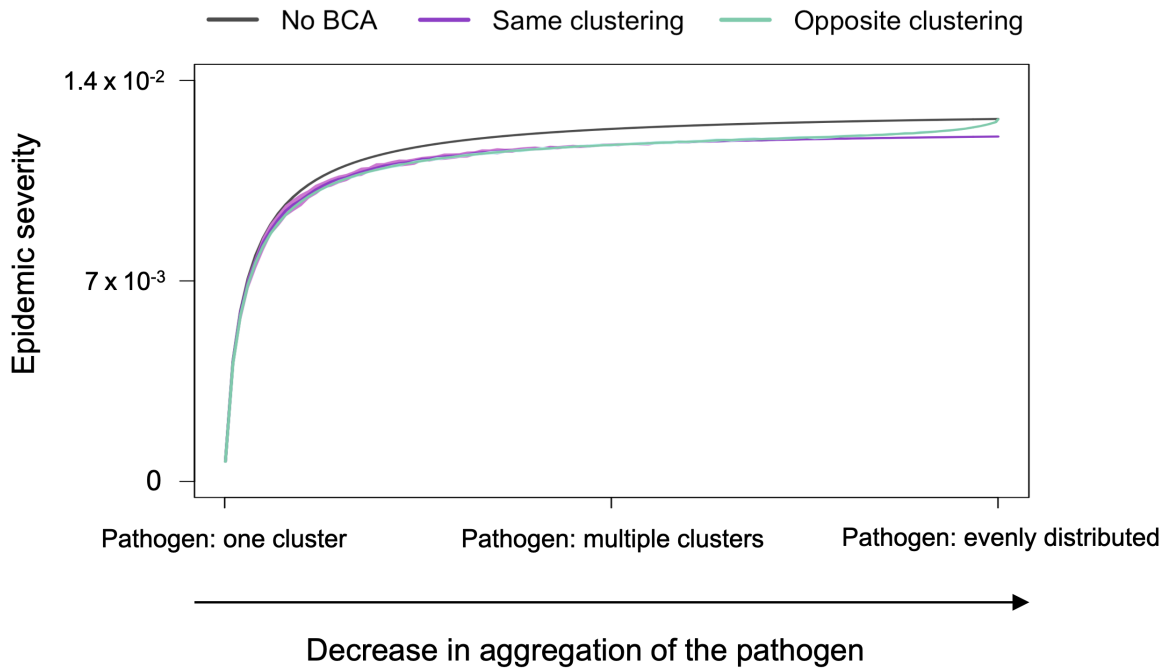

Fig. 7.10 Change in the epidemic severity for a one year simulation as the aggregation of the pathogen and the biocontrol agent (BCA) vary. Three strategies are compared: A) when only the pathogen is present, B) when both the pathogen and the biocontrol agent are present, and both have the same amount of aggregation, C) when both the pathogen and biocontrol agent are present, and have opposite aggregations. For C) as the pathogen becomes more aggregated, the biocontrol agent becomes less aggregated. Similarly, as the pathogen becomes less aggregated, the biocontrol agent becomes more aggregated.The epidemic severity represents the mean value of epidemic severity across all plants included in a simulation. The scale parameter for between-season dispersal is fixed at 15cm. The mean value across 20 simulations is plotted as a darker line, with the range of values across these simulations shown by a lighter area behind this line. For both the pathogen and the biocontrol agent, the amount of clusters varies between one, with all pathogen or biocontrol agent in this cluster, and 1024, where the pathogen or biocontrol agent is evenly spread across the area.

The relationship between aggregation of the pathogen and biocontrol agent was explored further across a five year simulation in Figure 7.11. The same general pattern is seen across all three scale parameters for the between-season dispersal kernel (γ = 5cm, 15cm, or 30cm).

Epidemic severity was highest when the biocontrol agent was not included in the simulation, regardless of the aggregation of the pathogen or biocontrol agent. When aggregation of the pathogen is high, epidemic severity is reduced the most when the aggregation of the biocontrol agent is low. When aggregation of the pathogen is low, epidemic severity is reduced the most with low aggregation of the biocontrol agent. There is therefore always the greatest reduction in epidemic severity when the biocontrol agent is less aggregated and more evenly spread across the spatial landscape. This allows it to come into contact with a maximum amount of plants infected by the pathogen, as well as being able to colonise the roots of more plants and produce more free-living material from this interaction.

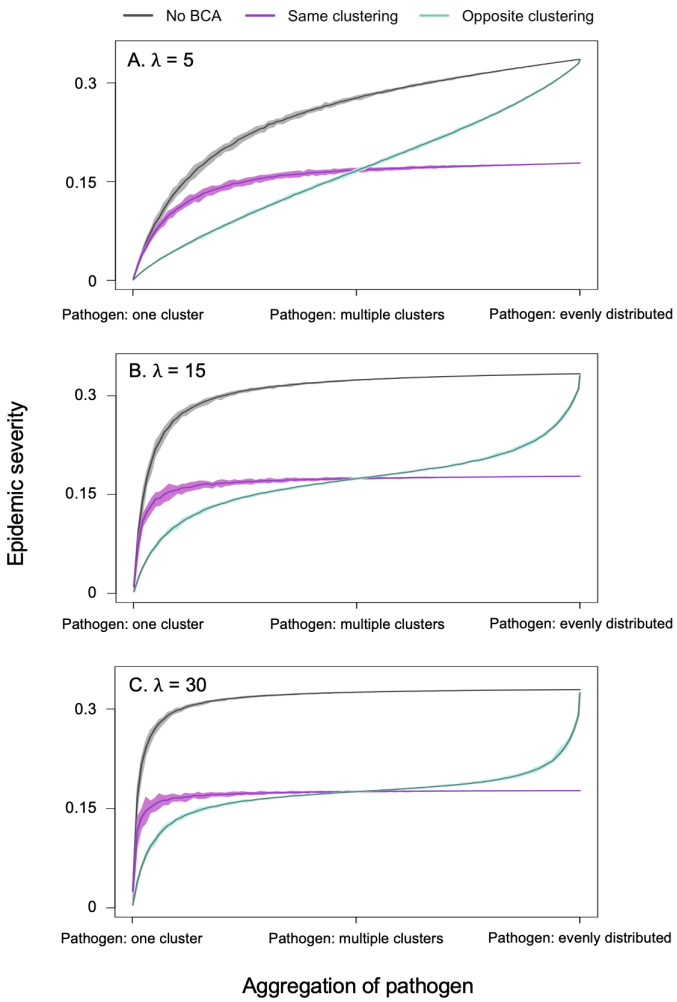

Fig. 7.11 Change in the epidemic severity for a five year simulation as the aggregation of the pathogen and the biocontrol agent (BCA), as well as between-season dispersal, vary. Three strategies are compared: i) when only the pathogen is present, ii) when both the pathogen and the biocontrol agent are present, and both have the same amount of aggregation, iii) when both the pathogen and biocontrol agent are present, and have opposite aggregations. For iii) as the pathogen becomes more aggregated, the biocontrol agent becomes less aggregated. Similarly, as the pathogen becomes less aggregated, the biocontrol agent becomes more aggregated.The epidemic severity represents the mean value of epidemic severity across all plants included in a simulation. Between-season dispersal occurs through an exponential dispersal kernel with the scale parameter fixed at either A) 5cm, B) 15cm, or C) 30cm. The mean value across 20 simulations is plotted as a darker line, with the range of values across these simulations shown by a lighter area behind this line. For both the pathogen and the biocontrol agent, the amount of clusters varies between one, with all pathogen or biocontrol agent in this cluster, and 1024, where the pathogen or biocontrol agent is evenly spread across the area.

7.5 Discussion

7.5.1 Effect of pathogen aggregation on epidemic severity

The spatial aggregation of a pathogen was found to reduce the amount of host plants that it can come into contact with, therefore reducing the total number of plants that can become infected. If a pathogen is highly aggregated within a field, there may be large areas where the pathogen is not present and cannot cause infection. This is especially likely with soil-borne pathogens as they can often only spread minimal distances through the soil (Gosme and Lucas, 2011; Paulitz et al., 2002; Prew, 1980a). Increased aggregation of the pathogen also reduces the number of plants that are available as host material for the pathogen to bulk up on. Aggregation of the pathogen creates a restriction on the upper limit of its population size and minimises epidemic severity (Ferrin and Mitchell, 1986).

The results in this chapter found that low movement of soil-borne pathogens within a growing season restricted their ability to infect nearby plants and reduced epidemic suppression. However, dispersal between growing seasons greatly increased the distribution of a pathogen, especially if the kernel scale parameter was large. This causes a large expansion of the size of clusters (Cotterill and Sivasithamparam, 1988; Gosme et al., 2007). If the range of dispersal was large enough, or if there were several consecutive growing seasons, clusters began to overlap. This can change an initially aggregated pathogen population to one with a uniform incidence across a field. As pathogen aggregation can limit epidemic spread and severity, reducing between-season dispersal as much as possible could be key to pathogen suppression.

There is growing interest in no-tillage agriculture due to its environmental benefits by reducing soil erosion and increasing efficiency of water and fertiliser use (Phillips et al., 1980; Teasdale et al., 2007; Triplett and Dick, 2008). No- or low-tillage agriculture will reduce the spread of the pathogen between growing seasons due to a reduced disruption to

the soil. A reduction in tillage has previously been found to decrease the effect of soil-borne diseases on wheat (Parylak, 2004; Rothrock, 1987). The incorporation of no- or low-tillage methods should therefore be considered when growing wheat, especially if the previously planted crop experienced clusters of infection by a soil-borne disease like take-all.

7.5.2 Impact of aggregation on the success of a biocontrol agent

This research found that the homogeneous spread of a biocontrol agent was more effectively able to suppress a pathogen than when it was highly aggregated. A homogeneous distribution allows the biocontrol agent to come into contact with all infected plants and maximise epidemic suppression. These findings are the same as those found in Xu and Hu (2020), where increased spatial aggregation of the biocontrol agent reduced its potential to negatively affect the pathogen.

Gubbins and Gilligan (1997a) found that spatial homogeneity of a pathogen and biocontrol may be more likely to lead to extinction of the biocontrol agent compared to when they are heterogeneously mixed. The aggregation of a biocontrol agent may be beneficial if a certain population size is required for epidemic suppression. One example of this is with the pathogen *Gaeumannomyces graminis* var. *tritici* and biocontrol agent 2,4-DAPG fluorescent *Pseudomonas* spp., where the latter is required to have a population size greater than 10^5 CFU g^{-1} for pathogen suppression (Raaijmakers et al., 1999; Raaijmakers and Weller, 1998; Weller, 2007). Although greater dispersal of the biocontrol agent led to a smaller amount present within each cluster at the start of the first season, we found that the biocontrol agent could bulk up within these clusters and increase its population size by the next season. A decrease in biocontrol aggregation is therefore limited in its ability to suppress the pathogen during the first season. However, as it was able to bulk up on a large number of host plants during this first season, it will be able to reach the high population

size needed for suppression more quickly across a field. A large scale parameter for the dispersal kernel will both maximise the number of host plants that a biocontrol agent can bulk up on, as well as maximising its contact with the pathogen. It should therefore be noted that, although there may be minimal epidemic suppression in the first growing season after biocontrol application, this may lead to much more effective epidemic suppression than clustered application over subsequent years.

As is mentioned in Kessel et al. (2005), both a uniform distribution and a high density of the biocontrol agent are required to reduce epidemic severity. If a biocontrol agent is applied homogeneously but at a low dose, it may not be effective. In this case, the clustering of a biocontrol agent may allow it to increase in population size and cause a greater effect to the pathogen when they come into contact. This will be dependent on the biocontrol agent and how it interacts with the host plant and pathogen.

7.5.3 Optimising the application of a biocontrol agent

Successful application of a biocontrol agent should focus on producing a high and homogeneous population that is able to directly contact the pathogen throughout a field. There should be a focus on application methods that do this whilst reducing mechanical dispersal from any machinery needed. On a small scale, dispersal should be able to cover the roots of a plant and keep up with root growth throughout a growing season. On a large scale, improvements must be made to machinery such as commercial field spraying equipment to improve application coverage and biocontrol agent survival.

Biocontrol agents should also be chosen based on their ability to survive mechanical dispersal events and the ease to which they can be commercially produced and applied. There would also be a benefit of choosing biocontrol agents that have a high ability to spread from their original location and move towards pathogens. Knudsen et al. (1991) found that the addition of certain additives to the soil could enhance hyphal extension of a

fungal biocontrol agent. The biocontrol agent *Ulocladium atrum* is often used against plant pathogens due to its high growth rate (Li et al., 2003). The movement of a biocontrol agent would reduce the effect of clustered biocontrol agent and may lead to increased epidemic suppression.

This research examined how initial clustering of a pathogen and biocontrol agent can affect epidemic suppression. In the real world, application of a biocontrol agent may be more frequent and could occur once a year or multiple times a year. Increasing the amount of application times will decrease the effect of aggregation as each additional application is likely to reach more places across a field. Examining whether there is a benefit to frequent application could be analysed, both as the amount of free-living biocontrol agent applied, as well as the scale parameter for the dispersal kernel, were allowed to vary. This could allow for suggestions to be made to ensure that application is as successful as possible, even if initial application is patchy.

7.5.4 Conclusions

There is a strong effect of aggregation of both a biocontrol agent and a pathogen on epidemic spread and suppression. A successful biocontrol agent needs to be as homogeneously dispersed across a field as possible. This can be through uniform application, large between-season dispersal, or the ability to move large distances. The biocontrol agent must also be applied at a level that allows for large enough population sizes to suppress the pathogen. Mechanical dispersal is key in epidemic severity across successive seasons, and agricultural methods that limit this spread should be considered. Variability of biocontrol agents across field trials is likely to be affected by ineffective and patchy application. There should therefore be a focus on optimising methods used for application in order to allow biocontrol agents to be more commercially viable control strategies.

Chapter 8: Discussion

8.1 Overview

There has been a considerable amount of research on the use of biocontrol agents as viable control strategies against plant pathogens. However, their variability across field trials has resulted in minimal commercial uptake. The use of mathematical models can allow for a detailed examination of the interactions between a plant, a pathogen, and a biocontrol agent. The trajectory of an epidemic can be simulated across multiple years, and the effects of specific criteria can be analysed without the noisiness from data that often occurs due to external factors. In this thesis, our aim was to explore how the use of biocontrol agents can be optimised using modelling. Factors that are key to the success of a biocontrol agent were identified and analysed, exploring how to maximise epidemic suppression through successful application.

In Chapter 2, the SIX and SIXCA models were introduced. These formed the basis for all the modelling work in this thesis. The incorporation of the pathogen and biocontrol agent both as free-living in the soil, as well as on the roots of a plant, allowed for primary and secondary infection and colonisation to be modelled. Temporal heterogeneity was included to account for variation in the model dynamics throughout a season due to harvesting and planting of an annual crop. The SIXCA model was designed to be sufficiently flexible so that multiple mechanisms that the biocontrol agent could use to negatively affect the pathogen could be incorporated. These could allow for a wide variety of different biocontrol agents to be modelled, as well as for an examination of the effectiveness of specific mechanisms under different conditions.

These models were used in Chapters 3 and 4 to examine the phenomenon of take-all decline. Parameter values were obtained through fitting the models to data from Werker

et al. (1991) using maximum likelihood estimation. Parameters for root growth were determined first, using additional experimental data to determine the rate of growth and the carrying capacity. Chapter 3 focused on fitting the SIX model to the first year of the experimental data where winter wheat infected by take-all was grown. Through this, parameter values for the rate of primary and secondary infection were obtained for the pathogen. The initial SIX model was determined to be over-parameterised and was therefore simplified by removing two parameters. These parameters both had no impact on the ability of the model to fit to the data, and therefore their removal had no impact on the model's behaviour.

Chapter 4 then focused on obtaining parameter values for the biocontrol agent, fitting to a ten-year data set that experienced take-all decline. This task was extremely difficult due to a lack of sampling times, an absence of any data on the biocontrol agent or the free-living pathogen, and noisy data. A lack of information about the potential bounds for most parameter values resulted in a large area of parameter space that had to be examined. The model fitting process was performed multiple times with different initial values, and many of these solutions converged on local optima rather than the global optimum.

Multiple variants of the SIXCA model were fitted to the data, each time including a different mechanism that the biocontrol agent could use to negatively affect the pathogen. This allowed for an examination into which mechanism, or mechanisms, may be involved in the process of take-all decline. Five mechanisms out of ten were identified as potentially involved. These were identified using AIC values, which examine whether additional parameters significantly improve the ability of the model to fit to the data. These five mechanisms fit well with some of the known mechanisms used by 2,4-DAPG fluorescent *Pseudomonas* spp., which is the biocontrol agent attributed to causing take-all decline. This further suggests that this biocontrol agent was likely to have been the main microorganism involved in take-all decline during the experiment from Werker et al. (1991). Although the

model fitting landscape was complex for each variation of the SIXCA model, parameters were shown to be fully identifiable for two of these models, providing confidence intervals for these values. One model had a single rate parameter with no lower bound, and two models were fully unidentifiable. These models will require additional data or knowledge of the bounds of some of the parameters included in the model fitting process in order to calculate confidence intervals.

In Chapter 5, the SIXCA model and the obtained parameter values were then used to explore how application of a biocontrol agent could be optimised across a 20-year simulation. Four different application strategies were examined: applying once at the start of the first season, applying once at the start of every season, applying twice per season, and applying four times per season. Across these application strategies, applying the entire application amount at the start of the first season was often found to maximise epidemic suppression. This was because the biocontrol agent had maximum time to bulk-up in the soil and reach the threshold level that is required for take-all suppression (Raaijmakers et al., 1999; Raaijmakers and Weller, 1998; Weller, 2007). However, soil-borne microorganisms are known to be heavily influenced by environmental conditions. As these conditions are not included in the model, it is possible that more regular application in the real world may be more successful. A maximum level of application was determined, above which there was no additional reduction in epidemic severity.

Spatial dynamics were incorporated into Chapter 6 to examine the transmission of infection between individual plants. The minimal spread of soil-borne pathogens such as *Gaeumannomyces graminis* var. *tritici* within a growing season results in small clusters of infected plants that can be heavily influenced by the spatial arrangement of a crop. We found that evenly spaced plants, or plants in rows with 12.5cm space between them, experienced lower epidemic severity than when they were planted in rows with 25cm or 50cm space between them. However, this benefit was removed in the second year of

a simulation when a large-scale dispersal event representing mechanical dispersal from agricultural machinery was included. Large scale spatial dynamics were examined in Chapter 7, analysing how between-season dispersal and aggregation of a pathogen and biocontrol agent can affect epidemic severity. We found that the biocontrol agent was most effective when it was homogeneously distributed across a field, allowing it to have maximum contact with the pathogen.

8.2 Relevance of work to agronomic practice

8.2.1 Successful application

It is well known that soil-borne microorganisms including pathogens often have a patchy distribution in the soil. We found that it is vital for the application of a biocontrol agent to be as evenly spread across a field as possible, allowing it to have maximum contact with the pathogen. This is especially key for soil-borne biocontrol agents like fungi and bacteria that can only travel small distances and cannot move far to come into contact with the pathogen. There should therefore be a focus on how application methods can be optimised to allow for uniform dispersal of the biocontrol agent across a field. This should not involve the production of new and complex machinery, or the refinement of laboratory procedures that do not work in large scale field trials. Instead, machinery that is already available and used by farmers should be optimised. For sprays, this may be looking at the type of nozzle used. For application to the soil, it may be looking at how thorough mixing of the biocontrol agent to the soil can be achieved.

The amount of application can have a significant impact on epidemic suppression. Too little was found to have little to no effect on the pathogen, whereas too much resulted in a waste due to no significant improvement to epidemic suppression. Minimal work has been done on the effective application of biocontrol agents in field trials, and it is likely that

some of the application will not reach the rhizosphere and have a chance of interacting with a pathogen. Even with a high application and optimised application methods, there is still likely to be some aggregation of the biocontrol agent and patches of the field where it does not persist. We would therefore recommend high application amounts, especially if previous field trials have found minimal effect of the biocontrol agent on epidemic severity at a lower application amount. Determining how high this should be will require additional experimental work, where epidemic severity is examined as application amount varies.

However, we are aware that an increased application amount will increase the overall cost. It therefore remains to be seen how many biocontrol agents would become too costly to use if applied at the optimal, or close to optimal, dose. This will involve further experimental and modelling work, examining the profit obtained from a higher crop yield compared to a loss of profit from increased application costs. Ensuring that there are no detrimental impacts from large applications is also vital, determining if there is a reduction in yield after a certain application amount is exceeded.

We found that a single application of a biocontrol agent at the start of the first growing season was often best for epidemic suppression across a 20-year simulation. This gives maximum time for the biocontrol agent to bulk-up in the soil, as occurs naturally with take-all decline. One reason for a reduced success of biocontrol agent application may be due to only examining the impacts of a biocontrol agent over a single year, whilst they may require longer to become fully effective. However, we are aware that it would not be practical to ask farmers to wait multiple years before they see a reduction in disease. Likewise, our modelling work does not take into account legislation in the UK that prevents the application of a biocontrol agent if it is known to persist long-term within the environment (Köhl et al., 2019a; Scheepmaker and Butt, 2010; Sundh and Goettel, 2013). It does not consider environmental changes that can have significant effects on microorganism in the soil. It also does not consider the requirements for frequent crop rotation, which has been found by this

research to have an impact on the ability of a biocontrol agent to persist and bulk-up in the soil. We would therefore not suggest a single large application unless application is done in a country that allows this. Instead, it is suggested that multiple applications throughout the season would be most effective at epidemic suppression. Multiple applications would reduce the impact of biocontrol aggregation or the effect of variation to environmental conditions throughout the growing season, but it does require more manual effort. This could be further examined by including environmental variability into a model, which can affect the ability for the pathogen and biocontrol agent to survive. A further examination into this variability would allow for a more detailed analysis as to how application frequency is affected by external factors, and therefore what should be recommended as the optimal application frequency.

Depending on the mechanisms included in the SIXCA model that the biocontrol agent could use to negatively affect the pathogen, we found that a certain population size of the pathogen was required for the biocontrol agent to successfully bulk-up in the soil. If the pathogen was present at a very low population size, the biocontrol agent was often unable to bulk-up and therefore remained at a low population size itself. This means that applying the biocontrol agent in the first growing season, when the pathogen is only present at low levels in the soil, limits its ability to bulk-up and negatively affect the pathogen. There may therefore be a benefit to delaying the application of a biocontrol agent until the second growing season, when the pathogen is more established in the soil. This gives the biocontrol agent maximum opportunity to come into contact with the pathogen and suppress it. However, it is likely that this would be a difficult application strategy to convince crop growers to use, as it requires a high epidemic severity before any control strategy is implemented. Due to this, combining this strategy with another more proactive one may be more suitable.

We also recommend the use of responsive application when possible, where application of a biocontrol agent only occurs after examining a field and finding a disease over a specific threshold level. This is due to the fact that it can often result in a reduction in cost of application. Responsive application can allow for a reduction in the amount of biocontrol agent applied whilst maximising epidemic suppression. However, we are aware that responsive application requires increased effort as a field has to be examined for disease before application can occur. This is especially difficult for soil-borne plant pathogens as they often have no or minimal above-ground symptoms. The benefit of an increased profit should therefore be weighed against the increased manual labour and the time taken to thoroughly inspect a field for disease.

8.2.2 Reducing the variability in success of a biocontrol agent

One of the main reasons why biocontrol agents are often not seen as commercially viable is due to their variability across different environmental conditions (Abbott et al., 2015; Clarkson and Polley, 1981; Hornby et al., 1989; White and Gilligan, 1998). These were not included in our model due to a focus on successful application and the spread of an epidemic without the complexity of additional external influences.

We do not disagree that there is an effect of environmental conditions on the success of biocontrol agents, and we believe that this would be an interesting area for future modelling work. However, we also believe that a lot of the variability seen may be due to inconsistent methodology and a focus on application methods that are only possible in small-scale laboratory experiments. We found that a biocontrol agent was able to suppress a pathogen across a variety of different scenarios. However, certain conditions had to be met such as high enough application amount and minimal aggregation of the biocontrol agent. We believe that a more consistent methodology of how and when to apply, how much to apply compared to in laboratory experiments, and how to ensure uniform distribution,

could produce significant improvements to biocontrol success across a variety of different environmental conditions. We must also ensure that uniform distribution of the biocontrol agent is at a high enough dosage to allow it to effectively bulk-up and not be restricted by low population sizes. Some research on these topics has already been performed (Irtwange, 2006; Stiling and Cornelissen, 2005; Tsegaye et al., 2018), but much more is needed as well as ensuring that this work is used to optimise future experiments. It is hoped that this work can be used to encourage others to consider the use of biocontrol agents more seriously and put more thought into experimental design and implementation.

8.2.3 The impact of between-season dispersal

Experiments that examine the effect of plant pathogens will often last a single growing season. Even when multiple growing seasons are included, the effect of between-season dispersal is not considered. However, we found that between-season dispersal can have a significant impact on epidemic spread and severity. This is important for any field where crops are planted and harvested every year, as is the case for most agricultural fields.

Our research examined how mechanical dispersal can increase epidemic severity by spreading a pathogen across a larger area than it would be able to travel on its own. In the absence of a biocontrol agent, it is therefore suggested that agricultural methods are used that reduce disruption to the soil as much as possible. There is growing interest in the use of no-till or low-till agricultural systems at the moment (Ashworth et al., 2017; Phillips et al., 1980; Teasdale et al., 2007; Triplett and Dick, 2008). We would further recommend low tillage as it results in less disruption to the soil, restricting pathogen dispersal (Marshall and Brain, 1999). However, the addition of a biocontrol agent makes the use of reduced tillage systems more complex. Although increased dispersal of the pathogen increases epidemic severity, it also increases epidemic suppression by a biocontrol agent through increased contact with the pathogen. Although we suggest reduced tillage in the absence

of a biocontrol agent, we believe that more research is needed to determine the impact of between-season dispersal on epidemic spread and suppression.

8.2.4 Integrated pest management

There is growing interest in using a combination of multiple control methods to more effectively suppress plant diseases. This is known as integrated pest management, and often focuses on environmentally friendly strategies (Lewis and Papavizas, 1991; Singh et al., 2019; Stenberg, 2017). These different strategies are assumed to work in synchrony to suppress a pathogen more effectively than would be possible using just a single strategy. This idea is very appealing and could be used to increase the effectiveness of biocontrol agents. However, we found that the combination of a biocontrol agent and a break crop led to a decrease in the ability for the biocontrol agent to suppress a pathogen. Although a break crop works by removing the host for a free-living pathogen and reducing its ability to persist in the soil, it may also do the same for a biocontrol agent (Baker and Cook, 1982; Cook and Rovira, 1976). Xu et al. (2011) also found that the combined use of two biocontrol agents was less effective than expected due to possible antagonistic interactions between the two. We therefore suggest that care should be taken when using integrated pest management, as there may be conflict between the combined strategies, resulting in less epidemic suppression than if they had been used separately. Modelling work could examine this through incorporating single control strategies into a simulation and examining their effects on epidemic suppression, before comparing these effects when combined with at least one other strategy. If the combination of strategies is determined to be unsuccessful, there should be a further analysis as to why this has occurred, as well as an identification of successful combinations of strategies.

8.2.5 Reducing the time taken for suppression to occur during take-all decline

There have been previous attempts to speed up the suppression that occurs after take-all decline by addition of 2,4-DAPG fluorescent *Pseudomonas* spp. to the soil whilst winter wheat is grown in monoculture (Cook, 2001; Mathre et al., 1999; Weller and Cook, 1982). However, these experiments did not have much success. This thesis found that the time taken until suppression caused by take-all decline could be significantly affected by the amount of biocontrol agent in the soil, and to a lesser extent the application strategy. We suggest that field trials where take-all decline does not occur, or where it takes a long time to occur, are likely to be due to low population sizes of 2,4-DAPG fluorescent *Pseudomonas* spp. in the soil. This may be due to a variety of factors such as antagonistic microorganisms within the soil, choosing crop cultivars that cannot sustain large population sizes of 2,4-DAPG fluorescent *Pseudomonas* spp., or environmental conditions that increase the decay rate of the biocontrol agent. Although one or multiple high applications of 2,4-DAPG fluorescent *Pseudomonas* spp. have the possibility to decrease the time until suppression after take-all decline occurs, other factors such as soil type, crop cultivar, previous cropping history, soil fertility, and environmental conditions may also have a significant impact. We therefore recommend that not only should initial application of a biocontrol agent be high, but that consideration for the interactions between the plant, pathogen, and biocontrol agent are required to reduce the time taken until suppression occurs.

8.3 Suggestions to improve future experimental work

One of the most challenging aspects of this thesis was obtaining parameter values through model fitting. The available data did not contain enough information to easily locate the global optimum without extensive exploration of parameter space and a detailed analysis of

results. Multiple initial sets of starting parameter values led to very poor fits of the SIX and SIXCA models to the data, and careful analysis of the obtained results were required to understand the output. These complications have led to us making some suggestions to improve the ability of future experimental work to be used for model fitting. However, we are aware that data collection can be time consuming and expensive, and therefore some of the suggestions will not be feasible for specific experiments. Although there is a focus on soil-borne experiments during this discussion, several of these points can be used to improve experimental work across a variety of different systems.

The first suggestion is simply that a greater amount of data needs to be collected. This can be both through increasing the number of data collection times, as well as repeating the experiment more than once. A greater amount of data can help the model fitting process to converge on the global optimum, as well as reducing the effect of noisy data points. The latter point is especially important for experiments performed across multiple years, where environmental conditions can vary significantly. Experiments that have occurred across multiple years will often detect at least one year where the data does not fit the same trend as the rest that has been collected. A greater amount of data can reduce the effect of outliers, as well as increasing confidence in any conclusions drawn. Although we did not test this in our thesis, in principle we could generate a large amount of artificial data by performing a model simulation using a set of parameter values. The model could then be refitted to this data to examine how much data would be required to significantly reduce any model fitting challenges.

One of the major limitations of the data from Werker et al. (1991) is that it did not contain any information on the biocontrol agent, either on colonised roots or free-living in the soil, as well as no data collected on the free-living pathogen. This created severe limitations in the ability of the SIX and SIXCA models to fit to the available data and required some parameter values to be fixed rather than included in the fitting process.

Advances in recent years have improved the ability to detect microorganisms in the soil and establish population sizes through the use of DNA arrays (Lievens et al., 2006; Lievens and Thomma, 2005; Tsui et al., 2011). For example, a population size of over 10^5 CFU g^{-1} for 2,4-DAPG fluorescent *Pseudomonas* spp. has been determined as necessary for suppression of *Gaeumannomyces graminis* var. *tritici* (Raaijmakers et al., 1999; Raaijmakers and Weller, 1998; Weller, 2007). This experimental work required accurate calculations of 2,4-DAPG fluorescent *Pseudomonas* spp. populations in the rhizosphere of wheat plants. Although collecting information on both the roots of a plant and the microorganisms in the rhizosphere requires more time and manual labour, it is the only way to accurately establish the interactions occurring between a plant, pathogen, and biocontrol agent in the soil. It would also have been beneficial to examine the population size of 2,4-DAPG fluorescent *Pseudomonas* spp. in the soil for Werker et al. (1991) to establish that they were responsible for take-all decline rather than general suppression or specific suppression by another microorganism.

Experimental work related to soil-borne systems provides additional challenges. When examining a soil-borne pathogen, above ground symptoms may overestimate the severity of the epidemic (Werker et al., 1991). Although it is more challenging, data collection should therefore focus on the roots of a plant. Soil-borne pathogens and other microorganisms are known to have a patchy distribution throughout the soil. Care should therefore be taken to ensure that enough measurements are obtained to accurately represent below-ground dynamics.

Another suggestion would be for more collaboration between research groups, allowing single experiments to examine a multitude of different questions. This is especially important for field trials that may span multiple years, such as those required for examining take-all decline. It is significantly less effort to collect two types of data from a single experiment than it is to perform the same experiment twice and collect one type per experiment. This

suggestion would require communication between researchers and additional planning but could significantly reduce the overall effort required to collect data, as well as allowing the data to be used by more people. The success of collaboration between groups has been successfully seen throughout the COVID-19 epidemic, where scientists from across the world that specialise in different disciplines have come together to optimise epidemic suppression (Bedford et al., 2019; Fry et al., 2020). The commitment required for experiments such as those that examine take-all decline across multiple years is large, and therefore any way to make this easier would be highly beneficial.

This section should act as a warning for anyone attempting to fit a model to data in the future. The process of fitting a model to biological data is commonly done, allowing for parameter values to be obtained that reflect real-world dynamics. However, the model fitting process is often not described in detail, making it unclear how much analysis has gone into the obtained results. An exploration of the model fitting landscape and the identification of local and global optima is uncommon, although Fernández Slezak et al. (2010) do examine this in detail. Biological data is often noisy and contains few data points, both of which will complicate the model fitting process. There must be a detailed examination of the results obtained through model fitting, exploring variability in results and obtaining confidence intervals for parameters. If model fitting is rushed, there is a high chance of locating a suboptimal solution or finding parameter values that do not accurately represent the biological system. Having access to a large amount of data, as well as knowledge about some of the bounds on parameters, can never eliminate these problems, but it can help to reduce them significantly.

8.4 Scope for future work

8.4.1 Additions to the spatial work

Both large- and small-scale spatial dynamics were explored within this thesis. However, there is scope for more spatial analysis of take-all and take-all decline. Hornby et al. (1989) found that clusters within a field in the first year of growing wheat infected by take-all were very small and separated, before increasing in size in the second year, and overlapping to create uniformly distributed infection in the third year. These clusters were then found to reform and start to reduce in size from the fourth year onwards, as free-living biocontrol agent living in the soil build up and begin to suppress the pathogen. This pattern was also seen in Mac Nish and Dodman (1973), where highly infected areas of take-all disease begin to contract after the third of fourth year of consecutively growing wheat. The suppression of *Gaeumannomyces graminis* var. *tritici* therefore results in increased aggregation of the pathogen as the clusters of infected plants get smaller. Using the large-scale spatial SIXCA model to analyse this interaction could provide more insight into how take-all decline occurs and how the biocontrol agent acts to suppress the pathogen. It could provide us with more information as to how aggregation of the pathogen and biocontrol agent can affect pathogen suppression, and may provide further insights into how a biocontrol agent can be applied to effectively suppress take-all or other soil-borne diseases.

Although take-all is known to occur most frequently in wet conditions, it is also prevalent throughout drier soils. These two systems are often referred to as wetland take-all and dryland take-all (Cook, 2003). Wetland take-all allows for both primary and secondary infection to occur, resulting in patches of infection as the disease spreads through the roots of nearby plants through secondary infection. Dryland take-all does not permit secondary infection and therefore each plant must be individually infected from pathogen inoculum. This means that the patches of disease that are common for wetland take-all are not seen

for dryland take-all (Cook 2003). Another addition to our spatial work could therefore be to simulate both dryland and wetland take-all, removing the possibility for dryland take-all to infect neighbouring plants through secondary infection. Hornby (1992) hypothesised that dryland take-all would not be able to experience take-all decline, or that any suppression would be short-term when wheat was grown under dry conditions. Examining how both dryland and wetland take-all affect epidemic spread and suppression by a biocontrol agent, as well as what impact dryland take-all has on the presence and prevalence of take-all decline, would be an interesting topic for future research.

Although it would be optimal to examine a large area through a spatial model, such as a whole field, there are computational limits on this. Increasing the area would therefore likely require division of it into larger sections. This may over-estimate the effect of between-season dispersal for the large-scale model, and prevent the examination of plant-to-plant infection for the small-scale model. There is therefore an important trade-off between the focus area and the computational power required.

8.4.2 Impacts of environmental variability

A lot of the variability in the success of biocontrol agents across field trials has been attributed to differing environmental conditions. Microorganisms in the soil are known to be affected by factors such as precipitation, temperature, and light (Dewan and Sivasithamparam, 1989; Fellows and Ficke, 1932). Multiple experiments have examined these effects on specific biocontrol agents in controlled laboratory experiments (Bowers and Parke, 1993; Kemp et al., 1992; O'Callaghan et al., 2001; Vandenhove et al., 1991; Wessendorf and Lingens, 1989). However, it is often more difficult to determine their effects in the field due to multiple confounding variables. Modelling would give a way to examine these factors in a more controlled way, identifying which environmental factors have the greatest impacts on the success of specific biocontrol agents. This work could be used when selecting

biocontrol agents, only selecting ones that are resistant to the environmental factors that cause the greatest impacts to the success of the biocontrol agents. It could also be used to identify which environmental conditions are most likely to impact take-all decline, examining how the presence of take-all decline and the duration until suppression are dependent on specific conditions. This research would initially require a literature review to determine how individual environmental conditions affect different biocontrol agents.

There could also be a more general focus on the impact of variation to rate parameters on biocontrol success and epidemic severity. It would be useful to identify how small changes to parameter values can affect the behaviour of a biocontrol agent. If very small fluctuations to rate parameters can result in large changes to model outputs, this may help to explain the difference in success between biocontrol agents in controlled laboratory experiments compared to when they are used in field trials. Commercial success of biocontrol agents is dependent on their ability to be effective across a range of environmental conditions, and the identification of hardy biocontrol agents that are less affected by external conditions would be highly beneficial for their future use.

8.4.3 Focusing on different plant-pathogen-biocontrol agent systems

This thesis focused on the infection of wheat plants by *Gaeumannomyces graminis* var. *tritici* and suppression by the biocontrol agent 2,4-DAPG fluorescent *Pseudomonas* spp. This allowed for a set of rate parameters to be obtained that could be used for further model analysis. It also allowed for an examination of take-all decline, which is known to be one of the most successful cases of specific suppression. However, the SIX and SIXCA models can be used across any system where infection and colonisation occur both through a reservoir of free-living material as well as through contact between different plants. This should allow it to be used across many soil-borne systems such as such as with other *Pseudomonas* spp.

(Weller, 2007), *Streptomyces* spp. (Vurukonda et al., 2018), *Trichoderma* spp. (Harman, 2006), and *Fusarium* spp (Fravel et al., 2003).

An examination of different plant-pathogen-biocontrol agent systems can allow for two things. The first is that it can allow for conclusions to be drawn that are specific to a particular system. This can allow for more confidence in any suggestions that are made for successful biocontrol application. The SIXCA has multiple mechanisms that can be incorporated to allow the biocontrol agent to negatively affect the pathogen, and these can be chosen depending on the biocontrol agent of focus. Secondly, it allows for an examination of what results seem to be specific to a particular system and which are applicable across a range of systems. The latter can provide insights that can be applied to all biocontrol use and may help to produce a set of rules that should be followed to enhance overall biocontrol success.

8.4.4 Incorporating stochasticity

The models used within this thesis are deterministic. Incorporating stochasticity would allow for the pathogen and biocontrol agent to become extinct in certain simulations, which is closer to what would be seen in real life. Currently, the free-living pathogen and biocontrol agent can never completely decay and be removed from the system. Allowing for stochasticity may affect factors such as application timing, as increasing the number of times that application occurs will reduce the chance of biocontrol extinction. It may also reduce the effect of low application amounts as the applied biocontrol agent may be removed from the system before it has had time to bulk-up and colonise the host. The results from a stochastic model would be more representative of those from a field trial and may help to explain some of the variability seen across them.

8.5 Concluding remarks

This thesis has shown that soil-borne biocontrol agents can be successful at controlling soil-borne plant pathogens across a variety of different conditions. We believe that they have the potential to be seen as commercially viable control methods, as long as careful consideration is taken with their application. A detailed understanding of the interactions between a plant, a pathogen, and a biocontrol agent are vital to ensuring that application can be as effective as possible. Care should also be taken when incorporating a biocontrol agent into integrated pest management to ensure that it is not negatively affected by other control methods. A considerable amount of research is still needed to optimise the use of biocontrol agents. However, we believe that they should be a key player in the future control of plant diseases. Hopefully the research and suggestions in this thesis can be used to enhance the overall success of soil-borne biocontrol agents within agriculture.

Bibliography

Abbott, K. C., Karst, J., Biederman, L. A., Borrett, S. R., Hastings, A., Walsh, V., and Bever, J. D. (2015). Spatial Heterogeneity in Soil Microbes Alters Outcomes of Plant Competition. *PLOS ONE*, 10(5):e0125788.

Abdullah, A., Deris, S., Anwar, S., and Arjunan, S. N. V. (2013a). An Evolutionary Firefly Algorithm for the Estimation of Nonlinear Biological Model Parameters. *PLoS ONE*, 8(3):e56310.

Abdullah, A., Deris, S., Mohamad, M. S., and Anwar, S. (2013b). An Improved Swarm Optimization for Parameter Estimation and Biological Model Selection. *PLoS ONE*, 8(4).

Abeysinghe, S. (2009). Efficacy of combine use of biocontrol agents on control of Sclerotium rolfsii and Rhizoctonia solani of Capsicum annuum. *Archives Of Phytopathology And Plant Protection*, 42(3):221–227.

Abichou, M., de Solan, B., and Andrieu, B. (2019). Architectural Response of Wheat Cultivars to Row Spacing Reveals Altered Perception of Plant Density. *Frontiers in Plant Science*, 10:999.

Abodayeh, K., Raza, A., Arif, M. S., Rafiq, M., Bibi, M., and Fayyaz, R. (2020). Numerical analysis of stochastic vector borne plant disease model. *Computers, Materials and Continua*, 63(1):65–83.

Adams, P., Marois, J., and Ayers, W. (1984). Population dynamics of the mycoparasite, Sporidesmium sclerotivorum, and its host, Sclerotinia minor, in soil. *Soil Biology and Biochemistry*, 16:627–633.

Adams, P. B. and Ayers, W. (1981). Sporidesmium sclerotivorum: Distribution and Function in Natural Biological Control of Sclerotial Fungi . *Phytopathology*, 71(1):90.

Adams, P. B. and Ayers, W. (1982). Biological Control of Sclerotinia Lettuce Drop in the Field by Sporidesmium sclerotivorum . *Phytopathology*, 72(5):485.

AHDB (2018). Wheat growth guide. Technical report.

Akaike, H. (1973). Information Theory and an Extension of the Maximum Likelihood Principle. In Petrov, B. and Csaki, F., editors, *Proceedings of the Second International Symposium on Information Theory*, pages 267–281.

Alexandratos, N. and Bruinsma, J. (2012). World agriculture towards 2030/2050: the 2012 revision. *ESA Working Paper*, 12-03.

Alford, D. (2008). *Pest and Disease Management Handbook* . Wiley-Blackwell.

Ali, Y., Haq, M., Tahir, G. R., and Ahmad, N. (1999). Effect of Inter and Intra Row Spacing on the Yield and Yield Components of Chickpea. *Pakistan Journal of Biological Sciences*, 2(2):305–307.

Alori, E. T. and Babalola, O. O. (2018). Microbial inoculants for improving crop quality and human health in Africa. *Frontiers in Microbiology*, 19(9):2213.

Andrade, O., Campillo, R., Peyrelongue, A., and Barrientos, L. (2011). Soils suppressive against Gaeumannomyces graminis var. tritici identified under wheat crop monoculture in southern Chile. *Ciencia e Investigacion Agraria*, 38(3):345–356.

Angus, J. F., Kirkegaard, J. A., Hunt, J. R., Ryan, M. H., Ohlander, L., and Peoples, M. B. (2015). Break crops and rotations for wheat. *Crop and Pasture Science*, 66(6):523–552.

Antoun, H. and Prévost, D. (2006). Ecology of plant growth promoting rhizobacteria. In *PGPR: Biocontrol and Biofertilization*, pages 1–38. Springer Netherlands.

Ardakani, S. S., Heydari, A., Khorasani, N. A., Arjmandi, R., and Ehteshami, M. (2009). Preparation of new biofungicides using antagonistic bacteria and mineral compounds for controlling cotton seedling damping-off disease. *Journal of Plant Protection Research*, 49(1):49–55.

Arnold, T. W. (2010). Uninformative Parameters and Model Selection Using Akaike's Information Criterion. *The Journal of Wildlife Management*, 74(6):1175–1178.

Asher, M. and Shipton, P. (1981). *Biology and control of take-all*. Academic Press, London.

Ashworth, A. J., DeBruyn, J. M., Allen, F. L., Radosevich, M., and Owens, P. R. (2017). Microbial community structure is affected by cropping sequences and poultry litter under long-term no-tillage. *Soil Biology and Biochemistry*, 114:210–219.

Ashyraliyev, M., Fomekong-Nanfack, Y., Kaandorp, J. A., and Blom, J. G. (2009). Systems biology: parameter estimation for biochemical models. *The FEBS Journal*, 276(4):886–902.

Atkinson, G. (1892). Some Diseases of Cotton. *Agricultural Experiment Station of the Agricultural and Mechanical College*, 41.

Aylor, D. E. (1990). The Role of Intermittent Wind in the Dispersal of Fungal Pathogens. *Annual Review of Phytopathology*, 28(1):73–92.

Bae, Y. S. and Knudsen, G. R. (2007). Effect of sclerotial distribution pattern of Sclerotinia sclerotiorum on biocontrol efficacy of Trichoderma harzianum. *Applied Soil Ecology*, 35(1):21–24.

Bahme, J. B. (1988). Effect of Inocula Delivery Systems on Rhizobacterial Colonization of Underground Organs of Potato. *Phytopathology*, 78(5):534.

Bailey, D. and Gilligan, C. (1997). Biological control of pathozone behaviour and disease dynamics of Rhizoctonia solani by Trichoderma viride. *The New Phytologist*, 136(2):359–367.

Bailey, D. and Gilligan, C. (1999). Dynamics of primary and secondary infection in take-all epidemics. *Phytopathology*, 89(1):84–91.

Bailey, D., Gosme, M., Lucas, P., Paveley, N., Spink, J., Cunniffe, N., and Gilligan, C. (2006). Developing a rationale to integrate take-all control measures, reduce disease impact and maximise wheat margins. *HGCA (Home-Grown Cereals Authority)*, 398.

Bailey, D., Kleczkowski, A., and Gilligan, C. (2004). Epidemiological dynamics and the efficiency of biological control of soil-borne disease during consecutive epidemics in a controlled environment. *New Phytologist*, 161(2):569–575.

Bailey, D., Otten, W., and Gilligan, C. (2000). Saprotrophic Invasion by the Soil-Borne Fungal Plant Pathogen Rhizoctonia solani and Percolation Thresholds on JSTOR. *The New Phytologist*, 146(3):535–544.

Bailey, D., Paveley, N., Spink, J., Lucas, P., and Gilligan, C. (2009). Epidemiological analysis of take-all decline in winter wheat. *Phytopathology*, 99(7):861–868.

Bailey, D. J. and Gilligan, C. A. (2004). Modeling and analysis of disease-induced host growth in the epidemiology of take-all. *Phytopathology*, 94(5):535–540.

Bailey, D. J., Paveley, N., Pillinger, C., Foulkes, J., Spink, J., and Gilligan, C. A. (2005). Epidemiology and chemical control of take-all on seminal and adventitious roots of wheat. *Phytopathology*, 95(1):62–68.

Bailey, K. L., Lafond, G. P., and Domitruk, D. (1998). Effects of row spacing, seeding rate and seed-placed phosphorus on root diseases of spring wheat and barley under zero tillage. *Canadian Journal of Plant Science*, 78(1):145–150.

Baker, K. and Cook, R. (1982). *Biological Control of Plant Pathogens*. American Phytopathological Society, San Francisco.

Bakker, P. A., Berendsen, R. L., Doornbos, R. F., Wintermans, P. C., and Pieterse, C. M. (2013). The rhizosphere revisited: Root microbiomics. *Frontiers in Plant Science*, 4(165):1–7.

Bauer, A., Fanning, C., Enz, J. W., and Eberlein, C. V. (1984). *Use of growing-degree days to determine spring wheat growth stages*. Co-operative Extension Service Bulletin, North Dakota State University, Fargo, North Dakota.

Beale, R., Phillion, D., Headrick, J., O'Reilly, P., and Cox, J. (1998). MON6550: A uniquie fungicide for control of take-all in wheat. In *Brighton Conference—Pest and Diseases*, pages 343–350, British Crop Protection Council Symposium Proceedings, Surrey, UK: Farnham.

Bedford, J., Farrar, J., Ihekweazu, C., Kang, G., Koopmans, M., and Nkengasong, J. (2019). A new twenty-first century science for effective epidemic response. *Nature*, 575(7781):130–136.

Beres, B. L., Turkington, T. K., Kutcher, H. R., Irvine, B., Johnson, E. N., O'Donovan, J. T., Harker, K. N., Holzapfel, C. B., Mohr, R., Peng, G., and Spaner, D. M. (2016). Winter Wheat Cropping System Response to Seed Treatments, Seed Size, and Sowing Density. *Agronomy Journal*, 108(3):1101–1111.

Berger, R. D. (1975). Disease Incidence and Infection Rates of Cercospora apii in Plant Spacing Plots. *Phytopathology*, 65(4):485.

Bergsma-Vlami, M., Prins, M. E., and Raaijmakers, J. M. (2005). Influence of plant species on population dynamics, genotypic diversity and antibiotic production in the rhizosphere by indigenous Pseudomonas spp. *FEMS Microbiology Ecology*, 52(1):59–69.

Boland, G. J. and Hall, R. (1988). Relationships between the spatial pattern and number of apothecia of Sclerotinia sclerotiorum and stem rot of soybean. *Plant Pathology*, 37(3):329–336.

Bolker, B. M. (2008). *Ecological Models and Data in R*. Princeton University Press.

Bossio, D. A., Scow, K. M., Gunapala, N., and Graham, K. J. (1998). Determinants of Soil Microbial Communities: Effects of Agricultural Management, Season, and Soil Type on Phospholipid Fatty Acid Profiles. *Microbial Ecology*, 36:1–12.

Botelho, G. R. and Mendonça-Hagler, L. C. (2006). Fluorescent Pseudomonads associated with the rhizosphere of crops - An overview. *Brazilian Journal of Microbiology*, 37(4):401–416.

Bowers, J. H. and Parke, J. L. (1993). Colonization of pea (Pisum sativum L.) taproots by Pseudomonas fluorescens: Effect of soil temperature and bacterial motility. *Soil Biology and Biochemistry*, 25(12):1693–1701.

Brain, P. and Marshall, J. (1999). Modeling cultivation effects using fast fourier transforms. *Journal of Agricultural, Biological, and Environmental Statistics*, 4(3):276–289.

Brassett, P. and Gilligan, C. (1988). A model for primary and secondary infection in botanical epidemics. *Zeitschrift für Pflanzenkrankheiten und Pflanzenschutz / Journal of Plant Diseases and Protection*, 95(4):352–360.

Breiman, A. and Graur, D. (1995). Wheat evaluation. *Israel Journal of Plant Sciences,*, 43:58–85.

Brooks, D. H. and Dawson, M. G. (1968). Influence of direct-drilling of winter wheat on incidence of take-all and eyespot. *Annals of Applied Biology*, 61(1):57–64.

Brown, M. E. and Hornby, D. (1971). Behaviour of Ophiobolus graminis on slides buried in soil in the presence or absence of wheat seedlings. *Transactions of the British Mycological Society*, 56(1):95–IN10.

Brun, R., Reichert, P., and Künsch, H. R. (2001). Practical identifiability analysis of large environmental simulation models. *Water Resources Research*, 37(4):1015–1030.

Bull, C., Weller, D., and Thomashow, L. (1991). Relationship between root colonization and suppression of Gaeumannomyces graminis var. tritici by Pseudomonas fluorescens strain 2-79. *Phytopathology*, 81(9):954–959.

Burnham, K. and Anderson, D. (2003). *Model Selection and Multimodel Inference: A Practical Information-Theoretic Approach*. Springer, New York, 2nd edition.

Calvente, V., De Orellano, M. E., Sansone, G., Benuzzi, D., and Sanz De Tosetti, M. I. (2001). Effect of nitrogen source and pH on siderophore production by Rhodotorula strains and their application to biocontrol of phytopathogenic moulds. *Journal of Industrial Microbiology and Biotechnology*, 26(4):226–229.

Campbell, C. L. and Madden, L. V. (1990). *Introduction to plant disease epidemiology.* John Wiley & Sons., New York.

Campbell, C. L. and Noe, J. P. (1985). The Spatial Analysis of Soilborne Pathogens and Root Diseases. *Annual Review of Phytopathology*, 23(1):129–148.

Campbell, R. (1989). *Biological Control of Microbial Plant Pathogens*. Cambridge University Press.

Carmona, M., Sautua, F., Pérez-Hérnandez, O., and Reis, E. M. (2020). Role of Fungicide Applications on the Integrated Management of Wheat Stripe Rust.

Chellemi, D. O., Rohrbach, K. G., Yost, R. S., and Sonoda, R. M. (1988). Analysis of the Spatial Pattern of Plant Pathogens and Diseased Plants Using Geostatistics. *Phytopathology*, 78(2):226.

Chng, S., Cromey, M. G., Dodd, S. L., Stewart, A., Butler, R. C., and Jaspers, M. V. (2015). Take-all decline in New Zealand wheat soils and the microorganisms associated with the potential mechanisms of disease suppression. *Plant and Soil*, 397(1-2):239–259.

Christ, B. J. and Maczuga, S. A. (1989). The Effect of Fungicide Schedules and Inoculum Levels on Early Blight Severity and Yield of Potato. *Plant Disease*, 73(8):695.

Ciancio, A., Pieterse, C. M. J., and Mercado-Blanco, J. (2019). Editorial: Harnessing Useful Rhizosphere Microorganisms for Pathogen and Pest Biocontrol - Second Edition. *Frontiers in Microbiology*, 10(AUG):1935.

Clarkson, J. and Polley, R. (1981). Diagnosis, assessment, crop-loss appraisal and forecasting. In Asher, M. J. C. and Shipton, P. J., editors, *Biology and Control of Take-All*, page 251–269. Academic Press, London, UK.

Cook, Hims, and Vaughan (1999). Effects of fungicide spray timing on winter wheat disease control. *Plant Pathology*, 48(1):33–50.

Cook, R. (2003). Take-all of wheat. *Physiological and Molecular Plant Pathology*, 62(2):73–86.

Cook, R. J. (1981). The Influence of Rotation Crops on Take-All Decline Phenomenon. *Phytopathology*, 71(2):189.

Cook, R. J. (1988). Biological control and holistic plant-health care in agriculture. *American Journal of Alternative Agriculture*, 3(2-3):51–62.

Cook, R. J. (1993). Making greater use of introduced microorganisms for biological control of plant pathogens. *Annual Review of Phytopathology*, 31:53–80.

Cook, R. J. (2001). Management of wheat and barley root diseases in modern farming systems. *Australasian Plant Pathology*, 30(2):119–126.

Cook, R. J., Bruckart, W. L., Coulson, J. R., Goettel, M. S., Humber, R. A., Lumsden, R. D., Maddox, J. V., McManus, M. L., Moore, L., Meyer, S. F., Quimby, J., Stack, J. P., and Vaughn, J. L. (1996). Safety of microorganisms intended for pest and plant disease control: A framework for scientific evaluation.

Cook, R. J. and Rovira, A. D. (1976). The role of bacteria in the biological control of Gaeumannomyces graminis by suppressive soils. *Soil Biology and Biochemistry*, 8(4):269–273.

Cooksey, D. A. (1982). Biological Control of Crown Gall with an Agrocin Mutant of Agrobacterium radiobacter. *Phytopathology*, 72(7):919.

Cotterill, P. J. and Sivasithamparam, K. (1988). The effect of tillage practices on distribution, size, infectivity and propagule number of the take-all fungus (Gaeumannomyces graminis var. tritici). *Soil and Tillage Research*, 11(2):183–195.

Cunniffe, N. and Gilligan, C. (2010). Invasion, persistence and control in epidemic models for plant pathogens: The effect of host demography. *Journal of the Royal Society Interface*, 7(44):439–451.

Cunniffe, N. and Gilligan, C. (2011). A theoretical framework for biological control of soil-borne plant pathogens: Identifying effective strategies. *Journal of Theoretical Biology*, 278(1):32–43.

Cunniffe, N. and Gilligan, C. (2020). Chapter 12: Use of Mathematical Models to Predict Epidemics and to Optimize Disease Detection and Management. In *Emerging Plant Diseases and Global Food Security*, pages 239–266. The American Phytopathological Society.

Cunniffe, N. J., Cobb, R. C., Meentemeyer, R. K., Rizzo, D. M., and Gilligan, C. A. (2016). Modeling when, where, and how to manage a forest epidemic, motivated by sudden oak death in California. *Proceedings of the National Academy of Sciences of the United States of America*, 113(20):5640–5645.

Cunniffe, N. J., Koskella, B., E. Metcalf, C. J., Parnell, S., Gottwald, T. R., and Gilligan, C. A. (2015). Thirteen challenges in modelling plant diseases. *Epidemics*, 10:6–10.

Dandurand, L. M. C. and Knudsen, G. R. (1997). Sampling microbes from the rhizosphere and phyllosphere. *Manual of Environmental Microbiology.*, pages 391–399.

Daval, S., Lebreton, L., Gazengel, K., Guillerm-Erckelboudt, A.-Y., and Sarniguet, A. (2010). Genetic evidence for differentiation of Gaeumannomyces graminis var. tritici into two major groups. *Plant Pathology*, 59(1):165–178.

de la Pasture, L. and Allen-Stevens, T. (2017). Opportunities to profit in the spring. Technical report, Crop Production Magazine.

De Souza, J. T., Weller, D. M., and Raaijmakers, J. M. (2003). Frequency, diversity, and activity of 2,4-diacetylphloroglucinol-producing fluorescent Pseudomonas spp. in Dutch take-all decline soils. *Phytopathology*, 93(1):54–63.

Deacon, J. (1988). Biocontrol of soil-borne plant pathogens with introduced inocula. *Philosophical Transactions of the Royal Society of London. B, Biological Sciences*, 318(1189):249–264.

Dewan, M. M. and Sivasithamparam, K. (1989). Growth promotion of rotation crop species by a sterile fungus from wheat and effect of soil temperature and water potential on its suppression of take-all. *Mycological Research*, 93(2):156–160.

Durán, P., Jorquera, M., Viscardi, S., Carrion, V. J., Mora, M. d. l. L., and Pozo, M. J. (2017). Screening and Characterization of Potentially Suppressive Soils against Gaeumannomyces graminis under Extensive Wheat Cropping by Chilean Indigenous Communities. *Frontiers in Microbiology*, 8(AUG):1552.

Eilenberg, J., Hajek, A., and Lomer, C. (2001). Suggestions for unifying the terminology in biological control. *BioControl*, 46(4):387–400.

Elderfield, J. (2018). *Using epidemiological principles and mathematical models to understand fungicide resistance evolution*. PhD thesis, University of Cambridge, Cambridge.

Ellis, M. A. (1986). Evaluation of Metalaxyl and Captafol Soil Drenches, Composted Hardwood Bark Soil Amendments, and Graft Union Placement on Control of Apple Collar Rot. *Plant Disease*, 70(1):24.

Elsas, J., Dijkstra, A., Govaert, J., and Veen, J. (1986). Survival of Pseudomonas fluorescens and Bacillus subtilis introduced into two soils of different texture in field microplots. *FEMS Microbiology Letters*, 38(3):151–160.

Esker, P. D., Sparks, A. H., Antony, G., Bates, M., Dall' Acqua, W., Frank, E. E., Huebel, L., Segovia, V., and Garrett, K. (2008). Ecology and Epidemiology in R: Spatial Analysis. *The Plant Health Instructor*.

Ettema, C. H. and Wardle, D. A. (2002). Spatial soil ecology. *Trends in Ecology and Evolution*, 17(4):177–183.

Fan, J., McConkey, B., Wang, H., and Janzen, H. (2016). Root distribution by depth for temperate agricultural crops. *Field Crops Research*, 189:68–74.

Fang, J. G. (1995). Efficacy of Penicillium funiculosum as a Biological Control Agent Against Phytophthora Root Rots of Azalea and Citrus. *Phytopathology*, 85(8):878.

Fang, Y. and Ramasamy, R. P. (2015). Current and prospective methods for plant disease detection. *Biosensors*, 5(3):537–561.

Fedele, G., Bove, F., González-Domínguez, E., and Rossi, V. (2020). A Generic Model Accounting for the Interactions among Pathogens, Host Plants, Biocontrol Agents, and the Environment, with Parametrization for Botrytis cinerea on Grapevines. *Agronomy*, 10(2):222.

Fellows, H. and Ficke, C. (1932). Wheat take-all. *Kansas Agricultural Experiment Station Annual Report*, 34:95–96.

Fernández Slezak, D., Suárez, C., Cecchi, G. A., Marshall, G., and Stolovitzky, G. (2010). When the optimal is not the best: Parameter estimation in complex biological models. *PLoS ONE*, 5(10).

Ferrin, D. M. and Mitchell, D. (1984). Spatial pattern of Phytophthora parasitica var. nicotianae in infested tobacco field soil. *Phytopathology*, 74(839).

Ferrin, D. M. and Mitchell, D. (1986). Influence of Initial Density and Distribution of Inoculum on the Epidemiology of Tobacco Black Shank. *Phytopathology*, 76(11):1153.

Fischer, S. and Lewis, M. (2021). A robust and efficient algorithm to find profile likelihood confidence intervals. *Statistics and Computing*, 31(38):1–16.

Fox, R. (1990). Rapid methods for diagnosis of soil-borne plant pathogens. *Soil Use and Management*, 6(4):179–183.

Fox, R. T. (1997). The present and future use of technology to detect plant pathogens to guide disease control in sustainable farming systems. *Agriculture, Ecosystems and Environment*, 64(2):125–132.

Fravel, D., Olivain, C., and Alabouvette, C. (2003). Fusarium oxysporum and its biocontrol. *New Phytologist*, 157(3):493–502.

Fravel, D. R. (1992). Systems for Efficient Delivery of Microbial Biocontrol Agents to Soil. In *Biological Control of Plant Diseases*, pages 399–406. Springer US.

Fravel, D. R. (2005). Commercialization and implementation of biocontrol. *Annual Review of Phytopathology*, 43:337–359.

Fravel, D. R., Rhodes, D. J., and Larkin, R. P. (1999). Production and Commercialization of Biocontrol Products. In *Integrated Pest and Disease Management in Greenhouse Crops*, pages 365–376. Springer, Dordrecht.

Freeman, S., Minz, D., Kolesnik, I., Barbul, O., Zveibil, A., Maymon, M., Nitzani, Y., Kirshner, B., Rav-David, D., Bilu, A., Dag, A., Shafir, S., and Elad, Y. (2004). Trichoderma biocontrol of Colletotrichum acutatum and Botrytis cinerea and survival in strawberry. *European Journal of Plant Pathology*, 110(4):361–370.

Fry, C. V., Cai, X., Zhang, Y., and Wagner, C. S. (2020). Consolidation in a crisis: Patterns of international collaboration in early COVID-19 research. *PLOS ONE*, 15(7):e0236307.

Ganeshan, G. and Kumar, A. M. (2005). Pseudomonas fluorescens, a potential bacterial antagonist to control plant diseases. *Journal of Plant Interactions*, 1(3):123–134.

Gardner, P. A., Angus, J. F., Pitson, G. D., and Wong, P. T. (1998). A comparison of six methods to control take-all in wheat. *Australian Journal of Agricultural Research*, 49(8):1225–1240.

Gareth, J. (1983). *Cereal Diseases: Their Pathology and Control*. Wiley-Blackwell, 2nd edition edition.

Garrett, K. A., Kabbage, M., and Bockus, W. W. (2004). Managing for fine-scale differences in inoculum load: Seeding patterns to minimize wheat yield loss to take-all. *Precision Agriculture*, 5(3):291–301.

Garrett, S. D. (1936). Soil Conditions and the Take-All Disease of Wheat. *Annals of Applied Biology*, 23(4):667–699.

Gerlagh, M. (1968). Introduction of Ophiobolus graminis into new polders and its decline. *Netherlands Journal of Plant Pathology*, 74(2 Supplement):1–97.

Gibson, G., Gilligan, C., and Kleczkowski, A. (1999). Predicting variability in biological control of a plant-pathogen system using stochastic models. *Proceedings of the Royal Society of London B: Biological Sciences*, 266(1430):1743–53.

Gibson, G. J., Kleczkowski, A., and Gilligan, C. A. (2004). Bayesian analysis of botanical epidemics using stochastic compartmental models. *Proceedings of the National Academy of Sciences of the United States of America*, 101(33):12120–12124.

Gilligan, C. (2002). An epidemiological framework for disease management. *Advances in Botanical Research*, 38:1–64.

Gilligan, C. and van den Bosch, F. (2008). Epidemiological models for invasion and persistence of pathogens. *Annual Review of Phytopathology*, 46:385–418.

Gilligan, C. A. (1980). Zone of potential infection between host roots and inoculum units of Gaeumannomyces graminis. *Soil Biology and Biochemistry*, 12(5):513–514.

Gilligan, C. A. (1985). Probability Models For Host Infection By Soilborne Fungi. *Phytopathology*, 75(1):61.

Gilligan, C. A. (1990). Antagonistic interactions involving plant pathogens: fitting and analysis of models to non-monotonic curves for population and disease dynamics. *New Phytologist*, 115(4):649–665.

Gilligan, C. A. (1995). Modelling soil-borne plant pathogens: Reaction-diffusion models. *Canadian Journal of Plant Pathology*, 17(2):96–108.

Gilligan, C. A. and Kleczkowski, A. (1997). Population dynamics of botanical epidemics involving primary and secondary infection. *Philosophical Transactions of the Royal Society B: Biological Sciences*, 352(1353):591–608.

Gilligan, C. A., Truscott, J. E., and Stacey, A. J. (2007). Impact of scale on the effectiveness of disease control strategies for epidemics with cryptic infection in a dynamical landscape: An example for a crop disease. *Journal of the Royal Society Interface*, 4(16):925–934.

Glynne, M. (1951). Effects of cultural treatments on wheat and on the incidence of eyespot, lodging, take-all and weeds. *Annals of Applied Biology*, 38(3):665–688.

Gomez-Cabrero, D., Compte, A., and Tegner, J. (2011). Workflow for generating competing hypothesis from models with parameter uncertainty. *Interface Focus*, 1(3):438–449.

Gosme, M. and Lucas, P. (2011). Effect of host and inoculum patterns on take-all disease of wheat incidence, severity and disease gradient. *European Journal of Plant Pathology*, 129(1):119–131.

Gosme, M., Willocquet, L., and Lucas, P. (2007). Size, shape and intensity of aggregation of take-all disease during natural epidemics in second wheat crops. *Plant Pathology*, 56(1):87–96.

GRDC (2011). Crop Placement and Row Spacing: Fact Sheet. Technical report.

Grundy, A., Mead, A., and Burston, S. (1999). Modelling the effect of cultivation on seed movement with application to the prediction of weed seedling emergence. *Journal of Applied Ecology*, 36(5):663–678.

Gubbins, S. and Gilligan, C. (1996). Population dynamics of a parasite and hyperparasite in a closed system: model analysis and parameter estimation. *Proceedings of the Royal Society of London B: Biological Sciences*, 263(1373):1071–1078.

Gubbins, S. and Gilligan, C. (1997a). Biological control in a disturbed environment. *Philosophical Transactions of the Royal Society of London B: Biological Sciences*, 352(2364):1935–1949.

Gubbins, S. and Gilligan, C. (1997b). Persistence of host-parasite interactions in a disturbed environment. *Journal of Theoretical Biology*, 188(2):241–258.

Gubbins, S., Gilligan, C., and Kleczkowski, A. (2000). Population dynamics of plant–parasite interactions: thresholds for invasion. *Theoretical Population Biology*, 57(3):219–233.

Gubbins, S. and Gilligan, C. A. (1997c). A test of heterogeneous mixing as a mechanism for ecological persistence in a disturbed environment. *Proceedings of the Royal Society of London B: Biological Sciences*, 264(1379):227–232.

Gubbins, S. and Gilligan, C. A. (1997d). A test of heterogeneous mixing as a mechanism for ecological persistence in a disturbed environment. *Proceedings of the Royal Society of London B: Biological Sciences*, 264(1379).

Guetsky, R., Shtienberg, D., Elad, Y., Fischer, E., and Dinoor, A. (2002). Improving biological control by combining biocontrol agents each with several mechanisms of disease suppression. *Phytopathology*, 92(9):976–985.

Gutenkunst, R. N., Waterfall, J. J., Casey, F. P., Brown, K. S., Myers, C. R., and Sethna, J. P. (2007). Universally Sloppy Parameter Sensitivities in Systems Biology Models. *PLoS Computational Biology*, 3(10):e189.

Haas, D. and Défago, G. (2005). Biological control of soil-borne pathogens by fluorescent pseudomonads. *Nature Reviews Microbiology*, 3(4):307–319.

Haas, D. and Keel, C. (2003). Regulation of Antibiotic Production in Root-Colonizing Pseudomonas spp. and Relevance for Biological Control of Plant Disease.

Handelsman, J. and Stabb, E. (1996). Biocontrol of soilborne plant pathogens. *The Plant Cell*, 8(10):1855–1869.

Handford, C., Elliott, C., and Campbell, K. (2015). A review of the global pesticide legislation and the scale of challenge in reaching the global harmonization of food safety standards. *Integrated Environmental Assessment and Management*, 11(4):525–536.

Harman, G. E. (2006). Overview of mechanisms and uses of Trichoderma spp. In *Phytopathology*, volume 96, pages 190–194. The American Phytopathological Society.

Hays, W. and Boss, A. (1899). Wheat: varieties, breeding, cultivation. *Minnesota Agricultural Experiment Station*, Bulletin 6.

Heydari, A. and Pessarakli, M. (2010). A review on biological control of fungal plant pathogens using microbial antagonists. *Journal of Biological Sciences*, 10(4):273–290.

HGCA (2006). Take-all in winter wheat – management guidelines. Technical report, Caledonia House, London.

Homan, H. W. and Clausen, R. W. (1996). *Pacific Northwest Agricultural Insect & Plant Disease Study Manual*. University of Idaho (USA). Cooperative Extension System.

Hornby, D. (1975). Inoculum of the take-all fungus: nature, measurement, distribution and survival. *EPPO Bulletin*, 5:319–333.

Hornby, D. (1979). Take-all decline: A theorist's paradise. In Schippers, B. and Gams, W., editors, *Soil-Borne Plant Pathogens*, pages 133–156. Academic Press, New York.

Hornby, D. (1992). New Information about Take-All Decline and Its Relevance to Research on the Control of Take-All by Biological Control Agents. In *Biological Control of Plant Diseases*, pages 95–98. Springer US.

Hornby, D. (1998). *Take-all disease of cereals: a regional perspective*. CABI International, Wallingford, Oxon.

Hornby, D., Bateman, G. L., Payne, R. W., Brown, M. E., and Henden, D. R. (1989). An experimental design and procedures for testing putative controls against naturally-occurring take-all in the field. *Annals of Applied Biology*, 115(2):195–208.

Hoy, M. A. (1992). Biological control of arthropods: Genetic engineering and environmental risks. *Biological Control*, 2(2):166–170.

Htay, K. and Kerr, A. (1974). Biological Control of Crown Gall: Seed and Root Inoculation. *Journal of Applied Bacteriology*, 37(4):525–530.

Huang, H. C., Bremer, E., Hynes, R. K., and Erickson, R. S. (2000). Foliar application of fungal biocontrol agents for the control of white mold of dry bean caused by Sclerotinia sclerotiorum. *Biological Control*, 18(3):270–276.

Huang, H. T. and Yang, P. (1987). The Ancient Cultured Citrus Ant. *BioScience*, 37(9):665–671.

Huang, L., Körschenhaus, J. W., Heppner, C., and Buchenauer, H. (2001). Effects of seed treatments with a novel fungicide Latitude (silthiofam) on fluorescent pseudomonads and take-all of wheat. *Nachrichtenbl. Deut. Pflanzenschutzd*, 53(7):165–171.

Hussain, M., Mehmood, Z., Khan, M. B., Farooq, S., Lee, D.-J., and Farooq, M. (2012). Narrow row spacing ensures higher productivity of low tillering wheat cultivars. *International Journal of Agriculture and Biology*, 14:413–418.

Irtwange, S. V. (2006). Application of Biological Control Agents in Pre-and Postharvest Operations. *Agricultural Engineering International: the CIGR Ejournal*, (3).

Jain, A. and Das, S. (2016). Insight into the Interaction between Plants and Associated Fluorescent Pseudomonas spp. *International Journal of Agronomy*, (4269010):1–8.

Jamalizadeh, M., Etebarian, H. R., Aminian, H., and Alizadeh, A. (2011). A review of mechanisms of action of biological control organisms against post-harvest fruit spoilage. *EPPO Bulletin*, 41(1):65–71.

Jeger, M., Jeffries, P., Elad, Y., and Xu, X.-M. (2009). A generic theoretical model for biological control of foliar plant diseases. *Journal of Theoretical Biology*, 256(2):201–214.

Jeger, M. and Xu, X.-M. (2015). Modelling the dynamics of a plant pathogen and a biological control agent in relation to flowering pattern and populations present on leaves. *Ecological Modelling*, 313:13–28.

Jeger, M. J., Termorshuizen, A. J., Nagtzaam, M. P. M., and van den Bosch, F. (2004). The Effect of Spatial Distributions of Mycoparasites on Biocontrol Efficacy: a Modelling Approach. *Biocontrol Science and Technology*, 14(4):359–373.

Jeger, M. J. and Viljanen-Rollinson, S. L. H. (2001). The use of the area under the disease-progress curve (AUDPC) to assess quantitative disease resistance in crop cultivars. *Theoretical and Applied Genetics*, 102(1):32–40.

Jenkyn, J., Gutteridge, R., and White, R. (2014). Effects of break crops, and of wheat volunteers growing in break crops or in set-aside or conservation covers, all following crops of winter wheat, on the development of take-all (Gaeumannomyces graminis var. tritici) in succeeding crops of winter wheat. *Annals of Applied Biology*, 165(3):340–363.

Jones, D. L., Nguyen, C., and Finlay, R. D. (2009). Carbon flow in the rhizosphere: Carbon trading at the soil-root interface. *Plant and Soil*, 321(1-2):5–33.

Kabbage, M. and Bockus, W. W. (2002). Effect of placement of inoculum of Gaeumannomyces graminis var. tritici on severity of take-all in winter wheat. *Plant Disease*, 86(3):298–303.

Kassambara, A. and Mundt, F. (2020). factoextra: Extract and Visualize the Results of Multivariate Data Analyses.

Kemp, D. R., Auld, B. A., and Medd, R. W. (1983). Does optimizing plant arrangements reduce interference or improve the utilization of space? *Agricultural Systems*, 12(1):31–36.

Kemp, J. S., Paterson, E., Gammack, S. M., Cresser, M. S., and Killham, K. (1992). Leaching of genetically modified Pseudomonas fluorescens through organic soils: Influence of temperature, soil pH, and roots. *Biology and Fertility of Soils*, 13(4):218–224.

Kerr, A. (1980). Biological control of crown gall through production of agrocin 84. *Plant Disease*, 64:25–30.

Kessel, G. J., Köhl, J., Powell, J. A., Rabbinge, R., and Van Der Werf, W. (2005). Modeling spatial characteristics in the biological control of fungi at leaf scale: Competitive substrate colonization by Botrytis cinerea and the saprophytic antagonist Ulocladium atrum. *Phytopathology*, 95(4):439–448.

Kim, D. S., Weller, D. M., and Cook, R. J. (1997). Population dynamics of Bacillus sp. L324-92R12 and Pseudomonas fluorescens 2-79RN10 in the rhizosphere of wheat. *Phytopathology*, 87(5):559–564.

Kim, G. H., Lee, Y. S., Jung, J. S., Hur, J.-S., and Koh, Y. J. (2013). Optimal Spray Time, Interval and Number of Preventive Fungicides for the Control of Fruit Rots of Green and Gold Kiwifruit Cultivars. *Research in Plant Disease*, 19(1):1–6.

Kimmey, J. (1969). Inactivation of Lethal-Type Blister Rust Cankers on Western White Pine. *Journal of Forestry*, 67(5):296–299.

Kirkegaard, J., Christen, O., Krupinsky, J., and Layzell, D. (2008). Break crop benefits in temperate wheat production. *Field Crops Research*, 107(3):185–195.

Kirkland, K. J. (1993). Weed management in spring barley (Hordeum vulgare) in the absence of herbicides. *Journal of Sustainable Agriculture*, 3(3-4):95–104.

Kleczkowski, A., Bailey, D., and Gilligan, C. (1996). Dynamically generated variability in plant-pathogen systems with biological control. *Proceedings of the Royal Society B: Biological Sciences*, 263(1371):777–783.

Kleczkowski, A. and Gilligan, C. A. (2007). Parameter estimation and prediction for the course of a single epidemic outbreak of a plant disease. *Journal of the Royal Society Interface*, 4(16):867–877.

Klepper, B., Rickman, R. W., Zuzel, J. F., and Waldman, S. E. (1988). Use of Growing Degree Days to Project Sample Dates for Cereal Crops. *Agronomy Journal*, 80(5):850–852.

Knudsen, G., Eschen, D., Dandurand, L., and Wang, Z. (1991). Method To Enhance Growth and Sporulation of Pelletized Biocontrol Fungit. *Applied and Environmental Microbiology*, 57(10):2864–2867.

Knudsen, G. R. and Hudler, G. W. (1987). Use of a computer simulation model to evaluate a plant disease biocontrol agent. *Ecological Modelling*, 35(1-2):45–62.

Knudsen, I. M., Hockenhull, J., Funck Jensen, D., Gerhardson, B., Hökeberg, M., Tahvonen, R., Teperi, E., Sundheim, L., and Henriksen, B. (1997). Selection of biological control agents for controlling soil and seed-borne diseases in the field. *European Journal of Plant Pathology*, 103(9):775–784.

Köhl, J., Booij, K., Kolnaar, R., and Ravensberg, W. J. (2019a). Ecological arguments to reconsider data requirements regarding the environmental fate of microbial biocontrol agents in the registration procedure in the European Union. *BioControl*, 64(5):469–487.

Köhl, J., Kolnaar, R., and Ravensberg, W. J. (2019b). Mode of Action of Microbial Biological Control Agents Against Plant Diseases: Relevance Beyond Efficacy. *Frontiers in Plant Science*, 10:845.

Kolb, L. N., Gallandt, E. R., and Mallory, E. B. (2012). Impact of Spring Wheat Planting Density, Row Spacing, and Mechanical Weed Control on Yield, Grain Protein, and Economic Return in Maine. *Weed Science*, 60(2):244–253.

Koscelny, J., Peeper, T., Solie, J., and Solomon, Jr., S. (1990). Effect of Wheat (Triticum aestivum) Row Spacing, Seeding Rate, and Cultivar on Yield Loss from Cheat (Bromus secalinus). *Weed Technology*, 4(3):487–492.

Kuijken, R. C., Snel, J. F., Heddes, M. M., Bouwmeester, H. J., and Marcelis, L. F. (2015). The importance of a sterile rhizosphere when phenotyping for root exudation. *Plant and Soil*, 387(1-2):131–142.

Kumar, A. and Verma, J. P. (2019). The Role of Microbes to Improve Crop Productivity and Soil Health. In *Ecological Wisdom Inspired Restoration Engineering*, pages 249–265. Springer, Singapore.

Kwak, Y. S., Bakker, P. A., Glandorf, D. C., Rice, J. T., Paulitz, T. C., and Weller, D. M. (2009). Diversity, Virulence, and 2,4-Diacetylphloroglucinol sensitivity of gaeumannomyces graminis var. tritici Isolates from Washington State. *Phytopathology*, 99(5):472–479.

Kwak, Y. S., Bonsall, R. F., Okubara, P. A., Paulitz, T. C., Thomashow, L. S., and Weller, D. M. (2012). Factors impacting the activity of 2,4-diacetylphloroglucinol-producing Pseudomonas fluorescens against take-all of wheat. *Soil Biology and Biochemistry*, 54:48–56.

Kwak, Y. S., Han, S., Thomashow, L. S., Rice, J. T., Paulitz, T. C., Kim, D., and Weller, D. M. (2011). Saccharomyces cerevisiae genome-wide mutant screen for sensitivity to 2,4-diacetylphloroglucinol, an antibiotic produced by Pseudomonas fluorescens. *Applied and Environmental Microbiology*, 77(5):1770–1776.

Kwak, Y.-S. and Weller, D. M. (2013). Take-all of wheat and natural disease suppression: A review. *The Plant Pathology Journal*, 29(2):125–35.

Lafond, G., Irvine, B., Clayton, G., Derksen, D., Johnson, E., Johnston, A., McConkey, B., Miller, P., and Rourke, D. (1999). Wide Row Spacing: Is it Really Possible with No-Till - The Canadian Prairie Experience. In *Northwest Direct Seed Cropping Systems Conference Proceedings*.

Lafond, G. P. (1994). Effects of row spacing, seeding rate and nitrogen on yield of barley and wheat under zero-till management. *Canadian Journal of Plant Science*, 74(4):703–711.

Lan, X., Zhang, J., Zong, Z., Ma, Q., and Wang, Y. (2017). Evaluation of the Biocontrol Potential of Purpureocillium lilacinum QLP12 against Verticillium dahliae in Eggplant. *BioMed Research International*, 2017.

Landa, B. B., Mavrodi, O. V., Schroeder, K. L., Allende-Molar, R., and Weller, D. M. (2006). Enrichment and genotypic diversity of phlD-containing fluorescent Pseudomonas spp. in two soils after a century of wheat and flax monoculture. *FEMS Microbiology Ecology*, 55(3):351–368.

Larkin, R. P. and Fravel, D. R. (2002). Effects of varying environmental conditions on biological control of Fusarium wilt of tomato by nonpathogenic Fusarium spp. *Phytopathology*, 92(11):1160–1166.

Lawes, R. A., Gupta, V. V. S. R., Kirkegaard, J. A., and Roget, D. K. (2013). Evaluating the contribution of take-all control to the break-crop effect in wheat. *Crop and Pasture Science*, 64(6):563.

Le, S., Josse, J., and Husson, F. (2008). FactoMineR: A Package for Multivariate Analysis. *Journal of Statistical Software*, 25(1):1–18.

Leclerc, M., Doré, T., Gilligan, C. A., Lucas, P., and Filipe, J. A. (2013). Host Growth Can Cause Invasive Spread of Crops by Soilborne Pathogens. *PLoS ONE*, 8(5):63003.

Lee, C. and Herbek, J. (2010). Wheat in 15-inch and 7.5-inch Rows, Year 2. Technical report, Plant & Soil Sciences Department, University of Kentucky, Lexington and Princeton.

Legard, D. E., Xiao, C. L., Mertely, J. C., and Chandler, C. K. (2000). Effects of plant spacing and cultivar on incidence of Botrytis fruit rot in annual strawberry. *Plant Disease*, 84(5):531–538.

Lewis, J. A. and Papavizas, G. C. (1991). Biocontrol of plant diseases: the approach for tomorrow. *Crop Protection*, 10(2):95–105.

Li, B., Madden, L. V., and Xu, X. (2012). Spatial analysis by distance indices: an alternative local clustering index for studying spatial patterns. *Methods in Ecology and Evolution*, 3(2):368–377.

Li, F. R., Gao, C. Y., Zhao, H. L., and Li, X. Y. (2002). Soil conservation effectiveness and energy efficiency of alternative rotations and continuous wheat cropping in the Loess Plateau of northwest China. *Agriculture, Ecosystems and Environment*, 91(1-3):101–111.

Li, G. Q., Huang, H. C., and Acharya, S. N. (2003). Antagonism and biocontrol potential of Ulocladium atrum on Sclerotinia sclerotiorun. *Biological Control*, 28(1):11–18.

Lidert, Z. (2001). Biopesticides: Is there a path to commercial success? In Vurro, M., Gressel, J., Butt, T., Harman, G., and Pilegram, A., editors, *Enhancing Biocontrol Agents and Handling Risks*, page 283. IOS Press, Amsterdam.

Lievens, B., Brouwer, M., Vanachter, A. C., Cammue, B. P., and Thomma, B. P. (2006). Real-time PCR for detection and quantification of fungal and oomycete tomato pathogens in plant and soil samples. *Plant Science*, 171(1):155–165.

Lievens, B. and Thomma, B. P. (2005). Recent developments in pathogen detection arrays: Implications for fungal plant pathogens and use in practice. *Phytopathology*, 95(12):1374–1380.

Lithourgidis, A. S., Damalas, C. A., and Gagianas, A. A. (2006). Long-term yield patterns for continuous winter wheat cropping in northern Greece. *European Journal of Agronomy*, 25(3):208–214.

Liu, Y. C., Durrett, R., and Milgroom, M. G. (2000). A spatially-structured stochastic model to simulate heterogenous transmission of viruses in fungal populations. *Ecological Modelling*, 127(2-3):291–308.

López-Bellido, L., Fuentes, M., Castillo, J. E., López-Garrido, F. J., and Fernández, E. J. (1996). Long-Term Tillage, Crop Rotation, and Nitrogen Fertilizer Effects on Wheat Yield under Rainfed Mediterranean Conditions. *Agronomy Journal*, 88(5):783.

Lumsden, R. D. (1983). Effect of Composted Sewage Sludge on Several Soilborne Pathogens and Diseases. *Phytopathology*, 73(11):1543.

Maas, A. L., Dashiell, K. E., and Melouk, H. A. (2006). Planting Density Influences Disease Incidence and Severity of Sclerotinia Blight in Peanut. *Crop Science*, 46(3):1341–1345.

Mac Nish, G. C. and Dodman, R. L. (1973). Incidence of gaeumannomyces graminis var. Tritici in consecutive wheat crops. *Australian Journal of Biological Sciences*, 26(6):1301–1307.

Madden, L., Hughes, G., and Bosch, F. v. d. (2007). *The Study of Plant Disease Epidemics.* American Phytopathological Society (APS Press), St Paul, Minnesota.

Madden, L. V. and van den Bosch, F. (2002). A Population-Dynamics Approach to Assess the Threat of Plant Pathogens as Biological Weapons against Annual Crops: Using a coupled differential-equation model, we show the conditions necessary for long-term persistence of a plant disease after a pathogeni. *BioScience*, 52(1):65–74.

Manasfi, Y., Cannesan, M. A., Riah, W., Bressan, M., Laval, K., Driouich, A., Vicré, M., and Trinsoutrot-Gattin, I. (2018). Potential of combined biological control agents to cope with Phytophthora parasitica, a major pathogen of Choisya ternata. *European Journal of Plant Pathology*, 152(4):1011–1025.

Manschadi, A., Ahmad, M., Christopher, J. B., DeVoil, P. A., and Hammer C, G. L. (2006). The role of root architectural traits in adaptation of wheat to water-limited environments. *Functional Plant Biology*, 33:823–837.

Marshall, E. J. P. and Brain, P. (1999). The horizontal movement of seeds in arable soil by different soil cultivation methods. *Journal of Applied Ecology*, 36(3):443–454.

Martensson, A. M. (1990). Competitiveness of inoculant strains of Rhizobium leguminosarum bv. trifolii in red clover using repeated inoculation and increased inoculum levels. *Canadian Journal of Microbiology*, 36(2):136–139.

Massalha, H., Korenblum, E., Tholl, D., and Aharoni, A. (2017). Small molecules below-ground: the role of specialized metabolites in the rhizosphere. *Plant Journal*, 90(4):788–807.

Mathre, D. E., Cook, R. J., and Callan, N. W. (1999). From discovery to use: Traversing the world of commercializing biocontrol agents for plant disease control. *Plant Disease*, 83(11):972–983.

Mavrodi, O. V., Mavrodi, D. V., Thomashow, L. S., and Weller, D. M. (2007). Quantification of 2,4-diacetylphloroglucinol-producing Pseudomonas fluorescens strains in the plant rhizosphere by real-time PCR. *Applied and Environmental Microbiology*, 73(17):5531–5538.

Mazzola, M. (2002). Mechanisms of natural soil suppressiveness to soilborne diseases. *Antonie van Leeuwenhoek, International Journal of General and Molecular Microbiology*, 81(1-4):557–564.

Mazzola, M. and Freilich, S. (2017). Prospects for biological soilborne disease control: Application of indigenous versus synthetic microbiomes. *Phytopathology*, 107(3):256–263.

McBeath, T. M., Gupta, V. V. S. R., Llewellyn, R. S., Davoren, C. W., and Whitbread, A. M. (2015). Break-crop effects on wheat production across soils and seasons in a semi-arid environment. *Crop and Pasture Science*, 66(6):566.

McIntyre, J. L. and Press, L. S. (1991). Formulation, delivery systems and marketing of biocontrol agents and plant growth promoting rhizobacteria (PGPR). In *The Rhizosphere and Plant Growth*, pages 289–295. Springer Netherlands.

McLeod, J. G., Campbell, C. A., Gan, Y., Dyck, F. B., and Vera, C. (1997). Seeding depth, rate and row spacing for winter wheat grown on stubble and chemical fallow in the semiarid prairies. *Canadian Journal of Plant Science*, 76(2):207–214.

Mcquilken, Gemmell, and Lahdenpera (2001). Gliocladium catenulatum as a Potential Biological Control Agent of Damping-off in Bedding Plants. *Journal of Phytopathology*, 149(3-4):171–178.

Meentemeyer, R. K., Cunniffe, N. J., Cook, A. R., Filipe, J. A. N., Hunter, R. D., Rizzo, D. M., and Gilligan, C. A. (2011). Epidemiological modeling of invasion in heterogeneous landscapes: spread of sudden oak death in California (1990–2030). *Ecosphere*, 2(2):1–24.

Mertens, S. K. and Jansen, J. H. (2002). Weed seed production, crop planting pattern, and mechanical weeding in wheat. *Weed Science*, 50(6):748–756.

Meyer, J. B., Lutz, M. P., Frapolli, M., Péchy-Tarr, M., Rochat, L., Keel, C., Défago, G., and Maurhofer, M. (2010). Interplay between wheat cultivars, biocontrol pseudomonads, and soil. *Applied and Environmental Microbiology*, 76(18):6196–6204.

Mills, N. and Getz, W. (1996). Modelling the biological control of insect pests: a review of host-parasitoid models. *Ecological Modelling*, 92:121–143.

Mitchell, J. E. (1973). The mechanisms of biological control of plant diseases. *Soil Biology and Biochemistry*, 5(6):721–728.

Moles, C. G., Mendes, P., and Banga, J. R. (2003). Parameter estimation in biochemical pathways: A comparison of global optimization methods. *Genome Research*, 13(11):2467–2474.

Moore, K. J. and Cook, R. J. (1984). Increased Take-all of Wheat with Direct Drilling in the Pacific Northwest. *Phytopathology*, 74(9):1044.

Moore, L. (1979). Practical use and success of Agrobacterium radiobacter strain 84 for crown gall control. In Schippers, B. and Gams, W., editors, *Soil-borne Plant Pathogens*, pages 553–568. London, UK.

Morozov, A. Y., Robin, C., and Franc, A. (2007). A simple model for the dynamics of a host–parasite–hyperparasite interaction. *Journal of Theoretical Biology*, 249(2):246–253.

Muhammad, S. and Bdliya, S. (2015). Effects of fungicidal rate and intra-row spacing on Cercospora leaf spot disease of groundnut (Arachis hypogaea L.) in the Sudan savanna, north-eastern Nigeria. *Journal of Biology, Agriculture and Healthcare*, 5(20):133–143.

Mumford, J. D. and Norton, G. A. (1984). Economics of Decision Making in Pest Management. *Annual Review of Entomology*, 29(1):157–174.

Nagelkirk, M. and Pennington, D. (2019). Seeding the 2020 winter wheat crop.

Narayanasamy, P. (2013). Mechanisms of Action of Fungal Biological Control Agents. In *Biological Management of Diseases of Crops*, pages 99–200. Springer Netherlands.

Nash, J. C. (2014). On best practice optimization methods in R. *Journal of Statistical Software*, 60(2):1–14.

Nathan, R., Klein, E., Robledo-Arnuncio, J. J., and Revilla, E. (2012). Dispersal kernels: review. In Clobert, J., Baguette, M., Benton, T. G., and Bullock, J. M., editors, *Dispersal Ecology and Evolution*, chapter 15, pages 187–210. Oxford University Press, 1 edition.

Nega, A. (2014). Review on Concepts in Biological Control of Plant Pathogens. *Journal of Biology, Agriculture and Healthcare*, 4(27):33–54.

Newman, E. (1985). The rhizosphere: carbon sources and microbial populations. In Fitter, A., editor, *Ecological interactions in soil*, pages 107–121. Oxford.

Nyaku, S. T., Affokpon, A., Danquah, A., and Brentu, F. C. (2017). Harnessing Useful Rhizosphere Microorganisms for Nematode Control. In *Nematology - Concepts, Diagnosis and Control*. InTech.

O'Callaghan, M., Gerard, E., and Johnson, V. (2001). Effect of soil moisture and temperature on survival of microbial control agents. *New Zealand Plant Protection*, 54:128–135.

Oerke, E.-C. (2006). Crop losses to pests. *The Journal of Agricultural Science*, 144:31–43.

Okubara, P. A. and Bonsall, R. F. (2008). Accumulation of Pseudomonas-derived 2,4-diacetylphloroglucinol on wheat seedling roots is influenced by host cultivar. *Biological Control*, 46(3):322–331.

Okubara, P. A., Kornoely, J. P., and Landa, B. B. (2004). Rhizosphere colonization of hexaploid wheat by Pseudomonas fluorescens strains Q8r1-96 and Q2-87 is cultivar-variable and associated with changes in gross root morphology. *Biological Control*, 30(2):392–403.

Oliver, M. A., Heming, S. D., Gibson, G., and Adams, N. (2003). Exploring the spatial variation of take-all (Gaeumannomyces graminis var. tritici) for site-specific management. In *4th European Conference on Precision Agriculture*, pages 481–486. Wageningen Academic Publishers.

Omlin, M., Brun, R., and Reichert, P. (2001). Biogeochemical model of Lake Zürich: Sensitivity, identifiability and uncertainty analysis. *Ecological Modelling*, 141(1-3):105–123.

Osbourn, A. and Ridout, C. (2013). Engineering wheat for take-all resistance. Technical report, Online research grant. URL: http://gtr.rcuk.ac.uk/projects?ref=BB%2FK006746%2F1.

Otten, W., Filipe, J. A. N., Bailey, D. J., and Gilligan, C. A. (2003). Quantification and Analysis of Transmission Rates for Soilborne Epidemics. *Ecology*, 84(12):3232–3239.

Pal, K. K. and McSpadden Gardener, B. (2006). Biological Control of Plant Pathogens. *The Plant Health Instructor*.

Pandey, B. P., Basnet, K. B., Bhatta, M. R., Sah, S. K., Thapa, R. B., and Kandel, T. P. (2013). Effect of row spacing and direction of sowing on yield and yield attributing characters of wheat cultivated in Western Chitwan, Nepal. *Agricultural Sciences*, 04(07):309–316.

Park, A. W., Gubbins, S., and Gilligan, C. A. (2001). Invasion and persistence of plant parasites in a spatially structured host population. *Oikos*, 94(1):162–174.

Parnell, S., Gilligan, C. A., Lucas, J. A., Bock, C. H., and van den Bosch, F. (2008). Changes in fungicide sensitivity and relative species abundance in Oculimacula yallundae and O. acuformis populations (eyespot disease of cereals) in Western Europe. *Plant Pathology*, 57(3):509–517.

Parylak, D. (2004). Possibilities of root and stem base diseases limitation in continuous wheat under conventional tillage and no-tillage system. *Journal of Plant Protection Research*, 44(2):141–146.

Paulitz, T. C., Smiley, R. W., and Cook, R. J. (2002). Insights into the prevalence and management of soilborne cereal pathogens under direct seeding in the Pacific Northwest, U.S.A. *Canadian Journal of Plant Pathology*, 24(4):416–428.

Peck, S. L. (2004). Simulation as experiment: A philosophical reassessment for biological modeling. *Trends in Ecology and Evolution*, 19(10):530–534.

Perry, J. N. (1995). Spatial Analysis by Distance Indices. *The Journal of Animal Ecology*, 64(3):303.

Pertot, I., Giovannini, O., Benanchi, M., Caffi, T., Rossi, V., and Mugnai, L. (2017). Combining biocontrol agents with different mechanisms of action in a strategy to control Botrytis cinerea on grapevine. *Crop Protection*, 97:85–93.

Phillips, R. E., Blevins, R. L., Thomas, G. W., Frye, W. W., and Phillips, S. H. (1980). No-tillage agriculture. *Science*, 208(4448):1108–1113.

Piening, L. (1983). Effects of seed spacing on common root rot of some barley cultivars. *Canadian Journal of Plant Science*, 63(3):611–616.

Pliego, C., Ramos, C., de Vicente, A., and Cazorla, F. M. (2011). Screening for candidate bacterial biocontrol agents against soilborne fungal plant pathogens. *Plant and Soil*, 340(1):505–520.

Polley, R. W. and Clarkson, J. D. S. (1980). Take-all severity and yield in winter wheat: relationship established using a single plant assessment method. *Plant Pathology*, 29(3):110–116.

Pope, A. and Hornby, D. (1973). Rothamsted Experimental Station Report for 1973, Part 1. pages 128–130.

Pope, A. M. and Hornby, D. (1975). Decrease of take-all by a transmissible factor in take-all decline soils. *Annals of Applied Biology*, 81(2):145–160.

Pope, A. M. and Jackson, R. M. (1973). Effects of wheatfield soil on inocula of gaeumannomyces graminis (Sacc.) Arx & Olivier var. tritici J. Walker in relation to take-all decline. *Soil Biology and Biochemistry*, 5(6):881–890.

Popp, J., Pető, K., and Nagy, J. (2013). Pesticide productivity and food security: A review. *Agronomy for Sustainable Development*, 33(1):243–255.

Porter, J., Pickup, R., and Edwards, C. (1997). Evaluation of flow cytometric methods for the detection and viability assessment of bacteria from soil. *Soil Biology and Biochemistry*, 29(1):91–100.

Prew, R. D. (1980a). Studies on the spread of Gaeumannomyces graminis var. tritici in wheat. I. Autonomous spread. *Annals of Applied Biology*, 94(3):391–396.

Prew, R. D. (1980b). Studies on the spread of Gaeumannomyces graminis var. tritici in wheat. II. The effect of cultivations. *Annals of Applied Biology*, 94(3):397–404.

Pullen, N. and Morris, R. J. (2014). Bayesian model comparison and parameter inference in systems biology using nested sampling. *PLoS ONE*, 9(2):88419.

R Core Team (2019). R: A Language and Environment for Statistical Computing.

Raaijmakers, J. M., Bonsall, R. F., and Weller, D. M. (1999). Effect of population density of Pseudomonas fluorescens on production of 2,4-diacetylphloroglucinol in the rhizosphere of wheat. *Phytopathology*, 89(6):470–475.

Raaijmakers, J. M., Paulitz, T. C., Steinberg, C., Alabouvette, C., and Moënne-Loccoz, Y. (2009). The rhizosphere: A playground and battlefield for soilborne pathogens and beneficial microorganisms. *Plant and Soil*, 321(1-2):341–361.

Raaijmakers, J. M. and Weller, D. M. (1998). Natural Plant Protection by 2,4-Diacetylphloroglucinol-Producing Pseudomonas spp. in Take-All Decline Soils. *Molecular Plant-Microbe Interactions*, 11(2):144–152.

Raaijmakers, J. M. and Weller, D. M. (2001). Exploiting Genotypic Diversity of 2,4-Diacetylphloroglucinol-Producing Pseudomonas spp.: Characterization of Superior Root-Colonizing P. fluorescens Strain Q8r1-96. *Applied and Environmental Microbiology*, 67(6):2545–2554.

Raaijmakers, J. M., Weller, D. M., and Thomashow, L. S. (1997). Frequency of Antibiotic-Producing Pseudomonas spp. in Natural Environments. *Applied and Environmental Microbiology*, 63(3).

Rasmussen, I. S. and Thorup-Kristensen, K. (2016). Does earlier sowing of winter wheat improve root growth and N uptake? *Field Crops Research*, 196:10–21.

Reddy, P. P. and Reddy, P. P. (2014). Mechanisms of Biocontrol. In *Plant Growth Promoting Rhizobacteria for Horticultural Crop Protection*, pages 55–68. Springer India.

Robertson, L. D., Guy, S. O., and Brown, B. D. (2004). Southern Idaho Dryland Winter Wheat Production Guide Basic Recommendations Southern Idaho Dryland Winter Wheat Production Guide Chemical and Variety Disclaimer. Technical report, University of Idaho, College of Agricultural and Life Sciences.

Rotenberg, D., Joshi, R., Benitez, M. S., Chapin, L. G., Camp, A., Zumpetta, C., Osborne, A., Dick, W. A., and McSpadden Gardener, B. B. (2007). Farm management effects on rhizosphere colonization by native populations of 2,4-diacetylphloroglucinol-producing Pseudomonas spp. and their contributions to crop health. *Phytopathology*, 97(6):756–766.

Rothrock, C. S. (1987). Take-all of wheat as affected by tillage and wheat-soybean doublecropping. *Soil Biology and Biochemistry*, 19(3):307–311.

Royston, P. and Groups, S. M. (2007). Profile likelihood for estimation and confidence intervals. *The Stata Journal*, 7(3):376–387.

Ruano-Rosa, D. and Mercado-Blanco, J. (2015). Combining Biocontrol Agents and Organics Amendments to Manage Soil-Borne Phytopathogens. pages 457–478. Springer, Cham.

Salgado, J. D., Lindsey, L. E., and Paul, P. A. (2017). Effects of Row Spacing and Nitrogen Rate on Wheat Grain Yield and Profitability as Influenced by Diseases. *Plant Disease*, 101(12):1998–2011.

Salt, G. A. (1957). Effects of nitrogen applied at different dates, and of other cultural treatments on eyespot, take-all and yield of winter wheat (field experiment, 1953). *The Journal of Agricultural Science*, 48(3):326–335.

Sandler, L., Nelson, K. A., and Dudenhoeffer, C. (2015). Winter Wheat Row Spacing and Alternative Crop Effects on Relay-Intercrop, Double-Crop, and Wheat Yields. *International Journal of Agronomy*, 2015:ID 369243.

Sanguin, H., Sarniguet, A., Gazengel, K., Moënne-Loccoz, Y., and Grundmann, G. L. (2009). Rhizosphere bacterial communities associated with disease suppressiveness stages of take-all decline in wheat monoculture. *New Phytologist*, 184(3):694–707.

Savary, S., Willocquet, L., Pethybridge, S. J., Esker, P., McRoberts, N., and Nelson, A. (2019). The global burden of pathogens and pests on major food crops. *Nature Ecology and Evolution*, 3(3):430–439.

Scheepmaker, J. and Butt, T. (2010). Natural and released inoculum levels of entomopathogenic fungal biocontrol agents in soil in relation to risk assessment and in accordance with EU regulations. *Biocontrol Science and Technology*, 20(5):503–552.

Scherwinski, K., Wolf, A., and Berg, G. (2007). Assessing the risk of biological control agents on the indigenous microbial communities: Serratia plymuthica HRO-C48 and Streptomyces sp. HRO-71 as model bacteria. *BioControl*, 52(1):87–112.

Schillhorn van Veen, T., Forno, D., Joffe, S., Umali-Deininger, D., and Cooke, S. (1998). Integrated Pest Management: Strategies and Policies for Effective Implementation. In Lutz, E., editor, *Agriculture and the Environment: Perspectives on Sustainable Rural Development*, chapter 18, pages 242–253. World Bank, Washington DC.

Schippers, B., Bakker, A. W., and Bakker, P. A. H. M. (1987). Interactions of Deleterious and Beneficial Rhizosphere Microorganisms and the Effect of Cropping Practices. *Annual Review of Phytopathology*, 25(1):339–358.

Schlatter, D., Kinkel, L., Thomashow, L., Weller, D., and Paulitz, T. (2017). Disease suppressive soils: New insights from the soil microbiome. *Phytopathology*, 107(11):1284–1297.

Schoeny, A., Jeuffroy, M. H., and Lucas, P. (2001). Influence of take-all epidemics on winter wheat yield formation and yield loss. *Phytopathology*, 91(7):694–701.

Schoeny, A. and Lucas, P. (1999). Modeling of Take-All Epidemics to Evaluate the Efficacy of a New Seed-Treatment Fungicide on Wheat. *Phytopathology*, 89(10):954–961.

Schüler, C., Biala, J., Bruns, C., Gottschall, R., Ahlers, S., and Vogtmann, H. (1989). Suppression of Root Rot on Peas, Beans and Beetroots Caused by Pythium ultimum and Rhizoctonia solani through the Amendment of Growing Media with Composted Organic Household Waste. *Journal of Phytopathology*, 127(3):227–238.

Schüler, C., Pikny, J., Nasir, M., and Vogtmann, H. (1993). Effects of composted organic kitchen and garden waste on Mycosphaerella pinodes (Berk. et Blox) Vestergr., causal organism of root rot on peas (Pisum sativum L.). *Biological Agriculture & Horticulture*, 9(4):353–360.

Sharma, K. K., Singh, U. S., Sharma, P., Kumar, A., and Sharma, L. (2015). Seed treatments for sustainable agriculture: A review. *Journal of Applied and Natural Science*, 7(1):521–539.

Shipton, P. (1975). Take-all decline during cereal monoculture. In Bruehl, G., editor, *Biology and Control of Soil Borne Plant Pathogens International Symposium*, page 137–144. The American Phytopathological Society, St. Paul, MN.

Shipton, P. J. (1972). Take-all in spring-sown cereals under continuous cultivation: disease progress and decline in relation to crop succession and nitrogen. *Annals of Applied Biology*, 71(1):33–46.

Shoda, M. (2019). *Biocontrol of Plant Diseases by Bacillus subtilis: Basic and Practical Applications*. CRC Press, Boca Raton.

Sieczka, J. (1988). Some negative aspects of crop rotation on Effects of Crop Rotation on Potato Production in the Temperate Zones. In Vos, J., Van Loon, C., and Bollen, G., editors, *Effects of Crop Rotation on Potato Production in the Temperate Zones*, pages 259–272. Developments in Plant and Soil Science.

Simon, A. (1989). Biological control of take-all of wheat by Trichoderma koningii under controlled environmental conditions. *Soil Biology and Biochemistry*, 21(2):323–326.

Simon, A. and Sivasithamparam, K. (1989). Pathogen-suppression: A case study in biological suppression of Gaeumannomyces graminis var. Tritici in soil. *Soil Biology and Biochemistry*, 21(3):331–337.

Singh, A., Bhardwaj, R., and Singh, I. K. (2019). Biocontrol Agents: Potential of Biopesticides for Integrated Pest Management. In *Biofertilizers for Sustainable Agriculture and Environment*, pages 413–433. Springer, Cham.

Singh, V., Mawar, R., and Lodha, S. (2012). Combined effects of biocontrol agents and soil amendments on soil microbial populations, plant growth and incidence of charcoal rot of cowpea and wilt of cumin. *Phytopathologia Mediterranea*, 51(2):307–316.

Smiley, R. W. (1973). Relationship Between Take-all of Wheat and Rhizosphere pH in Soils Fertilized with Ammonium vs. Nitrate-Nitrogen. *Phytopathology*, 63(7):882.

Smiley, R. W. (1979). Wheat-rhizoplane pseudomonads as antagonists of Gaeumannomyces graminis. *Soil Biology and Biochemistry*, 11(4):371–376.

Smit, E., Leeflang, P., Gommans, S., Van Den Broek, J., Van Mil, S., and Wernars, K. (2001). Diversity and Seasonal Fluctuations of the Dominant Members of the Bacterial Soil Community in a Wheat Field as Determined by Cultivation and Molecular Methods. *Applied and Environmental Microbiology*, 67(5):2284–2291.

Soetaert, K. and Petzoldt, T. (2010). Inverse Modelling, Sensitivity and Monte Carlo Analysis in R Using Package FME. *Journal of Statistical Software*, 33(3):1–28.

Spadaro, D. and Gullino, M. L. (2005). Improving the efficacy of biocontrol agents against soilborne pathogens. *Crop Protection*, 24(7):601–613.

Spink, J. H., Blake, J. J., Bounds, P., Rosemaund, A., and Wynne, P. (2004). Take-all control with silthoifam (Latitude); Economic implications from a six-year rotation experiment. Technical report, HGCA.

Stacey, A. J., Truscott, J. E., Asher, M. J., and Gilligan, C. A. (2004). A model for the invasion and spread of rhizomania in the United Kingdom: Implications for disease control strategies. *Phytopathology*, 94(2):209–215.

Stapper, M. and Harris, H. C. (1989). Assessing the productivity of wheat genotypes in a Mediterranean climate, using a crop-simulation model. *Field Crops Research*, 20(2):129–152.

Steddom, K., Becker, O., and Menge, J. A. (2002). Repetitive applications of the biocontrol agent Pseudomonas putida 06909-rif/nal and effects on populations of Phytophthora parasitica in citrus orchards. *Phytopathology*, 92(8):850–856.

Steddom, K. and Menge, J. A. (2001). Evaluation of continuous application technology for delivery of the biocontrol agent Pseudomonas putida 06909-rif/nal. *Plant Disease*, 85(4):387–392.

Stenberg, J. A. (2017). A Conceptual Framework for Integrated Pest Management. *Trends in Plant Science*, 22(9):759–769.

Stiling, P. and Cornelissen, T. (2005). What makes a successful biocontrol agent? A meta-analysis of biological control agent performance. *Biological Control*, 34(3 SPEC. ISS.):236–246.

Strange, R. N. and Scott, P. R. (2005). Plant disease: A threat to global food security. *Annual Review of Phytopathology*, 43:83–116.

Sundh, I. and Goettel, M. S. (2013). Regulating biocontrol agents: A historical perspective and a critical examination comparing microbial and macrobial agents. *BioControl*, 58(5):575–593.

Sundheim, L. (1982). Control of cucumber powdery mildew by the hyperparasite Ampelomyces quisqualis and fungicides. *Plant Pathology*, 31(3):209–214.

Suslow, T. (1982). Role of root colonizing bacteria in plant growth. In Mount, M. and Lacy, G., editors, *Phytopathogenic Prokaryotes*, pages 187–223. Academic Press.

Sutton, J. C. and Peng, G. (1993). Manipulation and Vectoring of Biocontrol Organisms to Manage Foliage and Fruit Diseases in Cropping Systems. *Annual Review of Phytopathology*, 31(1):473–493.

Szczech, M. and Shoda, M. (2006). The Effect of Mode of Application of Bacillus subtilis RB14-C on its Efficacy as a Biocontrol Agent Against Rhizoctonia solani. *Journal of Phytopathology*, 154(6):370–377.

Tang, S., Xiao, Y., and Cheke, R. A. (2010). Dynamical analysis of plant disease models with cultural control strategies and economic thresholds. *Mathematics and Computers in Simulation*, 80(5):894–921.

Teasdale, J. R., Coffman, C. B., and Mangum, R. W. (2007). Potential Long-Term Benefits of No-Tillage and Organic Cropping Systems for Grain Production and Soil Improvement. *Agronomy Journal*, 99(5):1297–1305.

Teich, A. H., Welacky, T., Hamill, A., and Smid, A. (1993). Row-spacing and seed-rate effects on winter wheat in Ontario. *Canadian Journal of Plant Science*, 73(1):31–35.

Ten Eyck, A. (1899). Roots of plants. *North Dakota Agricultural Experiment Station*, Bulletin 3.

Thrall, P. H. and Burdon, J. J. (1999). The spatial scale of pathogen dispersal: Consequences for disease dynamics and persistence. *Evolutionary Ecology Research*, 1(6):681–701.

Tjamos, E., Papavizas, G., and Cook, R. (1992). *Biological Control of Plant Diseases*. Plenum Press, New York.

Transtrum, M. K. and Qiu, P. (2012). Optimal experiment selection for parameter estimation in biological differential equation models. *BMC Bioinformatics*, 13(1):181.

Triplett, G. B. and Dick, W. A. (2008). No-Tillage Crop Production: A Revolution in Agriculture! *Agronomy Journal*, 100(S3):S–153.

Truscott, J. E. and Gilligan, C. A. (2001). The effect of cultivation on the size, shape, and persistence of disease patches in fields. *Proceedings of the National Academy of Sciences of the United States of America*, 98(13):7128–7133.

Truscott, J. E. and Gilligan, C. A. (2003). Response of a deterministic epidemiological system to a stochastically varying environment. *Proceedings of the National Academy of Sciences of the United States of America*, 100(15):9067–9072.

Truscott, J. E., Webb, C. R., and Gilligan, C. A. (1997). Asymptotic analysis of an epidemic model with primary and secondary infection. *Bulletin of Mathematical Biology*, 59(6):1101–1123.

Tsegaye, Z., Assefa, F., Genene, T., and Tenkegna, T. (2018). Concept, Principle and Application of Biological Control and their Role in Sustainable Plant Diseases Management Strategies. *International Journal of Research Studies in Biosciences*, 6(4).

Tsui, C. K., Woodhall, J., Chen, W., Lévesque, C. A., Lau, A., Schoen, C. D., Baschien, C., Najafzadeh, M. J., and de Hoog, G. S. (2011). Molecular techniques for pathogen identification and fungus detection in the environment. *IMA Fungus*, 2(2):177–189.

Turkington, T. K., Beres, B. L., Kutcher, H. R., Irvine, B., Johnson, E. N., O'Donovan, J. T., Harker, K. N., Holzapfel, C. B., Mohr, R., Peng, G., and Stevenson, F. C. (2016). Winter Wheat Yields Are Increased by Seed Treatment and Fall-Applied Fungicide. *Agronomy Journal*, 108(4):1379–1389.

Undersander, D. J. and Christiansen, S. (1986). Interactions of water variables and growing degree days on heading phase of winter wheat. *Agricultural and Forest Meteorology*, 38(1-3):169–180.

Van Den Berg, F., Van Den Bosch, F., and Paveley, N. D. (2013). Optimal fungicide application timings for disease control are also an effective anti-resistance strategy: A case study for zymoseptoria tritici (mycosphaerella graminicola) on wheat. *Phytopathology*, 103(12):1209–1219.

van den Bosch, F. and Gilligan, C. A. (2008). Models of fungicide resistance dynamics. *Annual Review of Phytopathology*, 46:123–147.

van den Bosch, R., Messenger, P. S., and Gutierrez, A. P. (1982). *An Introduction to Biological Control*. Springer US.

Vandenhove, H., Merckx, R., Wilmots, H., and Vlassak, K. (1991). Survival of Pseudomonas fluorescens inocula of different physiological stages in soil. *Soil Biology and Biochemistry*, 23(12):1133–1142.

Venzon, D. J. and Moolgavkar, S. H. (1988). A Method for Computing Profile-Likelihood-Based Confidence Intervals. *Applied Statistics*, 37(1):87.

von Grebmer, K., Fritschel, H., Nestorova, B., Olofinbiyi, T., Pandya-Lorch, R., and Yohannes, Y. (2008). *Global Hunger Index: The Challenge of Hunger 2008*.

Vurukonda, S. S. K. P., Giovanardi, D., and Stefani, E. (2018). Plant growth promoting and biocontrol activity of streptomyces spp. as endophytes. *International Journal of Molecular Sciences*, 19(4):952.

Walker, J. (1975). Take-all disease of Gramineae: a review of recent work. *Review of Plant Pathology*, 54(3):113–144.

Warcup, J. (1957). Studies on the occurrence and activity of fungi in a wheat-field soil. *Transactions of the British Mycological Society*, 40(2):237–IN3.

Warne, D. J., Baker, R. E., and Simpson, M. J. (2019). Using Experimental Data and Information Criteria to Guide Model Selection for Reaction–Diffusion Problems in Mathematical Biology. *Bulletin of Mathematical Biology*, 81(6):1760–1804.

Weaver, J. (1926). Root habits of wheat. In *Root Development of Field Crops*. McGraw-Hill Book Company, Inc., New York.

Weaver, J. E., Kramer, J., and Reed, M. (1924). Development of Root and Shoot of Winter Wheat Under Field Environment. *Ecology*, 5(1):26–50.

Wehrle, V. M. and Ogilvie, L. (1956). Spread of Take-All From Infected Wheat Plants. *Plant Pathology*, 5(3):106–107.

Welbaum, G. E., Sturz, A. V., Dong, Z., and Nowak, J. (2004). Managing Soil Microorganisms to Improve Productivity of Agro-Ecosystems. *Critical Reviews in Plant Sciences*, 23(2):175–193.

Weller, D. (2007). Pseudomonas Biocontrol Agents of Soilborne Pathogens: Looking Back Over 30 Years. *Phytopathology*, 97(2):250–256.

Weller, D. and Cook, R. (1982). Suppression of take-all of wheat by seed treatments with fluorescent Pseudomonads. *Phytopathology*, 73(3):463–469.

Weller, D., Raaijmakers, J., McSpadden-Gardener, B., and Thomashow, L. (2002). Microbial populations responsible for specific soil suppressiveness to plant pathogens. *Annual Review of Phytopathology*, 40(1):309–348.

Weller, D., Zhang, B.-., and Cook, R. (1983). Application of a Rapid Screening Test for Selection of Bacteria Suppressive to Take-All of Wheat. *Phytopathology*, 69(8):463–469.

Weller, D. M. (1983). Colonization of Wheat Roots by a Fluorescent Pseudomonad Suppressive to Take-All. *Phytopathology*, 73(11):1548.

Weller, D. M. (1988). Biological Control of Soilborne Plant Pathogens in the Rhizosphere with Bacteria. *Annual Review of Phytopathology*, 26(1):379–407.

Weller, D. M. (2015). Take-all decline and beneficial pseudomonads. In *Principles of Plant-Microbe Interactions: Microbes for Sustainable Agriculture*, pages 363–370. Springer International Publishing.

Weller, D. M. and Thomashow, L. S. (1994). Current Challenges in Introducing Beneficial Microorganisms into the Rhizosphere. In *Molecular Ecology of Rhizosphere Microorganisms*, pages 1–18. Wiley-VCH Verlag GmbH, Weinheim, Germany.

Werker, A. R., Gilligan, C. A., and Hornby, D. (1991). Analysis of disease-progress curves for take-all in consecutive crops of winter wheat. *Plant Pathology*, 40(1):8–24.

Wessendorf, J. and Lingens, F. (1989). Effect of culture and soil conditions on survival of Pseudomonas fluorescens R1 in soil. *Applied Microbiology and Biotechnology*, 31(1):97–102.

Whipps, J. M. (2001). Microbial interactions and biocontrol in the rhizosphere. *Journal of Experimental Botany*, 52(suppl_1):487–511.

Whipps, J. M. and Davies, K. G. (2000). Success in Biological Control of Plant Pathogens and Nematodes by Microorganisms. In *Biological Control: Measures of Success*, pages 231–269. Springer Netherlands.

Whipps, J. M. and Gerlagh, M. (1992). Biology of Coniothyrium minitans and its potential for use in disease biocontrol. *Mycological Research*, 96(11):897–907.

White, K. and Gilligan, C. (1998). Spatial heterogeneity in three species, plant–parasite–hyperparasite, systems. *Philosophical Transactions of the Royal Society B: Biological Sciences*, 353(1368):543–557.

Wiese, M. (1987). *Compendium of Wheat Diseases*. APS Press, St. Paul, Minnesota.

Wildermuth, G. (1977). *Studies on suppressive soils in relation to the growth of Gaeumannomyces graminis var. tritici and other root pathogens of wheat.* PhD thesis, University of Adelaide.

Wildermuth, G., Warcup, J., and Rovira, A. (1984). Growth of Gaeumannomyces graminis var. tritici in soil in the presence and absence of wheat roots. *Transactions of the British Mycological Society*, 82(3):435–441.

Willocquet, L. and Lebreton, L. (2005). Focal spread of wheat take-all disease. *Phytopathology*, 95(S111).

Willocquet, L., Lebreton, L., Sarniguet, A., and Lucas, P. (2008). Quantification of within-season focal spread of wheat take-all in relation to pathogen genotype and host spatial distribution. *Plant Pathology*, 57(5):906–915.

Winder, L., Alexander, C., Griffiths, G., Holland, J., Woolley, C., and Perry, J. (2019). Twenty years and counting with SADIE: Spatial Analysis by Distance Indices software and review of its adoption and use. *Rethinking Ecology*, 4:1–16.

Workneh, F. and van Bruggen, A. H. (1994). Microbial density, composition, and diversity in organically and conventionally managed rhizosphere soil in relation to suppression of corky root of tomatoes. *Applied Soil Ecology*, 1(3):219–230.

Wright, H., Ashpole, J., Dicks, L., Hutchison, J., McCormack, C., and Sutherland, W. (2020). Some Aspects of Enhancing Natural Pest Control. In Sutherland, W., Dicks, L., Petrovan, S., and Smith, R., editors, *What Works in Conservation 2020*, pages 589–612. Open Book Publishers, Cambridge.

Xu, G. and Gross, D. (1986). Selection of Fluorescent Pseudomonads Antagonistic to Erwinia carotovora and Suppressive of Potato Seed Piece Decay. *Phytopathology*, 76(4):414.

Xu, X. and Hu, X. (2020). The effect of aggregation of pathogen and biocontrol microbe propagules on biocontrol potential: a simple modelling study. *Phytopathology Research*, 2(1):1–9.

Xu, X. and Madden, L. V. (2003). Considerations for the Use of SADIE Statistics to Quantify Spatial Patterns on JSTOR. *Ecography*, 26(6):821–830.

Xu, X.-M., Jeffries, P., Pautasso, M., and Jeger, M. (2011). A numerical study of combined use of two biocontrol agents with different biocontrol mechanisms in controlling foliar pathogens. *Phytopathology*, 101(9):1032–1044.

Xu, X.-M. and Jeger, M. (2013a). Combined use of two biocontrol agents with different biocontrol mechanisms most likely results in less than expected efficacy in controlling foliar pathogens under fluctuating conditions: A modeling study. *Phytopathology*, 103(2):108–116.

Xu, X.-M. and Jeger, M. (2013b). Theoretical modeling suggests that synergy may result from combined use of two biocontrol agents for controlling foliar pathogens under spatial heterogeneous conditions. *Phytopathology*, 103(8):768–775.

Xu, X.-M. and Madden, L. V. (2004). Use of SADIE statistics to study spatial dynamics of plant disease epidemics. *Plant Pathology*, 53(1):38–49.

Xu, X. M., Salama, N., Jeffries, P., and Jeger, M. J. (2010). Numerical studies of biocontrol efficacies of foliar plant pathogens in relation to the characteristics of a biocontrol agent. *Phytopathology*, 100(8):814–821.

Yang, M.-M., Mavrodi, D. V., Mavrodi, O. V., Bonsall, R. F., Parejko, J. A., Paulitz, T. C., Thomashow, L. S., Yang, H.-T., Weller, D. M., and Guo, J.-H. (2011). Biological Control of Take-All by Fluorescent Pseudomonas spp. from Chinese Wheat Fields. *Biology Institute of Shandong Academy of Sciences*, 101(12):1481–99163.

Yarham, D. (1986). Change and decay - the sociology of cereal foot rots. In *Brighton Crop Protection Conference - Pests and Diseases*.

Zhang, H., Su, M., and Georgescu, P. (2015). The global dynamics and optimal control of a plant epidemic model. *Commun. Math. Biol. Neurosci.*, 2015(0):Article ID 32.

Zogg, H. and Jäggi, W. (1974). VII. Contribution to the take-all decline (Gaeumannomyces graminis) imitated by means of laboratory trials and some of its possible mechanisms. *Journal of Phytopathology*, 81(2):160–169.

Appendix A: Appendix to Chapter 3

A.1 Fitting the SIX model to data in Werker et al. (1991) - including μ and τ_I^*

A.1.1 Methods

The SIX model, described in Chapter 2, simulates the interaction between a pathogen and the roots of a plant. A detailed description of the model fitting process can be found in Section 3.5. The four parameters included in the model fitting are listed in Table A.1, and the initial parameter values are selected from those listed in Table A.2

Table A.1 List of parameters that were included in the first model fitting attempt when fitting the SIX model to data from Werker et al. (1991).

Parameter	Definition	Units
β_P	Rate of primary infection of roots by the free-living pathogen	t^{-1}
β_S	Rate of secondary infection of roots	t^{-1}
μ	Death rate of roots due to infection	t^{-1}
τ_I^*	Units of pathogen present on an infected root that has died due to severe infection	

Table A.2 Bounds set on parameters during the first fitting attempt to fit the SIX model to the data in Werker et al. (1991).

Parameter	Lower bound	Upper bound
β_P	0	1
β_S	0	1
μ	0	1
τ_I^*	0	100

A.1.2 Results

The model fitting process was performed 5,000 times under randomly selected initial parameter values, and the fitting attempt that provided the parameters that fit best to the data can be seen in Table A.3 Using these parameter values to run a simulation of the SIX model over a single growing year gives the model trajectory seen in Figure A.1. The number of infected roots increases gradually over the growing season, resulting in a peak of 5.75 infected roots at 3250 degree days $> 0^{\circ}$C. The amount of free-living pathogen decays exponentially throughout a growing season. However, it is also replenished throughout the growing season as infected roots die due to severe infection, causing any pathogen on them to return to the free-living state. This results in a greater amount of free-living material at the end of a growing season compared to at the start.

Using the parameter values found in Table A.3, the SIX model fitted to the data from Werker et al. (1991) produced a collinarity value of 829 (Table A.4). This is significantly above the threshold value determined by Omlin et al. (2001) and Brun et al. (2001). Removing one parameter from the model still produces very high collinearity values, suggesting that the SIX model is currently not identifiable using this data. This can be further seen from the profile likelihoods for the four parameters. Only the rate of primary infection (β_P) has identifiable lower and upper 95% confidence intervals. For the rate of secondary infection (β_S) and the death rate of infected roots (μ), only the upper confidence interval is identifiable. For the number of root fragments produced from a dead infected root that has died due to severe infection (τ_I^*), neither the upper or lower 95% confidence intervals are identifiable.

Table A.3 Parameter values and their 95% confidence intervals obtained through the first attempt at fitting the SIX model to data over one year of growing winter wheat crop infected by take-all. Maximum likelihood model fitting was used, and the standard deviation (σ) that was calculated during this process is shown in the table. Data was obtained from Werker et al. (1991). Out of 5,000 model fitting simulations starting with different initial parameter values, these parameter values produced the highest log likelihood (LL) value.

		Confidence interval (95%)		
Parameter	Value	Lower	Upper	Units
β_P	1.32×10^{-3}	1.83×10^{-4}	3.94×10^{-3}	t^{-1}
β_S	8.85×10^{-7}	-	1.30×10^{-4}	t^{-1}
μ	1.38×10^{-5}	-	1.37×10^{-3}	t^{-1}
τ_I^*	1.71×10^{1}	-	-	t^{-1}
LL	-118			

Table A.4 Collinearity values for the first fitting attempt of the SIX model using the parameters found in Table A.3 fitted to data from Werker et al. (1991). Data was obtained from field experiments carried out over two consecutive years, where winter wheat infected by take-all decline was grown. The full model, and all versions of the model where one parameter value is excluded from the model fitting process, are shown.

β_P	β_S	μ	τ_I^*	Number of parameters	Collinearity value
✓	✓	✓	✓	4	829
✘	✓	✓	✓	3	302
✓	✘	✓	✓	3	760
✓	✓	✘	✓	3	181
✓	✓	✓	✘	3	197

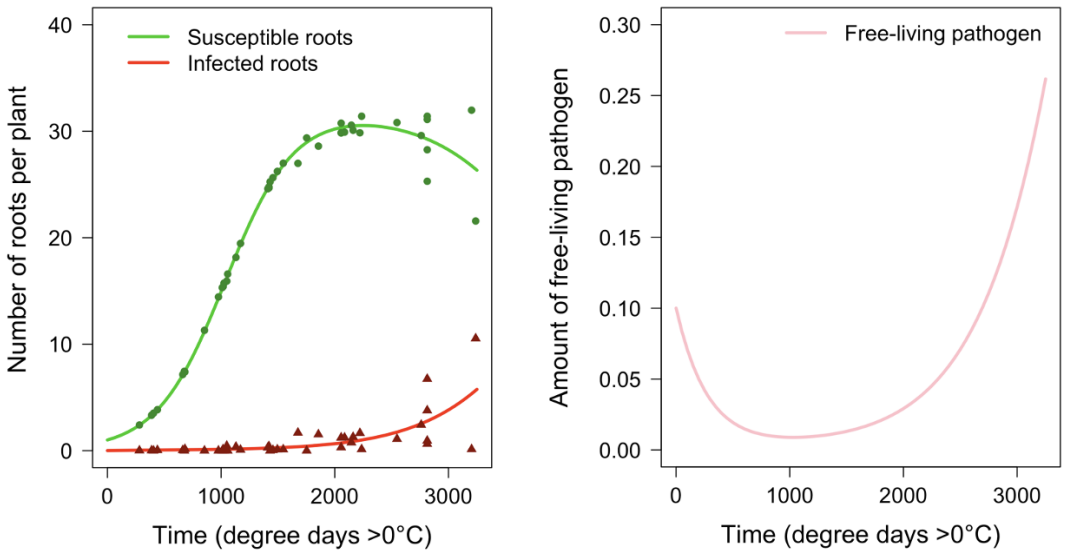

Fig. A.1 Simulation of the SIX model over one year using the parameter values found in Table A.3. Solid lines show the number of susceptible (green) and infected (red) roots, as well as the amount of free-living pathogen in the surrounding soil (pink). Data was obtained from field experiments carried out over two consecutive years, where winter wheat infected by take-all decline was grown (Werker et al. 1991). The data is shown for susceptible roots (green circles) and infected roots (red triangles).

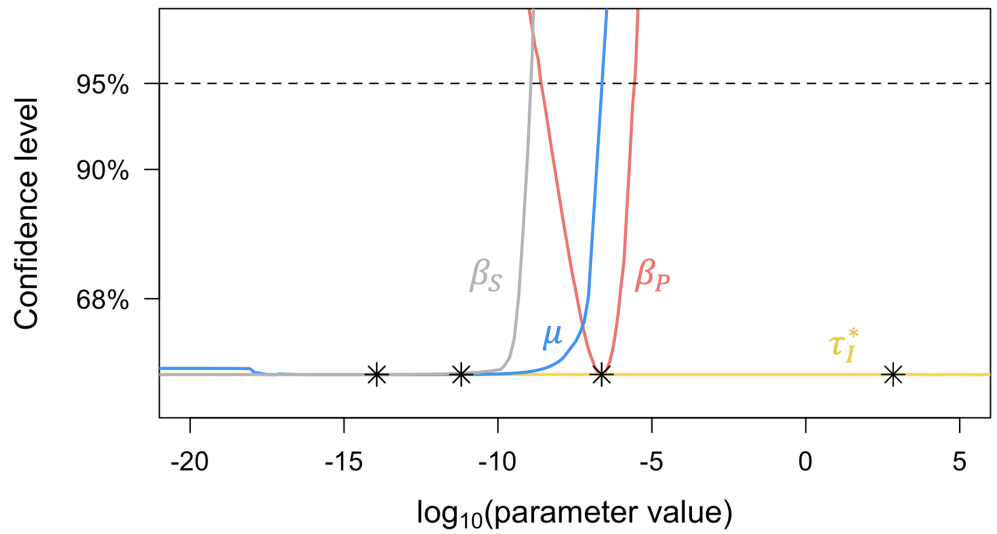

Fig. A.2 Profile likelihood plots for the first model fitting attempt of the SIX model. The best fitting parameter values from Table A.3 are marked on each profile likelihood curve by an asterisk.

A.1.3 Discussion

A simulation of the model using the parameters from Table A.3 shows that the model fits well to the data, with a gradual increase in the number of infected roots throughout a growing season (Figure A.1). However, the amount of free-living material is known to decay rapidly throughout a growing season, which does not occur with these parameter values. This is due to the high value of τ_I^*, which represents the units of pathogen present on an infected root that has died due to severe infection.

The parameter τ_I^*, as well as μ, which represents the death rate of roots due to infection, are highly collinear (Table A.4). This is further shown in the profile likelihood plot (Figure A.2), where τ_I^* is completely unidentifiable, with infinite upper and lower 95% confidence intervals. Both μ and β_S have an identifiable upper 95% confidence intervals but not a lower one. Due to this, it was determined that τ_I^* would be fixed at 0 and the analysis would be redone. The profile likelihood plot demonstrates that this will not have a significant impact on the ability of the model to fit to the data.

A.2 Fitting the SIX model to data in Werker et al. (1991) - including μ

A.2.1 Methods

The SIX model, described in Chapter (Reference chapter with all models here), simulates the interaction between a pathogen and the roots of a plant. A detailed description of the model fitting process can be found in Section 3.5. The three parameters included in the model fitting are listed in Table A.5 and the initial parameter values are selected from those listed in Table A.6.

Table A.5 List of parameters that were included in the second model fitting when fitting the SIX model to data from Werker et al. (1991).

Parameter	Definition	Units
β_P	Rate of primary infection of roots by the free-living pathogen	t^{-1}
β_S	Rate of secondary infection of roots	t^{-1}
μ	Death rate of roots due to infection	t^{-1}

Table A.6 Bounds set on parameters during the second attempt at fitting the SIX model to the data in Werker et al. (1991).

Parameter	Lower bound	Upper bound
β_P	0	1
β_S	0	1
μ	0	1

A.2.2 Results

The model fitting process was performed 5,000 times under randomly selected initial parameter values, and the fitting attempt which provided the parameters that best fit to the data can be seen in Table A.7. Using these parameter values to run a simulation of the SIX model over a single growing year gives the model trajectory seen in Figure A.3. The number of infected roots increases gradually over the growing season, resulting in a peak of 5.75 infected roots at 3250 degree days $> 0^{\circ}$C. The amount of free-living pathogen decays exponentially throughout a growing season , resulting in less than 1% remaining at 2000 degree days $>0^{\circ}$C.

Using the parameter values found in Table A.7, the SIX model fitted to the data from Werker et al. (1991) produced a collinarity value of 17.7 (Table A.8). This is below the threshold value determined by Omlin et al. (2001) and Brun et al. (2001), suggesting that the SIX model is identifiable using this data. However, the profile likelihoods could only determine upper and lower 95% confidence limits for primary (β_P) and secondary (β_S)

infection. The death rate of infected roots (μ) has an identifiable upper 95% confidence interval, but not a lower 95% confidence interval.

Table A.7 Parameter values and their 95% confidence intervals obtained through the second attempt at fitting the SIX model to data over one year of growing winter wheat crop infected by take-all. Maximum likelihood model fitting was used, and the standard deviation (σ) that was calculated during this process is shown in the table. Data was obtained from Werker et al. (1991). Out of 5,000 model fitting simulations starting with different initial parameter values, these parameter values produced the highest log likelihood (LL) value.

		Confidence interval (95%)		
Parameter	Value	Lower	Upper	Units
β_P	1.35×10^{-3}	2.1×10^{-4}	3.59×10^{-3}	t^{-1}
β_S	5.92×10^{-5}	4.22×10^{-5}	8.87×10^{-5}	t^{-1}
μ	4.96×10^{-14}	-	1.87×10^{-3}	t^{-1}
-LL	-118			

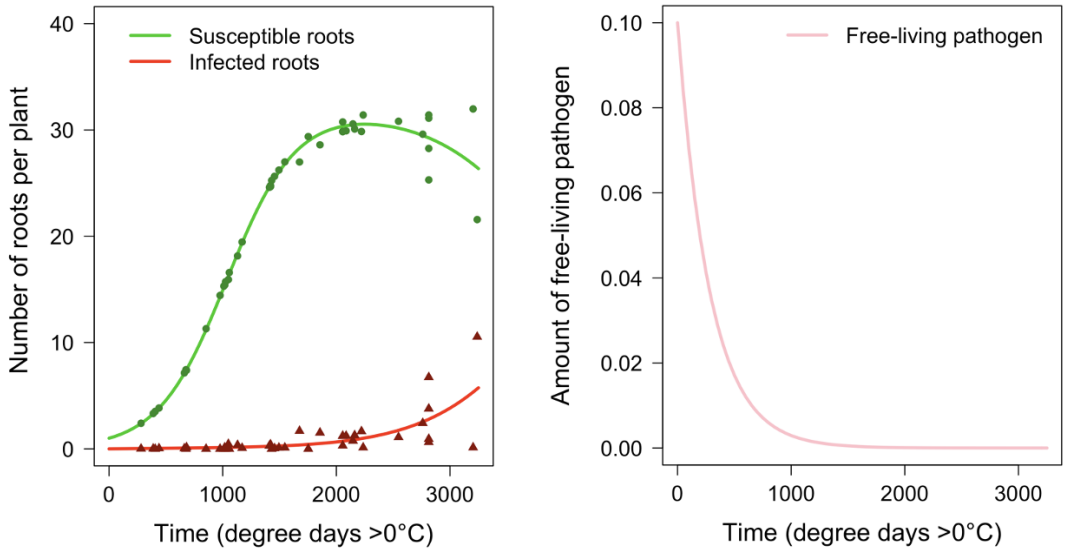

Fig. A.3 Simulation of the SIX model over one year using the parameter values found in Table A.7. Solid lines show the number of susceptible (green) and infected (red) roots, as well as the amount of free-living pathogen in the surrounding soil (pink). Data was obtained from field experiments carried out over two consecutive years, where winter wheat infected by take-all decline was grown (Werker et al. 1991). The data is shown for susceptible roots (green circles) and infected roots (red triangles).

Table A.8 Collinearity values for the second fitting attempt of the SIX model using the parameters found in Table A.7 fitted to data from Werker et al. (1991). Data was obtained from field experiments carried out over two consecutive years, where winter wheat infected by take-all decline was grown. The full model, and all versions of the model where one parameter value is excluded from the model fitting process, are shown.

β_P	β_S	μ	Number of parameters	Collinearity value
✓	✓	✓	3	17.7
✘	✓	✓	2	6.22
✓	✘	✓	2	2.44
✓	✓	✘	2	1.82

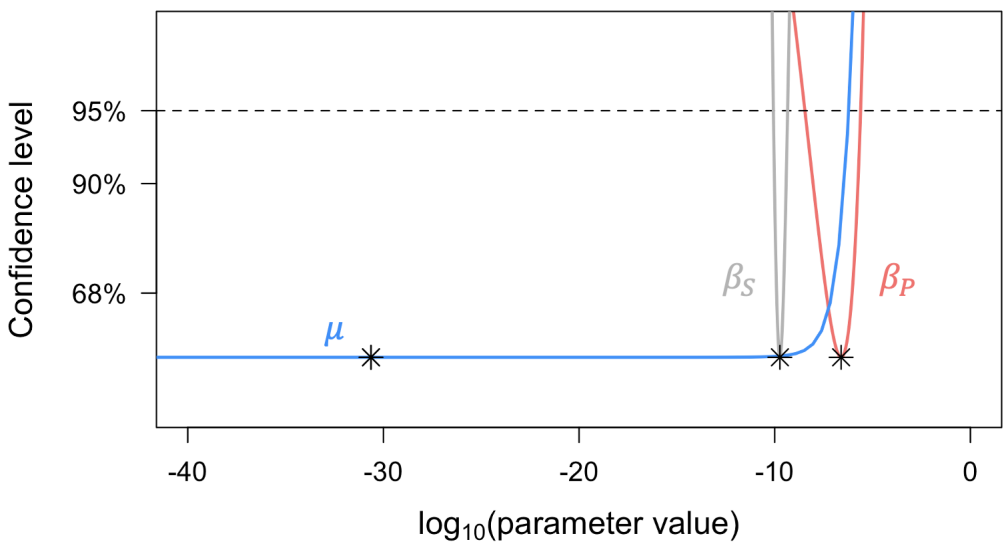

Fig. A.4 Profile likelihood plots for the second model fitting attempt of the SIX model. The best fitting parameter values from Table A.7 are marked on each profile likelihood curve by an asterisk.

A.2.3 Discussion

The SIX model in this section required three parameter values to be obtained through fitting the model to data from Werker et al. (1991). This was one fewer parameters than the version of the SIX model found in Section A.1. The negative log likelihood value for

these models, seen in Tables A.3 and A.7 are both -118, determining that removing this additional parameter from the model did not affect its ability to fit to the data.

A simulation of the model using the parameters in Table A.7 shows that the model fits well to the data (Figure A.3). The decay of free-living material has a trajectory consistent with the literature, with rapid decline over a growing season. The model is also determined to have low enough collinearity between the parameters for them to all be identifiable. However, this is not the case when looking at the profile likelihood plot. Although two of the rate parameters, β_p and β_s, have identifiable 95% confidence intervals, the lower bound for μ is unidentifiable. This suggests that removing μ from the SIX model doesn't have a significant impact on the ability of the model to fit to the data. This should therefore be done to prevent overfitting of the model and allow it to be as simple as possible.

A.3 Visualisation of the SIX model fitting results

The variation in log likelihood values across the solutions is explored in Figure A.5, where the variation in the values of β_P, β_S, and the log likelihood value are visualised. Unlike in Figure 3.9, the values of β_P and β_S can become negative during the model fitting process. There is a distinctive global optimum when either all the solutions are visualised (Figure 3.9A), or when only solutions with a log likelihood value of greater than -130 are visualised (Figure 3.9). This suggests that there is a distinct set of values for β_P and β_S that produce a much better fit to the data than any other values.

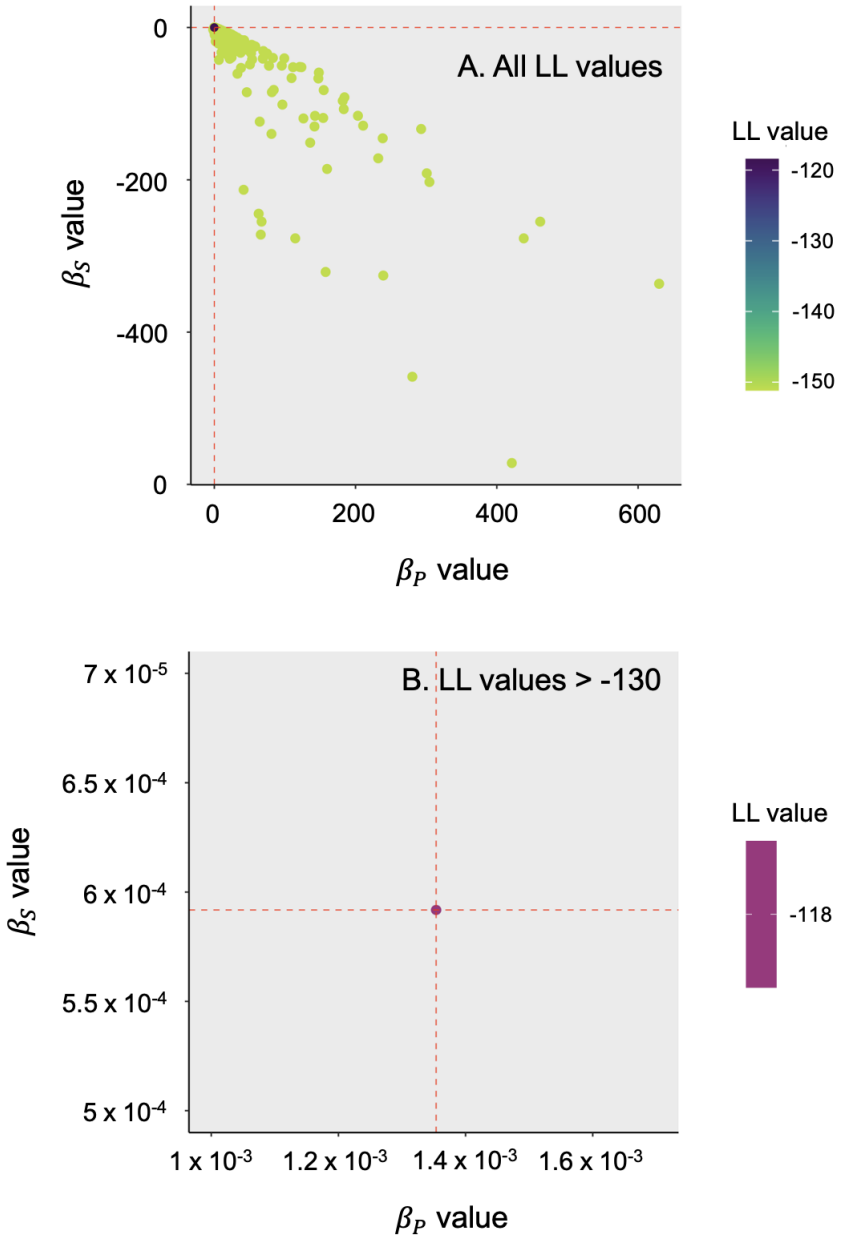

Fig. A.5 Variation in the values of β_P, β_S, and the log likelihood value across 5,000 model fitting attempts when the values of β_P and β_S are not constrained to being positive numbers during the fitting process. Either (A) all solutions, or (B) solutions with a log likelihood value greater than -130 are focused on. Out of all fitting attempts, the values of β_P and β_S that produced the highest log likelihood value are shown by red dashed lines.

Appendix B: Appendix to Chapter 5

B.1 Comparing regular and responsive application of a biocontrol agent

Regular application of the biocontrol agent four times a year, and responsive application, where a field is inspected for disease four times each year and application amount determined by Equation 5.5, were compared to examine their effects on epidemic severity (Appendix Figure B.1). The application time for regular application, and the inspection time and possible subsequent application time for responsive application, were the same for both strategies. The best strategy was determined if one strategy reduced the mean epidemic severity across all included years by over 5% compared to the other strategy. There is almost always no difference between the two application strategies. Responsive application never reduces the epidemic severity by greater than 5% compared to regular application, whereas regular application only does this compared to responsive application for moderate application amounts.

B.2 Variation in the initial amount of biocontrol agent present

When this initial amount of biocontrol agent present at the start of a 20 year simulation is allowed to vary between $A_S \times 10^{-10}$ and $A_S \times 10^{10}$, and there is no additional application after this, the epidemic severity for the four model variations can be seen in Figure B.2. For

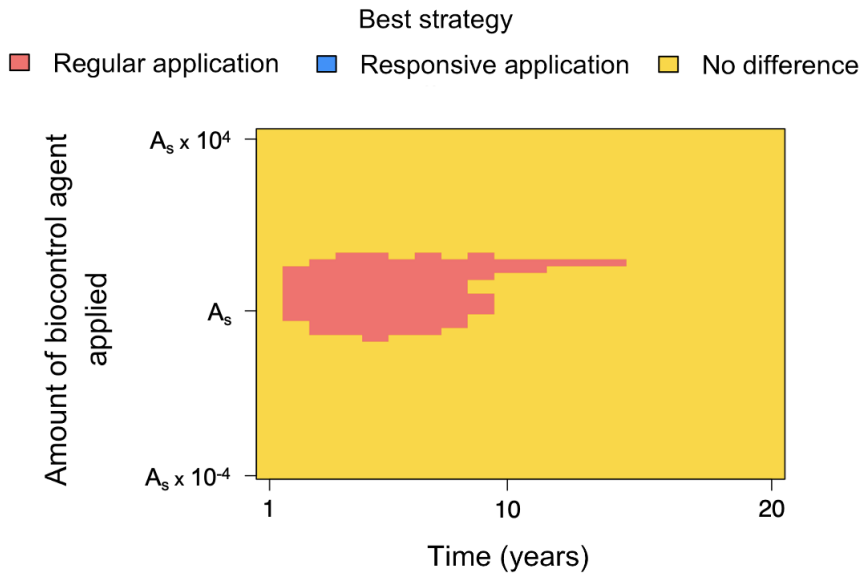

Fig. B.1 Identification of how well responsive and regular application can reduce epidemic severity, where the strategy is determined to be better than the other if it is able to reduce the epidemic severity by >5%. Both application strategies require visiting the crop four times a year, with regular application applying the same amount of biocontrol agent each time, whereas responsive application varies this amount dependent on the percentage of infected roots present (Model: "competition only").

high application amounts of the biocontrol agent for the "competition/out-competed by A" and "competition/out-competed by C" models, there is an increase in epidemic severity after several consecutive years of low epidemic severity. There is also an increase in epidemic severity for high application amounts of the biocontrol agent for the "competition/death of I" model. This is because the additional mechanisms included into these models that the biocontrol agent can use to affect the pathogen require the presence of the pathogen. As the pathogen is completely suppressed at high application amounts, the pathogen cannot bulk up from this interaction, and therefore steadily declines over successive years. It eventually reaches a low enough level that the pathogen can begin to infect the plant, therefore reducing the success of this strategy.

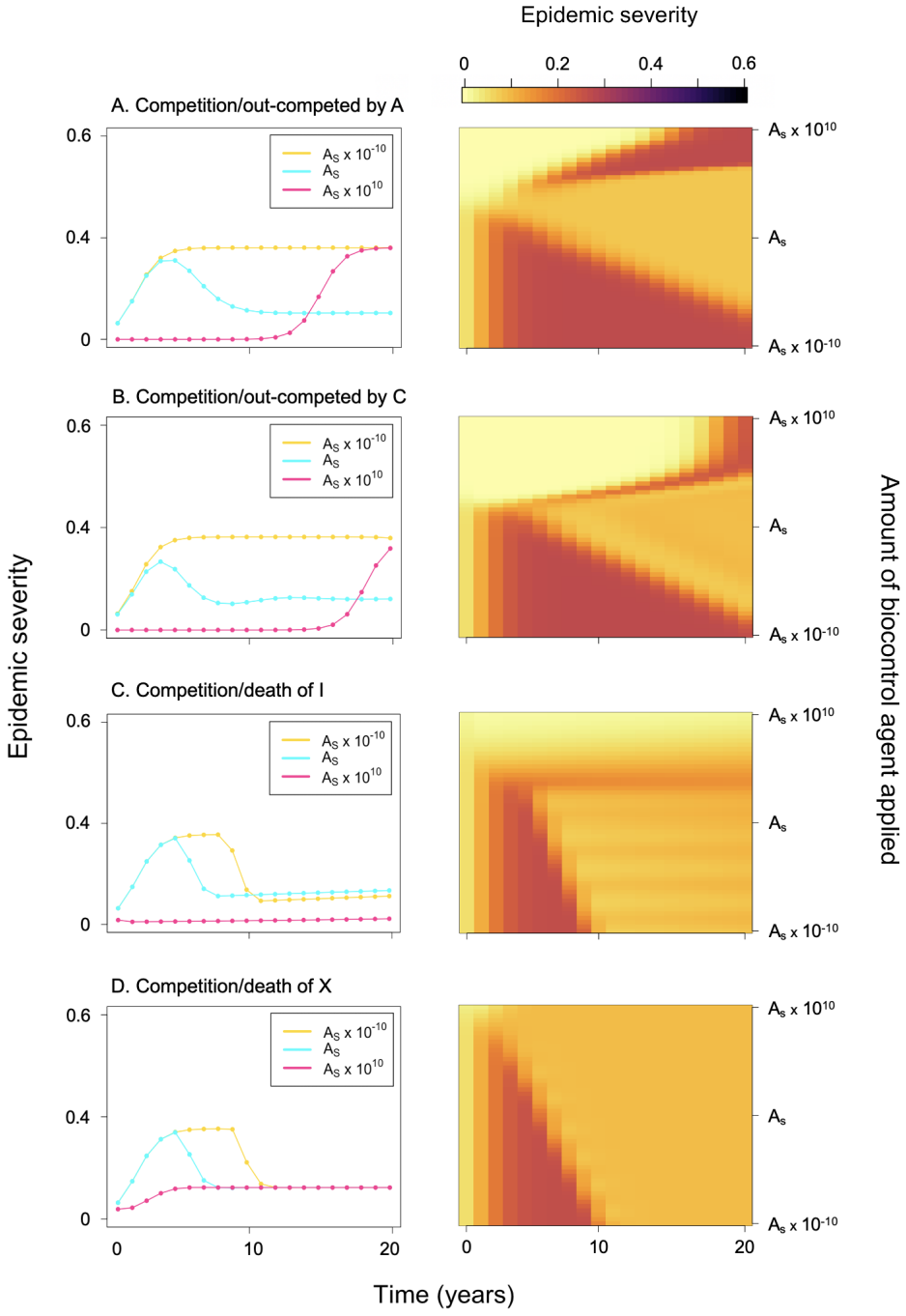

Fig. B.2 Change in epidemic severity across a 20 year simulation for four variations of the SIXCA model as the amount of biocontrol agent present at the start of the simulation is varied between $A_S \times 10^{-10}$ - $A_S \times 10^{10}$. The amount of biocontrol agent applied, shown on the y-axis for the four plots on the right hand side, is represented by a log scale.

B.3 Comparison of application methods for regular application of a biocontrol agent

For the "competition/out-competed by A" model across four application strategies, the only application strategy determined to be the most successful at reducing epidemic severity is when all of the biocontrol agent is applied at the start of the first season (Figure B.3A). The least successful application strategy was either when all of the biocontrol agent is applied at the start of the first season, or when the biocontrol agent is applied once at the start of every season. For the "competition/out-competed by C" model across four application strategies, there is never a most successful strategy (Figure B.3B). The least successful application strategy was either when all of the biocontrol agent is applied at the start of the first season, or when the biocontrol agent is applied once at the start of every season.

For the "competition/death of I" model across four application strategies, the only application strategy determined to be the most successful at reducing epidemic severity is when all of the biocontrol agent is applied at the start of the first season (Figure B.4A). The least successful application strategy was also identified as when all of the biocontrol agent is applied at the start of the first season. For the "competition/death of X" model across four application strategies, a most or least successful strategy is never identified (Figure B.4B).

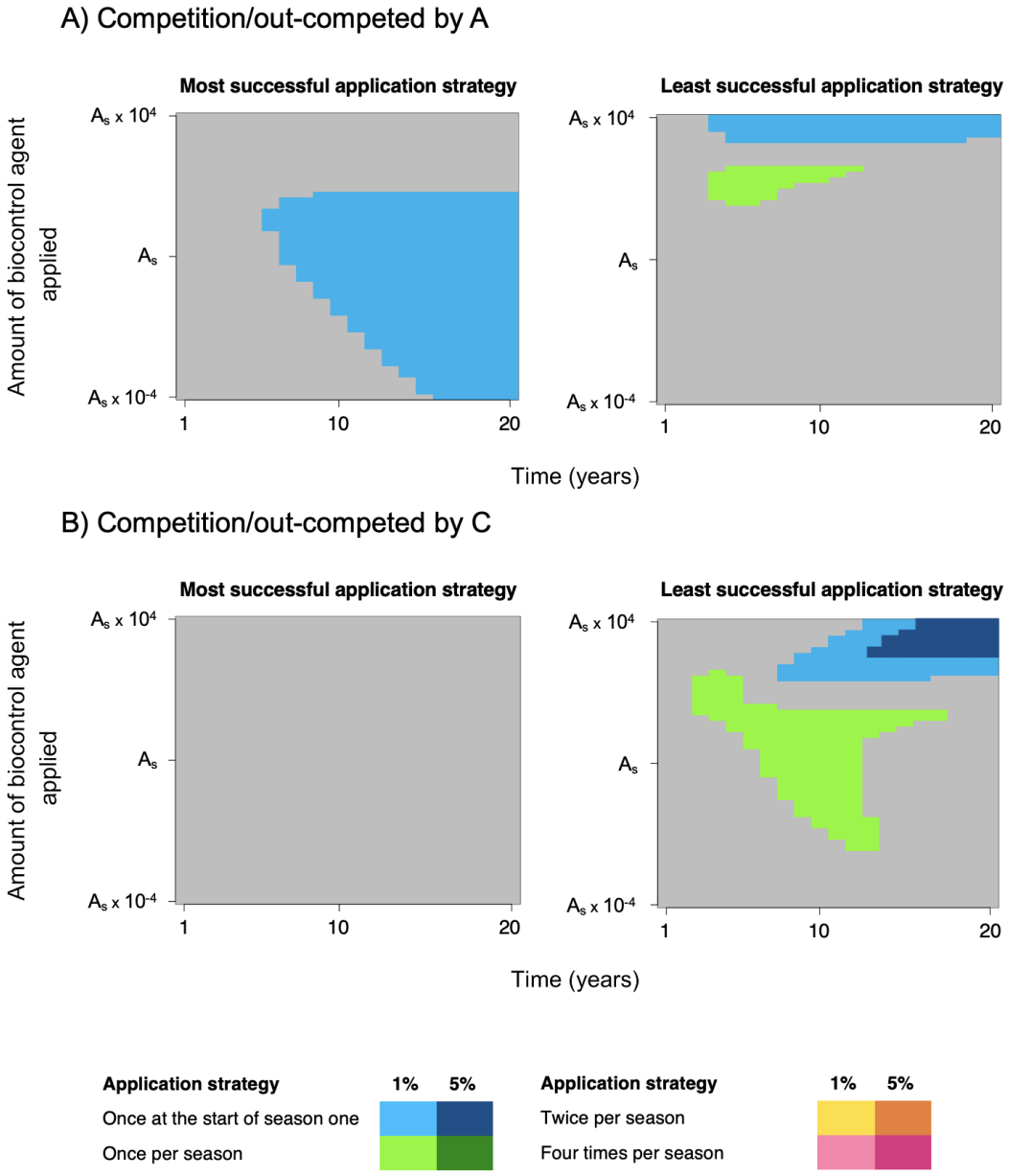

Fig. B.3 Most and least successful strategies for the application of a biocontrol agent to suppress epidemic severity. A strategy was determined to be the most successful if it reduced the mean epidemic severity by >1% or >5% compared to any other strategy. A strategy was determined to be the least successful if it increased the epidemic severity by >1% or >5% compared to any other strategy. The amount of biocontrol agent applied, shown on the y-axis, is represented by a log scale. (Models: " competition/out-competed by A " and "competition/out-competed by C")

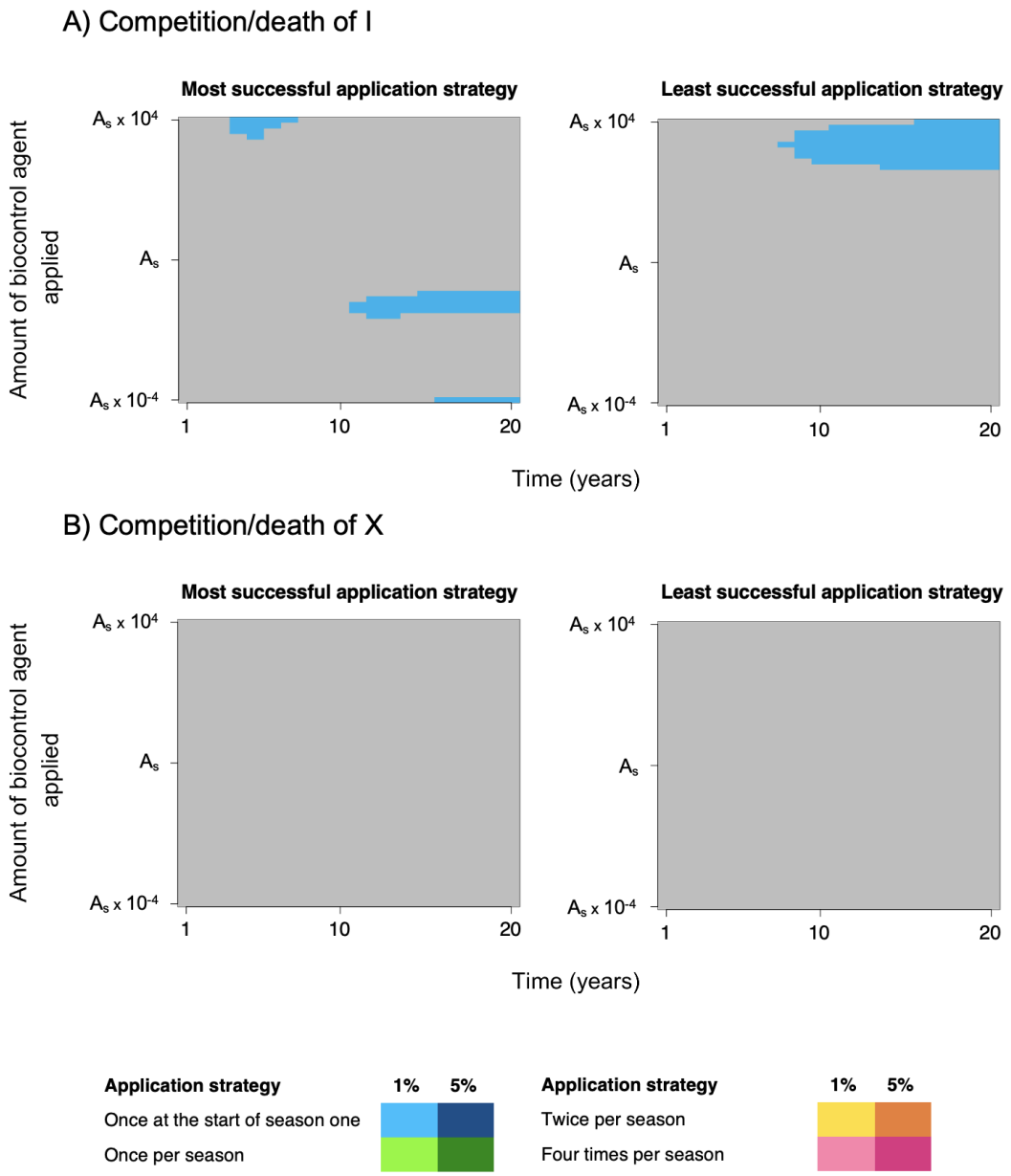

Fig. B.4 Most and least successful strategies for the application of a biocontrol agent to suppress epidemic severity. A strategy was determined to be the most successful if it reduced the mean epidemic severity by >1% or >5% compared to any other strategy. A strategy was determined to be the least successful if it increased the epidemic severity by >1% or >5% compared to any other strategy. The amount of biocontrol agent applied, shown on the y-axis, is represented by a log scale. (Models: " competition/death of I" and "competition/death of X")

Appendix C: Appendix to Chapter 6

C.1 Host growth

Figure C.1A shows that the time taken until crops with between 1-20cm spacing between them are in full contact with each other is always towards the start of a growing season, taking 75 degree days $> 0°$C for crops with 5cm spacing between them, and 522 degree days $> 0°$C for crops with 20cm between them. Due to this, most of the growing season will have crops with their roots in full contact with each other, and the rate of between-plant secondary infection will therefore be at a constant value whether host growth is included or not. Figure C.1B represents the value of the kernel for secondary infection as the distance between plants increases. The mean dispersal distance is 5cm, with a kernel value of 3.45×10^{-3} when crops are spaced 5cm apart from each other, and 8.54×10^{-6} when crops are spaced 20cm apart from each other. Figure C.1C represents how much infection from a single plant with no nearest neighbours occurs through primary infection and how much occurs through secondary infection. The blue dashed line represents the time in degree days $> 0°$C when plants that are spaced 20cm apart grow enough so that their roots are in full contact with each other, and the red dashed like represents the time in degree days $> 0°$C when plants that are spaced 5cm apart grow enough so that their roots are in full contact with each other. This occurs at 75 and 522 degree days $> 0°$C respectively, as seen in Figure C.1A. At the time when plants that are spaced 20cm apart have their roots in full contact with each other, the proportion of diseased roots that occur through secondary infection is 5.72×10^{-2}, and when the spacing is 5cm, the proportion of diseased roots that occur through secondary infection is 3.69×10^{-3}. Figure C.2 focuses on the

proportion of secondary infection that a plant with nearest neighbours will get from other roots within the same plant compared to between the roots of different plants. As the spacing between crops increases, the proportion of secondary infection that occurs between the roots of different plants decreases, with almost all infection occurring within a single plant when the crop spacing is 20cm.

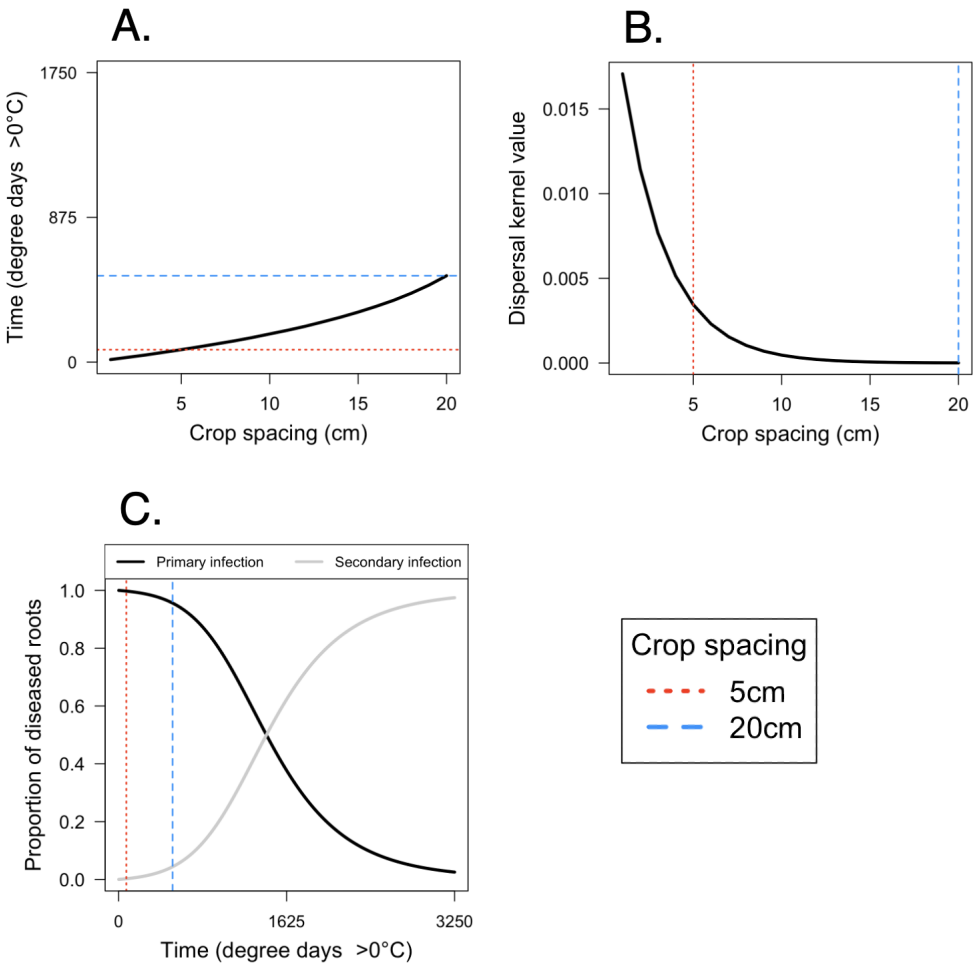

Fig. C.1 Analysis of the factors that determine the effect of host growth on epidemic severity for crops that are spaced 5cm or 20cm apart. A) Time taken before two neighbouring plants have grown enough for their roots to be in full contact with each other. A growing season lasts 3250 degree days $> 0°C$. B) Value of the secondary infection dispersal kernel as distance from the host plant to a neighbouring plant decreases. C) Variation in the proportion of roots that are infected throughout a growing season due to primary and secondary infection when no nearest neighbours are present (all infection occurs within a single plant). The blue dashed line represents a field of evenly spaced crops with 20cm between each plant, whereas the red dotted line represents a field of evenly spaced crops with 5cm between each plant.

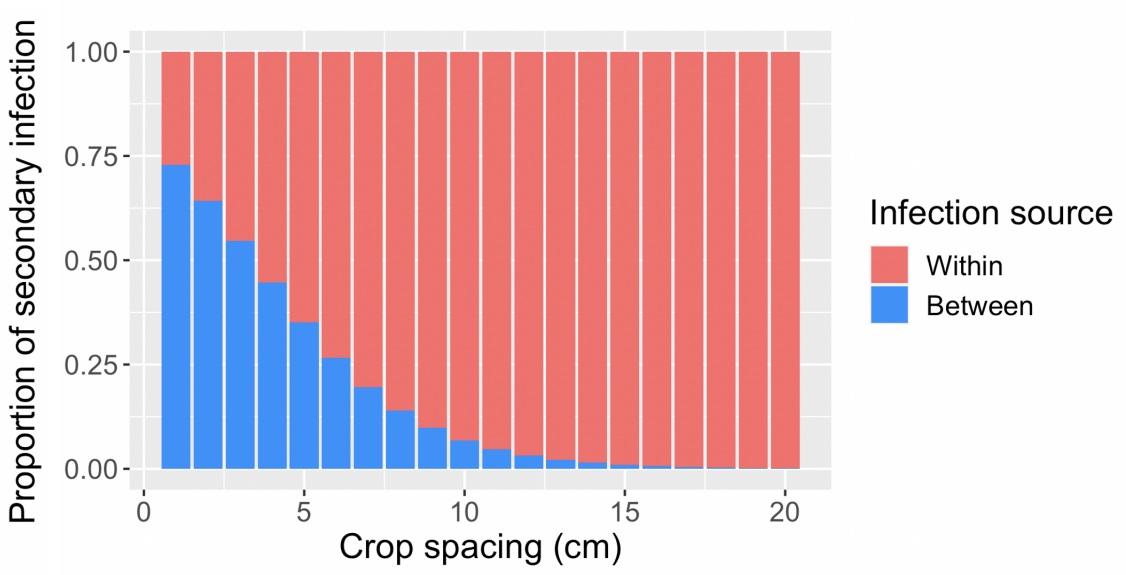

Fig. C.2 Proportion of secondary infection that occurs within the roots of a single plant compared to between the roots of different plants depending on the distance between evenly spaced crops. Infection spreads from a single source of inoculum at the centre of a 13x13 grid of 169 evenly spaced plants over a single growing season.